University of Dundee

University of Dundee

DOCTOR OF PHILOSOPHY

Quantifying soil reinforcement by fibrous roots

Loades, K. W.

Award date:
2010

Link to publication

General rights
Copyright and moral rights for the publications made accessible in the public portal are retained by the authors and/or other copyright owners and it is a condition of accessing publications that users recognise and abide by the legal requirements associated with these rights.

- Users may download and print one copy of any publication from the public portal for the purpose of private study or research.
- You may not further distribute the material or use it for any profit-making activity or commercial gain
- You may freely distribute the URL identifying the publication in the public portal

Take down policy
If you believe that this document breaches copyright please contact us providing details, and we will remove access to the work immediately and investigate your claim.

Download date: 05. May. 2023

DOCTOR OF PHILOSOPHY

Quantifying soil reinforcement by fibrous roots

K. W. Loades

2010

University of Dundee

Conditions for Use and Duplication
Copyright of this work belongs to the author unless otherwise identified in the body of the thesis. It is permitted to use and duplicate this work only for personal and non-commercial research, study or criticism/review. You must obtain prior written consent from the author for any other use. Any quotation from this thesis must be acknowledged using the normal academic conventions. It is not permitted to supply the whole or part of this thesis to any other person or to post the same on any website or other online location without the prior written consent of the author. Contact the Discovery team (discovery@dundee.ac.uk) with any queries about the use or acknowledgement of this work.

College of Art, Science and Engineering
School of Engineering and Physical Sciences
Department of Civil Engineering, University of Dundee

Quantifying soil reinforcement by fibrous roots

K. W. Loades

A dissertation submitted for the degree
of Doctor of Philosophy, June 2010

Declaration

This is to certify that, except where specific reference to other investigation is made, the work described in this dissertation is the result of the investigation of the candidate. Neither the dissertation, nor any part of it, has been presented or is currently submitted in candidature for any degree at any other university.

.....

Kenneth Wilhelmus Loades (candidate), Dundee, 7th June 2010

Acknowledgements

This project was a BBSRC standard research studentship project, BBS/S/K/2005/12211A, entitled 'Quantifying soil reinforcement by fibrous roots' and was carried out at the Scottish Crop Research Institute (SCRI) and the University of Dundee.

I would like to take this opportunity to thank all of my friends and family for their support during the course of my PhD. There have been many highs and a few lows but to have reached the end has been a (largely) enjoyable experience and not possible without you all!

Thanks to everyone at SCRI who has helped in answering questions from 'how does this work?' to 'where is the first aid kit?'. Special thanks must go to Dennis Gordon and my supervisors Dr Paul Hallett (SCRI), Dr Glyn Bengough (SCRI) and Dr Fraser Bransby (University of Dundee). Your guidance has been essential and your support and motivation, when things didn't quite work, invaluable.

A final note must go to Mum, you are always in my thoughts and I wish you were here to have seen what you always knew I was capable of.

Abstract

Reinforcement of soil by fibrous roots is crucial for preventing soil erosion and degradation, yet the underlying mechanisms are poorly understood. Without fully understanding root enmeshment within the soil matrix, and root biomechanical properties key for increasing soil shear strength, adoption in main stream civil engineering, understanding of natural systems and implications to agricultural soil management will be limited. Within this thesis the underlying processes that drive root reinforcement of soils were assessed through a variety of laboratory and field based experiments. This included recent advances in geotechnical engineering and model plant lines with specific root traits. Plant lines were barley (*Hordeum vulgare*) from a mapping population where differences in root hairs, tortuosity and lignin biosynthesis were previously identified by screening large numbers of mutants.

The initial hypothesis was that root numbers and area would control shear reinforcement, this was tested by altering planting density in both glasshouse and field experiments using one barley variety. After 5 weeks in the field, planting density was related to both reinforcement and root area ratio (RAR), with a 6.7 ±1.40 kPa, or 190%, increase in shear strength between 0 and 950/m^2. By 20 weeks in the field shear strength increased by only 29%. The glasshouse study showed an increase of 53%, with a positive correlation to planting density. Relationships between root number and shear strength were not explicit, however, highlighting further possible interactions between soil shear strength and root inclusions.

Various underlying processes were then investigated. Barley mutants, with differences in root hairs and tortuosity, were compared to parent lines. Hairless mutants had different root

tensile strength characteristics, but experimental difficulties (malfunctioning logging hardware) prohibited detection of impacts on shear strength. A refined study was then performed that also incorporated the influence of abiotic stress from compaction and water-logging. Barley with down-regulated lignin biosynthesis (Bowman 140) had increased nodal root tensile strength of 37% compared to the parent line (Bowman Line) under good growth conditions, but this changed to -31% for compacted and 26% for water-logged soil. In addition to abiotic stress, the age of the roots (measured as distance from root tip) type of root (seminal, nodal or lateral) had a large impact on biomechanical behaviour.

Orientation of roots and associated root movement during shear was assessed using Particle Image Velocimetry (PIV) techniques. PIV tracked movement of soil particles and roots at pixel resolution within a sequence of high definition digital images. Root deformation and strain were found to be dependant on root orientation to the shear force. A number of pre-failure changes in root form were also found and were dependant on orientation prior to ultimate failure, through roots either pulling out of the soil (pull-out) or breaking. Patterns of strain along root lengths were also shown to be influenced by orientation.

Conventional catastrophic failure mechanism models were compared to more recent fibre bundle models (FBMs) incorporating progressive failure. The earlier model significantly over predicted reinforcement in 75% of those modelled. Recently developed FBM models were shown to be more accurate, however, variability still existed. The strain based FBM over predicted reinforcement in 70% of the cores with the stress based FBM only over predicting in 46% of cores, highlighting increased model accuracy.

Table of contents

Figures

Chapter 2

Chapter 3

Chapter 4

Chapter 5

Chapter 6

Chapter 7

Tables

Chapter 2

Chapter 3

Chapter 4

Chapter 5

Chapter 6

BLANK PAGE

1. Introduction

Land management that removes vegetation can increase surface soil erosion and lead to landslides on slopes (Glade, 2003; Ziemer, 1981). Planting vegetation, on the other hand, can be a cost-effective and environmentally friendly solution to improve and remediate unstable soils. With an increase in awareness of the environment in which we live, sustainable and ecologically friendly solutions like this are being sought in order to solve problems in engineering. Eco-engineering has thus developed as a discipline - it involves the use of plants to restore unstable soils (Stokes et al., 2009). Such techniques replace hard engineering which uses man-made materials, such as concrete or metal soil nails, to stabilise previously unstable areas of land. Properties of man-made materials are well known and therefore quantifiable, thus providing engineers with the ability to understand and predict their performance under different environmental conditions. However, without being able to quantify the contribution of vegetation in increasing soil shear strength the application and use of vegetation in civil engineering will be limited.

Another important role of plant roots is the stabilisation of managed soils such as in agriculture or amenity surfaces. In agriculture, direct quantification of the impact of roots on mechanical stability has focussed mainly on very small-scale processes (e.g. aggregate stability), with much less conducted on larger-scale processes where roots provide mechanical enmeshment within the soil fabric. In amenity soils, such as sports fields and golf courses, the importance of plant roots is well accepted, but understanding of turf strength is highly qualitative.

In eco-engineering, most research has focused on the role of woody root systems in reinforcing soil (e.g. Abernethy and Rutherford, 1999; O'Laughlin and Ziemer, 1982; Wu et al., 1979). Hawthorn and Oak have been investigated for use in stabilising road embankments but due to the shallow rooting nature of Hawthorn, and the length of time Oak takes to establish using such species is site specific (Norris, 2005). Other trees species have been investigated within studies examining the effects of clear felling in forestry and the resulting effect on slope stability (e.g. Watson et al., 1999; Watson et al., 1997; Ziemer, 1981). Willow has been studied extensively in the field with assessments of their contributions to stream bank stability and highway embankment stability (Mickovski et al, 2009). Furthermore, laboratory based model experiments have investigated in greater detail failure mechanisms of Willow reinforced soil at different scales through the use of a centrifuge (Sonnenberg, 2008).

Much less research has considered fibrous root systems, which are smaller and more abundant in the soil surface. Theses roots may play an important role in reducing erosion and provide lateral reinforcement against cracking. Fibrous root systems of grasses were investigated by Pollen & Simon (2005), who proposed a new modelling framework that captures some of the major mechanisms of soil reinforcement by plant roots. However, a recent review by Stokes et al. (2009) highlighted a total of fifteen desirable root traits of importance when assessing potential soil stabilisation. Clearly, there is considerably more to learn about the mechanical interactions between roots and soil.

Investigating general modes of root reinforcement and the contribution of different attributes of root systems will increase knowledge of the manner of reinforcement. With an increased understanding of the fundamental concepts, a practitioner interested in soil reinforcement by

roots will be able to better identify technologies and predict their impact on soil stability. Engineering applications for this could include:

- River bank management
- Engineered embankments
- Flood defence
- River catchment management
- Sport surface technologies

With concise accurate data, improved models may be developed that utilise refined root parameters enabling better predictions of soil strength improvement. Through incorporation of vegetation root technologies in soil stabilisation, management and rehabilitation, reductions in potential management costs may be attained whilst allowing natural hydrological systems to operate. Concrete is impervious to water resulting in significant increases in surface run off following rain events. With low residence times for water on the surface, drainage channels and rivers can become over-burdened with water resulting in flooding. Utilising roots to reinforce soil both reduces overland flow, through friction, and also improves soil structure. Another advantage of roots is improved soil structure, increasing soil water storage capacity and also the infiltration rate, enabling water to recharge natural ground water supplies and minimising risk of flooding. Such problems have been documented as a significant secondary effect resulting from the adoption of concrete technologies. Climate change is likely to increase intense rainfall events exacerbating those effects that have already been observed to occur through the use of impermeable ground cover solutions.

1.1 Aims of the thesis

Understanding and predicting the reinforcement of soil by fibrous roots could be improved significantly by disentangling the underlying processes. The practical outcomes of such research could be stabilisation of agricultural soils, erosion control, river bank stabilisation and within engineered environments. Given the limited current understanding of the underlying processers, the aim of the thesis is to quantify root, soil and the root/soil interface properties that control reinforcement by fibrous roots.

Due to their rooting nature, fibrous root systems have the potential to significantly increase surface and shallow soil reinforcement. This shallow rooting is in contrast to woody vegetation, offering potential stability out with the scope of deeper rooting plants. Optimising the use of fibrous roots in increasing soil stability, however, requires more information.

Provision of a checklist of ideal root properties, and also those root properties that are key in increasing soil reinforcement, can currently not be provided to those who may seek to adopt ecological engineering techniques. Furthermore, modelling and predicting the long term stability of soils relies heavily on accurate and relevant data. Without knowing what the key root factors are to increasing soil stability model accuracy will be impeded. The key aim of this thesis is a better understanding of what is critical in optimising fibrous root contributions to soil stabilisation.

1.1.1 Objectives and hypotheses

To increase our understanding of fibrous root reinforcement of soils several experiments were performed to test specific hypotheses about roots, soil and the root/soil interface properties. The following outlines the objectives and hypotheses for each of the experiments conducted.

Objective 1 (Chapter 3) - Examine the relationship between root density and soil reinforcement.

Hypothesis

1: With increasing planting density, soil shear strength will increase as a function of the number of roots crossing the shear plane.

Methods

Both field and glasshouse experiments were conducted using a model fibrous root system (barley, *Hordeum vulare*) planted at five different densities in the field and eight in cores grown in a glasshouse environment. Following direct shear testing root diameters and the number of roots crossing the shear plane and their biomechanical properties were recorded to examine root contribution to increasing shear strength.

Objective 2 (Chapter 4) - Quantify the effects of root phenotypic trait to changes in soil shear strength.

Hypotheses

1: Root phenotypic trait, root hairs, will increase enmeshment of soil particles to roots increasing resistance to failure and shear strength.

2: Root tortuosity will increase soil/root contact increasing soil shear strength.

3: Decreases in effective stress due to increases in soil water content affect root contributions to soil shear strength.

Methods

Barley plants previously screened for root phenotypic properties were grown within an environmental chamber and sheared under differing effective stress conditions. Mutant barley plants, exhibiting differing root phenotypic trait, and soil effective stress conditions were controlled to compare and evaluate root contributions to observed shear strength.

Objective 3 (Chapter 5) - Investigate factors controlling root biomechanical properties of tensile strength and elastic modulus.

Hypotheses

1: Root tensile strength and elastic modulus will increase with root age.

2: Water logging and mechanical root impedance increases root tensile strength and elastic modulus.

3: Root cell composition, lignin down regulation, decreases root tensile strength and elastic modulus.

Methods

Plants were grown in soil of differing bulk density, one strong (dry bulk density of 1.4g/cm^3) and one weak (dry bulk density of 1.2g/cm^3). Following three weeks growth root biomechanics of seminal, lateral and nodal roots were assessed. Root biomechanical properties were also examined for plants grown in weak soil following water logging for a period of 7 days. Lignin barley mutants were also cultivated to examine the effects of root composition on biomechanics. Distance from the root tip to the region of the root biomechanically tested was recorded for all roots tested to examine the effects of root age on biomechanical properties.

Objective 4 (Chapter 6) - Visualisation of root failure and root strain development during shear using Particle Image Velocimetry (PIV) techniques.

Hypotheses

1: Direct observations of root failure in soil can be examined and strain quantified using time lapse photography and PIV image analysis.

2: Root orientation does not affect root failure mechanism but influences pre-failure conditions through stress localisation during direct shear.

Methods

Roots were excavated from soil and placed in three different orientations through the shear plane: 45° in compression; 45° in tension; Perpendicular to the shear plane. Direct shear tests were performed in Perspex boxes allowing root failure to be observed and captured using digital photographic techniques. Following direct shear tests root movement and strain development were quantified.

Objective 5 (Chapter 7) – Use quantitative data collected to examine the accuracy of models currently used in predicting root reinforcement of soils.

Hypothesis

1: Models that incorporate the most realistic failure mechanisms will provide the best predictions of root reinforcement.

Methods

Data collected throughout this thesis was incorporated into three key models for predicting reinforcement to assess model reliability. Models tested were the Fibre Bundle Models (FBM) which incorporates progressive failure of roots and the Wu et al. (1979) model. Wu et al. (1979) assume all roots fail catastrophically with no progressive failure. A further strain based FBM was developed and comparisons were made to the existing stress based FBM.

BLANK PAGE

2. Literature review

2.1 The root system

When first investigating root reinforcement of soils, differentiating the type of root system is key to understanding the differing contributions to soil stabilisation. Depending on the root system type, there can be markedly different root distributions with depth (Figure 2-1). Grasses, trees and shrubs have vastly different root architectures and thus differing roles in reinforcement.

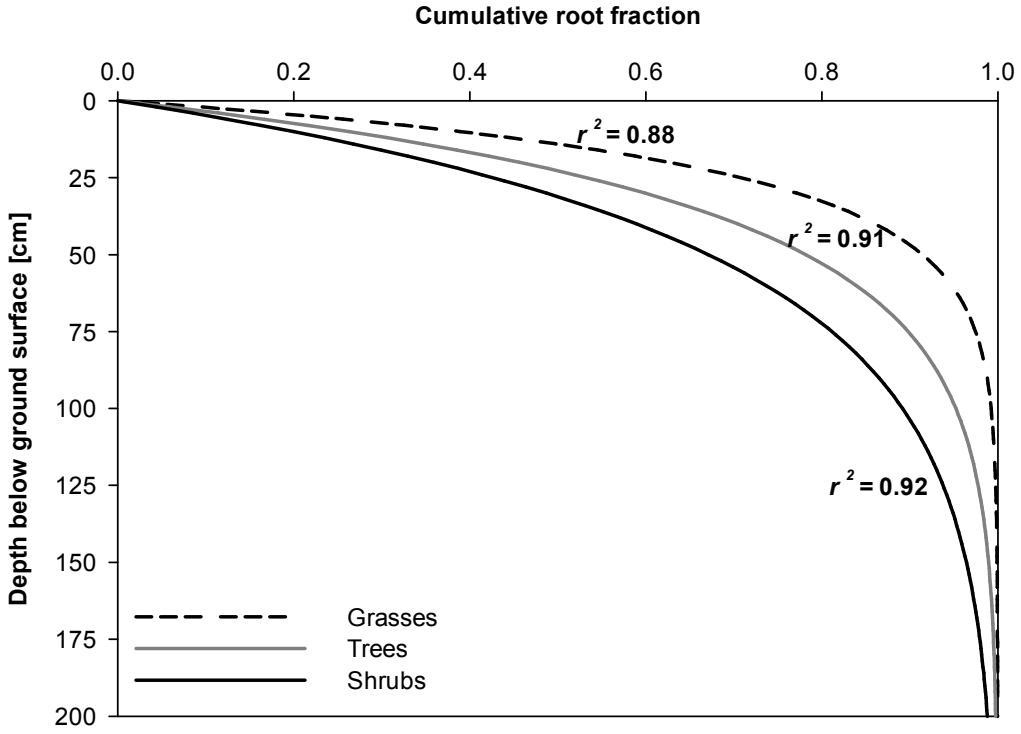

Figure 2-1: Global average root distribution for grasses, tree and shrubs (after Jackson et al., 1996)

Plants can be segregated into two main classes, dicots species and monocot species with each class increasing soil strength in different ways. Most woody rooted plants are dicots, typically with a tap root structure, and generally act to stabilise soil similarly to a soil nail used within the engineering industry for slope stability (Reubens et al., 2007). Fibrous

root systems generally root shallower than tap root systems, increasing surface soil reinforcement and reducing surface soil erosion (Gyssels et al., 2005). Fibrous root systems have multiple roots generated from the seed with a large number of branches (Figure 2-2 (A)). If tap roots are present they have a single main root axis with lateral roots originating from the main axis (Figure 2-2 (B)).

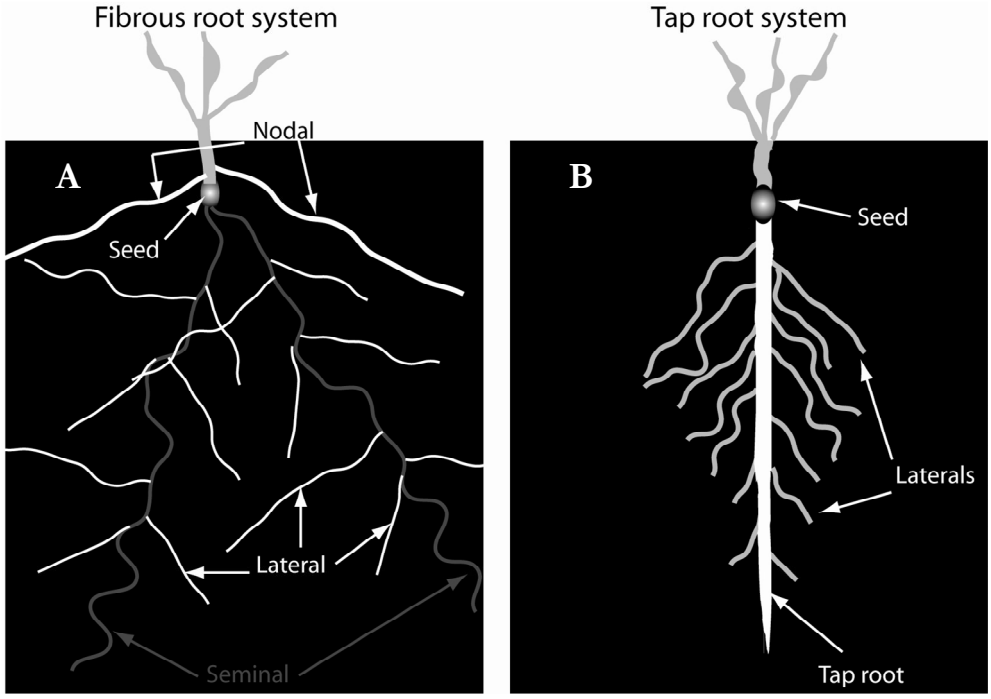

Figure 2-2: Two main root system types, fibrous root [**A**] and tap root [**B**]

One way in differentiating whether a root system is predominantly fibrous is to use root diameter class classifications as proposed by Melzer (1962) and modified by Böhm (1979) (Table 2-1). Typically fibrous root systems are those composed of roots within the very fine (<0.5mm) or fine (0.5-2.0mm) classes. It is important, however, to note that these classes should not be applied when roots are relatively young, as roots of woody tree species increase in diameter as they grow. Fibrous roots typically do not tend to increase in diameter as a function of age.

Root diameter [mm]	Classes of roots
<0.5	Very fine
0.5-2.0	Fine
2-5	Small
5-10	Medium
10-20	Large
>20	Very large

Table 2-1: Classes of roots based on root diameters (Bohm (1979) after Melzer (1962)

2.2 Soil and root interactions

Root and soil interactions are complex. By way of an example of the interactions, maize (*Zea mays* L.) was planted in nine different soils, both fertilized and unfertilized, with marked differences observed once root systems were excavated (Fehrenbacher et al., 1967 (In (Bohm, 1979)). Root mass was observed to differ between treatments, with differences also in the depth to which roots penetrated the soil (Figure 2-3). The interplay between the soil and roots works two ways. Roots impact on soil physical properties, for example affecting drainage, soil bulk density and aggregate stability. Soil also affects root properties, such as root length, diameter and root architecture. These are only some of the complex interactions with many others in the system (Figure 2-4) (Loades et al., 2010) which will be discussed further.

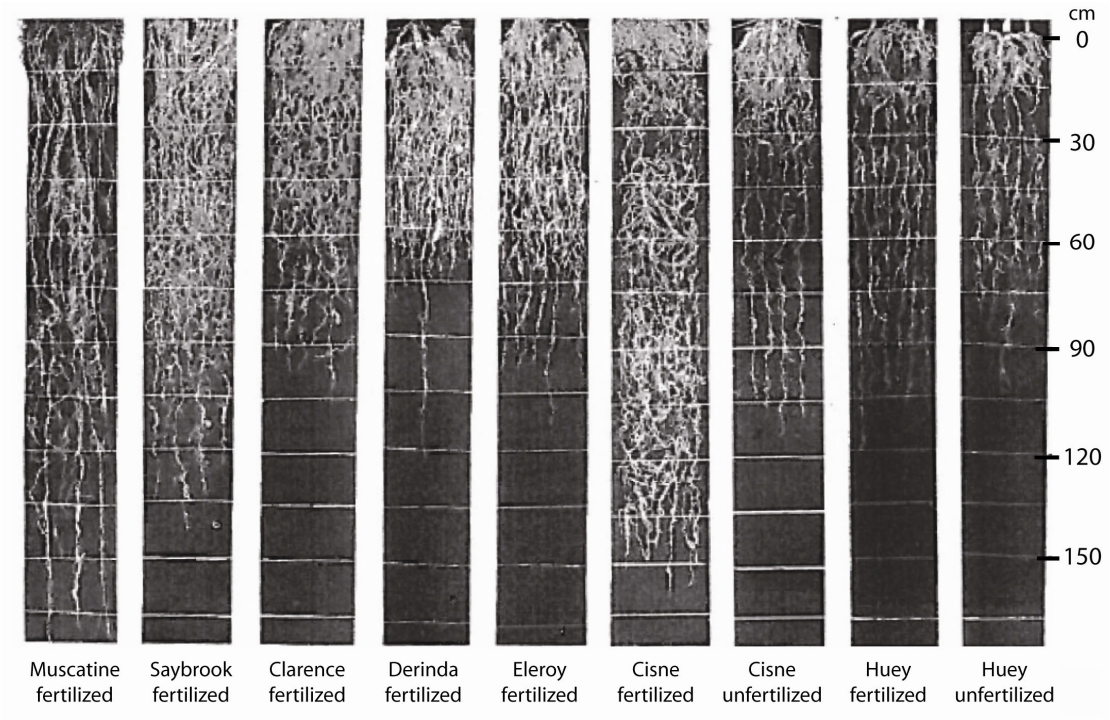

Figure 2-3: Changes in root system when grown within different soils and under different fertilizer regimes (Fehrenbacher et al., 1967 in Böhm, 1979)

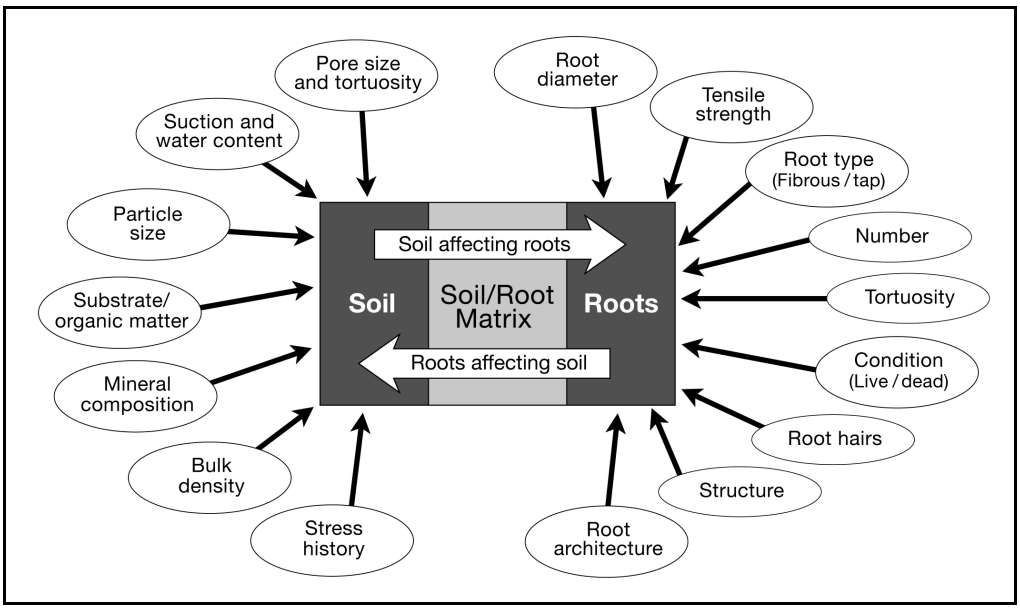

Figure 2-4: Schematic showing some of the factors affecting soil and root strength

2.2.1 Mechanical root impedance

Root growth depends considerably on physical constraints imposed by soil. The rate and extension of roots may be impeded by the structural degradation of soil pore spaces,

which can decrease porosity, hydraulic conductivity and air permeability. An example of degradation is wheeled traffic compacting soil and changing soil aggregate porosity. The impacts are variable depending on the depth of soil and the amount of traffic (Lipiec et al., 2009).

Considerable research has shown that compaction can not only impede root growth, through increased penetration resistance of soil, but may also alter root architecture and development. Increasing the penetration resistance results in a reduction in the root length density, the spatial distribution of roots and also soil water available to plants (Pardo et al., 2000). Roots elongate in soil as a result of 'hydrostatic pressure' and cell division within the meristem (Figure 2-5). In roots experiencing mechanical impedance, cell division can decrease by 40% at a penetration resistance of 0.34 MPa (Bengough and Mullins, 1990). Penetration resistance can also affect cell length. Soil penetration by roots can stop entirely at penetrometer resistances of 0.8-5.0 MPa as hydrostatic pressure is unable to force the root into the soil (Hamza and Anderson, 2005). The threshold penetration resistance for complete impedance varies with plant species. At smaller penetration resistances (i.e. <2.5 kPa), root elongation rates are also influenced, with the effect on root growth dependent on plant species.

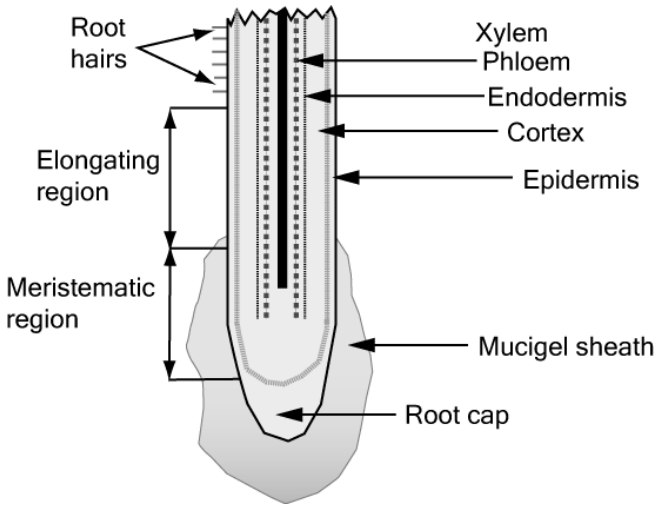

Figure 2-5: Root structure (After Bengough and Mullins, 1990)

There are many studies showing species specific impacts of penetration resistance on the biomechanical properties of roots. The impacts are due to the influence of penetration resistance on cell expansion and rate of root growth, as described previously. Goodman & Ennos (1999) performed bending tests on roots of various plant species grown in soils packed to prescribed densities, simulating weak and strong soils. Lateral root diameters were found to differ between sunflowers (*Helianthus annuus*) grown in loose (bulk soil density of 1.0 g/cm^3) and dense soil (bulk soil density of 1.4 g/cm^3), with root systems also having a greater angle of spread and tap-roots tapering more rapidly in strong soils. Sunflowers (*Helianthus annuus*) and maize (*Zea mays*) showed no significant difference regarding the weight and number of first-order lateral roots or in lignification which may affect root bending stiffness. Maize roots only differed in bending stiffness, with those in stronger soil being less stiff than those in weak soil, 709 MPa ± 45 and 958 MPa ± 74 respectively (Goodman and Ennos, 1999).

Mechanical impedance to root growth may depend on soil water potential, with short-term fluctuations in soil water content having a large influence on root development (Silva et al., 2003). Response times for root growth to resume following impedance are

dependant on the length of time the roots were impeded. Root growth rates change rapidly in response to even short periods of impedance (e.g. 10 minutes). Following impedance for longer periods (i.e. days) roots may take between 2 and 5 days to resume normal root elongation within loose soil (Bengough et al., 2006).

In addition to mechanical impedance, there are many other soil properties that influence root elongation rates and architecture. Nutrient impacts were already discussed briefly and demonstrated in Figure 2-3. Restrictions in the elongation of roots within soil have also been shown to increase the accumulation of *Pseudomonas* spp. around the tip of the root. *Pseudomonas* spp. are neutral, beneficial or restrictive to plant growth dependant on the density, environment or species (Watt et al., 2003).

2.2.2 Root growth effects on soil structure

Roots have an ability to modify the environment in which they live, improving soil structure and hydraulic conductivity (Angers and Caron, 1998). Changes can be direct, such as through root penetration improving hydraulic conductivity (Milleret et al., 2009; Pierret et al., 2007; Pollen-Bankhead and Simon, 2010) or indirectly through the aggregation of soil structure (Hallett et al., 2009). Roots can also provide substrate to microbes, leading to the production of extracellular compounds that 'glue' together soil particles.

Soil aggregation can improve the conditions for plant growth by improving the water retention and aeration characteristics of soil, thus allowing roots greater access to water to oxygen (Horn and Smucker, 2005). Aggregates are assemblages of primary soil particles and organic matter, with many researchers speculating a hierarchical structure ranging from micrometer size microaggregates to millimetre size macroaggregates.

Variations in aggregate sizes dictate the size of pores within soil and therefore the aerobic and hydrologic processes. Pores within aggregates >75 μm generally remain air-filled and hence aerobic, whereas pores 30-0.2 μm allow for water retention (Tisdall and Oades, 1982). A mixture of pore size classes provides a combination of aeration and retained water, thus providing important physical properties for root functioning in soil.

Plant roots can increase soil aggregate formation through multiple processes within soil (Caravaca et al., 2006; de Leon-Gonzalez et al., 2006). Root exudates may directly increase aggregate stability (Materechera et al., 1992) but also indirectly through their influence on soil microbial communities, such as arbuscular mycorrhizal fungi (Hallett et al., 2009). Secondary metabolites produced by microbes using root exudates as substrate lead to increased soil aggregation. The aggregation and penetration of soil by roots has been termed 'biological tillage' by some authors because it breaks up and restructures soil (Alakukka, 1998). In surface soils, fine roots have been found to decrease bulk density and also alter other soil properties, including an increase in the amount of water available for other plants (Milleret et al., 2009). Long term vegetation regeneration has been shown to affect soil structure through vegetation succession, following changes in land use. Soil porosity and the amount of water available for plants was observed to increase with changes through farmland-grassland-shrubs-forest with soil bulk density observed to decrease (Li and Shao, 2006). With increases in soil porosity, water is able to infiltrate and recharge ground water supplies, important for maintaining river flows during periods of drought and a key benefit of eco-engineering.

2.2.3 Root types and root architecture

Monocot species reinforce the top layers of soil (< 0.4m) due to the large number of roots acting as a mesh (Gyssels et al., 2005). These roots bind soil particles and have been shown to be more effective at controlling surface erosion processes by water. Dicot species typically have a smaller number of roots, however, with greater diameters and deeper penetration into the soil than monocot species. Each type of root plays a different role in soil stability, with maximum stability likely to be attained through a mixture of both monocot and dicot species. Due to differences in root structure, and the depth to which roots will penetrate, variability exists between both the root area ratio (RAR) and also root diameters between both species. RAR is defined as the *area* of roots in relation to the *area* of soil

Studies have used other terms to RAR such as the mean root volume (MRV) defined as the average root volume for a specified soil volume. Wynn et al. (2004) looked at median root volume ratio (MRV) and diameter distribution at different depths. MRV was significantly different at 0-15cm depth ($P<0.05$) with an almost two fold increase in the total root volume ratio (Figure 2-6). Root diameter was found be significantly different for roots in the very fine class (<0.5mm) to a depth of 60cm ($P<0.02$) with herbaceous roots having a total volume ratio of 0.593cm^3/cm^3 and forested roots having a total volume ratio of 0.173cm^3/cm^3 (Wynn et al., 2004). These findings are similar to those of van Beek et al. (2005) who reported similar differences between vegetation types.

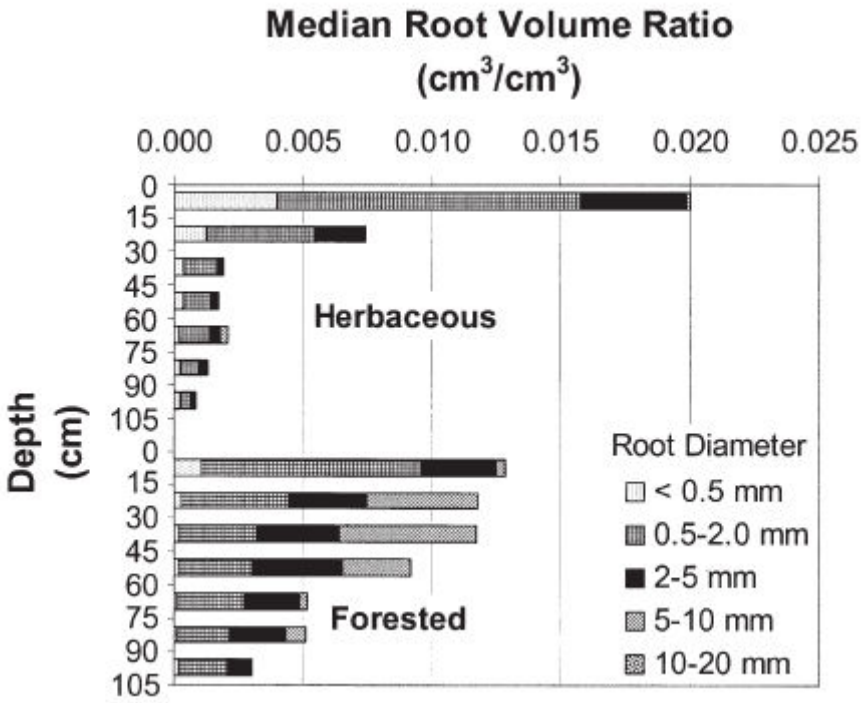

Figure 2-6: Changing median root volume ratio (RVR) with depth for herbaceous and forested stream bank sections (Wynn et al., 2004)

Root density within the soil is a major contributor to increasing shear strength of soil and as such research has used a variety of techniques to demonstrate this relationship. Researchers have used the ratio of root area to soil area across calculated shear planes (RAR) in order to attempt to quantify stresses that roots must be capable of withstanding (Waldron and Dakessian, 1981). Other researchers have looked more generally at 'root length density' (RLD) within soil and shown decreases in RLD with depth (Wynn et al., 2004). RLD has been used as an indicator of slope stability. Osman and Barakbah (2006) found that the top 10 cm contributed 72-88% of RLD for a variety of different species in Malaysia over a range of slope gradients. Results were derived from soil cores taken down to a depth of 70 cm from the surface. Assumptions were made so that the RLD and the soil water content (SWC) were usable as indicators of slope stability due to the stable slopes having a greater RLD and reduced SWC. Although results did indicate

linkages between RLD, SWC and slope stability (Osman and Barakbah, 2006), it may well be an overly simplistic approach due to potential vegetation diversity and inherent root strength of the species studied.

2.3 Root biomechanics

The mechanical properties of roots are important in controlling the contribution of roots to soil strength. Measured changes in applied force with the tensile extension or bending of roots are used to determine root strength and stiffness. Often tests are performed on roots of varying diameter to determine scaling behaviour.

Measuring root biomechanical properties, however, is fraught with complications because testing difficulties. A major problem is the clamping mechanism for holding roots when performing tensile tests and also the extension rate (Cofie and Koolen, 2001). Extension rate has been shown to alter measured fibre strength with strength increasing with increasing extension rate (Morton and Hearlé, 1976 (in Cofie and Koolen, 2001)). Cofie and Koolen (2001) reported the same response in beech roots (*Fagus sylvatica*) with stress increasing 8-20% with changes in extension rate from 10-400mm/min. Extension rates used in literature to date have varied. Examples of such variability are 1mm/min (Hepworth and Vincent 1998), 2mm/min (Genet et al., 2005; Norris, 2005), 3mm/min (Hamza et al., 2006) and 5mm/min (Ennos, 1990) for pull-out tests. It has been suggested that the potential error caused by extension rates used for biomechanical testing should be the same for field tests as used for laboratory tests used to develop root reinforcement models (Cofie and Koolen, 2001).

2.3.1 Root stiffness

Stiffness is the relationship between the stress and strain of a material. Materials of small stiffness, such as rubber, require little stress to extend. Stiffer materials, such as steel, require far greater stress to produce significant strains. Measuring stiffness in plant material is confounded as they have both elastic and plastic properties that are referred to as being biphasic in nature (Kohler, 2000). The elastic limit (yield point) is the region at which the root will return to its original length upon the release of applied load. Beyond the yield point plastic deformation occurs, and the root is unable to return to its original size and shape due to irreversible processes (Figure 2-7).

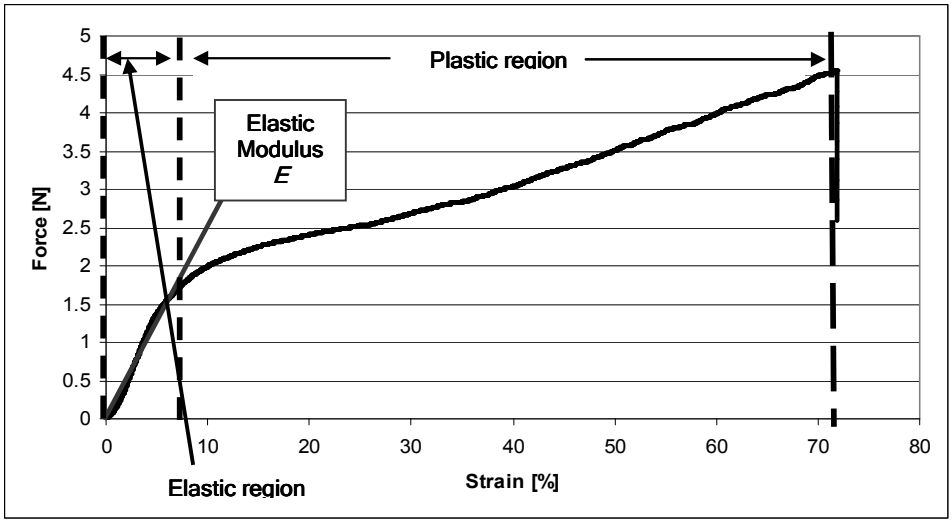

Figure 2-7: Stress versus strain curve for typical barley root tensile test, initial slope used to calculate Young's modulus (E).

The elastic region illustrated in Figure 2-7 can be used to measure axial stiffness, Young's modulus, E where:

$$\mathrm{E} = \frac{\sigma}{\varepsilon} = \frac{F / A}{\Delta L / L_o}$$

σ= stress; ε= strain; ΔL= change of length; L_o= original length; F= tensile force and A= cross-sectional area. Surface asperities, gripping, and root architecture can influence the

evaluation of *E*. Ennos (1990) suggested a critical length of roots must be selected in order to reach the peak contribution to soil reinforcement. He suggested that roots may localise stress at critical distances along the root before it breaks, with distal regions unlikely to localise any stress at all. If the elastic properties of the roots differ, for example as a result in root structural composition, stress may be localised further than would be expected for homogenous materials. This would only be true, however, if elastic properties differed along the length of the root, whilst peak strength did not differ. Weaker roots would still fail within a small spatial region at the point at which stress is being localised. Mobilisation of stress through the root will also been dependant of root architecture which will be discussed later.

2.3.2 Root strength

The tensile strength of roots is another key factor in the understanding and prediction of soil stabilization by roots. Tensile strength is 'the maximum force per unit area required to cause a material to break' (Genet et al., 2005). In plant roots it is assessed by stretching roots in tension until failure. This also provides information on tensile stress versus strain. The initial slope of this relationship is the *Young's modulus* (*E*), stiffness, discussed earlier. The standard unit for measuring force per unit area is Pa (N m^{-2}). However, some studies have reported tensile strength in terms of force only (Ennos, 1991; Toukura et al., 2006), a significant weakness within such studies as no information on root diameter was provided.

There have been a considerable number of studies that have quantified the biomechanical properties of wood plants. These have investigated many different species, primarily for investigations into slope stabilisation. However, research to date on

the tensile strength of fibrous roots is limited. Many of these studies are summarised in Table 2-2, which lists root strength for different species. Information on root stiffness is also provided for one study, but it can be seen that this property has rarely been measured in earlier studies. The interaction between root strength and stiffness in the reinforcement of soil will be described later.

2.3.3 Relationships between root biomechanics and root diameter

Root strength and stiffness are influenced considerably by root diameter. Surprisingly, the small diameter of fibrous root systems results in greater strength than woody systems, although this does not translate into greater soil reinforcement. Root strength versus diameter sometimes follows negative power-law relationship, which has lead to the widespread adoption of fitting these curves to strength-diameter data to describe scaling behaviour (Bischetti et al., 2005; Genet et al., 2005; Mickovski et al., 2009; Pollen and Simon, 2005). The power-law fits are then incorporated into reinforcement models. It has been observed, however, that power-law fits can exhibit large variability in relation to the raw data modelled (Beek et al., 2005; Hales et al., 2009). Hales et al., (2009) reported very poor fits (R^2 values <0.35) when fitting the power-function to a variety of hard wood trees and a native shrub. They also warned against auto-correlation as the derivation of strength is dependent on root diameter. Similarly for root stiffness, van Beek et al. (2005) reported power-function R^2 values of 0.22, with root stiffness decreasing with increasing root diameter. With such variability in fits, caution must be taken when incorporating such relationships into models.

Root Type	Species	Stiffness	Contribution to increasing shear strength	Tensile strength	Reference
Grasses	Setaria faberi Echinochloa crus-gali	n/a	n/a	1.40 ± 0.190 N 9.30 ± 1.230 N	Toukura et al., 2006
	Elymus (Agropyron) repens	n/a	n/a	7.2 – 25.3 MPa	Coppin and Richards, 1990
	Alopecurus geniculatus Poa pratensis	n/a	9.0 kPa 9.0 kPa	n/a	Tobias, 1995*
	Festucs pratensis; Festuca rubra; Poa pratensis	n/a	13.4 kPa	n/a	
	Agrostis stolonifera	n/a	5.2 kPa 4.8 kPa	n/a	
	Lolium mutiflorum; Agrostis stolonifera; Poa annua	n/a	-0.6 kPa 2.9 kPa	n/a	
	Vetiveria zizanioides	n/a	n/a	85.1 ± 31.2 MPa	Cheng and Liu, 2003
	Erimochioa ophiuroides	n/a	n/a	27.30 ± 1.74 MPa	
	Juncellus serotinus	n/a	n/a	24.50 ± 4.2 MPa	
	Paspalum dilatatum poir	n/a	n/a	19.74 ± 3.0 MPa	
	Paspalum notatum flugge	n/a	n/a	19.23 ± 3.59 MPa	
	Zoysia matrella merr	n/a	n/a	17.55 ± 2.85 MPa	
	Cynodon dactylon	n/a	n/a	13.45 ± 2.18 MPa	
	Lygeum spartum	n/a	n/a	37.8 ± 12.5 MPa	Mattia et al., 2005
	Grass	n/a	n/a	2-20 MPa	Cheng et al., 2003
	Moss	n/a	n/a	2-7 MPa	
Crop plants Crop plants	Triticum aestivum	Inner roots: 9.1 ± 1.7 N @ 7days old 17.5 ± 1.7 N @ 21days old Outer roots: 4.9 ± 2.8 N @ 7days old 9.5 ± 2.3 @21days old	n/a	Inner roots: 1.13 ± 0.29 N @ 7days old 2.51 ± 0.59 N @ 21days old Outer roots: 0.64 ± 0.23 N @ 7days old 1.09 ± 0.33 N @ 21days old	Ennos, 1991
	Hordeum vulgarum	n/a	n/a	15-31 MPa	Cheng et al., 2003

Table 2-2: Published results of root stiffness, shear strength and tensile strength of different plant species, (*) denotes those studies performed *in situ* within the field as opposed to laboratory testing

2.3.4 Root architecture

Root architecture is a complex property that is difficult to quantify. A simplistic interpretation is the root area ratio (RAR) described in section 2.2.3. It has been used to predict the contribution of roots to soil stability extensively and referred to as a measure of root architecture (Genet et al., 2008; Waldron and Dakessian, 1981). This approach allows for measurement just on the shear surface, which is much simpler than evaluating the properties of entire root systems. For trees, RAR at the shear plane has been related to soil reinforcement (Docker and Hubble, 2008). In fibrous root systems, however, this relationship is less clear.

Processes occurring away from the shear surface, such as the impact of root branching on pull-out resistance, require greater knowledge of root architecture. Moreover, failure surfaces in nature are not prescribed but occur at the weakest location. Determining the weakest zone in soil requires information of the entire root system. Hydroponic systems were used to investigate whole plant root systems in early research on plant physiology (Hackett, 1968). This work on nutrient deficiencies and root development found that deficiencies in potassium and phosphorous have significant effects on root length and architecture. Mickovski et al. (2007) used analogue roots comprising of three different architectures, tap, dichotomous and herringbone, to investigate fundamental changes in resistance to pull-out as affected by changing architecture. Such work has also been performed using Hawthorn roots where 3 distinct failure types were observed depending on root architecture (Norris, 2005). Roots were categorised into similar classes to the tap, dichotomous and herring bone roots described by Mickovski et al. (2007). A comparison of pull-out resistance between the two studies is not possible, however, as the root

analogues studied by Mickovski et al. (2007) were pulled out of sand, whereas Hawthorn roots studied by Norris (2005) were embedded in clay soils.

Changing the soil, however, highlighted different impacts from root architecture on pull-out. Pull-out force for roots embedded in clay gradually increased with root head displacement. Force increased, dependant on root architecture, to a peak before roots failed and force decreased (Norris, 2005). Conversely, the pull-out resistance of root analogues in sand initially increased rapidly with displacement, before failing in a more progressive way based on root architecture. Tap roots had the least resistance to pull-out and dichotomous roots were the most resistant (Mickovski et al., 2007). Such observed differences demonstrate that accurate predictions of the contribution of roots to reinforcement require soil properties, and their effects on bonds between roots and soil, in addition to information about root architecture

It is hypothesised that lateral roots and root hairs increase resistance to uprooting due to increases in surface area, and therefore friction, with the soil (Ennos, 1991; Operstein and Frydman, 2000). One study by Bailey et al. (2002) attempted to assess the contribution of root hairs to pull-out resistance with results proving inconclusive. This study used Arabadopsis, which has characteristically small root systems. Although root hairs did not increase pull-out resistance in this study, whereas lateral roots had a major impact, the authors did note that this may have been due to properties of the plant. They speculated that the very weak roots may have fractured before the influence of root hairs could be mobilised (Bailey et al., 2002).

2.3.5 Root composition

2.3.5.1 Cellulose

Plant cellulose microfibrils within plant root xylem are embedded within lignin with cellulose providing tensile strength and lignin affecting stiffness (Hepworth and Vincent, 1998). The cellulose content of plants has been show to affects plant mechanical properties. Links between cellulose content and root strength were shown by Penny and Hathaway (1975). Within six willow (*Salix*) and poplar (*Populus*) clones, the tensile strength of different root tissues was found to be affected by cellulose content. The strength of root cell walls were found to be positively correlated with increasing cellulose content. Correlations between the root stele strength and cellulose content was less clear (Figure 2-8). A study using sweet chestnut roots showed a decrease in both tensile strength and cellulose content with increasing root diameters (Figure 2-9) (Genet et al., 2005). The correlations between cellulose and lignin, however, were highly variable. Decreasing cellulose content in relation to increasing root diameter has also been found in other species, with further influence from topographic location (Hales et al., 2009).

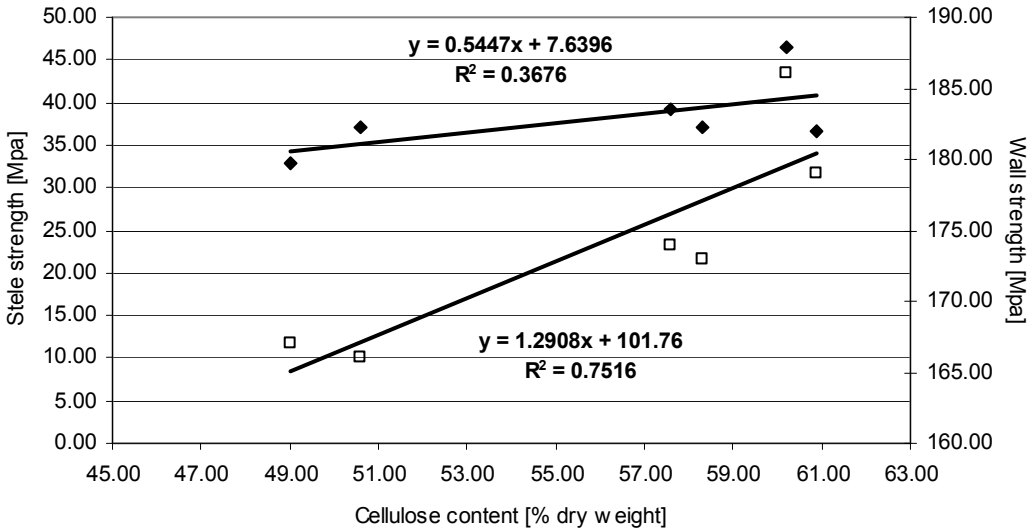

Figure 2-8: Stele (◆) and cell wall (□) tensile strength in response to changes in cellulose content within 3 *salix* and 3 *populus* clones with linear regression lines fitted (After Hathaway and Penny (1975).

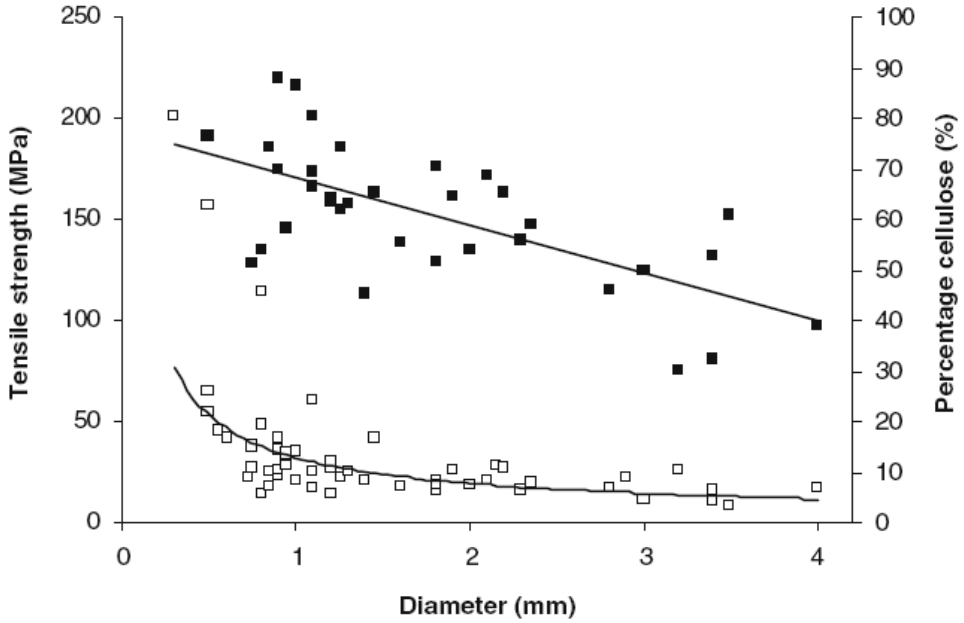

Figure 2-9: Decreasing root strength and cellulose content with increasing root diameter of Sweet chestnut. □- Tensile strength; ■ = Cellulose content (Genet et al., 2005).

A change in cellulose content within the above ground biomass of transgenic trees has been found to be affected by changes in lignin content (Figure 2-10). Within 8 transgenic aspen trees (*Populus tremuloides*), where lignin biosynthesis pathways were manipulated, the ratio of cellulose to lignin was found to increase from 2 to 4 in the most severely down regulated aspen trees (Hu et al., 1999). This is described in greater detail in the next section.

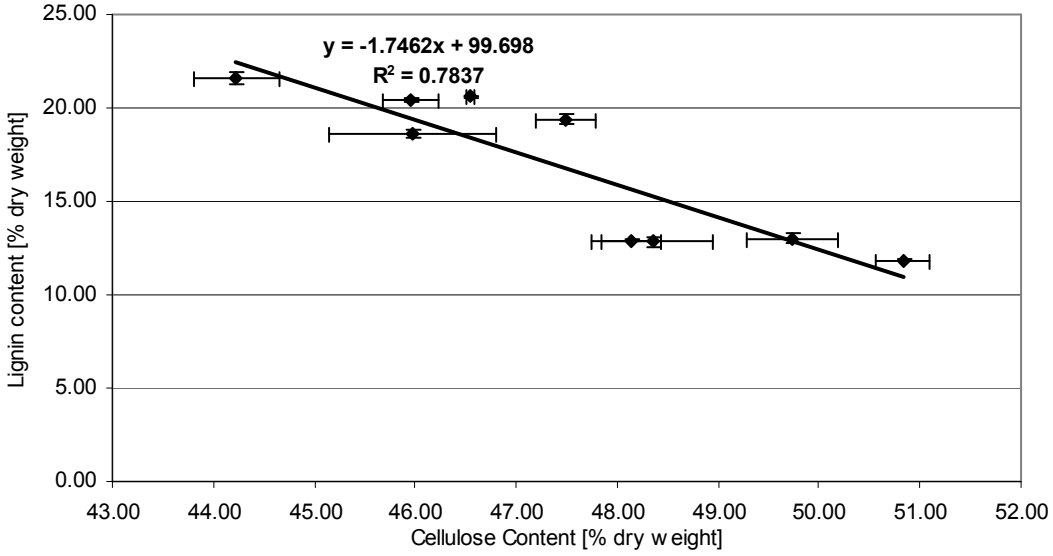

Figure 2-10: Decreasing cellulose content with increasing lignin within transgenic aspen with linear regression lines fitted, error bars indicate standard deviation (Hu et al., 1999).

2.3.5.2 Lignin

Research has begun to manipulate lignin and lignocellulosics, through genetic modification, to increase the value of plant raw materials within agro-industry practices (Boudet et al., 2003). Cellulose microfibrils are orientated by microtubules (Barlow and Baluska, 2000) and provide the framework for lignin and hemicellulose (Figure 2-11). With changes in cell wall structure, resulting from genetic mutations, the affects on plant root biomechanics may be significant and therefore have implications for root contributions to soil reinforcement. Quantification of these potential impacts should therefore be addressed before widespread commercial production. Moreover, these plants may provide a model to assess the influence of lignin and cellulose on root biomechanics.

One of the roles of lignin is in controlling water uptake. As lignin increases cell wall rigidity, it prevents the cell wall from collapsing inwards due to high suctions during water uptake and also, due to its hydrophobic properties, protects cellulose becoming wet which may lead to a reduction in tensile strength (Niklas, 1992).

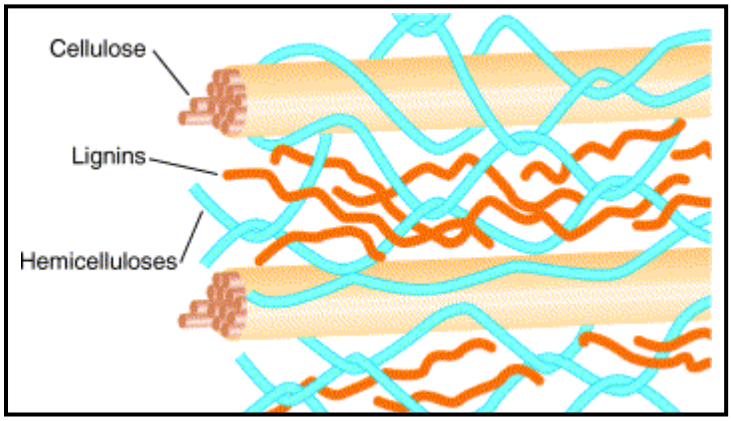

Figure 2-11: Basic schematic of a lignified secondary wall (Boudet et al., 2003)

Different plant species have been shown to vary considerably in lignin content (Table 2-3; Table 2-4) (Bilbro et al., 1991). Environmental stimulation is also known to impact lignin content (Cipollini, 1998; Niklas, 1998; Saidi et al., 2009; Scippa et al., 2006). Increased lignin deposition within cell walls has been found to be linked to environmental stimulation, such as wind, altering biomechanics through a process termed thigmomorphogenesis. Thigmomorphogenic responses were shown to inhibit stem elongation of barley (*Hordeum vulgare*) when rubbed (Jaffe, 1973) and have been also shown to impact plant tissue biomechecnics when above ground biomass was rubbed (Saidi et al., 2009), vibrated (Niklas, 1998) and stimulated by wind (Cipollini, 1998). Thigmomorphogenic responses have also been observed below ground in roots as a result of topology (Scippa et al., 2006). Spanish broom (*Spartium junceum*) increased its lignin concentration when grown on a slope, as opposed to on a horizontal plane, suggesting roots strengthened in response to the mechanical and gravitational loading (Scippa et al., 2006).

2.3.5.3 Silica

Silica is also thought to contribute to increasing plant root and stem strength. Silica is incorporated into cell walls, similar to lignin, and is a 'compression-resistant structural component' with only 3.7% of the energy required for incorporation in comparison to same unit weight of lignin (Epstein, 1994). Cowpea, *Vigna unguiculata*, has been shown to exhibit increases in stem tensile strength when grown hydroponically with increasing levels of silica supplied. Roots, however, were shown not to increase in tensile strength with increased silica (Dakora and Nelwamondo, 2003). Root tensile strength may have been unaffected due to little or no mechanical loading on the plant during hydroponic growth. Dakora and Nelwamondo (2003) suggest that silica is deposited to increase stem strength as a response to increasing stem loading and the necessity for improved mechanical strength within the plant. Many studies grow plants in ideal environments and therefore minimise disturbance and natural factors, such as wind, that may exert forces on the plant structure and alter root growth.

With lignin, cellulose and silica shown to affect plant mechanical strength, plants have been screened in order to measure differences in composition. Bilbro et al. (1991) highlighted lignin, cellulose and silica as 'possible criteria' when using plants for the control of soil erosion by wind. A variety of plants were screened from agricultural cultivars, such as wheat and barley, to a variety of grasses. The ranges of lignin, cellulose and acid detergent fibre ash (ADFA-silica being the major component) were highly varied. Gramineae, grass, species ranged from 6.2-29.8%, 28.8-54.9% and 0.2-16.6% for lignin, cellulose and ADFA respectively (Table 2-3). Wheat cultivars, *Triticum aestivum*, ranged from 6.0-8.5%, 28.9-33.5% and 7.3-18.7% for lignin, cellulose and ADFA

respectively (Table 2-4) (Bilbro et al., 1991). Such variability highlights differences in plant composition and highlights the need for further research in relating these changes to the relative contributions of different plants to soil reinforcement.

Name	Lignin (%)	Cellulose (%)	ADFA (%)
Switchgrass (Alamo) *Panicum virgatum L.*	16.2	38.2	2.7
Arizona cottontop *Trichachne California* (Benth.) Chase	14.9	34.4	2.7
Lovegrass ('Ermelo') *Eragrostis curvula* (Schrad.) Nees	14.1	43.8	1.2
Giant reed *Arundo donax L.*	13.1	40.1	3.2
Texas panicum *Panicum texanum* Buckley	6.2	28.8	16.6

Table 2-3: Lignin, cellulose and acid detergent fibre ash (ADFA) (with silica being the major component) percentage composition of various gramineae species (Bilbro et al., 1991)

Cultivar	Type*	Lignin (%)	Cellulose (%)	ADFA (%)
Turkey	HRW	8.5	32.2	11.2
TAM 105	HRW	8.4	32.9	8.6
Arkan	HRW	8.0	31.4	11.8
Blue Jacket	HRW	8.0	29.2	8.3
Chisholm	HRW	7.3	31.9	10.0
Centurk	HRW	7.2	32.7	10.0
Kanking	HRW	7.2	30.6	9.9
Scout 66	HRW	6.8	21.2	11.7
Hill 81	SWW	6.7	31.3	7.7
Wanser	HRW	6.7	31.4	10.9
MIT	HRW	6.6	31.4	11.9
Ponca	HRW	6.6	33.2	7.3
Stephens	SWW	6.3	30.1	11.1
Triumph 64	HRW	6.2	33.5	8.7
Yamhill	SWC	6.1	30.9	12.3
Paha	SWCL	6.0	28.9	18.7
Vona	HRW	6.0	30.5	12.4
Will	WB	5.2	30.4	13.3

Table 2-4: Lignin, cellulose and acid detergent fibre ash (ADFA) (with silica being the major component) percentage composition of various hard red winter wheat (HRW), soft white wheat (SWW), soft white club wheat (SWCL) and winter barley (WB) (Bilbro et al., 1991)

2.3.6 Changes in mechanical properties of roots with time

2.3.6.1 Effects of root age

During root growth, root biomechanical properties change over time as a function of root age. Information is known on the mechanisms by which these properties change through investigations into cell wall structure (Zeier et al., 1999). Less is known about the changes in biomechanical properties of strength and modulus of roots over time. Without such information, the effects of root age over time cannot be incorporated into root reinforcement models.

Root tips are the youngest root sections and therefore likely to be growing the deepest in the soil away from the plant stem. Current models used for predicting reinforcement with increasing depth use the RAR parameters and negative power law relationships for root strength (e.g. (Mattia et al., 2005)) with depth ignored in relation to root strength. With changes in root biomechanical properties with depth or age, these predictions of reinforcement are highly variable with many predictions based on a generic root strength plots irrespective of root age. It has previously been hypothesised that cellulose is responsible for increased resistance to tension and that cellulose content is greater in young roots (Genet et al., 2005). This has not been verified experimentally.

Root age is likely to have significant effects on vegetation regeneration. It has been noted before that the relative growth rate (RGR) of plants is important when plants are required to re-colonize soils, minimising potential erosion (Stokes et al., 2009). Viewing the time frame by which soil stability will increase on the RGR of plants, however, this could be misleading. Root strength development over time will interact with RGR to contribute to the change in soil reinforcement by roots over time. Studies have

investigated the effect of age on soil shear strength but this has been limited to examining general age of the plant population (Genet et al., 2008) as opposed to investigating specific root age and changing biomechanics. This is a major area requiring greater investigation so that planting strategies can be optimised to provide rapid reinforcement.

Research on plant anchorage variation with plant age could assist with the understanding of soil reinforcement over time as the underlying mechanical processes are similar. Crook et al. (1994) found that anchorage strength of wheat, planted in April, increased until early June and remained constant until early July when peak anchorage strength was recorded. From July until August anchorage strength decreased with two cultivars having different values for peak strength. The peak anchorage strengths for the two cultivars occurred during the same months of the growing season indicating differences in cultivar properties, and not in the time required to reach peak strength. To investigate this further, lignin within coronal roots was observed by cutting samples and staining with phloroglucinol followed by examination under a stereo microscope. Although lignin concentration in the tissues was not measured, there was obvious lignification and thickening after July. It was therefore suggested that anchorage strength diminished after July due to a lack of lignification affecting anchorage strength (Crook et al., 1994).

2.3.6.2 Effects of root decomposition

Decay rates following harvest, or vegetation removal for land management purposes, significantly impact the contribution made by roots on soil reinforcement. However, only limited information is available regarding root strength degradation and values of strength loss following tree felling or harvesting of agricultural or other commercial

crops. No study could be found that assessed decomposition of fibrous roots in relation to effects on root biomechanics.

O'Loughlin and Ziemer (1982) found that roots (>25mm diameter) from felled Radiata pine (*P. radiata*) and Kanuka shrubs (*Kunzea ericoides*) may degrade in strength by 300-500 kPa per month, from initial strengths of 10–60 MPa, with root biomass decreasing rapidly following felling. In contradiction to this, however, tensile strength of woody Kanuka roots increased for up to 12 months following cutting of the parent tree (Watson et al., 1999). Following this increase, root strength did not fall below that of the live wood until 24 months after cutting. In contrast, Radiata pine roots declined in strength by 5.9 MPa per year after felling of the parent tree (Figure 2-12) (Watson et al., 1999). There may be bias in these data, however, as root strength tests for Radiata pine were performed on increasing root diameters over the sampling period. As discussed previously, roots have been shown to be weaker with increasing root diameter and this may provide a possible explanation for the decrease in strength, with this relationship being exacerbated over time.

In the study by Watson et al. (1997) it was noted that roots shrunk following felling. This may compound errors by sampling larger root diameters over time. Increases in Kanuka root tensile strength were still observed despite an increase in root diameters being tested. Tensile strength was found to decrease from the initial peak despite reduced root diameter at 20 months. The study summarised that the changes in root tensile strength were attributed to the loss of root moisture. The onset of decay also affected tensile strength with softer roots from *P. radiata* decaying from as early as a few weeks after felling with Kanuka decay beginning in the order of 12 months after felling (Watson et al., 1997).

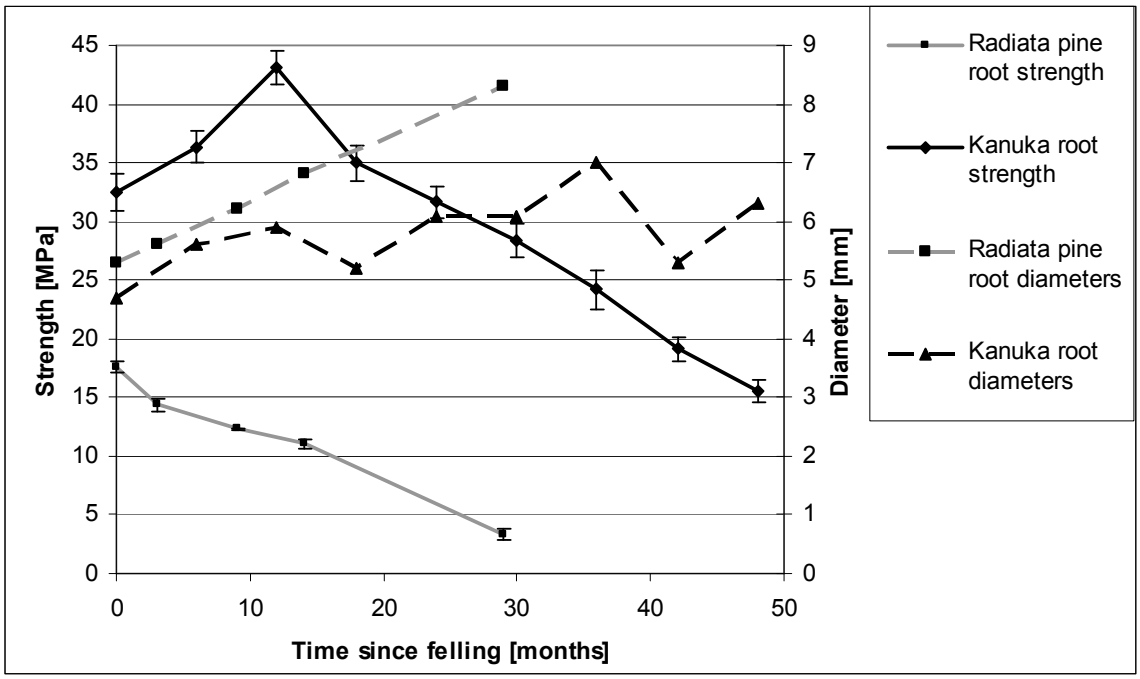

Figure 2-12: Decreases in root tensile strength of two tree species following felling (Adapted from Watson et al., 1999**)**

Decay rates of fibrous root systems have been studied with grass roots decaying quicker than pine roots (Guo et al., 2006). In thin roots (<3mm) strength may be reduced by damage to the root cortex, although this has not been studied. Plant maturity has also been linked to rates of decomposition within fibrous root systems. Barley root decay was found to be higher for roots produced at tillering than winter wheat (Swinnen et al., 1994). Damage may be caused by organisms within the soil feeding on fine roots causing a weakening or severing of the root fabric. No information on this was found in the published literature, but such interactions are likely to exist within the soil.

2.4 Mechanisms of root failure during the reinforcement of soils

When a load or force is placed on a soil block reinforced by plant roots, the stress is taken up by roots gradually until one of two failure mechanisms occur. Roots will either fail as a result of the interface between the root and soil shearing, pull-out failure (Waldron and Dakessian, 1981), or by the root breaking within the soil (Easson et al., 1995; Pollen, 2007). Breakage occurs in roots when the peak strength of the material has been exceeded. This may occur at a strain beyond the peak strength of the root i.e. the peak strength may have been reached and begun decreasing before breakage. Materials break or fracture either after reaching their peak tensile strength or exactly when mobilising peak tensile strength dependant on a range of processes. Two other stages of root movement may occur during shearing of reinforced of soil: root slippage before pulling out, and also root stretching. Although these contribute to reinforcement, they are intermediary stages prior to the peak shear strength of the soil and root matrix being reached. Contributions of these intermediary stages of failure have received relatively little attention in the literature to date.

The type of root failure is influenced by a number of different factors and also soil environment characteristics. Ennos (1990) showed that leek radicals failed as a result of root length with longer roots tending to fail through breaking. Pollen (2007) reported changes in failure mechanism dependant on diameter and also soil moisture conditions. Pollen (2006) looked at the pulling resistance of river birch (*Betulus nigra*) roots over a period of a year. Values for the critical root diameter were used to demonstrate changes from a predominant pull-out failure to breakage failure. When soils were wetter (moisture content 21.1%), in April, the root diameter threshold beyond which roots failed predominantly through breakage was 3.5 mm whereas when the soil was drier (11.3%), during July, roots were more likely to break when diameters exceeded 2.4 mm.

Some roots did, however, fail by either pull-out or breakage below those diameter thresholds reported (Pollen, 2007).

Poissons ratio suggests that as a material is placed under axial strain the centre decreases in diameter. With decreasing diameter of a root it is possible that this could then promote root failure by pull-out due to a decrease in soil and root contact. Ennos (1990) however suggest that root diameter decreases by about 5% and therefore 'should have little effect on the root in the soil' (Ennos, 1990). This suggests that the soil moisture condition is the predominant factor likely to contribute most to the mode of failure of a single root in soil, not including the potential effects resulting from root architecture. It must be noted that the study performed by Ennos (1990) used leek seedlings whereas Pollen (2006) used a woody species, river birch, with differences in root composition likely to significantly affect failure mechanisms.

2.5 Modelling root reinforcement of soil

2.5.1 Early models

The first simple model for predicting increases in soil shear strength containing roots was developed by Waldron (1977). The model was based on the Mohr-Coulomb equation for predicting soil shear strength (S_r), A term for increased soil strength due to the presence of roots (ΔS) was incorporated through:

$$S_r = c + \Delta S + \sigma_N \tan \varphi$$

Mohr-Coulomb equation components

$$\Delta S = T_r (A_R / A)(\sin \theta + \cos \theta \tan \varphi)$$

where c = apparent cohesion; σ_N = normal stress on shear plane and φ= soil friction angle. ΔS was calculated as a function of root area ratio (A_R (Area of roots) / A (Total Area)), tensile strength of roots (T_r) and incorporates root inclination in response to horizontal shear displacement ($\sin\theta + \cos\theta \tan\varphi$). Flexible roots with a uniform diameter were assumed to cross the shear plane perpendicularly with the position of the shear zone not changing during shear. Failures of roots within the model are assumed to be by breakage only. Pull-out is not considered so only one of the root failure mechanisms is considered.

Wu et al. (1979) further developed this model by examining the resisting component and root inclination. It was found that by varying the ranges of root inclination from 48-72°, results were insensitive and therefore a constant for this was produced of 1.2, simplifying the equation to:

$$\Delta S = 1.2(T_R(A_R / A))$$

The model proposed by Wu (1979) and Waldron (1977) tends to overestimate root derived reinforcement (Bischetti et al., 2009). One of the key reasons for this is that the model does not incorporate any form of progressive failure with all roots assumed to break simultaneously. As previously discussed in section 2.4, breakage is not the only failure mechanisms occurring under direct shear.

2.5.2 Fibre Bundle Model (FBM)

Recent developments within root reinforcement modelling have begun using models that apply stress gradually, allowing models to predict a more progressive failure. Such developments have investigated the use of fibre bundle models. Within fibre bundle

models, load is exerted on n fibres with each fibre supporting constant stress, x. When the load increases (i.e. through shearing) a fibre may reach its breaking stress resulting in the load being redistributed over n-1 fibres each carrying x constant stress (Daniels, 1945). Two outcomes may be observed: 1) Remaining fibres will support the total load resulting in no more failures and stress may be increased, or 2) Fibres break consecutively leading to total bundle failure (Daniels, 1945), progressive failure.

Fibre bundle models distribute load evenly through all of the fibres. Within fibre bundle models there are two main types, 'local load sharing' (LLS) and 'global load sharing' (GLS). GLS assumes that load is distributed uniformly through all of the fibres within the matrix composite. LLS incorporates a spatial dimension to the model with load exerted on individual fibres depending on the load on the neighbouring fibre (Hidalgo et al., 2002).

Fibre bundle model principles have been adapted for model soil reinforcement by roots through the design of the RipRoot model (Pollen and Simon, 2005) aimed at improving the accuracy of root reinforcement modelling in comparison to the Wu et al. (1979) model discussed earlier. RipRoot design uses GLS and does not incorporate root stiffness with fibres failing by tension rather than through pull out from soil. If pull out did occur, the model assumes that this failure is equal to the load required for root breakage (Figure 2-13) (Pollen and Simon, 2005). Pull out is likely to be significant within the modelling of fibrous root reinforcement (see section 2.4) and therefore the assumption that roots failing through pull out contribute as much to reinforcement as those failing by breakage may overestimate reinforcement. Empirical tests were performed to investigate this and it was shown that forces required to break roots exceeded those required to pull the root out for smaller diameter roots (Pollen, 2007).

The smallest diameter of root tested was however only 0.5mm with many fibrous roots being thinner. Roots tested were also only from river birch (*Betula nigra*) as these could be identified clearly from others present. With only woody roots being used to test the relationship between diameters and pull out, it is unclear whether fibrous roots would behave similarly within the soil. The peak stress required for root pull out has been shown to be dependant on soil water potential and the associated effective stress. The mode of root failure is likely to be through breakage in drier soils with pull out increasing with decreases in the effective stress of soil (Pollen, 2007).

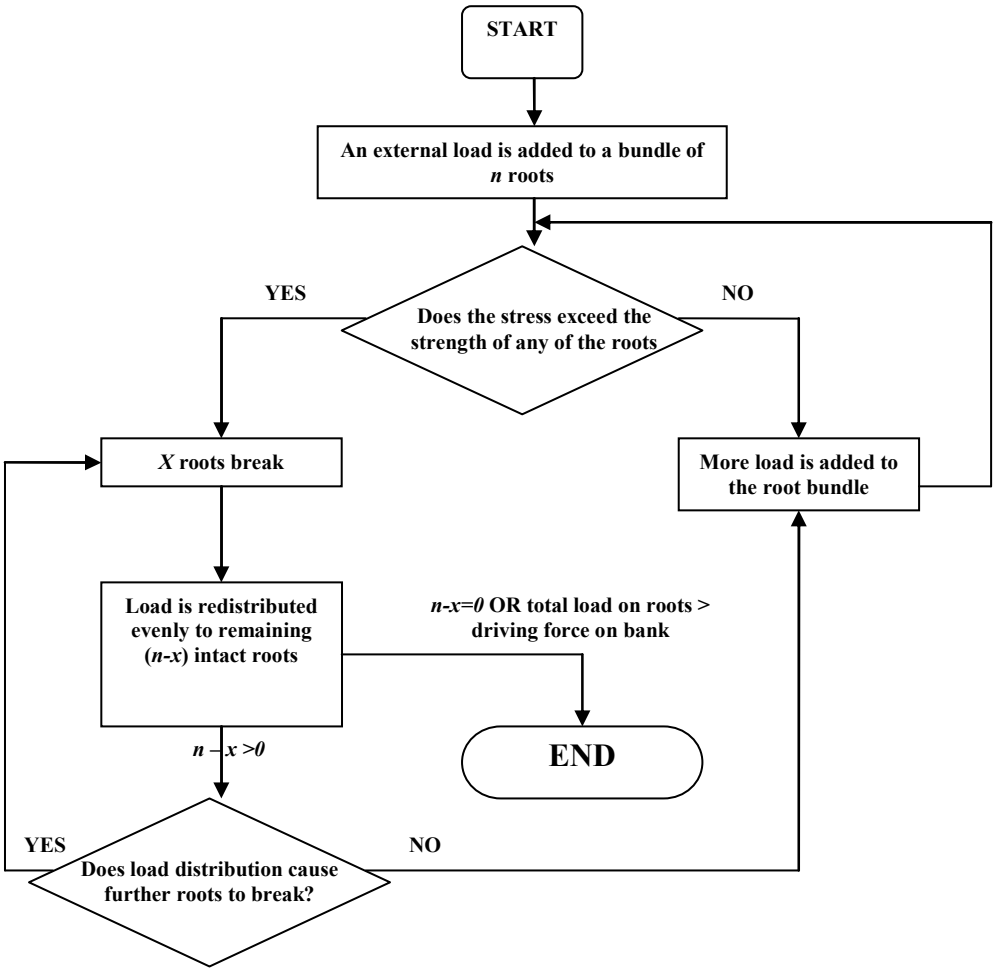

Figure 2-13: Flowchart showing rules within RipRoot model (Pollen and Simon, 2005)

BLANK PAGE

3. Influence of planting density on soil reinforcement by fibrous roots

A large proportion of this chapter has been published in:

Loades, K. W, Bengough, A.G., Bransby, M.F. and Hallett, P.D. (2010), Planting density influence on fibrous root reinforcement of soils. Ecological Engineering Vol. 36 (3), pp 276-284 (APPENDIX 1).

3.1 Introduction

Through increasing the planting density, root mass will increase resulting in increased root area ratio and root length density where an increase in shear strength would be expected. However, planting density has also been shown to change other root properties and as such questions must be asked as to whether such a relationship may be over simplified within such a complex environment. Soil reinforcement by plant roots has been related to the root area ratio (RAR) at the shear plane for numerous species of plants (Mickovski et al., 2009; Waldron, 1977). A greater RAR means more root area and hence greater soil reinforcement. Other contributory factors, however, may also influence soil shear strength greater than simply the quantity of roots, making use of RAR over simplistic. Root tensile strength, for instance, also influences reinforcement with much research showing a large dependency between root tensile strength and root diameter (De Baets et al., 2007; De Baets et al., 2008). RAR represents a general figure

for total root mass and does not incorporate root diameters individually. Reinforcement would be expected to be much different for soils with similar RARs but different distributions of root diameters and hence root strengths.

Within agricultural crops, for instance, root length density is influenced by the planting system (Aggarwal et al., 2006). Root mass of cereal crops is typically in shallow horizons of the soil, 0-15cm with 91.9-50.0% of total root mass in this region (Welbank et al., 1973). Seeds planted in beds compared to conventional sowing with a seed drill can differ in root length density soil water content and soil bulk density. Within both planting systems 50% of the root length was in the 0-15 cm region, however in the 0-30 cm region increased by nearly 22% when compared to conventionally sown plots. Soil bulk density was lower in the bed system with less water applied but the crop was more water efficient and also generated greater yield. The increases in both root length and soil bulk density can be explained by the bed system being 20cm above that of the conventional system with soil looser and easier to penetrate by roots. Under both systems ≥75% of roots were 0-0.3 mm in diameter (Aggarwal et al., 2006).

Root tensile strength is critical in influencing reinforcement with much research showing a large dependency between root tensile strength and root diameter (De Baets et al., 2007; De Baets et al., 2008). Planting density has been shown to affect root diameter, with potential implications on root system strength, within some cultivars of cotton (*Gossypium hirsutum*). Average root diameters were lower in one variety used at planting densities <6 plants/m^2, with root diameter also observed to differ dependant on developmental stage. Root length density was observed to be dependant on planting density, decreasing with increasing planting density (Zhang et al., 2006). It may therefore

be possible that competition for nutrients may result in decreased root length and reduced reinforcement derived from root inclusions within the soil.

RAR and the size distribution of roots can vary markedly depending on (1) planting density, (2) soil depth, (3) soil density and (4) other environmental variables such as nutrient and water availability. Plant type also has a large impact on the relationships between RAR, root size distribution and soil reinforcement, with woody plants having markedly different root structures to fibrous plants (Operstein and Frydman, 2000).

The aim of this study was to investigate how planting density influences soil reinforcement by fibrous roots. Due to competition between plants, it is hypothesised that planting density will increase reinforcement up to a threshold, beyond which increasing plant density will have no impact. The number, size and tensile strength of fibrous roots crossing a shear plane 50mm below the soil surface were measured so that the direct mechanical reinforcement of individual plant roots could be examined. Barley (*Hordeum vulgare* cv. Optic) was used in this study to represent a model fibrous root system and was planted at a range of densities in both the field and glasshouse. Barley has practical importance as a major arable crop in regions where soil erosion and structural degradation can be problematic, and is also a convenient model system with a wide range of genotypes. Data on RAR, root tensile strength, root diameter and soil shear strength were collected.

3.2 Methods

3.2.1 Soil

Field and glasshouse experiments consisting of barley (*Hordeum vulgarum* cv Optic) planted at different densities were used for this experiment. Both experiments used the same soil collected from the Scottish Crop Research Institute, Dundee (Lat 56°27'36.44"N; Long 3°4'21.74"W), which had been grown with spring barley for 2 years before this experiment. The soil was an undifferentiated sandstone (Eutric Cambisol, FAO) comprised of sand 71%, silt 19%, clay 10%, with a pH(H_2O) of 6.2, 1.9 %C, and 0.07 %N (Mickovski et al., 2009; White et al., 2000).

Soil for the glasshouse study was collected from 0-15 cm depth and then sieved to 2mm before storage under cover until used. Proctor compaction test, BS 1377-4 (1990), determined the optimal water content for packing. Soil was packed into a standard 1 litre proctor compaction mould and compacted with a 50 mm diameter 2.5kg hammer falling from a fixed height of 0.3m. Prior to testing, the soil moisture content was calculated with 6 batches of soil prepared with moisture contents ranging from 0.09 m^3 m^{-3} to 0.28 m^3 m^{-3}. A second degree polynomial curve was fitted to the results (R^2= 0.945) with optimal soil water content found to be 0.198 g/g (Figure 3-1).

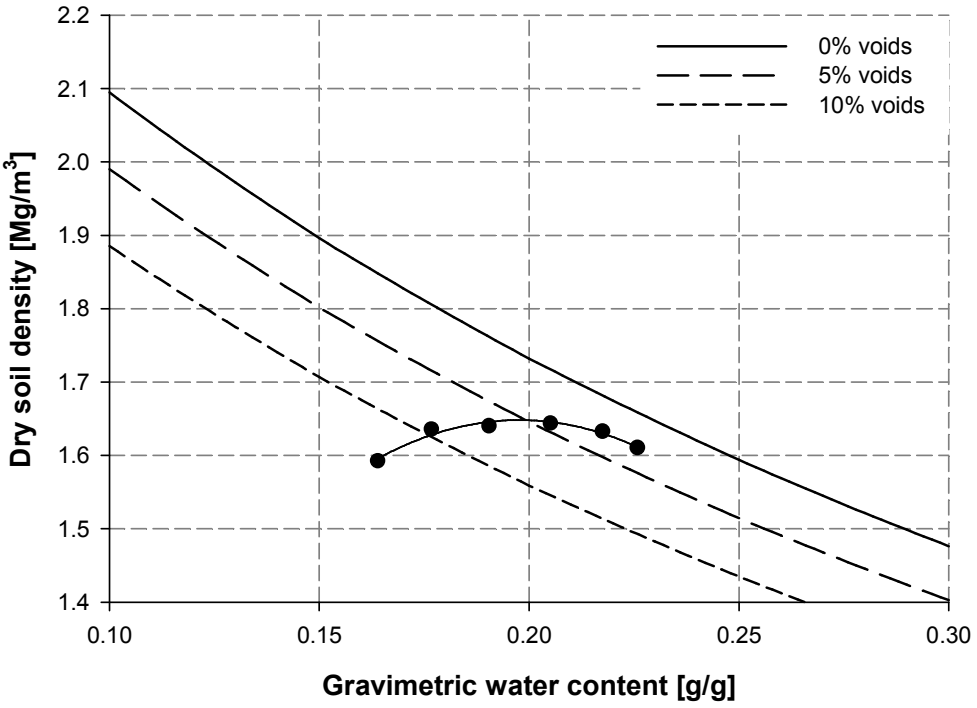

Figure 3-1: Proctor Compaction Curve for soil used within core and field experiments

Water retention was assessed on three replicate cores packed at 0.20 kg kg^{-1} water content to a dry density of 1190 ± 8.5 kg/m^3 and subjected to suctions ranging from 0.05 to 1500 kPa. Suctions 0.05 kPa to 5 kPa were applied using the sand box method (Eijelkamp, Giesbeek, Netherlands) from 10 kPa to 50 kPa using tension tables formed from a semi-permeable membrane (EcoTech, Bonn, Germany) and from 100 kPa to 1500 kPa using pressure plates (ELE International, Hemel Hempstead, UK). Once cores reached a stable weight, the moisture content of the cores was calculated to allow plotting of the water release characteristics (Figure 3-2).

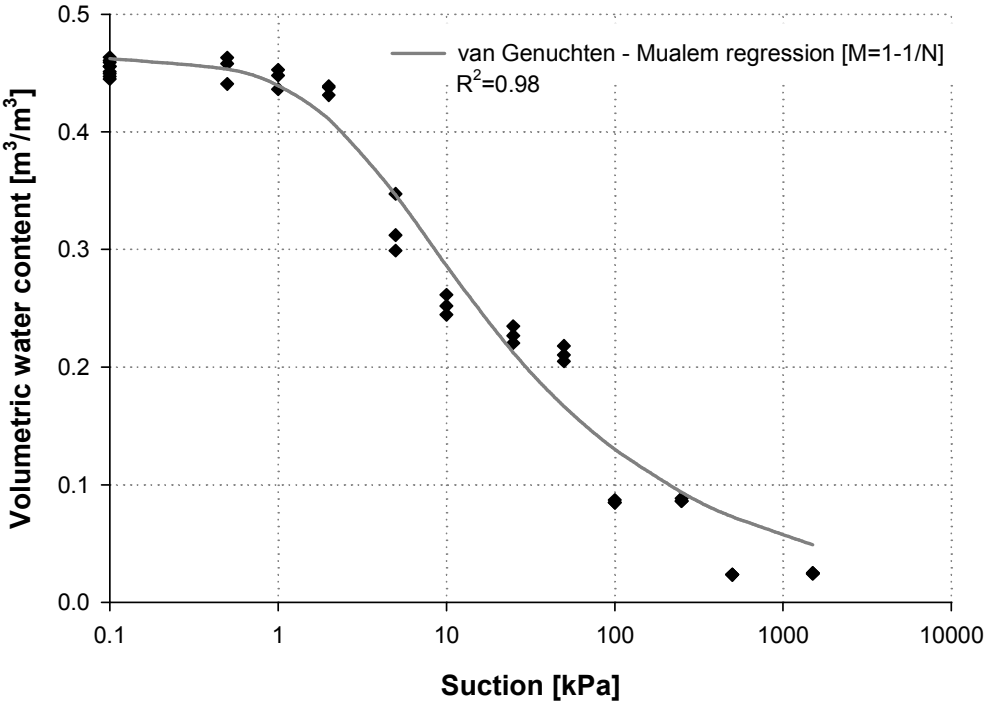

Figure 3-2: Water release curve for Bullion field soil sieved to 2 mm and repacked to 1.19 g cm^3

3.2.2 Field study

3.2.2.1 Field plots

Field plots 2.0m x 1.2m were sown on 7 April 2007 at four densities. There was a total of fifteen plots, consisting of 3 replicates of each of 0, 76, 304 570 and 950 plants/m^2. The standard agricultural sowing practice for this region is 380 plants/m^2 (New Farm Crops, 2007). The plots were prepared running South East (Lat 56°27'36.44"N; Long 3°4'21.74"W) to North West (Lat 56°27'37.46"N; Long 3°4'21.74"W). Planting densities were completely randomly distributed along the length of the trial site, one row, with a 0.5m gap between plots. The plots received standard fertiliser and pesticide inputs during the experiment. Fertilizer (Nitrogen: Phosphorus: Potassium) was applied ten days

prior to sowing at 160kg/ha (0-0-60) with a further application of 350kg/ha (22-4-14) seven days before sowing.

3.2.2.2 Sampling procedure

At 5 and at 20 weeks after sowing, soil cores were taken from each plot for mechanical testing in the laboratory. As soil matric suction affects soil shear strength, the sampling area was first brought to field capacity (approximately 0.45 m^3 m^{-3}; 5 kPa) to minimise the variability between sampling location or time. Twenty four hours prior to sampling, an individual grid square was enclosed within a 300 mm diameter 230mm height plastic tub with the bottom removed to allow localised watering of the sampling location. Water (2500cm^3) was poured into the tubs allowing percolation into the soil bringing the sampling location to near field capacity after 24 hours of drainage (Figure 3-3).

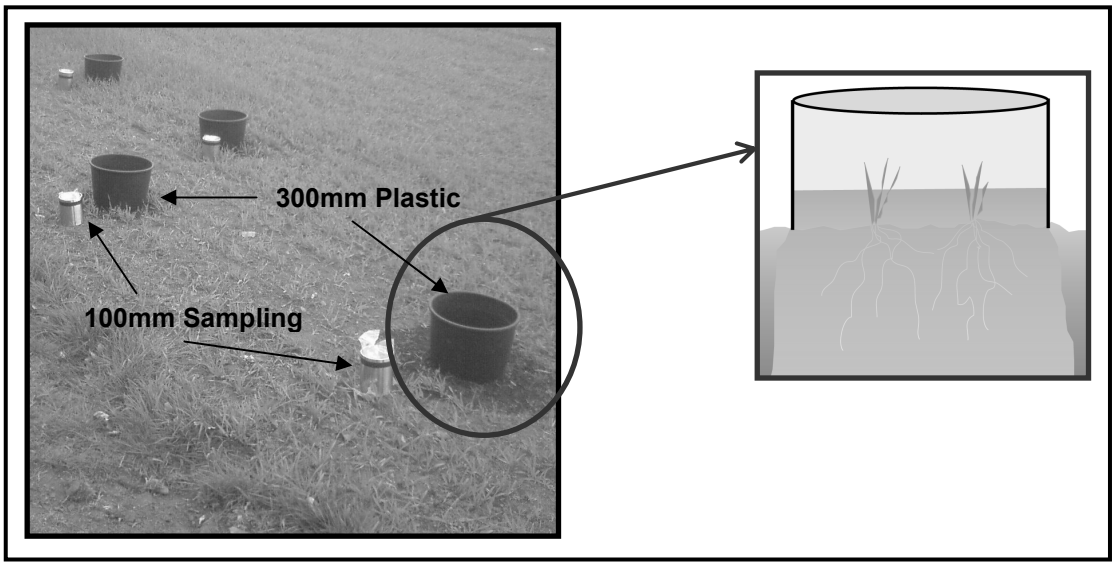

Figure 3-3: Preferential watering of sampling area with cores placed next to sampling point prior to core collection for shear testing. Cores taken from within black plastic watering bunds

Barley stems were cut 10mm above the soil surface prior to core collection to minimize water uptake from soil. Metal soil rings, 100 mm internal diameter x 100 mm height (ELE International, Hemel Hempstead, UK), were greased with pure petroleum jelly. They were inserted into the soil within the plastic wetting bunds by hammering lightly to ensure lateral movement was minimal. The rings filled with soil were extracted and stored in sealed bags prior to shearing.

At 5 weeks the barley plants had five leaves or more unfolded (HGCA, 2006). At 20 weeks, ears were completely emerged and drooping with soft dough developing within the grain. Each of the fifteen plots were sampled in a day, with four samples from each plot collected for each sampling period providing a total of sixty cores for each sampling period. The shear tests were conducted on the day of sampling.

3.2.2.3 Field shear testing

Prior to shear tests being performed, soil samples were collected from each of the samples to allow soil water content to be calculated. Shear tests were performed using a conventional direct shear rig (Model Number 25402, Wykeham Farrance, Tring, United Kingdom) fitted with a 100mm diameter circular shear assembly. The soil cores sampled from the field were extruded from the metal ring using a wooden disc, extruding directly from the core into the shear assembly. Once extruded, the soil was sheared at a depth of 50mm. This depth was selected from observations of washed root systems from the field site five weeks after sowing, where large numbers of roots were detected to 50 mm, with a progressive decrease at greater depths (Figure 3-4). The displacement rate was 1mm/min with no normal load applied. Force and displacement data were logged during shearing using a PMD-1608FS USB data acquisition system (Personal Measurement

Device™, Newport, United Kingdom) with real-time data observed during shearing using TracerDAQ software. Force was measured using a 500 ± 0.1 N S-beam load cell (RDP Model RLT0050Kg) and displacement was measured using a Pioden displacement transducer (PD20, Newport, United Kingdom). Both the load cell and displacement transducer were calibrated prior to shear testing.

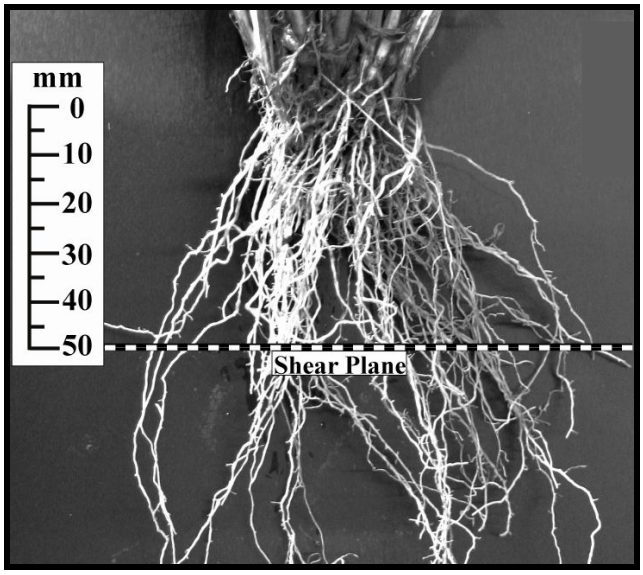

Figure 3-4: Washed root system of barley (*Hordeum vulgare* cv. Optic) showing shear region of root system adjacent to the shear plane

Shear strength for each core was calculated using BS 1377 (1990). Shear strength reported in this study was the peak value within each test, however, not all shear tests reached ultimate peak strength due to the constraints of the shear assembly. The calculation of strength did not account for decreasing shear surface area with increasing displacement, in accordance with guidelines outlined in BS 1377-7 (1990). Following shearing, the cores were stored at -20ºC for later analysis of roots transecting the shear plane and also root diameter distribution data.

3.2.2.4 Root data collection and biomechanical testing

The same procedure was used for collecting root material and biomechanical testing in both field and glasshouse experiment. Methods for biomechanical testing are found in section 3.2.4.

3.2.3 Glasshouse study

3.2.3.1 Core preparation

Cores were packed with sieved soil described in section 3.2.1 within 150 mm internal diameter x 210 mm height PVC drainage pipes. Tubes were pre-cut 50 mm below the top of the core to allow for shearing within the shear assembly at the same depth as that used for the field experiment. Edges of the upper and lower section of the tubes were sanded smooth to remove rough edges and greased with silicon to reduce friction at the interface between lower and upper sections of the tubes. Following preparation of the cores, the upper and lower sections were re-joined using ducktape©. Nylon mesh was affixed to the bottom of the core to retain soil once packed. Soil was packed at close to the optimum gravimetric water content, 0.198 g/g, assessed through a Proctor compaction test. Packing was performed in 10 layers with roughing of the surface between layers to allow for good connection between packed layers. Preliminary testing showed that 10 blows per layer from a 2.5kg proctor hammer falling from 0.3m (equivalent energy of 192.6kJ m^{-3}) achieved the required dry soil density. The dry density of the cores was 1260 ± 2 kg/m^3 (mean ± s.e.). Plastic beads were placed on the soil surface after packing and stem emergence to reduce soil surface drying and potential soil cracking. A lip was also created around the top of cores to eliminate surface runoff of water during irrigation which may have potentially led to changes in plant growth.

3.2.3.2 Plant growth

Cores were planted at nine densities including a control fallow. To ensure all sown seeds would grow within the cores, seeds were sterilised and germinated on filter paper prior to planting. The husks were removed as necessary before imbibing seed to make it easier to surface sterilise the seeds and facilitates more uniform germination. Seeds were soaked in de-ionised water for 3-4 hours changing water occasionally. Seeds were sterilised in 2% calcium hypochlorite solution (saturated), for 15 min followed by three rinses in de-ionised water. Seeds were left to then soak for a further 1-2 hours. Seeds were then placed in 10 cm x 10 cm square petri dishes with 3 layers of moist filter/blotting paper. Seeds were set in horizontal rows with embryos pointing downward. For the final germination petri dishes were placed almost vertical in a dark incubator at 12°C for 3 days. Only seeds with three roots emerging and signs of a shoot breaking through seed coat were then transplanted to cores.

Cores had a surface area of 0.0177m^2 with 0, 1, 4, 6, 8, 10, 14, 18, and 24 seeds per core relating to planting densities of 0, 76, 190, 304, 456, 570, 760, 950 and 1330 plants/m^2 respectively. Seeds were distributed uniformly within cores using a template (Figure 3-5) to ensure all cores of the same density had plants the same distance apart. There were three replicate cores of each planting density and three additional spare cores used for preliminary testing prior to commencement of full scale testing.

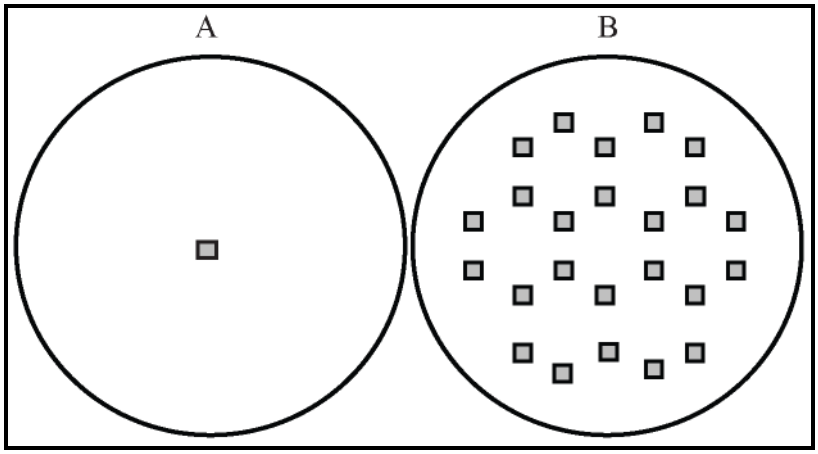

Figure 3-5: Example of planting templates for the lowest density (A), 76 plants/m^2, and highest planting density (B), 1330 plants/m^2

All cores were watered regularly and fertilised with Sinclair Sangral Universal Foliar and Root Food (1:1:1) in a 1:1000 solution applied through a watering can. Fertiliser was initially applied weekly and increased to daily after 2 weeks with continued feeding until sampling. Cores were planted on 30 March 2007, with shear testing commencing ten weeks after planting on 2 July 2007. Plant maturity after 20 weeks in the field was similar to the development observed at 10 weeks within glasshouse cores. All cores were randomly sampled over a two-week period.

3.2.3.3 Harvesting and shear testing

Plant stems were cut 10mm above the soil surface before testing. Shoot mass was determined after drying at 70^{o}C until a constant mass was reached. Cores were fully saturated before draining on tension tables to a suction of 5 kPa (field capacity) for at least 24 hours. Mini tensiometers (SWT4, Delta-T, Cambridge, United Kingdom) were placed within the soil cores at the surface to verify that correct suctions were obtained prior to shearing.

A specially designed shear table (Figure 3-6) was used for shearing these large diameter cores. Cores were placed on a platform and secured to the shear table by upper and lower braces. Direct shear was performed through displacement of the upper section by a screw jack actuator (Macks Group, UK). Force was measured with a 3 kN Tedea Huntleigh S beam load cell (Model No: 615). Displacement was monitored using a Linear Variable Differential Transformer (LVDT) manufactured by RDPE Group (Model LDC6000C). All data were captured using a Campbell Data Logger 21X with collection every second. Mickovski et al., (2009) provide a full description of the shear table and the test procedure.

Peak shear strength was calculated using British Standard 1377-7:1990. Root mass, above ground biomass and the number of heads produced within each of the eight planting densities were also recorded. Root dry mass was measured for roots washed over a 300μm sieve and dried at 70^{o}C until a constant mass was observed. During this process, some roots were kept aside for testing root biomechanical properties before also being dried for root mass. Root were washed gently to minimise mechanical damage of roots used for mechanical testing.

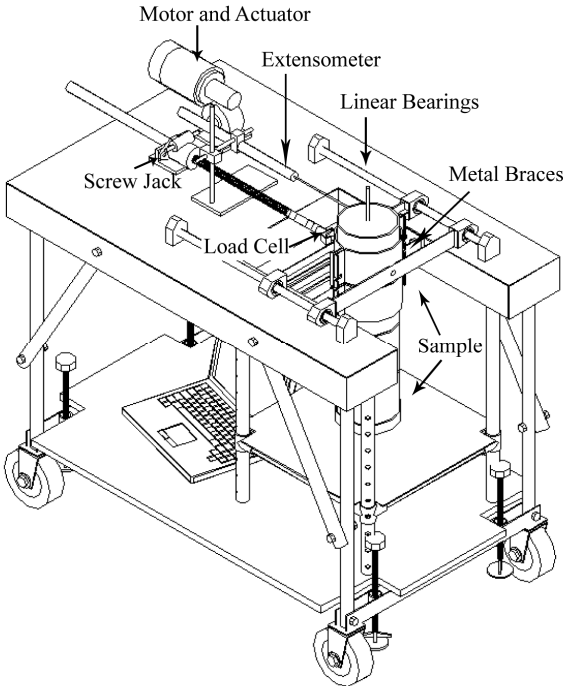

Figure 3-6: Direct shear testing table for large diameter cores. Cores secured to assembly with displacement and load logged to a computer during testing (reprinted from Mickovski et al., 2009)

3.2.4 Root measurements

Following shear testing the cores were frozen at -20°C. This allowed root properties to be measured at a later date. Frozen cores were cut through the shear plane with a diamond saw. Once cut, warm water was sprayed on the shear surface and the thin layer of thawed soil removed to expose cut root tips. Root diameter data was collected by using a stereo microscope and graticule at 7X magnification (Model SDZ (846108), Kyowa, Tokyo, Japan). A grid containing ten 10 mm x 10 mm grid squares was placed on the core surfaces and the diameters and numbers of all individual roots in each grid square was recorded.

Roots were collected for biomechanical testing from the area surrounding the sampling location at the time of core collection for shear tests. These root samples were still within the preferentially wetted sampling area to minimise the influence of spatial variability. An intact spade sample of soil was placed on a 300 micron sieve and sprayed with water to release roots from the soil with minimal mechanical disturbance. The sieve aperture was chosen to minimise the loss of roots during the soil removal process. Within 24 hours of extracting roots from soil they were mechanically tested in tension using a 2 kN universal mechanical test frame (Model 5544, Instron, High Wycombe, United Kingdom). The applied tensile load was measured with a 50 N load cell, accurate to 2mN at maximum load and the cross-head displacement rate was 1mm/min (the same as the shear rate of the cores). Data was logged to a PC and analysed with Bluehill 2 software (Instron, High Wycombe, United Kingdom). Root sections were 80mm in length and secured between upper and lower clamps to expose 60 mm of root (Figure 3-7). Each clamp was shaped as a cam to increase grip and friction on the root as strain increased. The central point between clamps corresponded to approximately 50 mm below the soil surface so that it was a similar depth to the shear plane. Roots were tested until failure, with samples failing close to the clamps or where pull-out was observed rejected. The diameter of the root at the location of failure was measured under a microscope using a graticule. Tensile strength (maximum load/root cross-sectional area) and modulus of elasticity were calculated for each root section tested. Glasshouse experiment roots were extracted from 150mm cores using the same procedure outlined for root removal from spade sampled field soil.

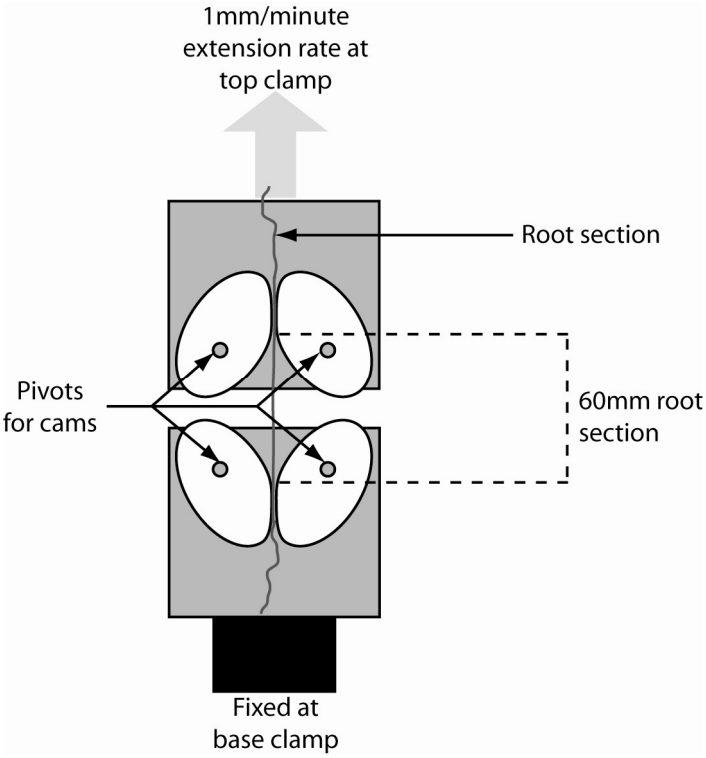

Figure 3-7: Clamping arrangement used to hold roots during biomechanical testing for ultimate tensile strength and elasticity. Clamp allowed increasing root grip as strain increased

Root diameters for tensile testing data for field study roots were measured using the same microscope as used for measuring the RAR, however, glasshouse root diameters for biomechanical testing were collected using Leica MZFLIII stereo microscope and graticule at 10X magnification (Leica, Milton Keynes, United Kingdom). Due to the technique used for measuring the root area ratio it was not possible to assess root structure and length following shear testing.

3.2.5 Data analysis

All data were tested for normality followed by linear regression analysis using Genstat (Tenth Edition) statistical analysis software (GenStat for Windows. (2007). 10th Edition. VSN International Ltd., Hemel Hempstead, UK). Relationships between root diameter and strength were fitted with power-law curves, as described in section 2.3.3. Significance

testing between root strength and sampling time was performed using a linear regression with groups following log transformation of strength and diameter data. Soil water content and dry bulk density between treatments and sampling time were tested for significance using a general analysis of variance. Differences were considered statistically significant when the probability value (P) was <0.05.

3.3 Results

3.3.1 Field study

Sampled soil cores had a dry bulk density of 1.35 Mg/m^3 ± 0.01 (mean ± standard error) and 1.41 Mg/m^3 ± 0.01 for sampling after 5 and 20 weeks respectively. With increased planting density, soil dry bulk density decreased after 20 weeks growth but the relationship was not significant after 5 weeks (Figure 3-8(A)). Dry soil density was significantly affected by sampling time (P<0.001) and also by planting density over time (P=0.037). Water content of cores collected from the field were 0.22 g/g ± 0.002 at 5 weeks and 0.24 g/g ± 0.002 at 20 weeks (Figure 3-8 (B)). Gravimetric water content was significantly affected by sampling time (P=<0.001) but not by planting density over time (P=0.156).

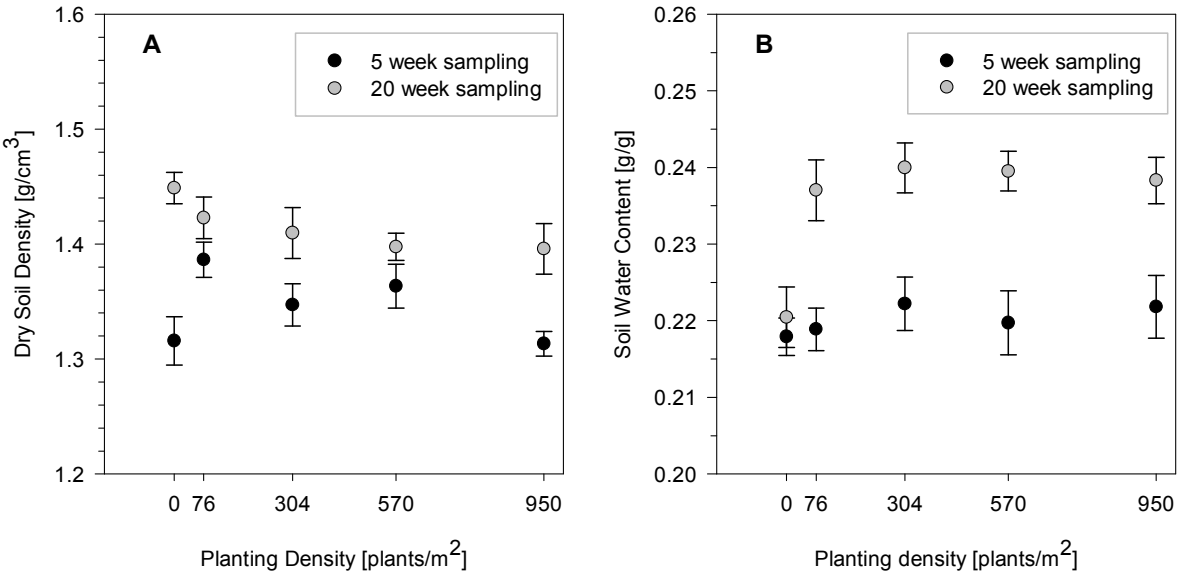

Figure 3-8: Dry soil bulk density (A) and gravimetric soil water content (B) for field samples collected after 5 and 20 weeks growth with error bars showing standard error

Direct shear tests on fallow soil cores found soil strength to be 7.5 ± 0.47 kPa at 5 weeks and 10.3 ± 0.42 kPa at 20 weeks. Shear strength of fallow cores was found to initially increase before decreasing to a residual strength post peak, this was observed at both sampling times of 5 and 20 weeks (Figure 3-9). Within vegetated core samples shear strength continually increased to the end of shear test with ultimate peak shear strength not reached (Figure 3-9). The number of roots crossing the shear plane significantly affected core strength with $P<0.05$ at five weeks and $P<0.01$ at twenty weeks. Planting density increased soil strength significantly by 6.7 ±1.40 kPa ($P<0.001$; adjusted r^2 of 0.3) after 5 weeks growth (Figure 3-10). Sampling after twenty weeks again showed an increase in soil strength, compared to fallow plots (Figure 3-10), of 3.0 ± 0.36 kPa ($P<0.001$) with 17% of variance accounted for by increased planting density.

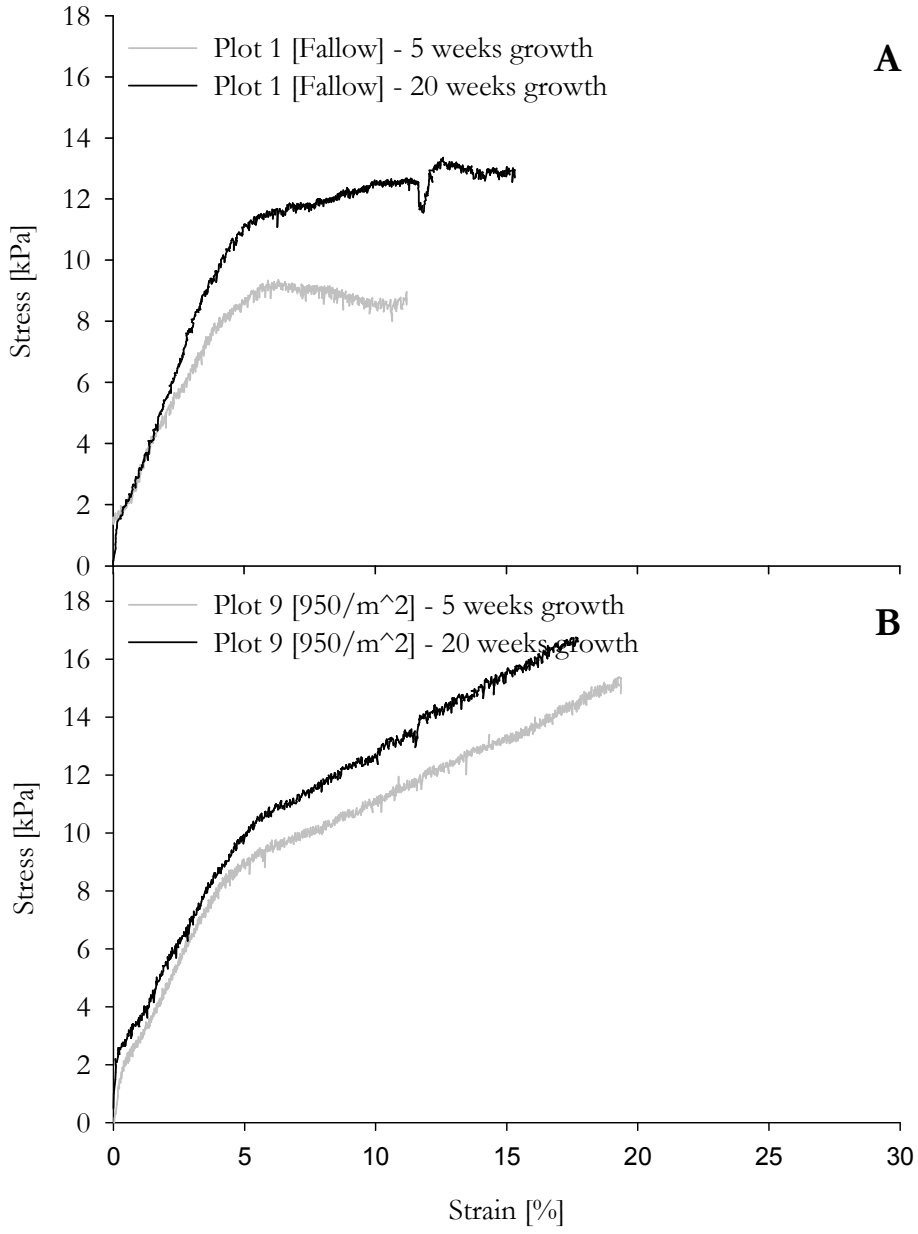

Figure 3-9: Typical shear test from a fallow (A) and planted core (B) sampled from the field after 5 and 20 weeks growth.

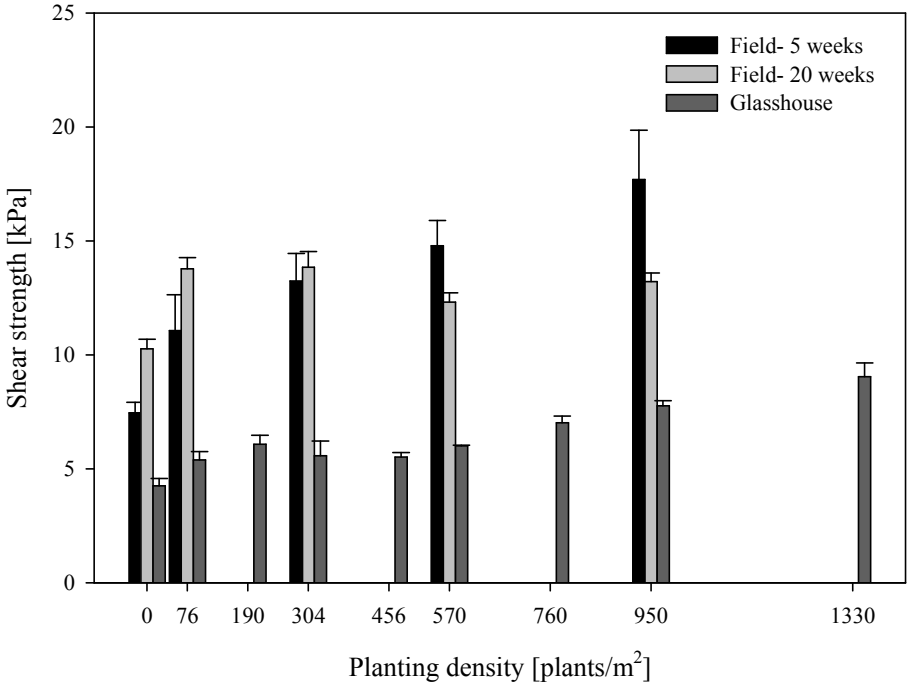

Figure 3-10: Soil core strength from glasshouse and field samples collected at 5 weeks and 20 weeks + standard error within each sampling density.

The mean root diameter per core increased between planting densities of 76 plants/m^2 and 304 plants/m^2 but, beyond these densities, the mean diameter decreased at greater planting densities (Figure 3-11). This trend was observed at both 5 and 20 weeks sampling, although root diameters were on average smaller at the later date (Figure 3-11). Root area ratio at the shear plane increased with increasing planting density when sampled at 5 weeks, with a large variation within densities (Figure 3-12). RAR at 20 weeks was significantly smaller ($P<0.001$) than at 5 weeks, with relatively little variation both within and also between densities (Figure 3-12). Comparison between root strength and sampling time, following log transformation and linear regression with groups, showed a significant relationship ($P<0.001$) with 46 % of variance accounted for. Root tensile strength decreased with increasing root diameter, although there was considerable scatter and a poor negative powerlaw relationship (Figure 3-13(A)).

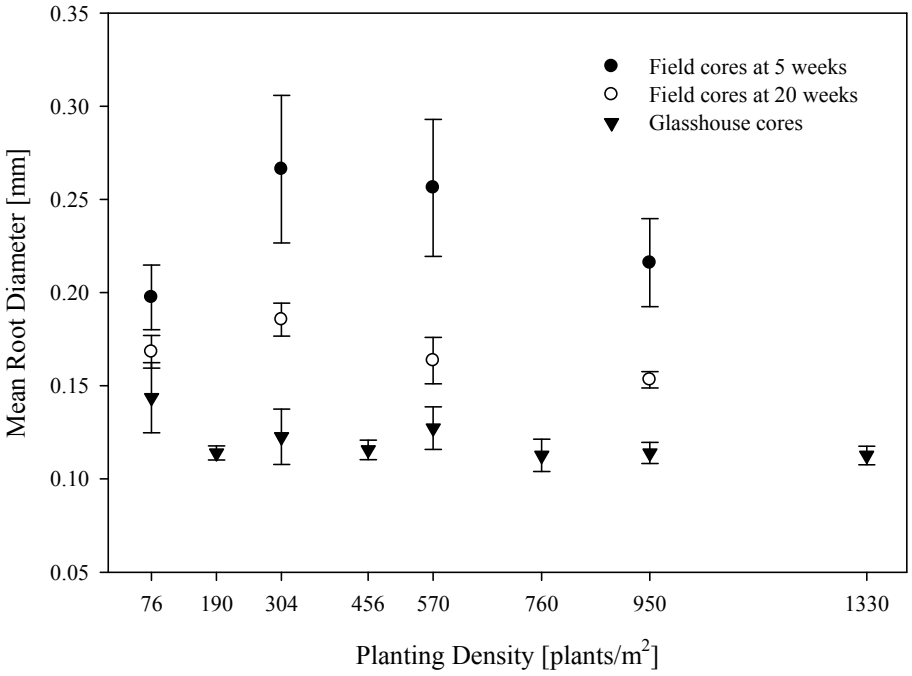

Figure 3-11: Mean root diameters for field and glasshouse cores ± standard error for each density

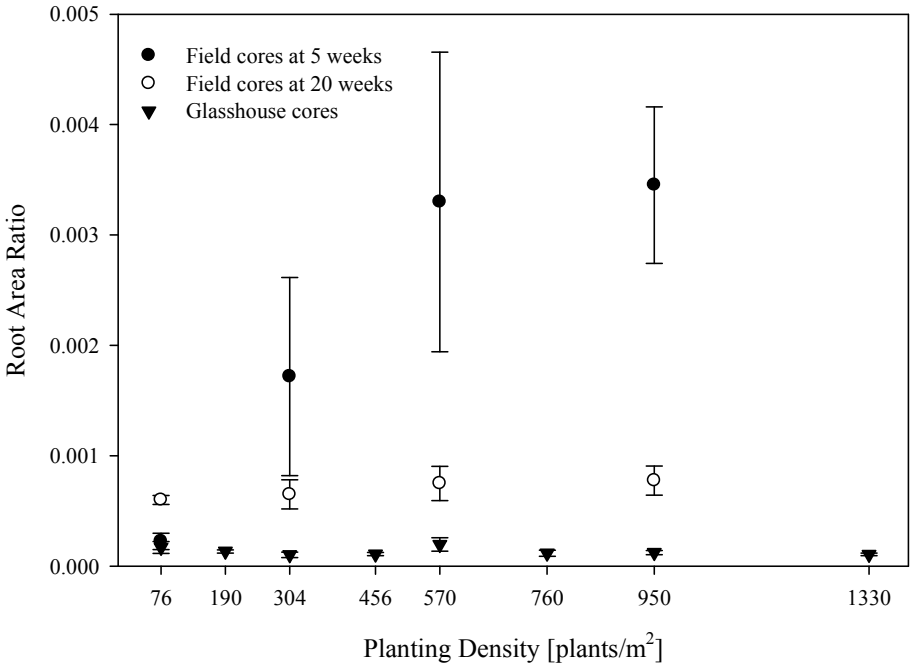

Figure 3-12: Relationship between root area ratio and planting density ± standard error

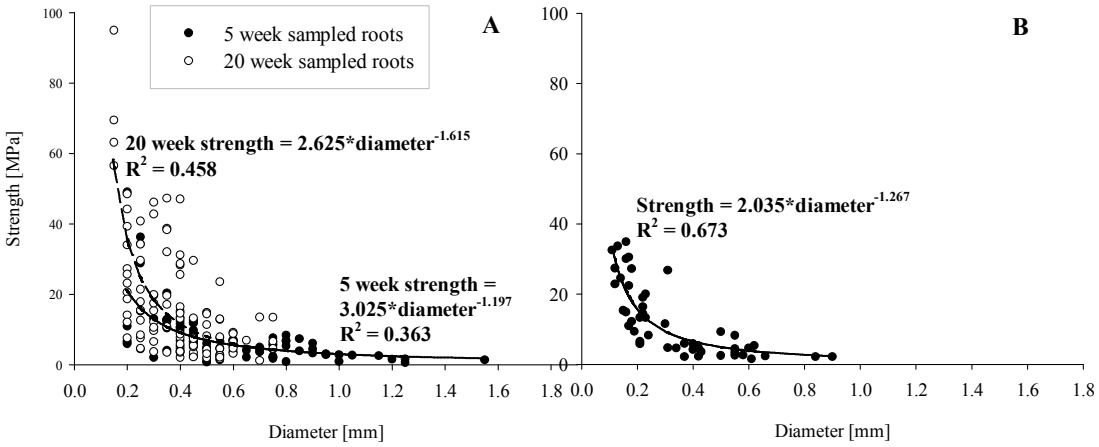

Figure 3-13: Strength diameter relationship for field experiment (A) and glasshouse (B) roots

3.3.2 Glasshouse study

Biomass data (Table 3-1) showed density treatments resulted in significant differences in the number of heads ($P<0.001$) and plant height ($P<0.001$). No significant differences were found in total above ground biomass ($P=0.249$). RARs within glasshouse cores were not significantly different between planting densities ($P=0.503$) with little spread within samples (Figure 3-12).

Density [plants/m²]	Biomass [g]	Number of heads	Plant height [mm]	Root mass [g]	Mean root diameter [mm]	Root diameter range [mm]
76	12.1 ± 0.40	6.3 ± 0.33	626.6 ± 32.83	0.96 ± 0.13	0.144 ± 0.033	0.06
190	13.7 ± 0.62	11.3 ± 0.88	581.6 ± 16.91	0.99 ± 0.30	0.114 ± 0.007	0.01
304	10.7 ± 0.32	12.3 ± 1.86	510.0 ± 18.93	0.53 ± 0.08	0.123 ± 0.026	0.05
456	15.5 ± 1.87	18.3 ± 1.45	521.6 ± 1.67	0.91 ± 0.20	0.116 ± 0.009	0.02
579	16.7 ± 2.48	22.0 ± 3.21	498.3 ± 18.78	1.06 ± 0.30	0.127 ± 0.020	0.04
760	10.8 ± 1.17	16.0 ± 1.00	396.6 ± 17.20	0.80 ± 0.19	0.113 ± 0.015	0.03
950	15.4 ± 1.19	20.67± 1.45	440.0 ± 10.41	0.78 ± 0.07	0.114 ± 0.010	0.02
1330	14.9 ± 2.75	26.3 ± 4.91	365.0 ± 32.79	1.90 ± 0.78	0.113 ± 0.009	0.02

Table 3-1: Glasshouse core plant data, mean ± standard error

Glasshouse results showed a significant relationship between planting density and core strength with $P<0.001$ and 76% of variance accounted for. Stress was observed to increase with increasing strain. Fallow cores reached a peak prior to returning to a residual stress with vegetated core stress continuing to increase to a peak at much greater strain (Figure 3-14). Soil shear strength was greater in all cores when compared to fallow, with a plateau reached between a planting density of 76 and 456 plants/m^2 (Figure 3-10). At planting density of >456 plants/m^2, core strength increased linearly with the greatest core strength observed at 1330 plants/m^2 (Figure 3-10). Core strength of the greatest planting density, 1330 plants/m^2, was significantly greater than at all but two of the other

planting densities (Table 3-2). At a planting density of 760 plants/m^2, core strength increased significantly when compared with fallow. In cores with a planting density of 950 plants/m^2, core strength differed significantly from both fallow cores and those at a planting density of 76 plants/m^2 (Table 3-2).

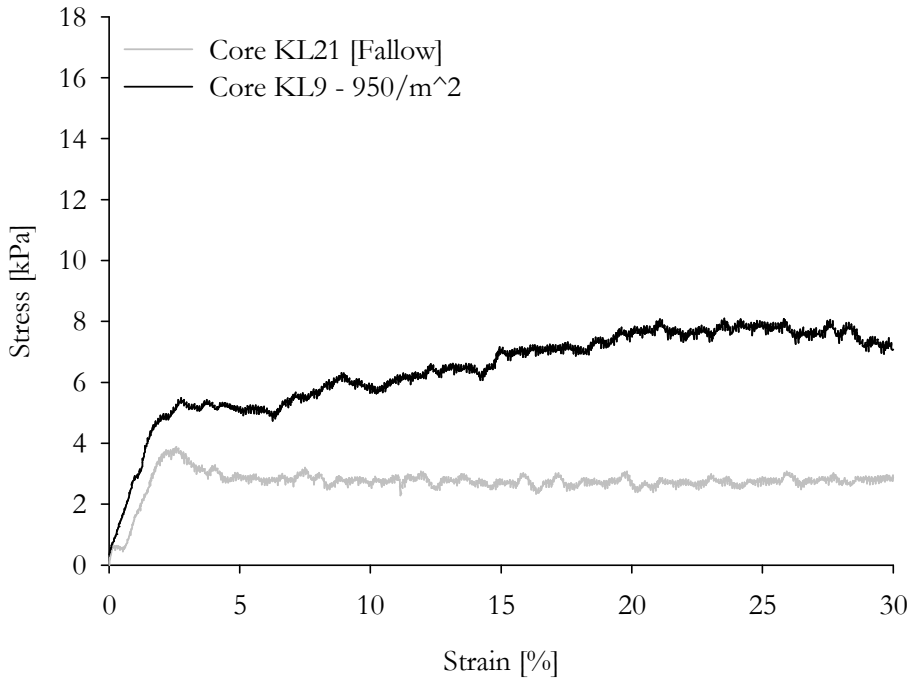

Figure 3-14: Typical shear test from a fallow (A) and planted core (B) following growth in a glasshouse environment.

Total root mass per core (Table 3-1) was not significantly correlated with core strength (P= 0.626). The number of roots at the shear plane also did not significantly affect core strength (P=0.466) with root mean diameters for each density not found to significantly affect reinforcement. As with the field study, root strength decreased with increasing diameter (Figure 3-13(B). Glasshouse root strength differed significantly from field root strengths at both field sampling times, P<0.001 (R^2= 0.536) at 5 weeks and P<0.001 (R^2=0.476) at 20 weeks.

76	1.13							
190	1.82	0.69						
304	1.31	0.18	0.151					
456	1.26	0.14	0.55	0.04				
570	1.74	0.62	0.07	0.44	0.48			
760	2.76*	1.64	0.94	1.45	1.50	1.02		
950	3.50**	2.38*	1.68	2.19	2.24	1.76	0.74	
1330	4.78**	3.65**	2.96*	3.47*	3.51*	3.03*	2.02	1.28
	0	**76**	**190**	**304**	**456**	**570**	**760**	**950**

Table 3-2: Differences in glasshouse core strength [kPa] between densities [*y* value – *x* value] (* =0.05% significant difference level; ** = 0.01% significant difference level)

Although mean root diameter was not found to significantly affect reinforcement (P=0.240), accounting for only 1.9% of variance, changes were observed in the spread of mean root diameters within each planting density when plotted (Figure 3-15).

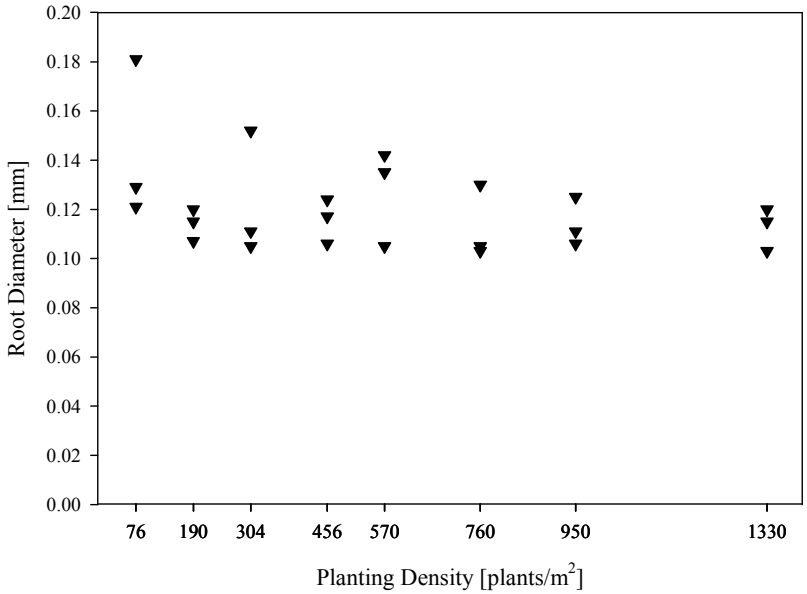

Figure 3-15: Effect of planting density on mean root diameter within glasshouse cores. Data for each replicate is shown

Quantification of root diameters at the shear plane showed cores with sparser planting densities (76, 190, 304 and 456 plants/m^2) fell into 6 root diameter categories, <0.072mm; <0.143mm; <0.215mm; <0.286mm; <0.429mm; <0.572mm. Roots measured from cores planted at higher densities fell within just four size categories with no roots greater than 0.286mm in diameter. Therefore, although significant differences in mean root diameter were not observed, there was evidence of density affecting root size distribution, through changes in mean root diameter variance at the shear plane within planting density replicates.

3.4 Discussion

Increasing soil shear strength was linked to increasing planting density, but the relationship was not as clear as originally expected. At 5 weeks in the field, RAR increased with increasing planting density and therefore may be the source of increased core strength between planting densities. At 20 weeks, however, this relationship between planting density and soil strength was not observed. One explanation could be that roots may weaken as the plant matures prior to harvest. Compared with fibrous roots, the effects of decay on woody roots have been widely reported in literature with some roots initially increasing in strength after trees had been felled and others decreasing directly following felling (Watson et al., 1997; Watson et al., 1999). Within some tree species, decreases in the tensile strength of small woody roots may be in the order of 300-500kPa per month following felling (O'Loughlin and Ziemer, 1982). Currently no information is available regarding the quantification of fibrous root decay on tensile root strength so more research is required to investigate the likely impacts. Within this study, RAR was much smaller at 20 weeks than at 5 weeks suggesting

significant decay had occurred although no significant differences between tensile tests were found for roots sampled at 5 and 20 weeks. RAR did not vary between planting densities at 20 weeks and this could be explained by depletion of soil resources limiting further root growth in this zone (Lopez-Bucio et al., 2003; Zobel et al., 2007).

The field experiment highlighted large variability in shear strength between specimens including those from the same treatment. A major source of variation will be in-field spatial variability induced by the structural heterogeneity of the seedbed and subsequent environmental impacts from weather and roots. Field tests of fallow soils at 5 weeks, however, showed much smaller variability of shear strength than for plots containing plants (Figure 3-10). Root penetration and proliferation changes soil structure, drainage and soil water content (Angers and Caron, 1998; Milleret et al., 2009; Pierret et al., 2007; Pollen-Bankhead and Simon, 2010), all factors known to affect soil strength. The extent to which soil structure will be affected may be influenced by increasing planting density. It is worth noting therefore that soil reinforcement may not solely be derived from fibre inclusions within the soil matrix, but also due to plant impact on soil structure (Milleret et al., 2009; Pierret et al., 2007). Merely subtracting the shear strength of rooted soil from that of fallow soil may not derive a value of reinforcement simply due to roots acting as fibre inclusions. Reinforcement of soil by roots must therefore be seen as a change to the whole soil system resulting in *ground improvement* rather than reinforcement *per se*. More work may provide a better understanding of the mechanisms by which plant roots increases soil strength and how this may be viewed, either as direct mechanical reinforcement or ground improvement increasing soil strength.

The glasshouse core study results indicated very little difference in RAR with increasing planting density, suggesting that RAR was not responsible for the observed increases in shear strength. Reinforcement significantly increased in cores with increasing numbers of plants only beyond a planting density of 570 plants/m^2. With little observed increases in RAR, one explanation of increasing reinforcement could be changes in root diameters. Smaller diameter roots have previously been shown to be stronger than larger diameter roots per unit area (Bischetti et al., 2005; Genet et al., 2005; Tosi, 2007). Cores of higher planting density resulted in thinner root diameters and this may explain increases in core strength. Soil nutrient content has been shown previously to affect root diameter distribution (Zobel et al., 2007), and root architecture (Lopez-Bucio et al., 2003). Root architecture is a key factor in increasing soil shearing resistance and has been shown to affect pull-out failure of roots (Mickovski et al., 2007), one of the shear failure processes within root reinforced soils. It is possible that the core grown plants were nutrient limited, resulting in changes in root diameter with planting density. With little evidence to suggest an alternative for observed increases in reinforcement, it is likely that increasing reinforcement was partly derived from changes in root diameter distribution.

Due to the number of very fine roots (<0.5mm), accurate diameter measurements of roots at the shear plane were very difficult to obtain. Previous studies have highlighted potential sources of error when utilising commercial root analysis software for measuring roots (Costa et al., 2001; Zobel, 2003). (Bauhus and Messier, 1999) recommended 'rigorous preliminary testing' in order to achieve the most accurate results. This study did not utilise root analysis software in an attempt to improve the accuracy of root diameter measurements. However, the resolution of the microscope graticule limited measurements to specific size classes rather than exact root diameters. Although a trend

was observed between root diameter and core strength in the glasshouse experiment, a clearer relationship may have been observed if measurement resolution was increased further. Through increased root measurement resolution, elucidation of potential links between root diameters within soil and soil strength may be possible. Previous research relating root diameter to strength has focussed mainly on woody plant species (Mickovski et al., 2009; Stokes et al., 2009). In the case of grasses considerable variability has been found regarding root diameter distributions (De Baets et al., 2008).

Fibrous root systems offer the potential to increase soil strength significantly and work at a different scale, in terms of rooting depth and mass, to woody root systems. Modelling of increasing soil strength with fibrous root inclusions requires more information than currently available due to the complexity of the interactions. Plant traits, such as root hairs and the root diameter distribution, will affect shear strength due to changes in failure mechanisms, e.g. through pull-out or breakage (Mickovski et al., 2007; 2009). Quantifying the conditions under which pull-out failure and root breakage occurs will also increase the predictability of root reinforced soil shear strength. Root composition, such as lignin and cellulose content, will also affect root strength (Genet et al., 2005) but without quantified data the inclusion of these factors into models is not possible.

BLANK PAGE

4. Effects of root phenotype on soil reinforcement

4.1 Introduction

During shear failure roots have been found to fail in one of two key ways, through either breakage failure, whereby the maximum tensile strength of the root is exceeded, or by pull-out failure where the bond between the root and soil has been exceeded. A variety of factors affect the failure mechanism of roots, some associated with soil properties (e.g. water content, bulk density, particle size) and others relating to root architecture or tortuosity.

Much could be learnt about the specific role of root traits on soil reinforcement and the failure mechanism by altering only key root traits. For instance, Bailey et al. (2002) used mutants of *Arabodopsis* to determine if root architecture had a much greater role than root hairs on the pull-out resistance of roots. They found a large impact from the amount of lateral roots but root hairs did not increase root pull-out resistance. This may have been due to *Arabidopsis thaliana* having weaker roots than the bond between root and sand. Mutants of other plants are available that would allow for specific traits to be isolated without the bias introduced by the small and weak root system of Arabidopsis. A large mutant population of barley has been developed at SCRI that has been screened for a range of specific traits. This provides the opportunity to extend the work of Bailey et al. (2001).

This study uses selected barley, *Hordeum vulgare*, mutants to investigate the influence of root hairs and architecture. The specific phenotypic root traits were hairlessness and increased tortuosity. By growing these plants in soil cores packed to the same densities and sheared under prescribed pore water suctions, it was possible to test the hypothesis that the phenotypic trait would affect soil shear strength. Through accurate manipulation of soil moisture conditions, the failure mechanism was also incorporated into the study with roots more likely to fail through pull-out in wet soil and more roots breaking in drier soil (Ennos, 1990). In order to minimise the effect of soil moisture content on soil strength a sand layer was incorporated into the cores at the shear zone, further enabling accurate data collection of root cross-sectional area at the shear plane.

4.2 Methods

4.2.1 Mutants and traits

All plants used in this study were from the same parent of *Hordeum vulgare* , cv Optic. A primary screen of mutant cultivars was performed through germination of seeds on filter paper. The plant traits selected were:

1. Wildtype – parent line used as the control.
2. Increased root tortuosity – natural mutant derived from the parent line
3. Hairless root – natural mutant derived from parent line

Two hairless mutants, 019-75 and 008-75, 036-50, a hairless root with increased tortuosity, and the parent were screened through growth in both soil and on filter paper

to ensure plants exhibited the desired mutation as they matured. Initial screening was performed through growth on filter paper of pre-germinated seeds. Optic 019-75 appeared not to have any root hairs however Optic 008-75 had a small number just below the seed (Figure 4-1). Due to these observations 019-75 was used within this experiment.

Germinated barley seeds were planted at 10 mm depth in 51mm diameter x 600mm length plastic tubes. The tubes were initially pre-cut vertically up the length of the tubes to create two 'u' shaped sections. Sections were then re-joined using Duck tape© and packed with Bullion field soil (described in section 3.2.1) to a bulk density of 1.17g/cm^3 ± 0.01. Plants were grown for a period of two weeks Tubes were then opened and the intact column of soil extracted. Instead of washing roots from soil, plants were gently agitated and lifted out of the soil to allow for any adhered soil to remain attached to the roots. Following removal it was possible to observe root hairs adhering to soil particles (Figure 4-2). Observations made of soil adhering to roots showed reduced quantities of soil on the hairless mutants when compared to the hairy plants.

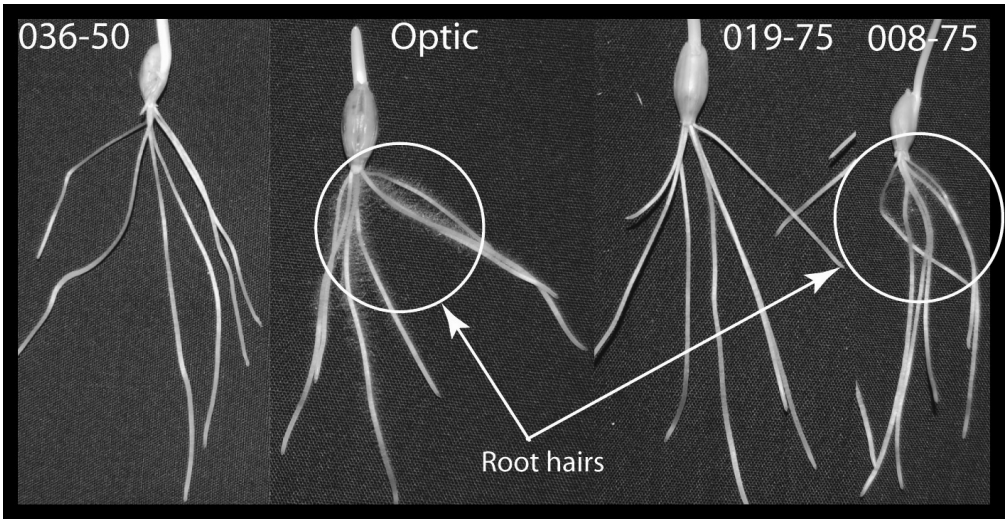

Figure 4-1: Initial screening of Optic cultivars, 036-50= Hairless and curly; Optic= Control; 019-75= Hairless; 008-75= Hairless. Mutant 008-75 grew some root hairs and was eliminated from the study. Note the clear sinuosity of 036-50 in comparison to both Optic and 019-75 mutants

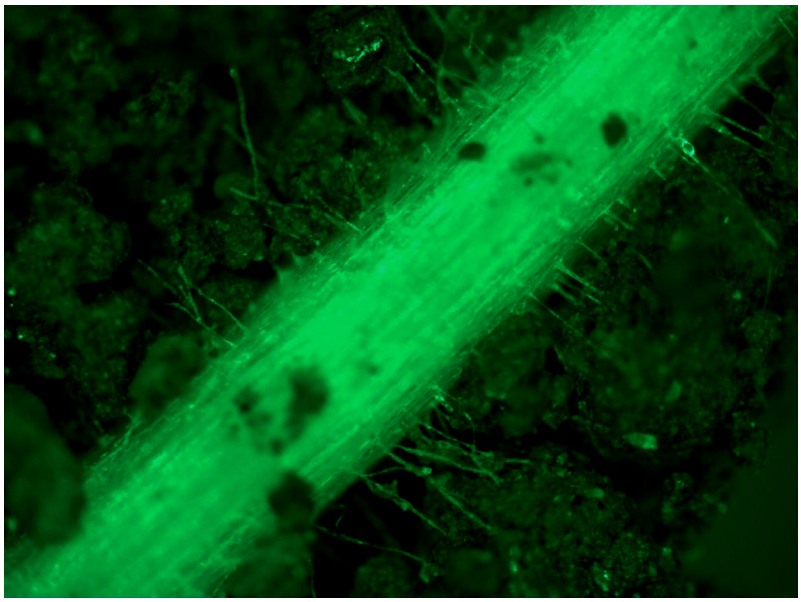

Figure 4-2: Root hairs adhering to soil particles, image captured using Leica MZFLIII stereo microscope

4.2.2 Soil preparation and packing

Bullion field soil, passed through a 2mm sieve, was packed into a circular metal cores 100mm diameter x 130mm height to a depth of 100mm. Cores were 30mm taller than the soil volume inside due limitations in the shear assembly whereby only 100mm height soil cores could be shear tested. Metal cores were first greased with petroleum jelly before being lined with acetate sheets to aid in the removal of the soil core for shear testing. In order to gain accurate root data at the shear plane, sand was packed 5mm above and below the shear plane, with 45mm of soil above and below (Figure 4-3). The sand used was Redhill 110, a sand with a d_{50} of 120μm (Kelly et al., 2004). Soil was packed to a density of 1.2g/cm^3, thereby enabling easy penetration of the soil by roots so that growth would be unimpeded. Packing was performed using a compaction plate (Figure 4-4) and 2.5kg proctor hammer falling from a height of 170mm, 130mm lower

than the standard proctor drop of 300mm. This reduced height allowed accurate packing of the soil cores to the correct density, as found through preliminary testing. The energy required for packing was calculated as being 21.23 kJ/m^3. The moisture content of the soil used for packing was 13.3 ± 0.13 g/100g. Once cores were packed they were saturated from the top with 300ml of water 24 hours prior to planting with germinated seeds. The method used for seed germination may be found in section 3.2.3.2.

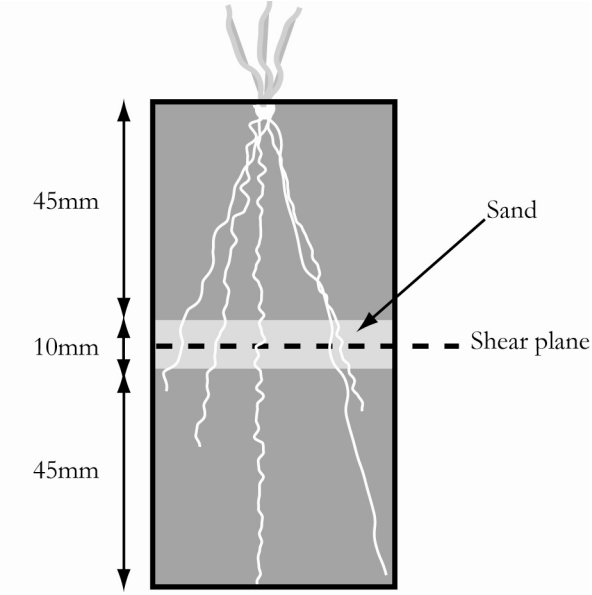

Figure 4-3: Example of packed core with sand shear plane

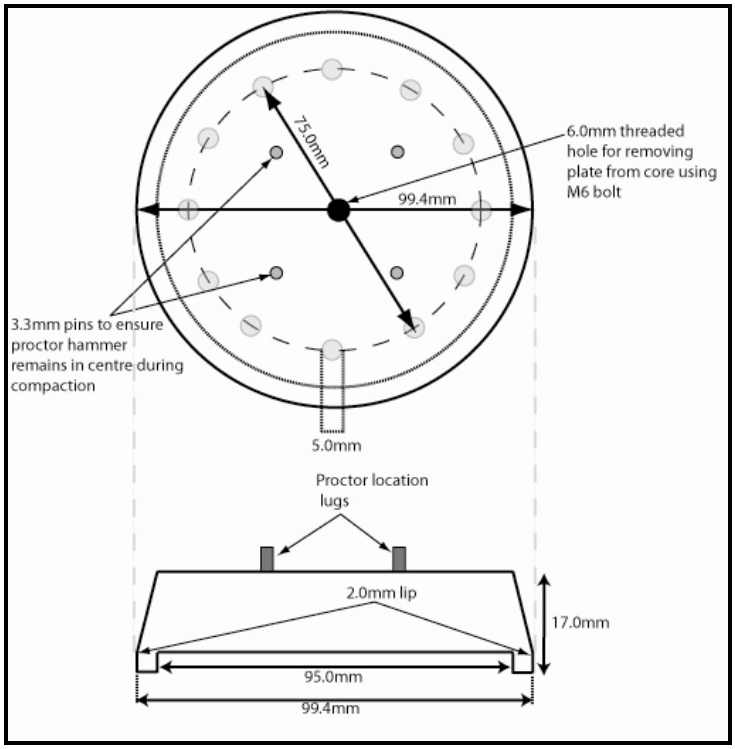

Figure 4-4: 100mm compaction plate used packing soils to specific soil density

Cores were then placed on top of four tubs containing soil packed to the same density as that in the cores. As a result, roots could grow into the soil blocks below with root growth only constrained laterally and not vertically. The soil block was also formed from Bullion field soil, but it was only passed through a 4mm sieve. Soil was packed into a 365 mm width, 550 mm length and 330 mm depth tub (internal dimensions) in 8 layers at a soil moisture content of 13.6 g/100g with energy required calculated as 14.13 kJ/m^3. This was less than that required for the soil cores because edge friction was smaller. Prior to the placement of cores on the surface of the soil block, 6.78 l of water was applied to the block with a watering can to bring the soil water content close to field capacity of 45 g/100 g.

A total of 48 cores (+ 2 spare for preliminary testing of shearing procedure) were prepared with 12 cores placed on the surface of each of the 4 tubs (Figure 4-5). Cores

were planted with pre-germinated seeds, with each treatment factor randomly distributed in each of the prepared cores. Three seeds were planted in each core, with planting density derived from the agricultural standard planting density of 380 plants/m^2. A total of 12 treatments were prepared (Table 4-1) and grown in 4 tubs with treatments randomly distributed within tubs (Figure 4-6). Randomisation was performed using the 'Spread'-'Randomize Rows' command in Genstat (GenStat for Windows. (2007). 10th Edition. VSN International Ltd., Hemel Hempstead, UK).

Figure 4-5: Cores grown on soil tubs to reduce sampling influence on soil structure

Treatment Factor	Cultivar and Trait	Soil Shearing Suction
1	Optic [*Control*]	1 kPa
2	Optic [*Control*]	5 kPa
3	Optic [*Control*]	10 kPa
4	Optic 019-75 [*Hairless*]	5 kPa
5	Optic 019-75 [*Hairless*]	10 kPa

Treatment Factor	Cultivar and Trait	Soil Shearing Suction
6	Optic 036-50 [*Hairless and Curly*]	5 kPa
7	Optic 036-50 [*Hairless and Curly*]	10 kPa
8	Fallow	1 kPa
9	Fallow	5 kPa
10	Fallow	10 kPa

Table 4-1: Treatment factors used within this study, highlighted areas denote treatments being used to assess failure mechanisms

Tub 1 [Planted 26/09/2008]			
1-4	2-4	1-3	9-2
3-6	2-3	6-2	8-3
10-1	6-4	3-5	3-4

Tub 2 [Planted 29/09/2008]			
5-4	10-4	10-8	3-7
10-3	10-7	7-3	1-2
5-2	7-4	3-1	7-2

Tub 3 [Planted 03/10/2008]			
3-8	4-2	10-6	4-3
2-2	1-1	8-4	6-3
10-5	10-2	7-1	9-1

Tub 4 [Planted 06/10/2008]			
9-3	8-1	4-1	2-1
3-2	8-2	3-3	6-1
5-1	5-3	9-4	4-4

Figure 4-6: Random distribution of cores within the 4 tubs used during growing period prior to shearing (**x-x refers to 'treatment – replicate'**)

The preparation of cores was staggered to ensure that all shear tests were performed on the cores following identical periods of growth. Cores were planted on 26 September, 29

September, 3 October and 6 October 2008, with shear testing performed 18 days after planting. Controlled preparation and growth of plants in cores on top of soil blocks minimised potential changes in soil structure associated with the collection process. Such changes may have occurred in the field trial experiment discussed in Chapter 3.

4.2.3 Plant growth

Plants were grown in a controlled environment room with prescribed light, temperature and humidity conditions that reflect local summer conditions. Night temperatures were 12°C for 6 hours followed by day temperatures of 18 °C for 18 hours. Sodium lights provided photosynthetic active radiation of 320 micromols . All cores were watered daily with 200ml H_2O. Once the plants reached a height of 20mm, 60g of gravel was placed on the soil surface to reduce surface drying. Surface drying of the soil may lead to desiccation and development of preferential flow paths to be formed. Prior to shear testing, plant height data were recorded for each of the 3 plants grown in each core.

4.2.4 Shear testing

Cores were removed from the surface of the soil tubs 18 days after initial planting and fully saturated with de-aired water, from the bottom, for a period of 24 hours. The removal of cores was performed using a thin stainless steel plate with a sharpened bevelled edge to cut roots crossing the boundary between the core and soil tub. Samples were then transferred to large sintered glass funnels for equilibration to 1kPa suction, sand tables for 5 kPa suction, and ceramic tension tables for 10 kPa suction. Different methods of equilibration were used to increase the accuracy of equilibration.

Shear testing was done following the same procedure outlined in section 3.2.2.3. The test conditions were identical, however, the method in which samples were extruded from metal cores differed to minimise soil disturbance as much as possible. Soil was pushed from the surface into the shear assembly with the soil core supported at the bottom by a hydraulic jack (Figure 4-7 (a)). A wooden plate on the soil surface was used to push out the soil core, with holes drilled to ensure the plant stem was not loaded during the transfer (Figure 4-7 (b)). Using the jack enabled the passage of the core into the shear assembly to be as smooth as possible (Figure 4-7 (c)) with no danger of the core separating. Particular care was necessary because of the sand at the shear plane. Finally the roots that had travelled along the boundary of the soil and metal core were cut using a scalpel blade to ensure that only roots within the soil core were sheared (Figure 4-7 (d)).

During shear testing errors occurred in the data acquisition USB interface card connecting the shear table load cell and LVDT to the computer. Errors meant that it was not possible to record consistent data during the course of the shear tests with data not recorded in all shear tests beyond 9mm displacement, 9% strain. For the purposes of this study all data are reported from the first 9mm of direct shear tests. After shear testing soil cores were extruded from the shear assembly into the original metal cores, tensiometers were then used to measure soil suction and data recorded. Following measurements of soil suction cores were frozen at -18 ^{o}C for later shear plane analysis.

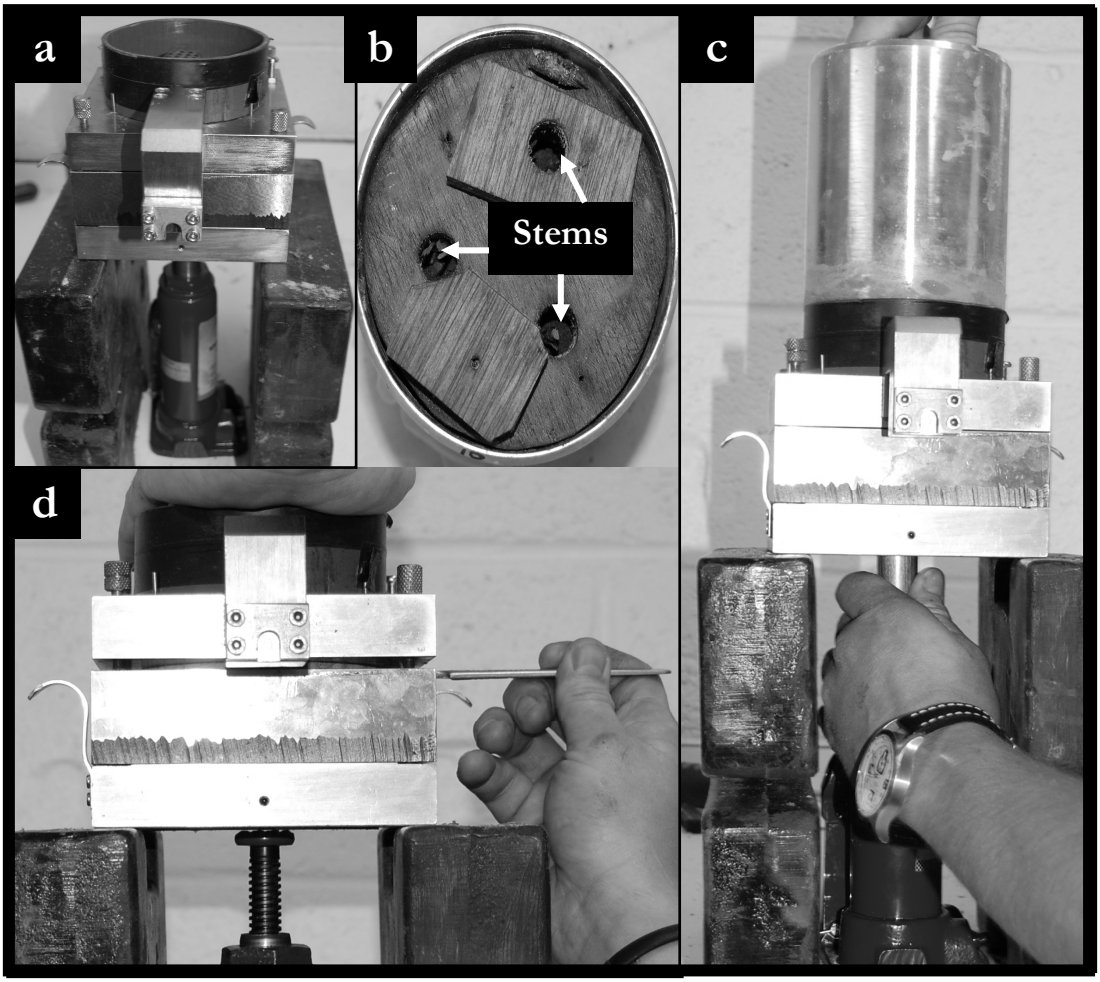

Figure 4-7: Soil core extrusion causing minimal soil disturbance using a hydraulic jack to control extrusion rate (a), a pushing plate to eliminate plant stem loading (b) allowing smooth transfer of core to shear assembly (c) before cutting roots travelling along the outside of the soil core at the shear plane (d)

4.2.5 Root area ratio measurement

Frozen metal cores were removed from the freezer at the time of measurement of the roots crossing the shear plane. The soil was removed from the cores whilst still frozen. It was then cut in half horizontally across the sand at the shear plane using a diamond circular saw lubricated with water. Following cutting of the shear plane, warm water was applied to the exposed sand shear zone to expose cut roots (Figure 4-8). A grid was then placed over the shear plane and root numbers and diameters recorded through the use of

a microscope and graticule. Calculation of the cross-sectional area of each root allowed for the RAR to be calculated.

Figure 4-8: Exposed roots at the shear plane following removal of sand. Grid used as an aid in recording root diameter and location

4.2.6 Statistical analysis

All data were tested for normality followed by linear regression analysis using Genstat (Tenth Edition) statistical analysis software (GenStat for Windows. (2007). 10th Edition. VSN International Ltd., Hemel Hempstead, UK.). Relationships between root diameter and strength were fitted with power-law curves, as discussed in Chapter 2 section 2.4.3. Significance testing between root strength and cultivar was performed using a linear regression with groups following log transformation of strength and diameter data. The effect of cultivar on plant height was examined using analysis of variance (ANOVA). Differences were considered statistically significant when the probability value (P) was <0.05. A polynomial fit was applied to the peak strength of fallow cores, under different suctions, to derive values of reinforcement. This method was chosen to smooth fallow soil strength data and elucidate any observable reinforcement better.

4.3 Results

4.3.1 Plant biomass

Differences in above ground biomass production during the growing period was not found to be significant between cultivars (P=0.055). Plant height for control Optic was 351.9mm ± 10.98, which was greater than that of other cultivars with differing root traits (Figure 4-9); 319.0mm ± 10.65 for cultivar 036-50 and 302.4mm ± 23.58 for cultivar 019-75. Such differences in plant height indicate potential pleiotrophy where changes in a single gene are found to have multiple phenotypic effects (Lobo, 2008), in this case reduced plant height.

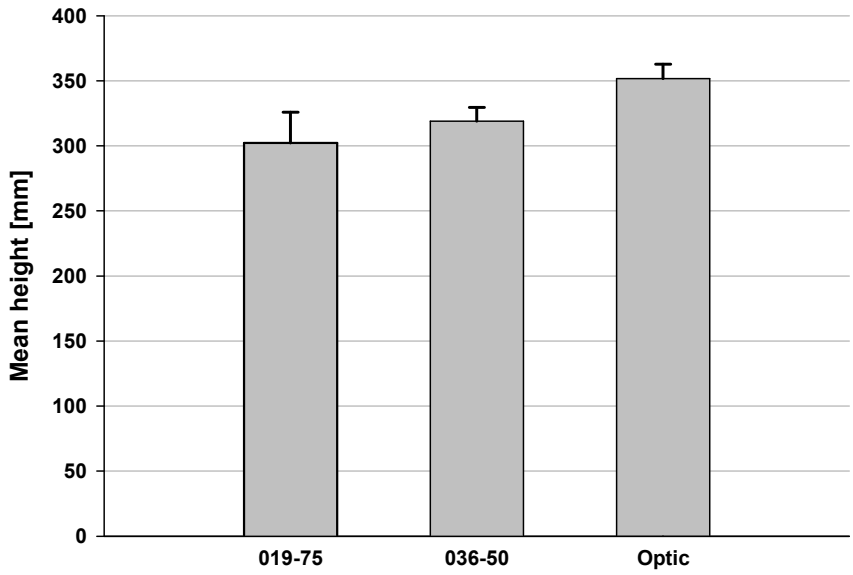

Figure 4-9: Mean aboveground plant height of the three Optic barley cultivars, 019-75 = Hairless; 036-50 = Hairless and curly; Optic = Wild Type (control)

4.3.2 Shear strength

After soil water equilibration, there were no differences in soil suctions within treatments and also between planted and fallow cores, with the values measured being very close to the equilibration suctions of 1kPa, 5kPa and 10kPa (Figure 4-10). An example of plots

derived from shear strength and strain data may be found in Figure 4-11 for cores sheared at 1 and 5kPa. Mean peak shear strength of each treatment (Figure 4-12) showed no measurable reinforcement by roots compared to the fallow treatment (P=0.634) and no differences in reinforcement between cultivars (P=0.329). Shear strength in all cores tested increased from 1kPa to 5 kPa soil suction, but then decreased at 10kPa suction (Figure 4-13). Trends were seen in both rooted and fallow soil cores with suction found to have a significant effect on peak shear strength (P<0.05).

A quadratic polynomial regression was fitted through data for peak shear strength of fallow soil cores (Figure 4-14). Using the polynomial regression it was possible to calculate predicted peak shear strength of fallow cores and subtract this from rooted cores to calculate root derived reinforcement (Figure 4-15). Cultivar type was not found to have a significant effect on reinforcement (P=0.260). Soil suction was found to significantly affect reinforcement (P<0.05) however this was not cultivar dependant (P=0.893).

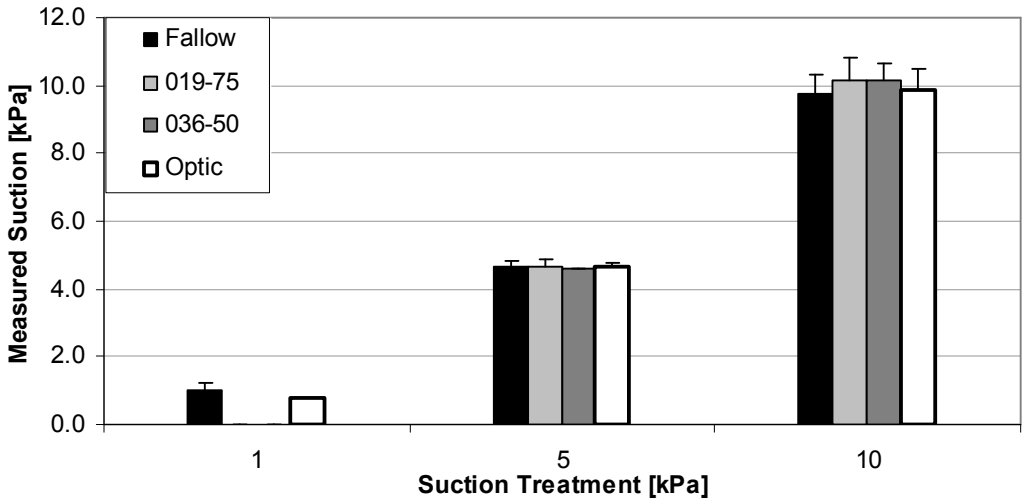

Figure 4-10: Measured suction of each treatment prior to shear testing

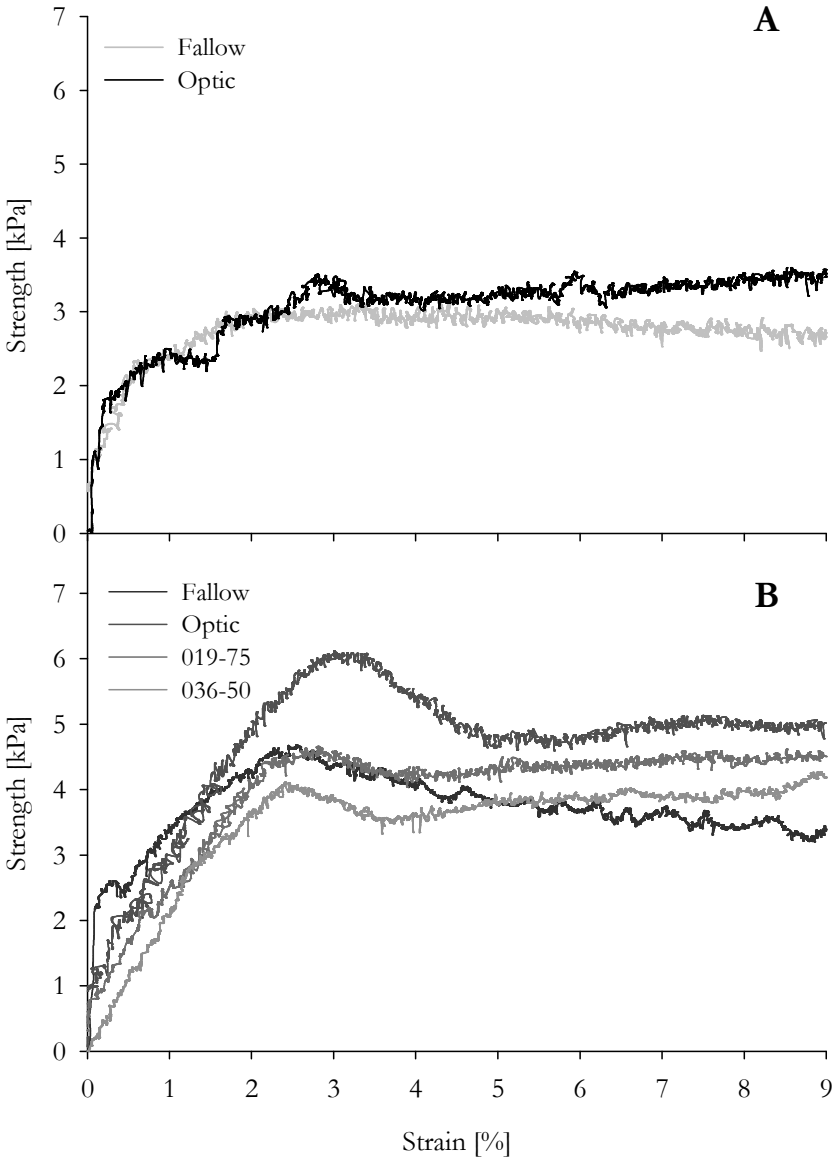

Figure 4-11: Example of shear curves for cores sheared at 1 kPa (A) and at 5 kPa (B) suction.

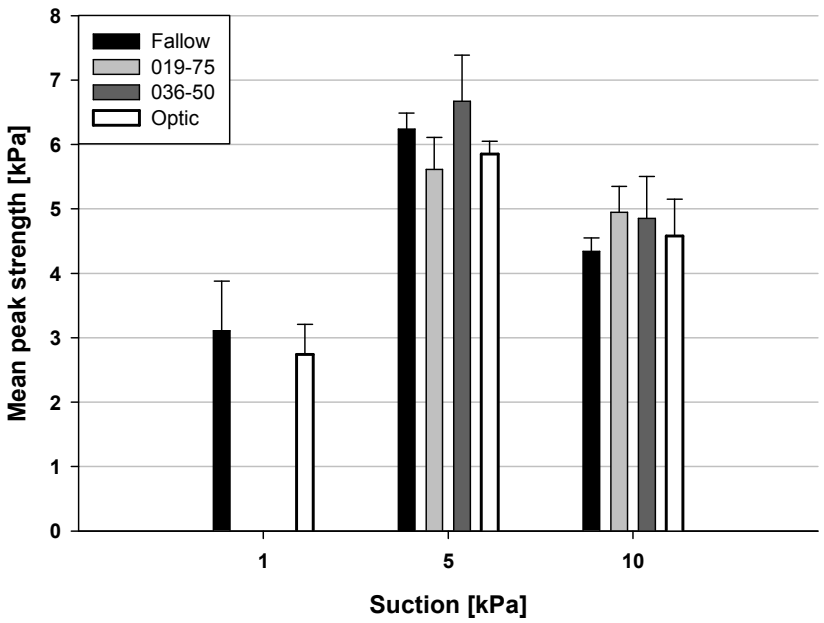

Figure 4-12: Mean peak shear strength of rooted and fallow soil cores shear under different soil moisture conditions, error bars indicate standard error

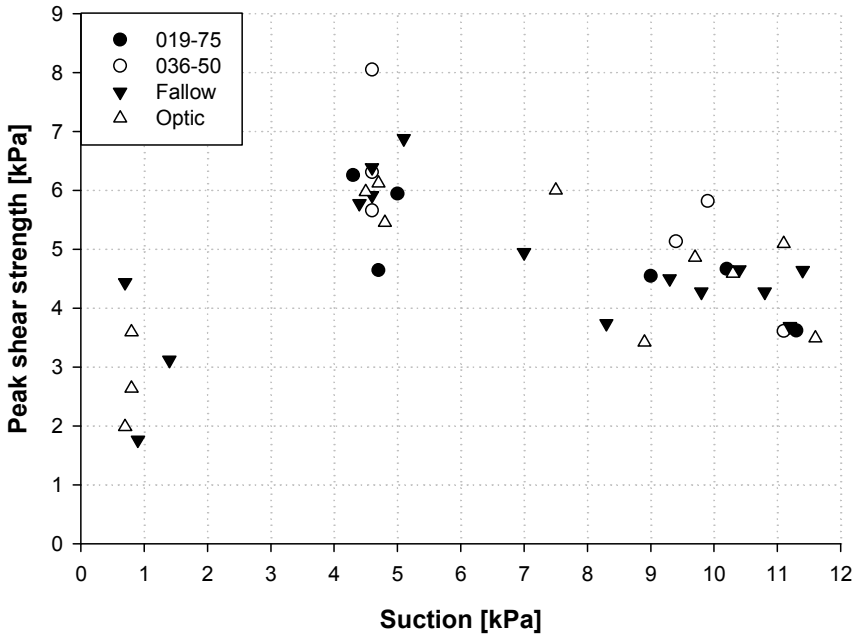

Figure 4-13: Peak shear strength after 9mm displacement of rooted and fallow soil cores sheared under different matric potentials

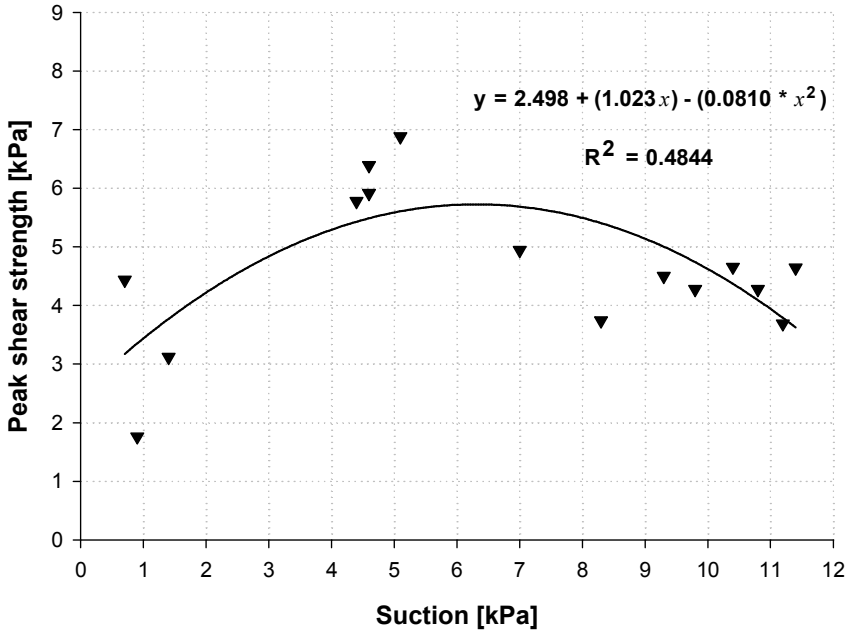

Figure 4-14: Polynomial regression fit of peak shear strength of fallow cores under different matric potentials

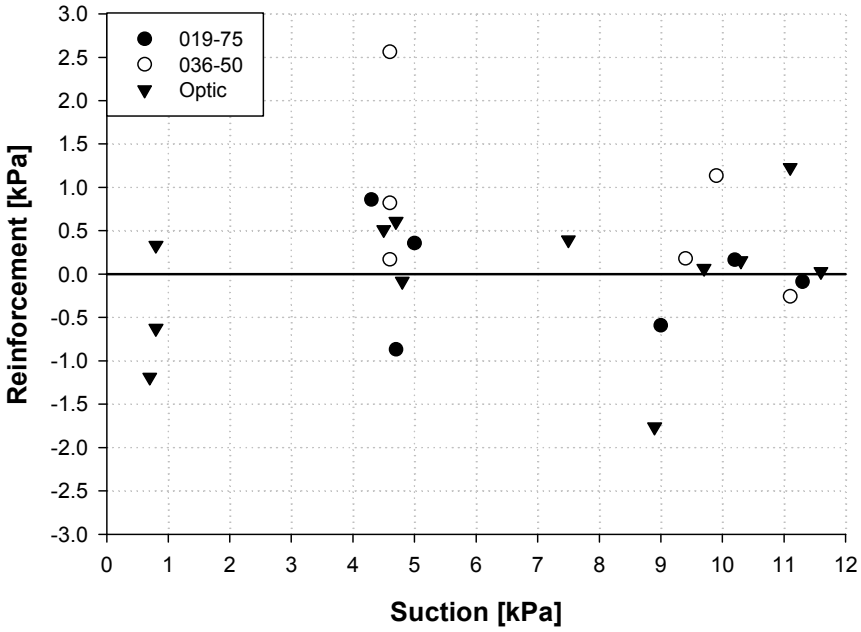

Figure 4-15: Root reinforcement of soil cores of 3 cultivars sheared under different matric potentials

Increasing reinforcement was not related to root area ratio (RAR) (Figure 4-16) (P=0.457) with RAR not found to be significantly different between cultivars (P=0.659).

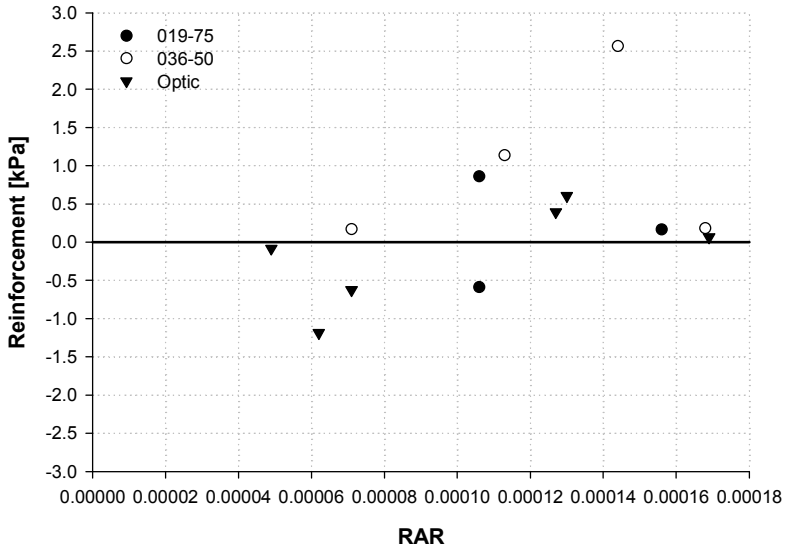

Figure 4-16: Effect of root area ratio (RAR) on reinforcement

4.3.3 Root tensile strength

Analysis of variance showed significant differences between root strength and cultivar ($P<0.001$; 108 df). Plots showed evidence of relationships between root strength and diameter (Figure 4-17). Root strength data were log transformed prior to linear regression analysis showing root diameter significantly affected root tensile strength ($P<0.001$). A T-test was performed to extract further interactions between cultivars and root strength. Optic root strength was significantly different to 019-75 ($P=<0.001$; 75 df) but not 036-50 ($P=0.300$; 76 df). Cultivar 036-50 was significantly different to 019-75 ($P=<0.001$; 61 df).

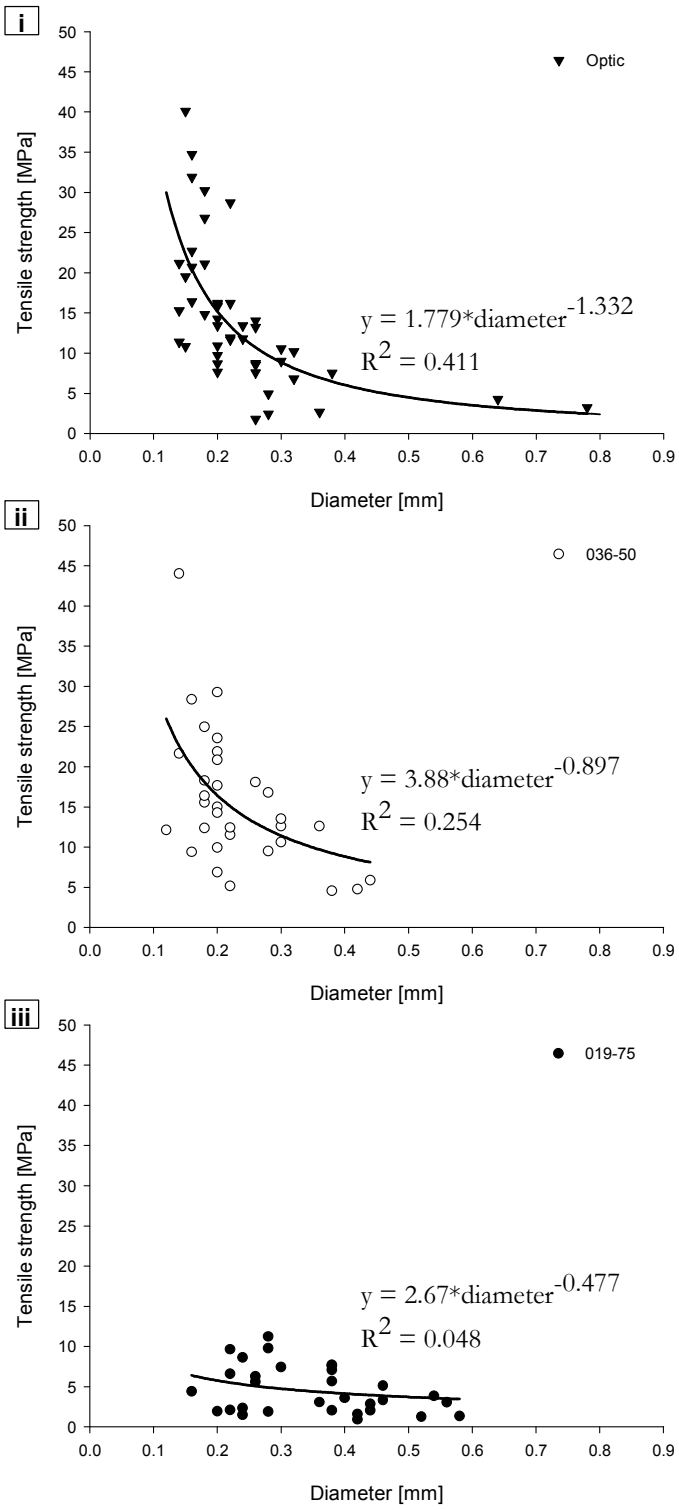

Figure 4-17: Root strength diameter relationship for cultivars, **i=**Optic (Control); **ii=**036-50 (Hairless and curly); **iii=**019-75 (Hairless)

4.4 Discussion

One of the difficulties in all experiments on plant roots is the accurate measurement of the diameter of roots that intersect the shear plane. It is widely acknowledged that measuring fine roots, 0.5-2.0 mm in diameter (Bohm, 1979), and very fine roots, <0.5mm (Bohm, 1979), is problematic with large errors associated with the use of scanning equipment due to pixel sizes in relation to root diameter (Bauhaus and Messier, 1999). For fine root measurement the most accurate and widely used is that of microscopic measurement **(**De León-González et la., 2007; Bohm, 1979; Melhuish, 1968). Using this technique requires root tips to be seen, but as fine young roots can be nearly translucent, visualisation can be difficult (Zobel, 2003). Being able to easily separate the soil from the roots allows for much better visualisation during measurement.

Due to the use of sand at the shear plane, to enable better quantification of the root area ratio, the shear strength recorded was that of sand and not the soil. Depending on sand properties, shear stress initially increases with increasing matric suction before decreasing as pores empty and effective stress is reduced (Fredlund et al., 1996). This was observed during this study. Although sand shear strength was measured, with soil shear strength likely to exhibit markedly different trends in relation to suction, it is still likely that changes in failure mechanism would have been observed were tests not compromised by data collection problems. It is possible that data beyond the 9% strain recorded may have shown changes in reinforcement derived from differing plant traits and soil conditions. Due to a capillary boundary formed by desaturated sand, soil below the shear plane may have equilibrated to different effective stress conditions associated with different levels of suction. Changes in effective stress would therefore alter the failure mechanism of roots present in the soil below and above the sand layer. There were no changes in

reinforcement associated with changing failure mechanism. One explanation for it not being possible to elucidate changes in reinforcement, based on root trait, may be due to problems encountered during shear testing, restricting shear strength data available from displacements >9mm (9% strain),. For example, if roots had increased tortuosity, displacement would have to be greater in order to localise stress down the length of the root. Previous root tensile tests in Chapter 3 were found to require approximately 40% strain before breaking in direct tension when already straightened. If roots were tortuous it would suggest that a strain value >40% is required before peak strength, and therefore any root derived reinforcement, would be reached.

The shear strength of rooted cores tested in Chapter 3, collected from the field site, were observed to differ between fallow and rooted samples even at the same levels of displacement which samples were displaced here (For example Figure 4-18). Such an observation may suggest a potential influence of the sand, used at the shear plane in this study, having an effect on stress localisation, when compared to soil. Sand may allow roots to 'pull' through with very little stress development during this process. Pull-out tests performed on root analogues have shown that soil close to the root is disturbed less in sand than in a sandy loam, indicating smaller root-soil friction in sand (Mickovski et al., 2007). This observation suggests that roots may take longer to localise stress during direct shear in pure sand due to the ability of roots to 'move' more freely through the sand layer incorporated into the soil cores used in this study. To further complicate possible results in this study, roots have also been shown to affect sand shear zone width (Abe and Ziemer, 1991). Further work in this area is needed to investigate the effects sand content on stress localisation during shear. With a large amount of research investigating root pull-out resistance and root reinforcement of sands (e.g Mickovski et al., 2007; Shewbridge and Sitar, 1996; Stokes and Mattheck, 1996) stress localisation may

be significantly affected by soil composition indicating further work is required for use of such studies in predicting the effects of roots on soil reinforcement.

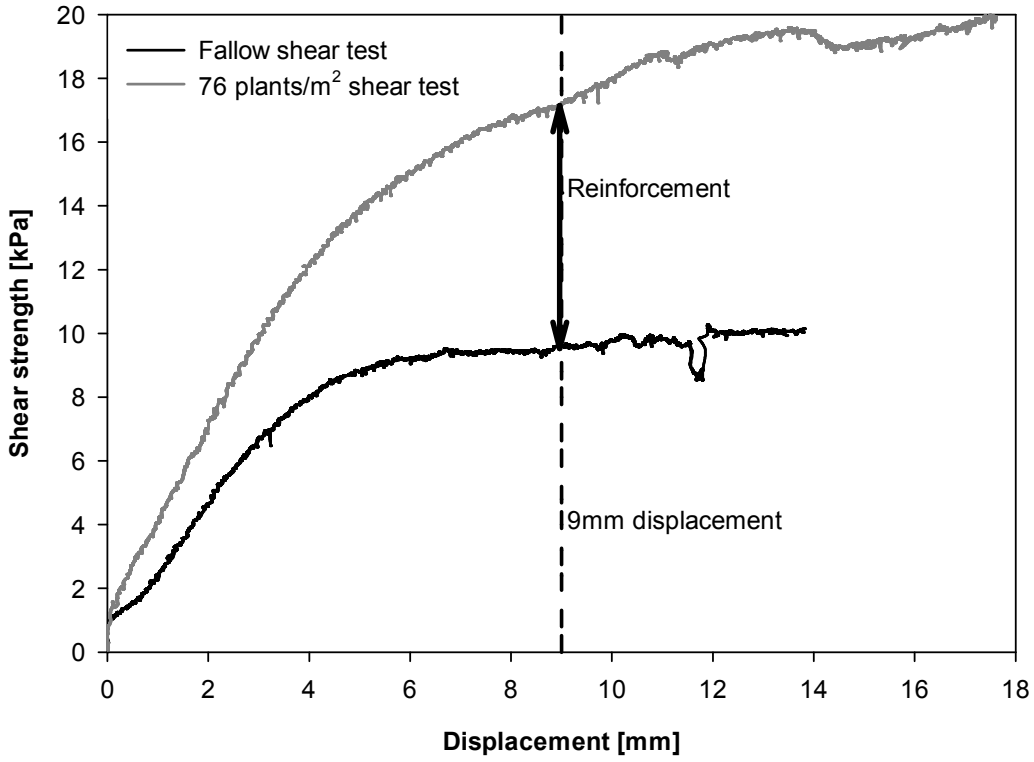

Figure 4-18: Example of shear test from Chapter 3 highlighting observed reinforcement at 9mm displacement

The significant difference in root biomechanical properties between the barley mutant 019-75 (hairless) and both Optic control and the 036-50 (hairless and curly) mutant indicates further possible evidence of pleiotrophy, first indicated through changes in above ground biomass. With no differences in tensile strength properties between the standard Optic cultivar and 036-50, these lines could be used in future research to isolate the impact of root hairs and tortuosity on pull-out resistance and root derived reinforcement without complications arising from different tensile strengths. This would enable a much better understanding of the role of root hairs in surface soil stabilisation. In the study of Bailey et al. (2001), root hairs of *Arabidopsis thaliana* did not increase resistance to uprooting. Roots, however, were found to break, as opposed to pull-out,

with the authors stating that 'the grip that the root is able to exert on the sand is greater than the strength of the root' (Bailey et al., 2001). Such a conclusion implies that a stronger root may have increased anchorage, and pull-out resistance, derived from root hairs. One weakness of the Bailey et al. (2001) study is that no root biomechanical properties were measured. No data are available for comparing the root strength of *Arabidopsis thaliana* to other plant roots. One study has performed tensile tests on *Arabdopsis* roots (Ryden et al., 2003) but root diameter was not recorded making comparisons impossible.

4.5 Conclusions

All efforts were made to setup a robust experiment to observe changes in reinforcement derived from changes in failure mechanism. Despite this, equipment errors during the collection of shear data resulted in it not being possible to quantify changes in reinforcement.

It is highly likely that were there not any problems with data collection results would still have been inconclusive regarding failure mechanism. Incorporation of a sand layer will have influenced the localisation of root stress during shear greater than expected. Also, it is likely that some potential evidence of root trait affecting reinforcement would have been seen in the data collected. With this not being the case it also possible that the effects of root trait may not be as important to the mode of failure as originally hypothesised. Traits examined in this study were assumed to potentially influence failure mechanism. However, the extent to which the 'curly' mutants exhibited their trait in soil is difficult to quantify and verify when plants are grown in soil.

Changes in root trait may also have resulted in pleiotropic effects on the plants themselves, however, the extent of these effects is again difficult to quantify. Thorough screening of model plant mutants is therefore recommended, especially the biomechanics, in order to eliminate pleiotropic effects. Further study into the effects of changing failure mechanism, and root derived reinforcement, would be highly beneficial in producing more accurate models for predicting reinforcement. The use of better screened cultivars, previously shown not to have pleiotropic effects on plant growth and biomechanics would be key for such studies. Through the use of screened cultivars and experimentation in a system, such as that described in this chapter, a variety of different root properties, and their contribution to soil reinforcement, could be studied. Variation in water content is, however, important within some environments where root reinforcement is likely to be highly variable due to fluctuating soil water content. River bank environments are typical examples of this and an application where research such as this would improve predictions in long term stability.

BLANK PAGE

5. Factors controlling biomechanics of plant roots: root type, root age, genetics and environmental stress

5.1 Introduction

Currently a great deal of research is being performed into second generation biofuel production. First generation biofuel production uses food crops, such as maize, for the production of biofuel via fermentation processes with authors arguing that such uses may increase food costs and increase food scarcity (Escobar et al., 2008). Second generation biofuel production would utilise waste from arable farming, such as barley (*Hordeum vulgare*) straw, to reduce pressures on the use of food crops. Currently use of such wastes is hindered due to costs, both environmentally, through the use of acids, and economically, through increased production costs, of removing lignin in order to allow complete digestion of cellulose and hemicellulose from straw material. Within barley straw cellulose accounts for 44% of the plant, hemicellulose accounting for 30% and lignin the remaining 26%. Increased biofuel production efficiency could be achieved by improving the quantities of both cellulose and hemicellulose, but this technology is currently not available. Altering lignin quality so it is more easily digestible has been found to reduce production costs and increase the yield of cellulose and hemicellulose. Down regulation of lignin is therefore the most promising method of increasing biofuel energy yield and reducing production costs.

Within plants lignin plays a key role within plant secondary wall structure (Boudet et al., 2003) and with increasing down regulation potential exists for significant effects on plant fitness (Pedersen et al., 2005). Plant secondary cell walls are predominantly composed of cellulose, hemi-cellulose and lignin (Boudet et al., 2003). Roots with greater cellulose content have been found to have greater tensile strength (Genet et al., 2005; Hathaway and Penny, 1975). Altering lignin to cellulose ratios may impact of root biomechanical properties key in contributing to soil stabilisation and plant anchorage. Links exist between lignin and cellulose contents with reduced lignin improving growth and increasing cellulose accumulation within trees (Hu et al., 1999). Effects of decreasing lignin on yield have been studied previously with decreases in lignin content increasing bio fuel production efficiency from agricultural straw waste (Pedersen et al., 2005).

Recently mutant cultivars have been developed enabling unique novel investigations to be performed to compare biomechanical properties between mutants and control 'wild type' plant in response to changing lignin concentrations. Prior to the availability of isolines, plants whose only genetic difference was that of the trait being studied, researchers have been limited in being able to perform studies into the secondary impacts of potential changes in biomechanics through alteration of cell wall composition. Cell wall composition has been shown to vary with age. Within maize roots lignin content increases in relation to the distance along the root within the endodermal cell walls with a similar relationship in the hypodermal cell walls (Zeier et al., 1999). Root lignin type, *p*-hydroxyphenyl, guaiacyl and syringyl, was also found to differ in content between root zones within endodermal cells (Zeier et al., 1999).

Lignin content affects the root biomechanical properties. However, this depends on species (Kohler, 2000; Kohler and Spatz, 2002). Kőhler (2000) found that *Aristolochia macrophylla* and *Aristolochia brasiliensis* stems became stiffer with increasing lignin content. Biomechanical properties of flax have also exhibited similar responses with stem tensile strength and Young's modulus increasing with decreasing lignin content. Manipulation of the CAD gene, one of the two main genes responsible for lignin production, altered the lignin/cellulose resulting in a 40% reduction in lignin content (Wrobel-Kwiatkowska et al., 2007). It must be noted that plants were grown in tissue culture with biomechanical properties calculated from only five replicates. Wróbel-Kwiatkowska et al. (2007) suggest that cellulose is a 'fibrous element' within plant tissues whereas lignin, pectin and hemi-cellulose are 'matrix components'. An increase in the ratio of lignin to cellulose both increases stem tensile strength and bending stiffness in flax (Wróbel-Kwiatkowska et al. (2007) and also bending stiffness in wheat (Wang et al., 2006). Such observations suggest cellulose is more responsible for increasing strength and stiffness within some plant species.

Currently little research has investigated the effects of lignin modification within roots below ground and more specifically on root biomechanical properties. With such a key role in plant cell structure the experiment presented in this Chapter aims to investigate both changes in root strength and also potential negative impacts to plant fitness under waterlogged conditions. With climate change models predicting more frequent intense rainfall events, water logging may increase. With increasing flooding there will be the requirement to develop more cultivars with increased resistance to water logging (Bates et al., 2008) however with potential changes in root structural properties questions must be asked on what these effects might have on root reinforcement of soils.

As previously mentioned, plant biomechanics are affected by changes in lignin quality with lignin deposition associated also with root age. Effects of lignin reduction on plant biomechanics may be exacerbated when plants are subjected to environmental stress. The aim of this chapter is to investigate this and the effects of root age. Novel mutants will be used and grown in ideal conditions, hydroponically, and also subjected to environmental stress caused by water logging and mechanical impedance of the roots. Through study of these effects it will be possible to increase our understanding of the impacts associated with altering cell wall structure and also increase our understanding on the effects of age on root biomechanics.

5.2 Methods

5.2.1 Plants and growing conditions

5.2.1.1 Plants

This study used a range of barley (*Hordeum vulgare*) lignin mutants (Table 5-1). Cultivars had previously been back crossed with the respective wild type cultivar following screening for natural mutations of lignin down regulation (J Stephens per comm.). The use of natural mutations allows for further screening of mutations to limit the likelihood of pleiotropy, changes within the plant out with those of the desired trait, within the plant genetic structure. Bowman 140 is the most thoroughly screened of the mutations available with no known pleiotropic effects resulting from lignin down regulation (J Stephens, per comm). Shoot lignin content of Bowman 140 and wild type has previously been quantified through Klasson lignin analysis with Bowman 140 showing a 13% reduction in lignin (Table 5-2).

An initial screening was performed in order to isolate which mutations exhibited biomechanical changes assumed to be as a response to reduced lignin within the plant. This screen involved an examination of shoot material only. Three point bending tests were performed between nodes on the main stems with flexure and peak stress recorded.

Optic	Emir	Bowman
Wild Type	Wild type	Wild Type
003	894	140
180	-	862
-	-	869

Table 5-1: Three screened cultivars showing the plants, wild type and mutations, tested

	Mean (g lignin/100g dry mass)	Standard error
Bowman WT	**17.53**	**0.18**
Bowman 140	**15.20**	**0.29**

Table 5-2: Klason lignin analysis of shoots of Bowman cultivars, each sample was analyzed as independent triplicates (J Stephens, 2009 (Per comm))

5.2.1.2 Plant growth

Plants were grown in a variety of different systems to elucidate potential changes in root biomechanics related to the growth environment. Plants for the initial screening process were grown in compost. Plants used for biomechanical testing were grown within a hydroponic setup and also in soil packed to two different densities. A control soil density of 1.2g/cm^3 was used with a further compacted treatment of 1.4 g/cm^3. The compacted

soil treatment was used to cause mechanical root impedance. Water logging was only performed on the control soil treatments.

5.2.1.2.1 Compost

Emir, Optic and Bowman wild type and mutant cultivars were pre-germinated (method outlined in section 3.2.3.2) and grown in a standard compost mix. This method was used for both the initial screening of barley cultivars for stem bending tests and also for the assessment of plant growth between lignin mutants and the control, wild type, cultivars.

5.2.1.2.2 Hydroponics

Lengths of 1m x 50mm diameter MUPVC waste pipe were sealed using a rubber bung and supported vertically within a controlled environment chamber. Light and temperature was controlled automatically with 16h of daylight, 8h of darkness, and with temperatures of 18°C and 12°C for daylight and dark periods respectively. This represents typical summer growing conditions in Scotland. Tube volume was calculated as 0.002m^3 with each tube holding 2 litres of nutrient solution. Tubes were filled to the top with a complete nutrient solution for growing barley (*Hordeum vulgare*) (Table 5-3) and topped up daily to replace losses through evaporation.

Seeds were pre-germinated (outlined in section 3.2.3.2) before being wrapped in plastic non-toxic foam and suspended so roots could easily touch the hydroponic solution. Air stones, attached to a compressor, were placed 80cm below the surface of the solution within each tube to aerate roots, thus ensuring root growth was not inhibited due to hypoxia.

	Stock solution concentration	Quantity (ml) per 2000ml tube
Stock solution		
NH_4Cl	0.3M (100X)	7.06
$Ca(NO_3)_2$	0.4M (100X)	7.06
KNO_3	0.4M (100X)	7.06
$MgSO_4$	0.3M (100X)	7.06
FeEDTA	0.1M (1000X)	1.40
KH_2PO_4	1M (200X)	14.12
Micronutrients		
$MnCl_2$	6mM (1000X)	
H_3BO_3	23mM (1000X)	
$ZnCl_2$	0.6mM (1000X)	
$CuSO_4$	1.6mM (1000X)	
Na_2MoO_4	1.0mM (1000X)	
$CoCl_2$	1.0mM (1000X)	2.00
Distilled H_2O		1954.24
TOTAL		2000.00ml

Table 5-3: Nutrient solution used for growing barley cultivars hydroponically

5.2.1.2.3 Soil

Bullion field soil (characterised in section 3.2.1), as used in Chapters 3 and 4, was packed in to plastic pipes 1m length x 50mm diameter. Pea gravel was placed in the bottom of each tube to a depth of 20mm with 980mm of soil packed above this layer. Soil was packed to dry bulk density of 1.2g/cm^3 (control treatment) and 1.4 g/cm^3 (compacted treatment). Packing was performed using a metal plunger weighing 2.78 kg dropped from a height of 20mm and 80mm for densities of 1.2g/cm^3 and 1.4 g/cm^3 respectively. Soil was packed in 25 layers for 1.2g/cm^3 and 50 layers for 1.4 g/cm^3. To minimise the potential risk of the silo effect, soil was packed in 25 and 50 layers for the lower and

higher soil densities respectively. The energy required for packing was found to be 7.08 kJ/m^3 and 113.22 kJ/m^3 for soil densities of 1.2g/cm^3 and 1.4g/cm^{3}respectively. Soil surfaces between each layer were roughened to ensure a homogenous column of soil eliminating the potential for a greater density of soil at the interface between layers (Figure 5-1). Following packing, four of the 50mm diameter tubes were placed in each of four 160mm diameter containers (16 soil filled tubes in total). After 7d of initial growth the tubes were flooded to 50mm below the soil surface (Figure 5-2). Waterlogged conditions were maintained for a period of 1 week before water was drained through a tap in the bottom of the containers used to hold the soil tubes. The soil tubes not receiving a water logging treatment were sealed at the base to ensure no uncontrolled water ingress occurred. These tubes were also immersed in water to ensure soil temperature was the same in all tubes as root growth has been shown to be temperature dependant (Vincent and Gregory, 1989).

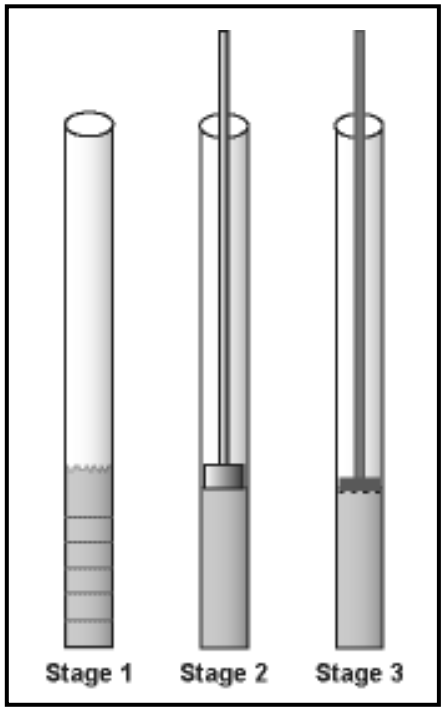

Figure 5-1: 50mm soil tube packing for water logging and root growth impedance study. Stage 1- Soil pluviated into tube in 20mm and 40mm layers for 1.2g/cm^3 and 1.4g/cm^3 soil densities respectively; Stage 2- Soil compacted with a plunger weighing 2.78 kgs; Stage 3- Surface of packed layer roughened to ensure a final homogenous column of soil is prepared

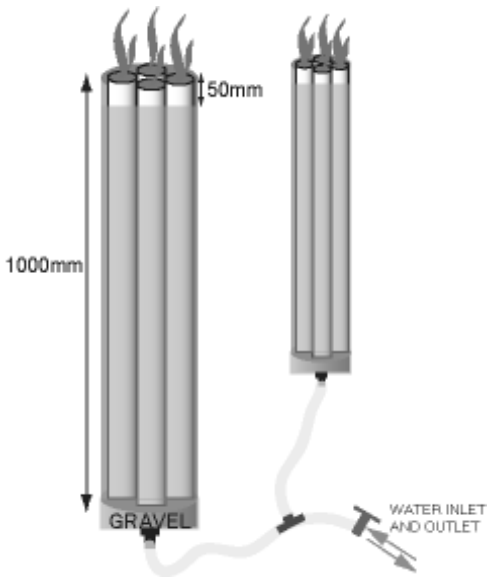

Figure 5-2: Water logging setup with four 50mm tubes within each 160mm containment tube. Tubes were flooded and drained through a valve in the base with non-waterlogged tubes sealed at the bottom

5.2.2 Mechanical testing

5.2.2.1 Stem bending and flexure

Flexure tests were performed using a single column universal testing machine, Instron 5544. Stems were placed on two 12mm diameter cylindrical rollers situated 80mm apart with the central intermodal point of the stem situated directly under the upper anvil. An upper cylindrical anvil, 18mm in diameter, deflected the centre of the stem at a rate of 5mm/min (Figure 5-3) with load and deflection recorded. The load cell had a capacity of 5 N and was accurate to 0.001N.

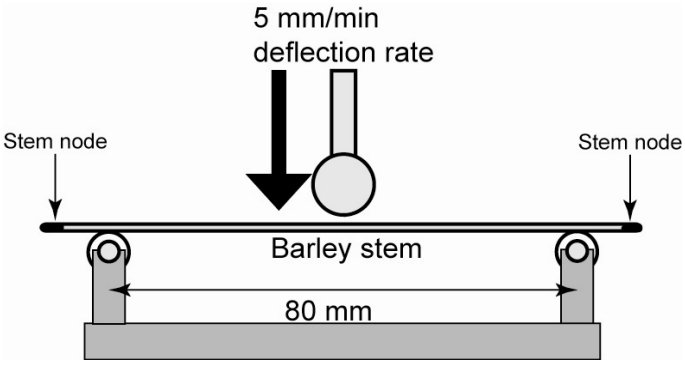

Figure 5-3: Schematic of three point bending and flexure testing setup for measuring barley stem mechanical properties at intermodal points

5.2.2.2 Tensile testing

Root tensile data was collected using the same procedure outlined in section 3.2.2.4 with an extension rate of 1mm/min. This is the same as the shear displacement rate in Chapter 3.

5.2.3 Statistical analysis

All data were tested for normality followed by linear regression analysis using Genstat (Tenth Edition) statistical analysis software (GenStat for Windows,(2007) 10th Edition. VSN International Ltd., Hemel Hempstead, UK). Relationships between root diameter and strength were fitted with power-law curves, as described in section 2.3.3. Significance testing between root strength and cultivar was performed using a linear regression with groups following log transformation of strength and diameter data.

The impact of cultivar, treatment and growing medium on plant biomass was assessed using repeated measures ANOVA. Significance was tested for all soil grown plants

separately to hydroponically grown plants. Differences were considered statistically significant when the probability value (P) was <0.05.

5.3 Results

5.3.1 Stem biomechanics of screened barley cultivars

Stem biomechanics varied with the height above the stem base and hence plant age. Emir and Optic cultivars were stiffest at the first node, oldest stem section, with decreasing flexure modulus for nodes further from the stem base (Figure 5-4). Contrary to this observation the Bowman 140 had increasing flexure modulus with increasing distance from the stem base. The results of the stem flexure tests (Figure 5-4) indicated that Bowman 140 had a markedly smaller stem flexure modulus compared with Bowman WT ($P<0.001$), and the node section also had a significant effect on flexure modulus ($P<0.05$). Optic 003 and Optic WT were also significantly different in flexure stiffness at each internode but as they had not been fully tested for other pleiotropic effects they were not used in the subsequent experiments.

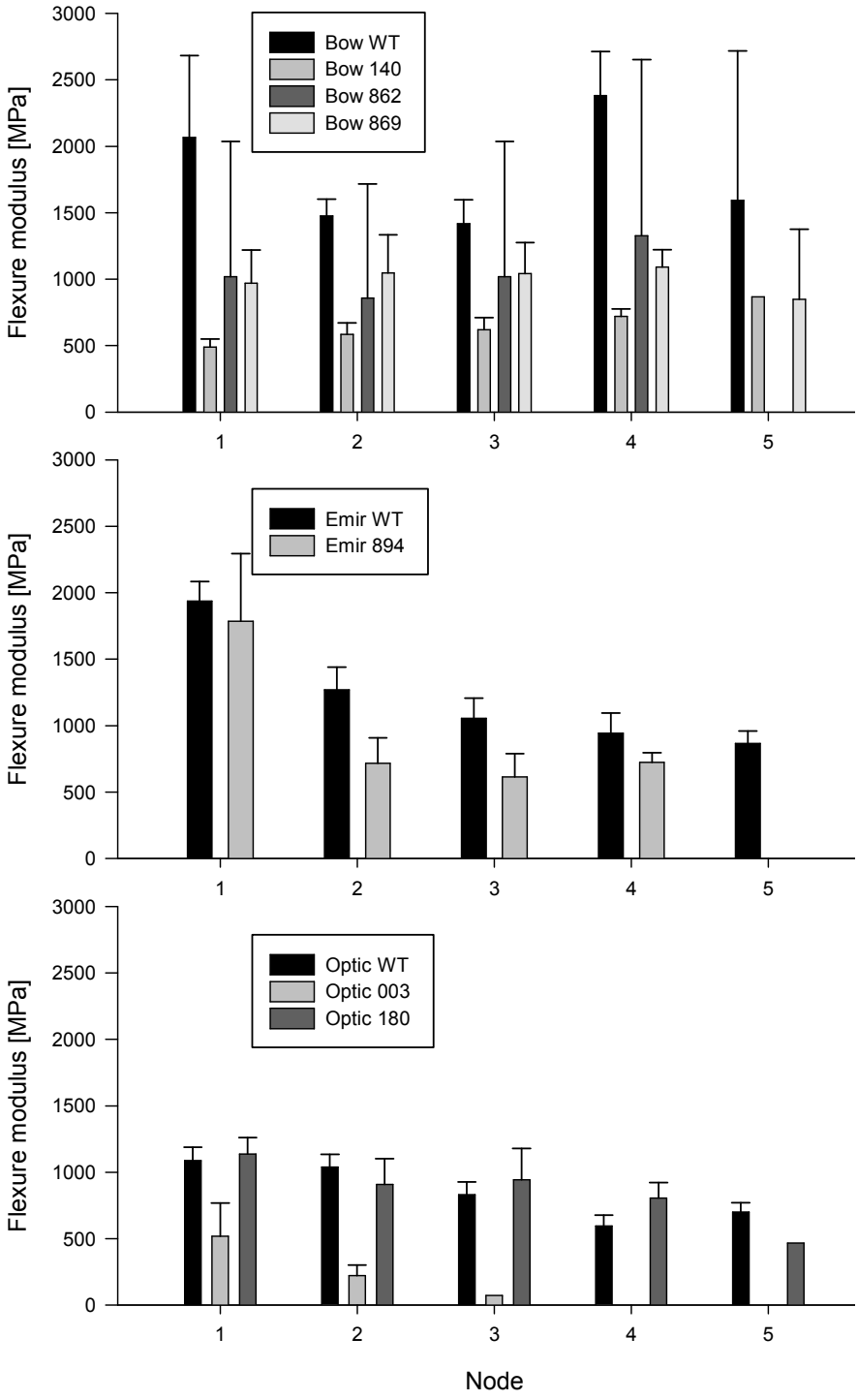

Figure 5-4: Flexure modulus for three point bending tests of stem tissue for Bowman, Emir and Optic cultivars. 'WT' refers to the wild type with other varieties previously screened for reduced lignin production, tests performed at inter-nodes e.g. 2 = between nodes 1 and 2

5.3.2 Plant biomass

Compost and hydroponically grown plants increased in height over time ($P<0.001$), however Bowman 140 grew much worse when grown hydroponically in comparison to Bowman WT (Figure 5-5). Plant height was found to significantly differ between cultivars ($P<0.01$) and also between treatment ($P<0.01$).

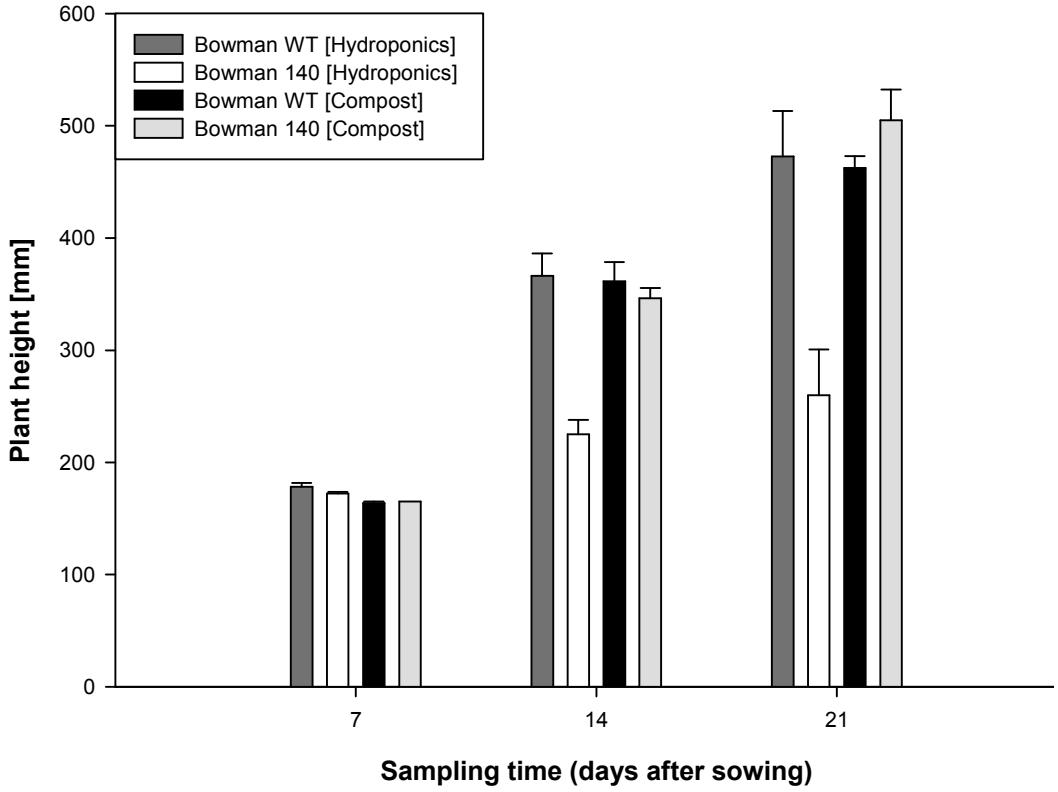

Figure 5-5: Effects of soil treatment and cultivar type on plant height for Bowman wild type (WT) barley and lignin modified, Bowman 140, when grown in compost and hydroponically. Error bars shown indicate standard error

Barley cultivars that were grown in soil increased in height over time ($P<0.001$) (Figure 5-6) with no significant difference between cultivars ($P=0.109$). Plants grown in soil of a normal density (control), compacted soil and waterlogged soil had significantly different plant heights ($P=0.01$).

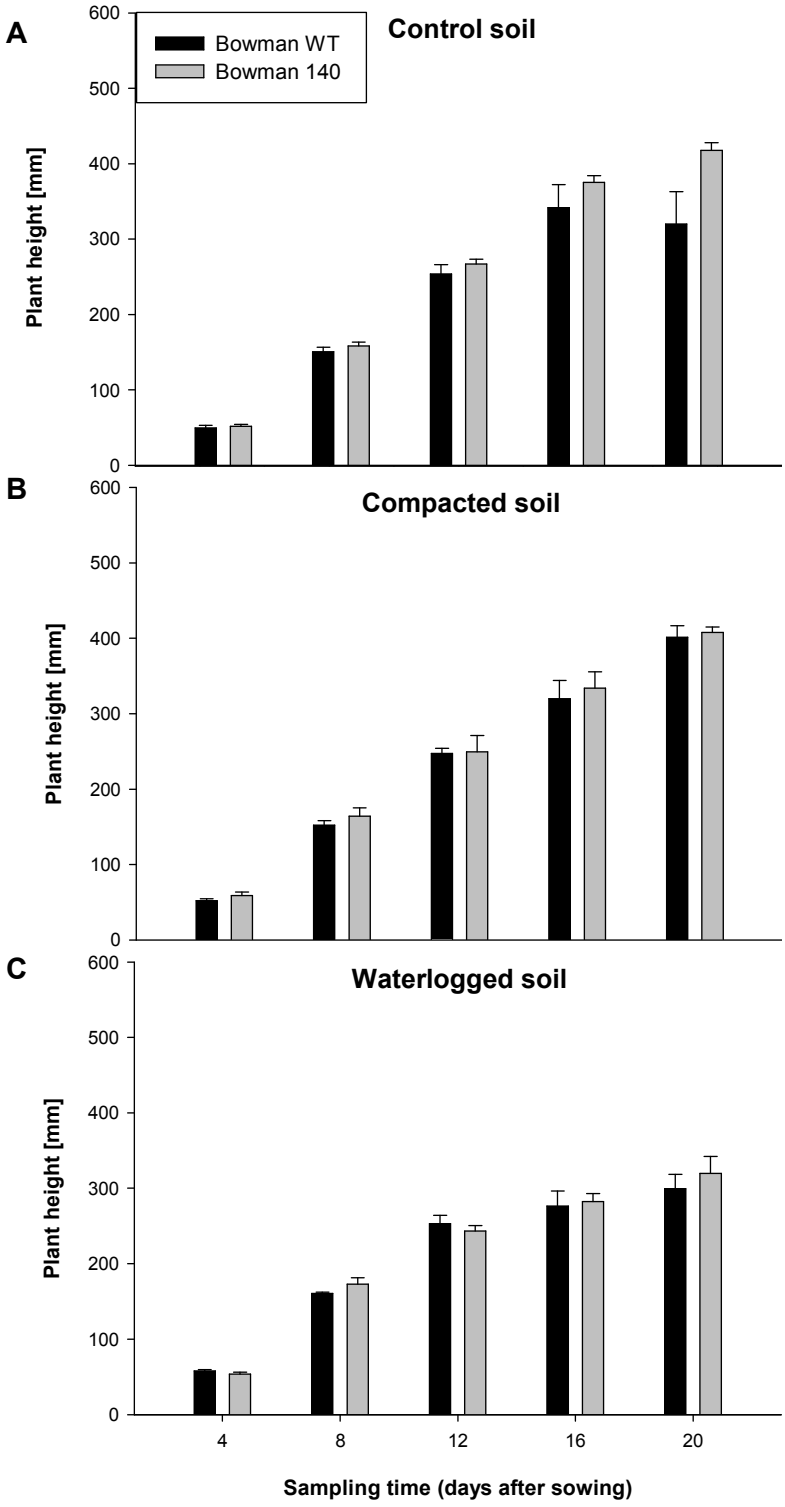

Figure 5-6: Effects of soil treatment and cultivar type on plant height, mean ± standard error

5.3.3 Root biomechanics

5.3.3.1 Soil grown root biomechanics

Interestingly, an increase in the mean flexure modulus and strength of roots resulted in a linear increase in standard deviation (Figure 5-7). Such a relationship highlights variability within biological materials with increasing strength and modulus properties resulting in a greater spread within the measured property.

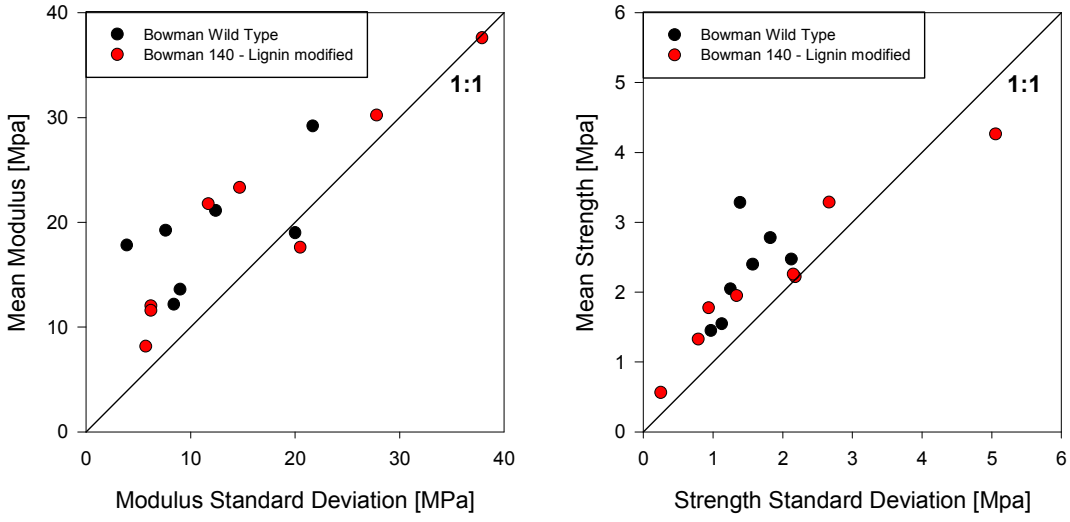

Figure 5-7: Linear relationship between standard deviation and means of root mechanical properties, strength and modulus, for Bowman wild type and lignin down regulated cultivars

A summary of changes in modulus and strength (Table 5-4) highlighted differences between all root types (seminal, nodal and lateral) and treatment. Within the control soil both Bowman 140 seminal and nodal roots were stronger and stiffer. The same trend was found for Nodal roots in waterlogged soil. In contrast, however, all root types of Bowman 140 were weaker and less stiff than Bowman WT when grown in compacted soil.

		Modulus	Strength
Control	Seminal	28.81%	53.40%
	Nodal	148.4%	37.08%
	Lateral	*	*
Compact	Seminal	**-7.3%**	**-10.16%**
	Nodal	**-32.49%**	**-31.25%**
	Lateral	**-14.84%**	**-8.38%**
Waterlogged	Seminal	*	*
	Nodal	21.16%	26.11%
	Lateral	*	*

Table 5-4: Differences in strength and modulus between Bowman WT and Bowman 140, positive values indicate Bowman 140 had increased strength or stiffness compared to Bowman WT with negative values indicating a decrease

Analyses of root strength and modulus data were performed on the whole root dataset for each soil treatment as it is likely that a natural root population, at a particular depth, will comprise of both young and old roots. Root type and treatment were separated to compare differences within each of the growing condition treatments. The output is listed in Table 5-5.

Root strength of plants grown in soil was found to significantly increase with decreasing diameter in all seminal roots, with cultivar not found to affect root strength (Table 5-5). Lateral root strength, when grown in compacted soil, was significantly affected by diameter with no relationship with cultivar. Nodal roots in both control and compacted soil were not significantly influenced by diameter (Table 5-5).

		P values for differences between cultivar strength and diameter			
Treatment	**Root**	**Diameter**	**Cultivar**	**Diameter and cultivar**	**PVAF [%]**
Compacted	*Seminal*	**<0.001*** **	0.695	0.730	68.5
	Nodal	-	-	-	-
	Lateral	**<0.001*** **	0.825	0.649	77.5
Control	*Seminal*	**<0.001*** **	0.778	0.511	45.1
	Nodal	0.195	0.791	0.762	2.6
	Lateral	-	-	-	-
Waterlogged	*Seminal*	**0.004** **	0.156	0.168	16.6
	Nodal	0.982	0.578	0.437	0.8
	Lateral	-	-	-	-

Table 5-5: Significance testing results for root strength and diameter/cultivar relationship for soil grown plants, ***** = P<0.001; ****** =P<0.01; ***** =P<0.05. PVAF (Percentage Variance Accounted For, or adjusted R^2) for diameter and cultivar relationship

Root tensile modulus of seminal roots in control and compacted soil was found to be significantly affected by diameter, however, this effect was not seen in seminal roots subjected to water logging for a 7 day period (Table 5-6). Seminal root modulus, when subjected to water logging, however, differed significantly between cultivars (Table 5-6).

		P values for differences between cultivar modulus and diameter			
Treatment	**Root**	**Diameter**	**Cultivar**	**Diameter and cultivar**	**PVA [%]**
Compacted	*Seminal*	**<0.001*** **	0.689	0.413	43.9
	Nodal	-	-	-	-
	Lateral	**<0.001*** **	0.580	0.683	48.1
Control	*Seminal*	**<0.001*** **	0.901	0.934	28.9
	Nodal	0.569	0.376	0.587	21.0
	Lateral	-	-	-	-
Waterlogged	*Seminal*	0.239	**0.021***	**0.021***	8.0
	Nodal	0.941	0.650	0.694	-
	Lateral	-	-	-	-

Table 5-6: Significance testing results for root modulus, diameter and cultivar effects for soil grown plants, ***** = P<0.001; ****** =P<0.01; ***** =P<0.05. PVAF (Percentage Variance Accounted For, or adjusted R^2) for diameter and cultivar relationship

Root strength and diameter relationships could be fitted with a negative power law relationship when significance was found between strength and diameter in all soil treatments (Figure 5-8). Although significant relationships were found R^2 values ranged between 0.22 and 0.95 indicating fits were variable despite common adoption of fitting this relationship to root strength data. Negative exponential power law relationships were also observed between modulus and diameter when significance testing highlighted significant effects of diameter (Figure 5-9).

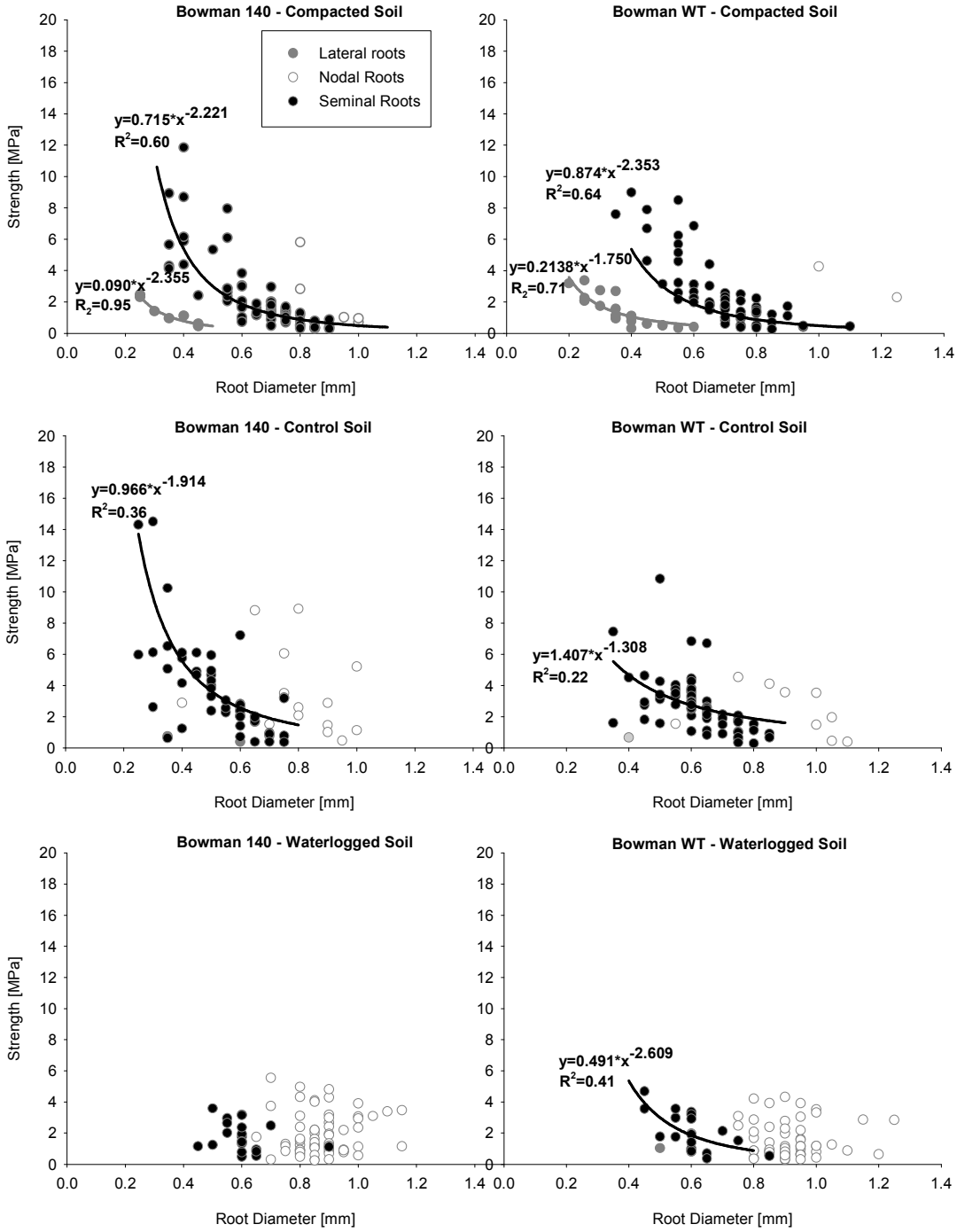

Figure 5-8: Effects of diameter on root strength of plants grown in compacted soil (1.4g/cm³), normal soil density (1.2g/cm³) and soil waterlogged for a period of 7d. Plotted regression lines indicate statistically significant relationship ($P<0.05$) between strength and diameter

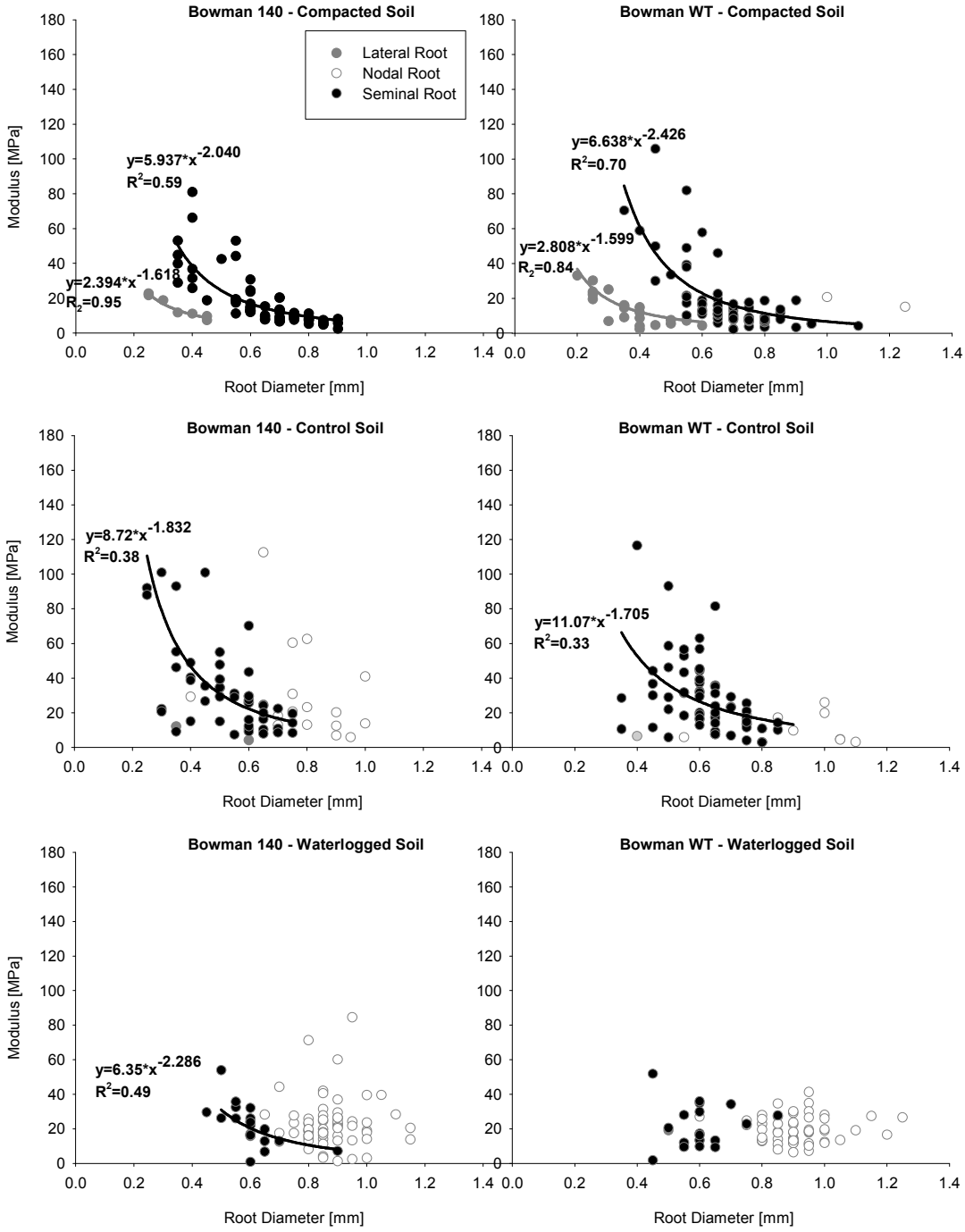

Figure 5-9: Effects of diameter on root modulus of plants grown in compacted soil (1.4g/cm^3), control soil (1.2g/cm^3) and soil waterlogged for a period of 7d. Plotted regression lines indicate statistically significant relationship ($P<0.05$) between modulus and diameter

Nodal and seminal root modulus and strength, when grown in the control soil, were the only root populations found to be significantly different between cultivar ($P<0.05$). All

root populations were found to be significantly affected by distance from root tip with roots increasing in strength with increasing distance from root tip ($P<0.05$) (Table 5-7; Table 5-8). Roots were observed to penetrate the soil to a maximum depth of 0.865m in the control soil (Figure 5-10). Plants grown in waterlogged soil produced the shortest seminal roots, 0.21m, when compared to those in either compacted soil, 0.51m or the control soil.

The strongest roots of Bowman WT were those situated closest to the stem base (furthest from the root tip) with strength increasing with increasing distance from the root tip. Root stiffness was also found to increase with increasing distance from the root tip for the Bowman WT roots; however, this was not as pronounced in waterlogged root samples (Figure 5-10). Bowman 140 exhibited similar trends to Bowman WT with both modulus and strength increasing with increasing distance from root tip. Standard error for the strength and modulus of each was greatest in control soil with less variation in both waterlogged and compacted soils.

As with seminal roots, nodal roots were observed to increase in strength and stiffness with increasing distance from the root tip (Figure 5-11). In waterlogged soil, the maximum nodal root length was found to be longer than seminal roots under the same treatment regime, 0.39m as opposed to 0.21m for seminal roots. Maximum lengths of nodal roots grown in control soil were shorter than seminal roots, 0.21m as opposed to seminal maximum root length of 0.51m. Due to a limited number of nodal roots in compacted soil, it was not possible to compare root biomechanics to waterlogged and control soil treatments (Figure 5-11).

		P values for differences between cultivar root strength and distance from root tip			
Treatment	**Root**	**Distance from root tip**	**Cultivar**	**Distance from root tip and cultivar**	**PVAF [%]**
Compacted	*Seminal*	**<0.001*** **	0.403	0.936	49.0
	Nodal	-	-	-	-
	Lateral	-	-	-	-
Control	*Seminal*	**<0.001*** **	0.122	0.672	54.4
	Nodal	**0.002** **	**0.043***	**0.019***	51.4
	Lateral	-	-	-	-
Waterlogged	*Seminal*	**0.024***	0.591	0.553	21.7
	Nodal	**<0.001*** **	0.268	0.742	64.2
	Lateral	-	-	-	-

Table 5-7: Linear regression analysis with groups results for root strength and distance from root tip relationship for soil grown plants, ***= P<0.001; **=P<0.01; *=P<0.05. PVAF (Percentage Variance Accounted For, or adjusted R^2) for diameter and cultivar relationship

		P values for differences between cultivar root modulus and distance from root tip			
Treatment	**Root**	**Distance from root tip**	**Cultivar**	**Distance from root tip and cultivar**	**PVAF [%]**
Compacted	*Seminal*	**<0.001*** **	0.960	0.969	37.7
	Nodal	-	-	-	-
	Lateral	-	-	-	-
Control	*Seminal*	**<0.001*** **	**0.020***	0.111	36.7
	Nodal	0.292	0.533	0.800	-
	Lateral	-	-	-	-
Waterlogged	*Seminal*	0.370	0.529	0.633	-
	Nodal	0.062	0.813	0. 400	3.9
	Lateral	-	-	-	-

Table 5-8: Linear regression analysis with groups results for root modulus and distance from root tip relationship for soil grown plants, ***= P<0.001; **=P<0.01; *=P<0.05. PVAF (Percentage Variance Accounted For, or adjusted R^2) for diameter and cultivar relationship

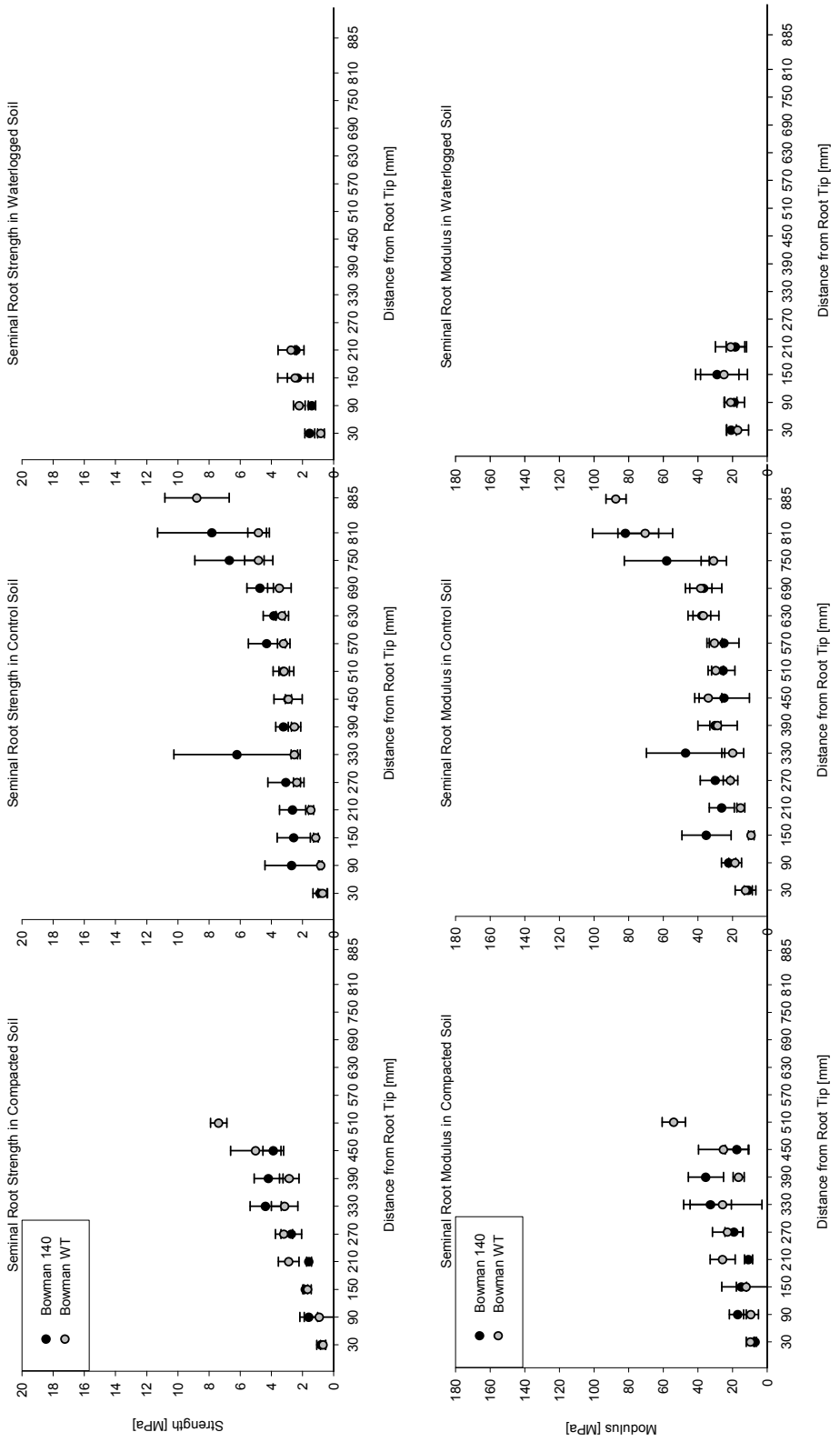

Figure 5-10: Effects of distance from root tip for seminal root biomechanical properties, elasticity and strength (mean ± standard error). Plants were grown in compacted soil (1.4g/cm^3), control soil density (1.2g/cm^3) and normal soil waterlogged for a period of 7 days

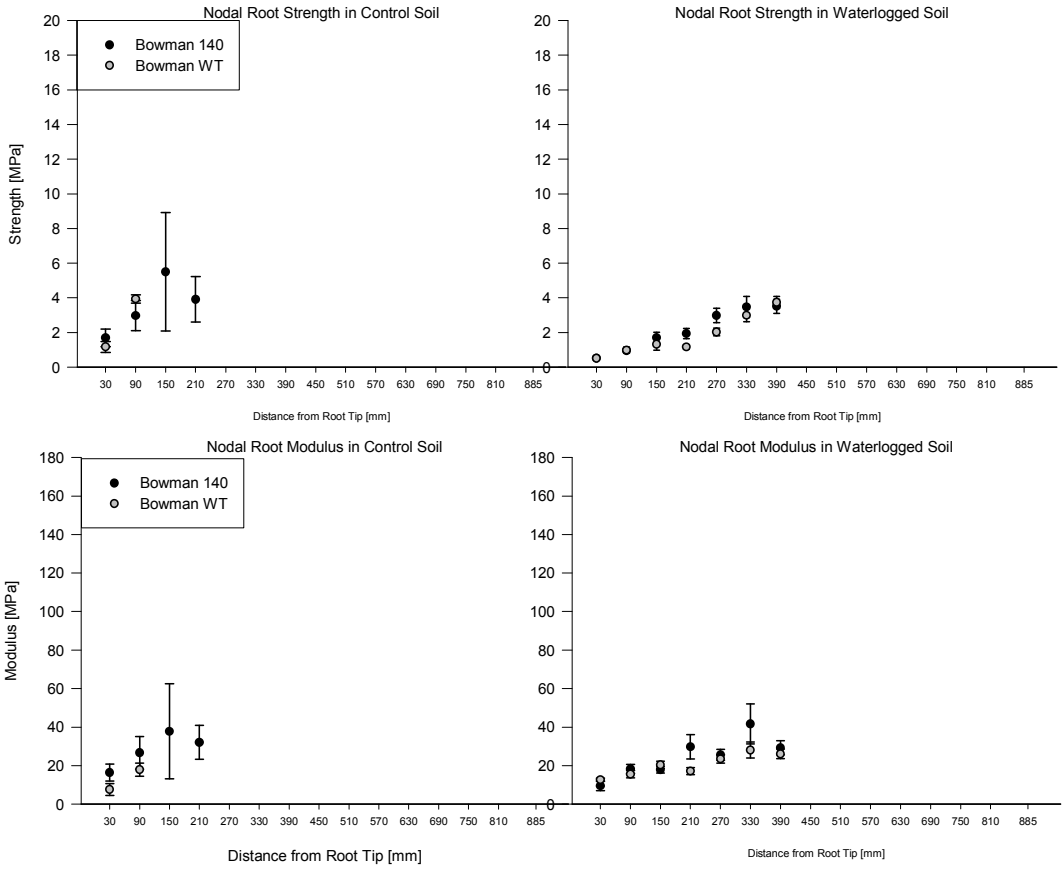

Figure 5-11: Root strength and modulus as a function of distance from root tip (mean ± standard error). Plants were grown in control soil density (1.2g/cm^3) and a normal soil density waterlogged for a period of 7 days

With changes in root strength and stiffness, as a function of distance from root tip, root diameter may be affected by distance along the root influencing this relationship. There was however no significant relationship between root diameter and distance from root tip (Figure 5-12). Data were analysed using ANOVA with root diameter affected by root type, cultivar and treatment ($P<0.001$). The distance from the root tip was not significant ($P=0.093$).

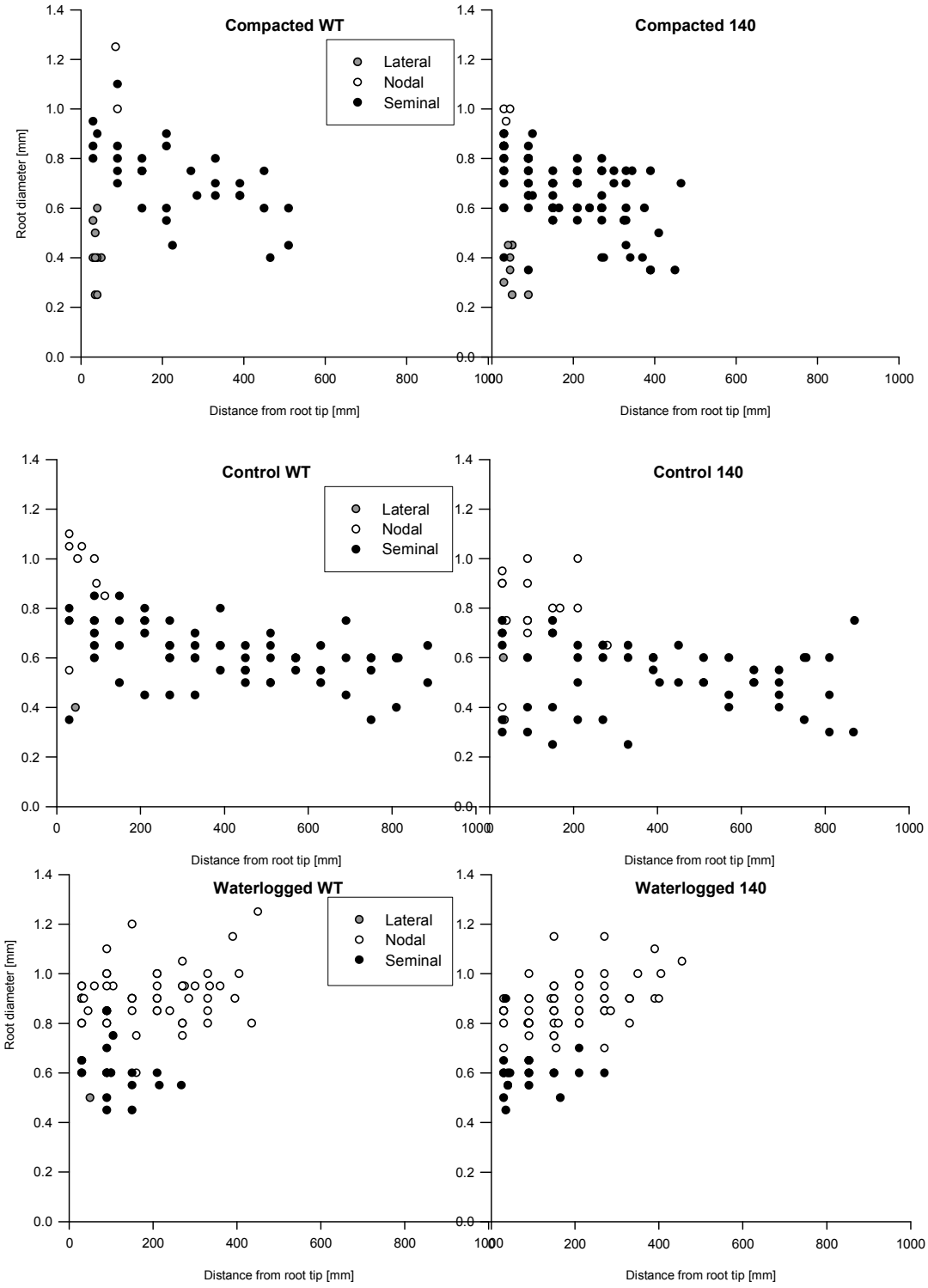

Figure 5-12: Effects of distance from root tip on root diameter for soil grown cultivars

5.3.3.2 Properties of hydroponically grown plant root biomechanics

Similar relationships between root strength and diameter were observed in hydroponically grown roots as were observed in soil. Seminal root strength was significantly affected by diameter ($P<0.001$), but this was not significant for nodal and lateral roots. Only lateral root strength was found to be affected by cultivar ($P<0.01$) (Table 5-9). The results were similar for root modulus, with seminal roots affected by diameter ($P<0.001$), but not nodal or lateral roots. Nodal and lateral roots were significantly different between cultivars ($P<0.05$), unlike seminal roots (Table 5-10).

		P values for differences between cultivar strength and diameter			
Treatment	**Root**	**Diameter**	**Cultivar**	**Diameter and cultivar**	**PVAF [%]**
Hydroponics	Seminal	**<0.001*** **	0.138	0.138	47.8
	Nodal	0.375	0.145	0.261	14.0
	Lateral	0.562	**0.002** **	**0.004** **	35.1

Table 5-9: Significance testing results for root strength and diameter/cultivar relationship for hydroponically grown plants, ***= P<0.001; **=P<0.01; *=P<0.05. PVAF (Percentage Variance Accounted For, or adjusted R^2) for diameter and cultivar relationship

		P values for differences between cultivar modulus and diameter			
Treatment	**Root**	**Diameter**	**Cultivar**	**Diameter and cultivar**	**PVAF [%]**
Hydroponics	Seminal	**<0.001*** **	0.168	0.285	49.9
	Nodal	0.652	**0.019***	**0.025***	19.6
	Lateral	0.079	**0.018***	**0.005** **	34.7

Table 5-10: Significance testing results for root strength and diameter/cultivar relationship for hydroponically grown plants, ***= P<0.001; **=P<0.01; *=P<0.05. PVAF (Percentage Variance Accounted For, or adjusted R^2) for diameter and cultivar relationship

ANOVA highlighted root strength and modulus as significantly different between root types (lateral, seminal and nodal), P<0.001 (Figure 5-13). Strength and modulus of different root types was not significantly affected by cultivar, P=0.117 and P=0.391 respectively.

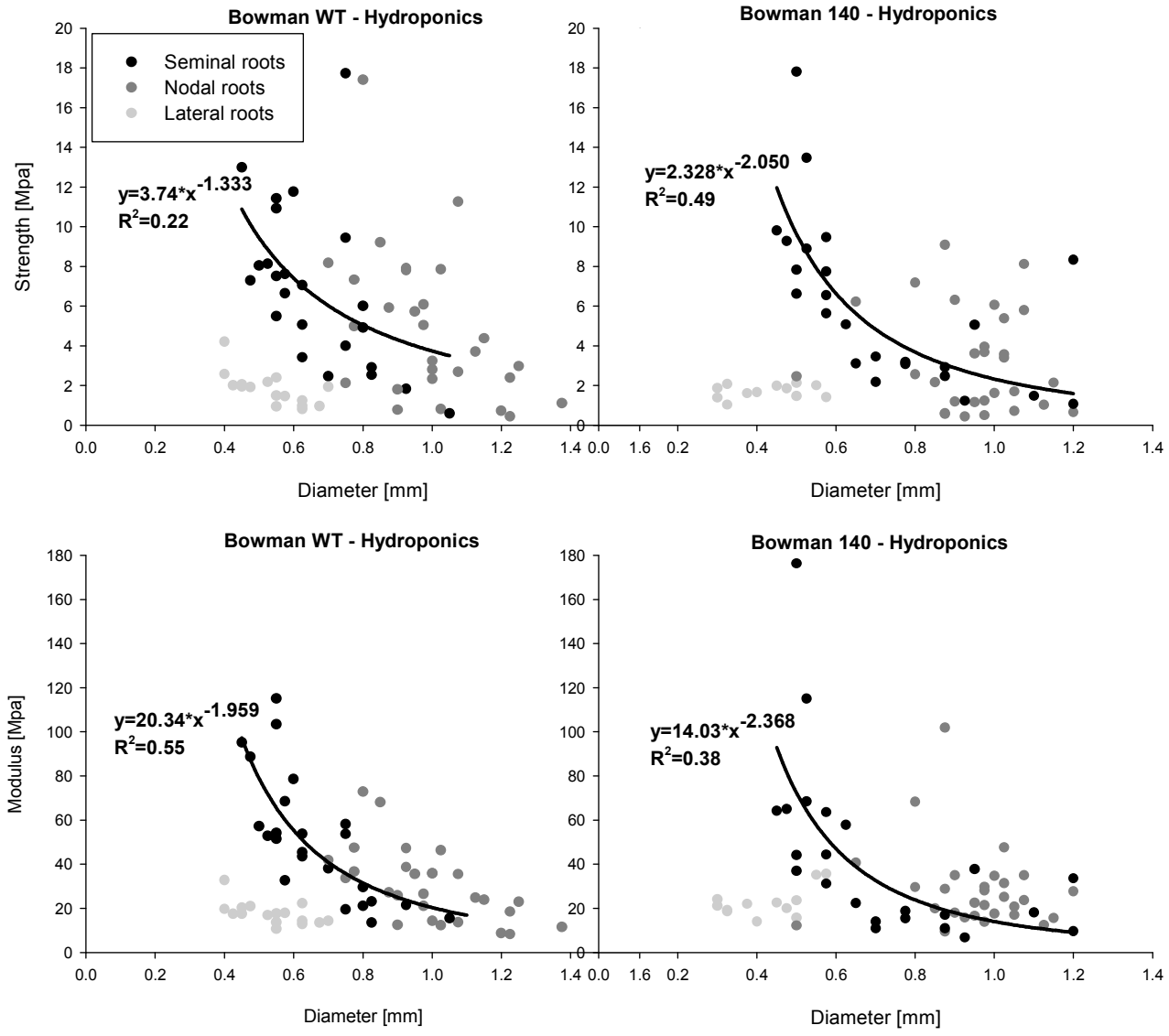

Figure 5-13: Effects of diameter on biomechanical properties, elasticity and strength, of seminal and nodal plant roots grown hydroponically

The strength and modulus of all root types was found to be significantly affected by distance from root tip and age ($P<0.05$) (Table 5-11; Table 5-12). Neither root strength nor modulus was found to be affected by cultivar.

The mean root strength as a function of the distance from root tip was found to increase with increasing distance from the root tip in both nodal and seminal roots (Figure 5-14). Nodal roots were observed to be the longest roots with a maximum root length of 0.57m long, whereas seminal roots were slightly shorter, 0.45m long. Those roots closest to the stem base, furthest from the root tip, were both strongest and also stiffest for both root types measured.

		P values for differences between cultivar root strength and distance from root tip			
Treatment	**Root**	**Distance from root tip**	**Cultivar**	**Distance from root tip and cultivar**	**PVAF [%]**
Hydroponics	*Seminal*	**0.011***	0.725	0.214	25.6
	Nodal	**<0.001*****	0.123	0.894	51.0
	Lateral	-	-	-	-

Table 5-11: Significance testing results for root modulus and distance from root tip relationship for hydroponically grown plants, ***= P<0.001; **=P<0.01; *=P<0.05. PVAF (Percentage Variance Accounted For, or adjusted R^2) for diameter and cultivar relationship

		P values for differences between cultivar root modulus and distance from root tip			
Treatment	**Root**	**Distance from root tip**	**Cultivar**	**Distance from root tip and cultivar**	**PVAF [%]**
Hydroponics	*Seminal*	**0.036***	0.213	0.715	9.7
	Nodal	**0.002****	0.858	0.770	23.3
	Lateral	-	-	-	-

Table 5-12: Significance testing results for root modulus and distance from root tip relationship for hydroponically grown plants, ***= P<0.001; **=P<0.01; *=P<0.05. PVAF (Percentage Variance Accounted For, or adjusted R^2) for diameter and cultivar relationship

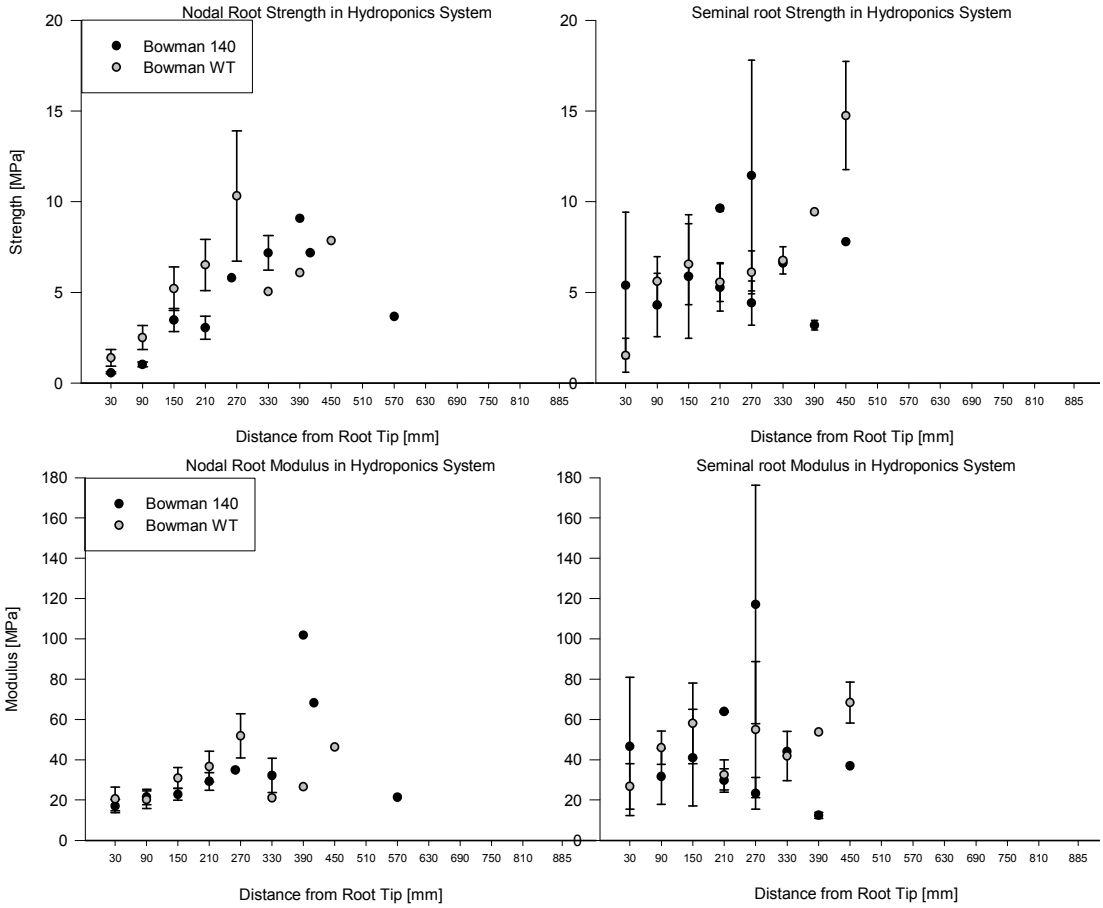

Figure 5-14: Effects of distance from root tip for nodal and seminal root biomechanical properties, elasticity (modulus) and strength, plotted with standard error for plants. Plants were grown hydroponically in an aerated nutrient solution

Hydroponically grown roots were found to have the same relationships as soil grown roots with root type found to have a significant effect on root diameter ($P<0.001$) following ANOVA testing. In contrast to soil grown plants, the diameter of roots of hydroponically grown plants were significantly affected by distance from root tip ($P<0.05$) (Figure 5-15).

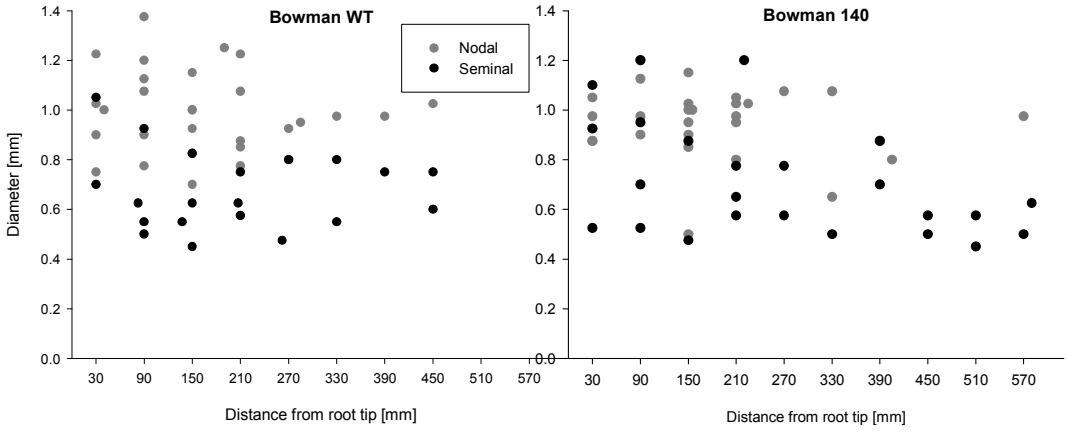

Figure 5-15: Effects of distance from root tip on root diameter for hydroponically grown cultivars

5.4 Discussion

When investigating differences between cultivars based on specific traits or genetic mutations it is important to ensure that pleiotropy is not responsible for observed differences between plants. Pleiotropic effects are other phenotypic changes associated with a mutation other than the trait being assessed e.g. another phenotypic change other than lignin down regulation. Within this study biomass data showed no significant differences between cultivars when plants were grown in all soil treatments. However, when plants were grown hydroponically, differences in biomass were observed and found to be cultivar dependant. One potential explanation for this observation may be the role in which lignin plays in the cell wall. Cell wall hydrophobicity is influenced by the deposition of lignin polymers that improve compressive strength of water transport vessels (Campbell and Sederoff, 1996). Lignin also increases xylem resistance to compression, minimising collapse due to high suction (Niklas, 1985), so if these vessels

are impaired as a result of lignin down regulation, plants would function more poorly, affecting biomass and yield.

Lignin is a key structural compound within the root cell wall with root submersion shown to increase cell wall thickening, through deposition of cellulose, lignin and/or suberin, and altering aerenchyma (Baruch and Merida, 1995; Silva et al., 2003). Aerenchyma are air filled channels within the root allowing gas exchange between root and shoot which when damaged have been shown to reduce grain yield and ear production (Dickin and Wright, 2008). With lignin playing such a key role in plants subjected to flooding, plant growth of those containing reduced lignin may be impacted as shown in this study after a flooding treatment of only 7 days. With climate change predicting increased rainfall and flooding, such a response in yield of lignin reduced cultivars should be investigated further.

Results of root modulus and strength show large variations within all soil treatments and also between cultivars. It has been previously suggested that this results from biological variation, possibly linked to variation in the angle of fibres within the root structure (Kőhler, 2000). Relationships between root strength and diameter were not found to be affected by the different cultivars used in this study. Authors have previously suggested that cellulose is the key structural component responsible for root strength (Genet et al., 2005; Tosi, 2007) with this study further agreeing with this hypothesis. For plant stems and shoots, however, this hypothesis is not supported. Wang et al. (2006) reported that it was more likely that in *Triticum aestivum*, cellulose was responsible for driving stem strength due to the strong fibrillar network. With cellulose content responsible for root strength, the ratio of lignin to cellulose has been suggested as a factor influencing root

stiffness (Hathaway and Penny, 1975). Cell wall thickening, through lignin deposition, has also been hypothesised to increase plant root stiffness (Hamza et al., 2006). As water-logging increases cell wall thickness (Da Silva et al, 2003; Baruch and Mérida, 1995) plants with reduced lignin should therefore have reduced stiffness resulting from reduced lignin deposition.

The results highlighted changes in root strength and modulus in response to increasing distance from the stem base, showing an age effect. Age effects have also been shown in previous studies with strength decreasing as a function of the distance from the base of the stem (Easson et al., 1995). Zeier (1999) reported that increases in root strength within different root regions were found to correlate with changes in lignin deposition. Results agreed with the findings of Eason et al. (1995). There are potential applications of these findings into root architecture models to predict changes in soil reinforcement with depth. Lignin down-regulation was not shown to affect root strength or modulus between mutants and wild type cultivars except in nodal roots subjected to water logging or grown hydroponically. Nodal root structural composition differs when compared to seminal root composition. Seminal roots have central and multiple peripheral xylem tracheary elements (XTE), whilst nodal roots have a central pith surrounded by both inner and peripheral XTE (Figure 5-16) (Watt et al., 2008). Such significant changes in root structure, between different root types, may provide some explanation into observed differences in root bio-mechanics due to changes in cell wall composition.

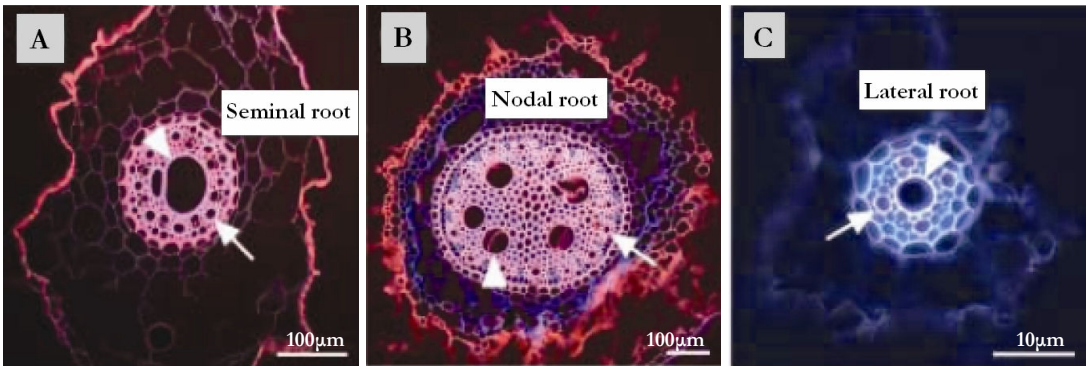

Figure 5-16: Structure of different root types of barley. Arrowheads indicate central or inner XTE with arrows indicating peripheral XTE (Source: Watt and McCully, 2008)

Significant differences in the relationship between root diameter and seminal root modulus were observed between cultivars for roots grown in waterlogged soil. Within this study most of the significant results were achieved through plants grown in the hydroponics setup. This system, although used extensively in previous studies, must be viewed as an idealised condition that exerts limited environmental stress on roots. It has been shown in this chapter that root bio-mechanics change as a result of growth in soil and also environmental stresses, highlighting the necessity for root studies to be performed using plants grown in soil. Growth of plants in other media provides good fundamental results. However, it may not be possible to transfer such results to larger natural scales due to possible changes associated with abiotic stresses on roots and thigmomorphogenesis.

5.5 Conclusions

This work has highlighted potential changes in root bio-mechanics in response to alteration of cell wall composition. Plants were only grown for a short period of time and

it was not possible to perform soil shear tests to compare root bio-mechanics to derived reinforcement. Such information would provide invaluable data for reinforcement model validation. Root strength was found to increase as a function of root age and distance from root tip however this may vary over a growing season with roots dying, potentially reducing in strength. In some tree species this has been proven not to be the case with root strength increasing (Watson et al., 1997). Whether this occurs in fibrous root systems is not clear with any new data improving long term predictions of soil reinforcement.

Research into the effects that root structure and other abiotic factors have on root biomechanics is critical in generating reliable predictions of soil reinforcement and stability. Root structure has been shown to affect biomechanics, however, more work is now required to understand in greater detail root structures of other plant species and the associated biomechanics. With the changing face of the agriculture industry and the development of crops with altered tissue composition biomechanical effects must be assessed. Were such research not performed there is an inherent risk that such affects may result in increased mass wasting and erosion of soils. Greater biomechanical understanding of root behaviour is key in better informing engineers, land managers and those managing fluvial environments of other, previously unknown, contributory factors to soil reinforcement.

BLANK PAGE

6. Measurement of soil and root displacement under direct shear using Particle Image Velocimetry

6.1 Introduction

Previous chapters have highlighted the effect roots have on reinforcing soil. Reinforcement has already been shown to increase with increasing planting density in both field trials and a glasshouse experiment. Reinforcement was derived from increasing numbers of roots crossing the shear plane, with potential links to changes in root diameter. However, the contribution from roots to soil strength was found to be highly variable and the experiments gave relatively little insight into understanding root failure mechanisms during direct shear. How roots fail and interact with soil undergoing shear are key in quantifying the contributions roots make to reinforcement (Hamza et al., 2007).

With traditional shear tests, it is impossible to isolate processes that could contribute to variability. One driver will be the mechanisms by which roots fail within soil. In research by Mickovski et al. (2007), root pull-out mechanisms were investigated by visualising roots through Perspex boxes filled with soil. It should be possible to adapt shear boxes to visualise the movement of soil and roots under increasing shear displacements.

This chapter will investigate root movement and strain localisation of long and short lengths of roots during direct shear testing. Root length has been shown to affect the failure mechanism, with shorter roots having a smaller contact area with the soil and thus a lower frictional pull-out resistance and therefore increasing likelihood of pull-out failure as described by Abe and Ziemer (1991). Barley roots will be used in this study and varied by age and type (seminal or nodal) to examine any effects they may have on strain localisation and failure mechanisms. Another variable is root orientation, as it has long been established as a factor in soil reinforcement and has been shown to affect stress localisation (Gray and Ohashi, 1983). Roots in this study will be orientated in tension (45^{o} to the shear plane), compression (45^{o} to the shear plane) and perpendicular to the shear plane to further investigate displacement under direct shear.

Root antecedent conditions prior to failure will also be investigated to discover pre-failure conditions in which roots may contribute to reinforcement prior to ultimate failure. Roots will only contribute to reinforcement if the bond between root and soil is strong enough to transmit stress down the root length (Fan and Su, 2008). It is widely acknowledged that roots fail during shear in one of two key ways, through breakage or pull-out failure. Observations and comments on factors influencing the failure of roots in soil have been performed previously. A variety of factors, such as various soil and root characteristics, have been highlighted as causing the lodging of cereal crops, with lodging described as the 'displacement from their vertical stance' of the stem (Berry et al., 2004). More recently x-ray computed tomography has been used to visualise, in 3D, root failure associated with lodging of cereal crops (Mooney et al., 2006). The technique has been shown to allow visualisation of the processes involved in root lodging well but only provide a snap shot at the moment of image capture. To date there are currently no

studies that have directly visualised, in real time, roots failing in soil. Abe and Ziemer (1991) performed studies using *Pinus contorta* (Dougl. var. *contorta*), a woody rooted species, in sand summarising that roots initially stretched before failing through pull-out with reinforcement increasing during pull-out failure. More recently, studies have investigated the effects of root biomechanical and architectural properties on pull-out resistance of root analogues in sand (Mickovski et al., 2007; Stokes and Mattheck, 1996). The key weakness in these recent studies has been the use of root analogues and sand as opposed to real roots and soil.

Abe and Ziemer (1991) used video recording equipment to view how roots changed position during shear. Advances have since been made allowing use of high resolution time lapse images to be analysed through tracking of variations in brightness of specific areas of interest. This technique is called Particle Image Velocimetry (PIV). PIV originated in the field of fluid dynamics allowing '*accurate, quantitative measurement of fluid velocity vectors at a very large number of points simultaneously'* (Adrian, 1991). PIV may simply be described as an image analysis method for estimating displacement of patches of texture within a defined area between successive images. More recently the technique has been adopted for geotechnical engineering applications i.e. GeoPIV. Prior to GeoPIV development, planar deformation investigations required the use of artificial targets, such as coloured beads (White et al., 2003). With GeoPIV the need for the use of specific targets was overcome resulting in increased accuracy and precision (White et al., 2003).

Plants roots have been analysed during tensile testing with PIV to characterise root mechanical properties (Hamza et al., 2006). PIV has also been used to investigate deformation and stress on roots during pull-out failure (Mickovski et al., 2007; Bransby

et al., 2006) and also during centrifuge testing of root reinforced slopes (Sonnenberg et al., 2007). PIV has been shown to be a useful tool when examining geotechnical problems. No work to date, however, has used the technique to look at root interactions with soil during direct shear testing.

6.2 Experimental Methods

Direct shear tests were conducted on soils containing segments of real roots. The approach was extended from Mickovski et al. (2007), who used a narrow box with roots growing along a Perspex front face to visualise pull-out mechanisms. In my experiment the box had an upper and lower section, so that a direct shear displacement could be controlled by displacing the upper section relative to the bottom. The box allowed for homogeneous packing of soil, control of matric potential and careful placing of root segments. Each side of the boxes was transparent to allow for photographic observation of root and soil movement during shear.

6.2.1 Shear boxes and testing

6.2.1.1 Shear boxes

The design of the shear box is illustrated in Figure 6-1. A Perspex front face allowed for visualisation of roots and soil during shear. They were constructed in two sections; upper sections were 300mm x 50mm x 50mm in size with lower sections 300mm x 50mm x 150mm (Figure 6-1). To ensure minimal friction whilst direct shear tests were performed, the shearing surfaces of the boxes were sanded with P120 and P800 wet sand paper and final polishing using Perspex Polish No. 2. A thin coating of silicone grease

(SGM494, RS 283-404) was applied to the shearing surfaces of the box prior to soil packing to ensure an airtight seal between upper and lower sections, critical for soil moisture equilibration prior to testing. The grease also acted as a lubricant to reduce friction and as a barrier to prevent the ingress of moisture/water during equilibration prior to shearing.

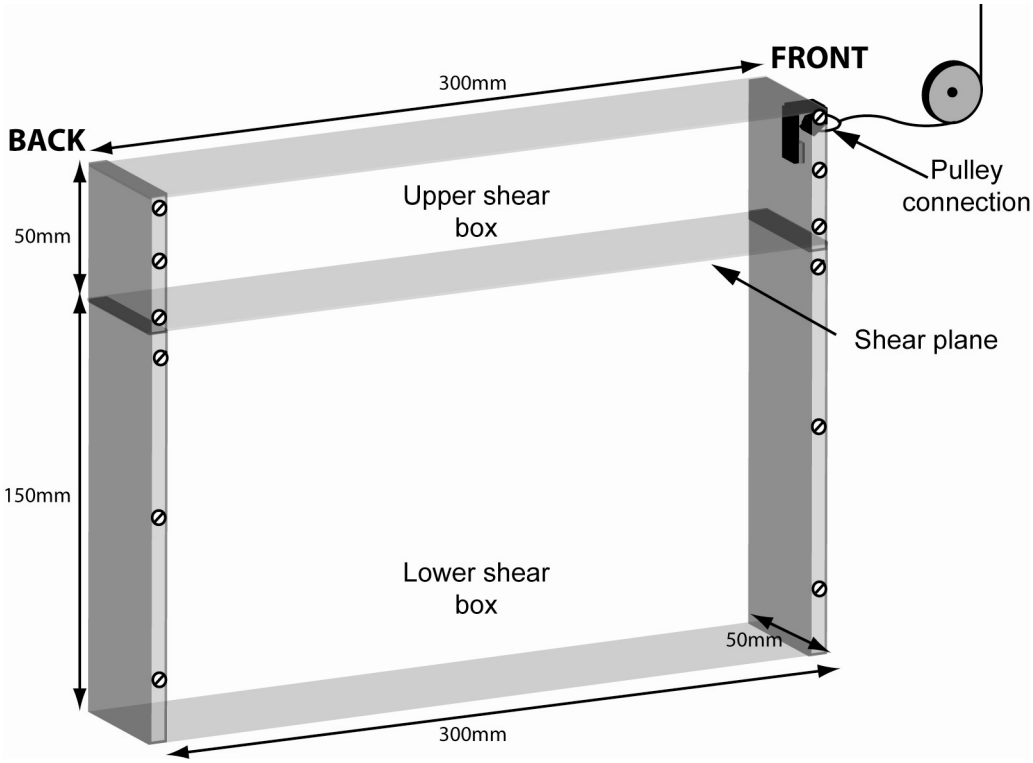

Figure 6-1: Shear box used for PIV shear testing

The Perspex surfaces were lined with acetate sheets to reduce the risk of scratching when the soil was packed. Scratching of the Perspex may result in inaccurate PIV analysis due to the software registering scratch texture as opposed to root and soil texture. Before packing, two braces per box side were attached to the exterior; one 75% down the depth of the box and a second at the shear plane (Figure 6-2:). Braces were attached for three key reasons:

1. packing could cause the walls of the box to expand, thus increasing box volume with a resulting decrease in soil density;
2. a good seal was required at the interface between upper and lower sections of the shear assembly for soil moisture equilibration; and
3. braces enabled easy transportation of shear boxes once packed, so the risk of possible pre-shearing of the soil was reduced.

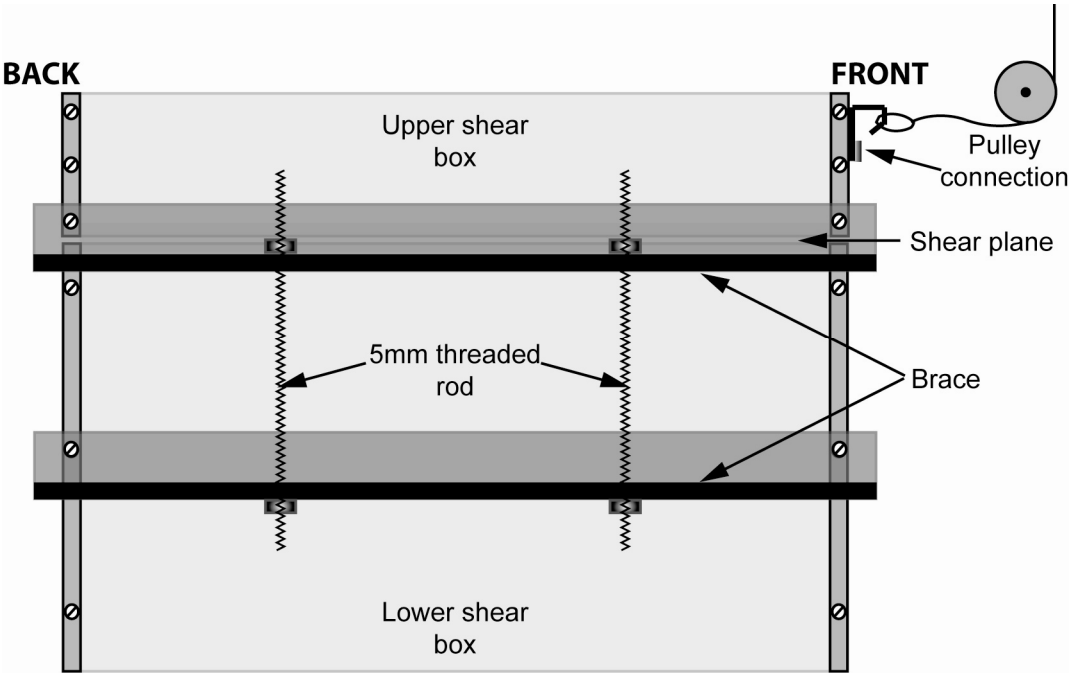

Figure 6-2: Shear box assembly used for packing to retain shear box integrity. The braces were removed prior to shear testing

6.2.1.2 Shear box soil packing

Bullion field soil (characterised in section 3.2.1) used throughout this thesis was used again within this study. After sampling from the field, soil was air-dried to approximately 0.2g/cm^3 water content and then sieved to 2mm. As mentioned previously, shear boxes were lined with acetate sheets (section 6.2.1.1), and packing was performed in 10 layers, 20 mm thick, to obtain a uniform soil density. Due to the potential of lower shear

strength interfaces developing between compacted layers, soil was roughened at the interface between layers before packing of the next layer. The shear box volume was 2758 cm^3 and required 3309.6 g of dry soil to achieve a dry bulk density of 1.2 g/cm^3. A soil density of 1.2 g/cm^3 was chosen as this is often assumed to be similar to soil densities found in an agricultural soil with a similar texture that does not suffer from compaction. Soil moisture content was measured prior to packing and the total mass of soil was calculated to achieve the required dry density (Table 6-1). Packing was performed by volume, as opposed to energy, and the soil was fully saturated from the base for 12 hours following completion of the compaction process.

PIV box code	Box volume [cm^3]	Gravimetric Water Content at Packing [g/cm^3]	Mass soil packed [g]	Wet soil density [g/cm^3]	Dry soil density [g/cm^3]	Soil suction when sheared [kPa]
PIV 3	2758	0.05	3486.9	1.26	1.2	4.8
PIV 4	2758	0.05	3485.4	1.26	1.2	5.1
PIV 6	2758	0.05	3485.8	1.26	1.2	4.7
PIV 7	2758	0.05	3486.1	1.26	1.2	4.8
PIV 8	2758	0.10	3665.3	1.33	1.2	4.6
PIV 9	2758	0.10	3665.3	1.33	1.2	4.7

Table 6-1: PIV shear box soil properties

Prior to shear testing, the soil was equilibrated to field capacity, by first fully saturating the soil in the box from the bottom for 24 hours before draining to 5 kPa suction using a silica flour sand table until drainage ceased (24 hrs). Boxes were removed from the sand table prior to shearing and miniature tensiometers (SWT4, Delta-T, Cambridge, United Kingdom) were inserted in the soil at the top surface to confirm the correct matric

suction conditions had been reached (Table 6-1**).** Boxes contained a uniformly packed soil on which root inclusions were placed prior to shear testing.

6.2.1.3 Plant growth and root inclusions

Barley plants were grown in a growth room environment in 1 metre long PVC tubes packed with Bullion field soil to a dry density of 1.2 g/cm^3. A full description of the packing process and growth room conditions may be found in Chapter 5. Plants were grown for a period of 3 weeks and washed out of the soil 24 hours prior to performing the first group of PIV shear tests incorporating root segments. Further details on root washing used to extract the roots from soil may be found in Section 3.2.4.

Roots used in this study were both old and young roots with age determined as a function of the distance from the root tip. Root segments collected at the distal region from the stem were young roots with old root segments those collected at the base of the plant stem. Two different root types were used, seminal and nodal. Chapter 5 has previously highlighted the changing effects of age and root type on root biomechanics, highlighting potential for changes in the mode of root failure.

To ensure that soil packed within the shear boxes was not stressed during the addition of root inclusions, 'F' clamps were placed to hold top and bottom together securely. Top and bottom exposed soil surfaces were also covered with wooden shims to enable shear boxes to be laid horizontally for clamp removal and addition of root segments (Figure 6-3 (A)). Root inclusions were placed on the soil surface by first disassembling shear boxes through the removal of the Perspex face (Figure 6-3 (B)) and acetate sheeting (Figure 6-3 (C)). The Perspex panels were then cleaned thoroughly with a soft cloth and a

thin smear of silicon applied to the shear surfaces before being re-attached to the soil block (Figure 6-3 (D)). This same procedure was repeated for the opposite side. After re-orientation back to the vertical position, clamps were removed and the box was transferred to the shear assembly. During the transfer process, the bottom shim was left in place and only removed once the shear boxes were installed in the shear assembly. This ensured that the soil block could not slip down the shear boxes during transfer.

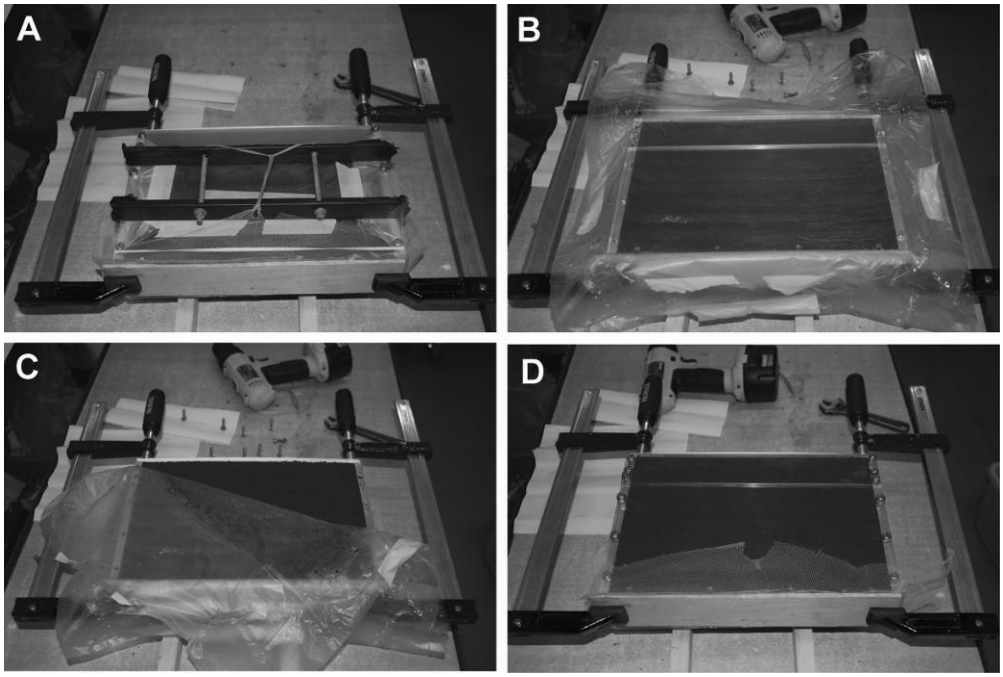

Figure 6-3: Preparation of shear boxes for PIV testing. A – Box clamped with shims placed top and bottom to contain soil when laying flat; B – Brackets removed holding top and bottom of box together; C – Plastic sheeting removed, used to reduce scratching on Perspex during soil packing; D – Perspex reinstalled onto soil surface with box ready for shearing

Root inclusions were placed on the soil surface and orientated in three directions: (1) Compression at 45º from vertical; (2) Vertical; or (3) Tension at 45º from vertical (Figure 6-4). There was only one root orientation direction on each shear box side. As shear force was not recorded, it was possible to have different orientations on the opposing Perspex surfaces, thus allowing different root orientations to be investigated simultaneously photographically. The interaction between roots between the Perspex

surfaces was assumed to be negligible because the typical diameter was 1/20th of the box width.

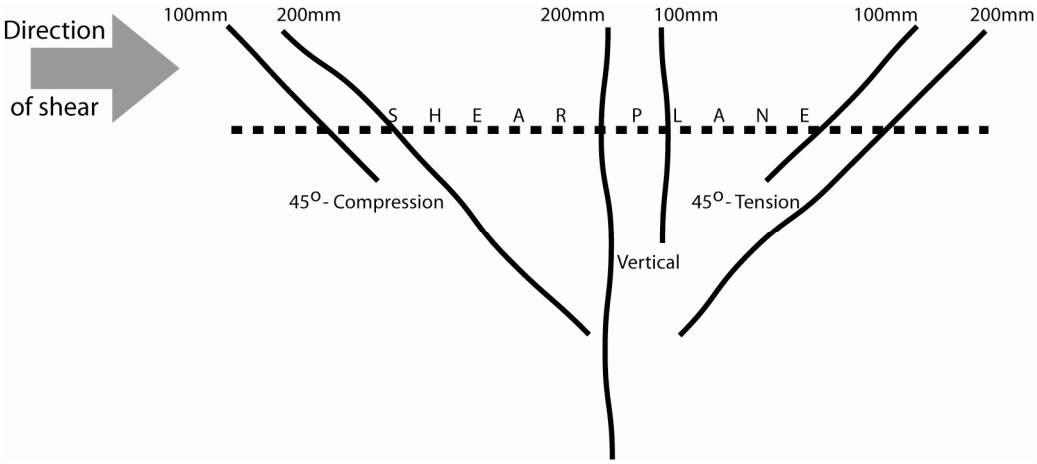

Figure 6-4: Root orientations used in shear tests for assessing failure mechanisms

6.2.1.4 Shear testing

Boxes were sheared using a mechanical test frame, Instron 5544**,** connected to the top section of the shear assembly. Four strands of plaited wire were connected between the test frame crosshead and the shear box via a pulley (Figure 6-5). The wire had a stiffness several orders of magnitude greater than the shear box assembly, so the amount of strain generated in the wire during shear tests was negligible. Both load and displacement were measured, although load data were not used because of testing artefacts described later. The shear rate was 1 mm min-1 and controlled through vertical movement of the crosshead connected to the wire assembly.

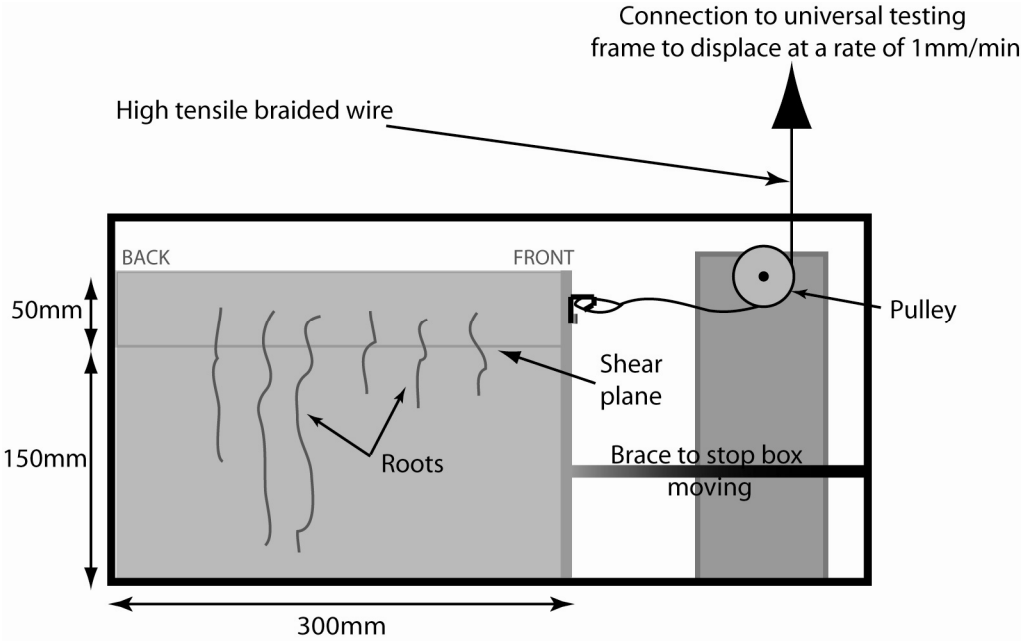

Figure 6-5: Shear box assembly for visualisation of root failure during direct shear testing using PIV

Soil dilation may have affected friction between roots and soil. To minimise soil dilation during shear testing a Perspex lid was placed on top of the box and located within runners connected to the main shear assembly frame. The lid minimised potential vertical pull-out of roots, caused by dilation, and also ensured the upper shear box section remained aligned to the bottom section. Lateral movement of the top section may have caused the transfer of stress to roots other than in the primary horizontal shear direction. Runners were thinly coated with silicon grease to reduce friction.

6.2.2 Image capture

Images were captured using two Nikon D300 digital cameras fitted with Nikkor 60 mm macro lenses. Tripods were placed on either side of the shear box, with cameras mounted on each so that they were perpendicular to the shear assembly to reduce

potential image errors and necessity for photogrammetric correction. Reflection was minimised through the extinction of all external light from the test laboratory. Two Bowens 500 studio flashes (BW4805) with Softlite diffusers (BW1899) were synchronised to the cameras using Elastolite wireless radio transmitters. Studio flashes were setup to provide light from an approximate angle of 45° so that reflection from box sides was minimised (Figure 6-6). The camera bodies and tripods were covered in non-reflective black card, with non-reflective material also draped over the camera to further reduce camera reflection in images. Prior to each shear test, a calibration grid containing 5 mm x 5 mm squares, was placed over the region being photographed in order to spatially calibrate images. All focusing was performed manually before the start of the test.

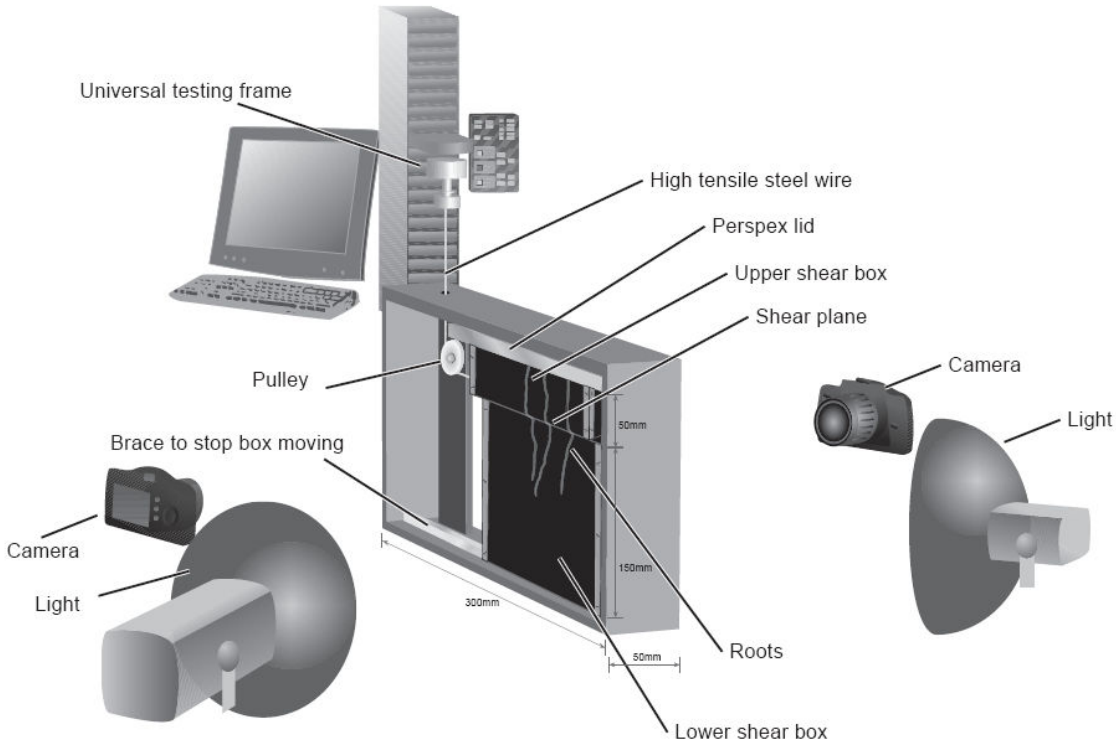

Figure 6-6: PIV shear testing assembly for image capture

During early testing one of the synchronising wireless flash units was faulty, causing inconsistent exposure on some photographs. As a result, hard wiring between flash and camera was used in subsequent tests. Due to the necessity for clear and correctly exposed

images, polarising filters were also removed for the later tests. Filters were found to be manufactured by different companies resulting in different levels of polarisation between camera and lens packages. Following removal of the polarising filters it was possible to have identical image capture parameters for both Nikon D300 cameras (Table 6-2).

Software Tab	Camera parameter	Setting
EXPOSURE 1	Exposure mode	Manual
	Shutter speed	1/100sec
	Aperture	f/20
	Exposure compensation	0 ev
EXPOSURE 2	ISO	200
	White balance	Flash
STORAGE	Format	JPEG (8 bit)
	Quality	Fine
	JPEG compensation	Size priority
	Image size	Large (4288 x 2848)
IMAGE PROCESSING	Picture control	Standard
	Colour	sRGB
	Active D lighting	Off
	Long exposure noise reduction	Off
	High ISO noise reduction	On (normal)

Table 6-2: Camera control pro software settings for images captured for PIV analysis

Cameras were connected to a desktop computer using Nikon Capture Control Pro software enabling time lapse photography. Images were captured every 30 seconds and stored on the computer for later PIV analysis. Test images were collected prior to shear testing to verify focus, to confirm correct exposure settings and to ensure that there were no reflections from the camera and flashlight setups onto shear assemblies. It was

essential to minimise reflection wherever possible due to the potential for error during post image analysis using the PIV software.

6.2.3 Particle image velocimetry analysis

Software has been developed for use specifically within the geotechnical research environment, GeoPIV (White et al. 2003), with three key processes involved: pre-processing, PIV analysis using Matlab software and post processing of output files by the user. Pre-processing requires three files consisting of:

- a launcher file - providing information on images and other variables required for analysis of each run
- a mesh file - defining the area size and co-ordinates to be investigated
- a set of images – a group of time-lapse images to be analysed

GeoPIV software runs within Matlab producing ASCII files containing information on images analysed and the co-ordinates of original and subsequent new patch location on successive images. These files require calibration in order to quantify movement of patches between images. A flow chart of the processes involved is shown (Figure 6-7).

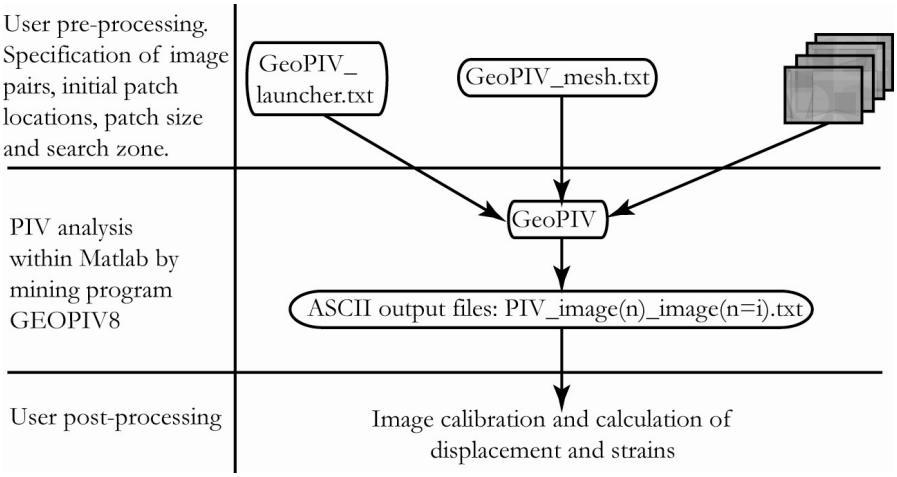

Figure 6-7: Particle Image Velocimetry analysis sequence (White and Take, 2002)

If necessary, cropping was performed using Faststone Image Viewer (*Freeware software [http://www.faststone.org]*), allowing batch cropping of consecutive images to a specified region of the image. Following image preparation, GeoPIV was run within Matlab© software. A full description on how to perform PIV analysis may be found in White and Take (2002). The software analysed changes between images through examining movements of patches superimposed onto images. The programme records the original x, y co-ordinate (u_0 and v_0) of the patch in pixels and records the location of the same patch on the next image in the sequence being analysed (u_f and v_f) (White et al., 2003). The locations of these patches are compared between images by an autocorrelation function to track movement. For analysis of root movement, patches were placed manually along the root length using the *mousemeshrandom* command. The patch size was 20 x 20 pixels, selected since Sonnenberg (2008) found a large impact of smaller patch sizes on accuracy (Sonnenberg, 2008). Patches were placed along the root dependant on root sinuosity with patches on bends to ensure an imaginary straight line between patches could be superimposed over the root (Figure 6-8). Patches were sparsely distributed along the root length in order to best calculate strain directly from the data.

Patches closer together may have resulted in greater error, reducing observable trends in strain along the root length.

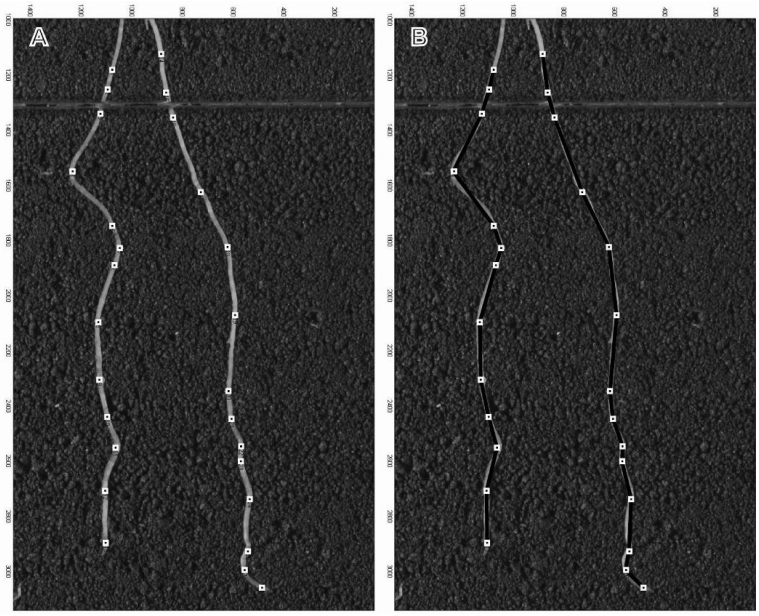

Figure 6-8: Example of patch overlay on roots for particle image velocimetry analysis, A= patch location; B= example simulated root location based on patch location

When assessing soil movement and shear zone development during shear, a grid was placed over the soil surface with 2 strips containing 50 x 50 pixel patches at opposite ends of the shear assembly: the front strip was located towards the pulley. Strips were orientated vertically through the shear plane and encompassed the whole depth of image captured. Patch movement was recorded and lateral displacement (Δu) calculated using**:**

$$\Delta u = \frac{\left(u_f - u_o\right)}{px}$$

where px = scale factor calibration value (pixels/mm), u_f= original x co-ordinate and u_o = x co-ordinate of patch in next image. Vertical patch (Δv) movement was calculated using:

$$\Delta v = \frac{\left(v_f - v_o\right)}{px}$$

where y = scale factor calibration value (pixels/mm), v_f= original y co-ordinate and v_o = co-ordinate of patch in next image.

Strain (ε) was calculated from PIV image analysis using movement in both x and y recorded between patches:

$$n^1 = \sqrt{(u_f - u_o)^2 + (v_f - v_o)^2}$$

$$n^2 = \sqrt{(u_f' - u_o')^2 + (v_f' - v_o')^2}$$

where n_1 = original distance between patches; n_2=distance between patches on image 2 following displacement. Strain (ε) is then calculated as:

$$\varepsilon = \frac{n^2 - n^1}{n^1} x100$$

y is the vertical coordinate measured from the top of the image. Following PIV analysis, vector plots were created to visualise root and soil movement during shearing.

6.2.4 Root visualisation recording

Following shear testing, images were viewed using Image J software to enable successive images from time-lapse photographs to be viewed. Notes were recorded on root movement during shear, failure mode of the root and also any evidence of failure in the soil, e.g. cracking. Using initial shear test images, containing a 5 mm x 5 mm calibration grid, it was possible to use the Image J measurement tool to record shear plane depth and thickness. The tool measured the number of pixels between two points enabling simple calculation of the number of pixels per mm to be performed. This method was also used to calculate displacement rates over consecutive images captured for each test.

6.3 Results

6.3.1 Soil responses to direct shear

Vector plots produced by GeoPIV software showed a complex movement of soil at the commencement of tests (Figure 6-9 and Figure 6-10). Following initiation of the tests, soil can be seen to initially dilate at the rear of the box (right hand side of plots) and also move laterally, both above and below the shear plane (Figure 6-9 and Figure 6-10). At subsequent displacements no further movement of soil patches below the shear plane was observed (Figure 6-9 (ii and iii)). This observation was again seen in another fallow shear test where vector plots show soil dilating and displacing at the rear of the box after test initiation (Figure 6-10 (i)). Unlike the previous fallow test, further soil movement was observed below the shear plane with a second failure plane developing at subsequent displacements (Figure 6-10 (ii; iii)).

Soil displacement was measured at the front and the rear of the image sequences to ensure displacement rates were the same. Initial discontinuity was observed, as seen in vector plots, however displacement rates were found to be the same at both the front and rear of the boxes following the start of tests (Figure 6-11). Displacement rates may have been affected initially because of the large compressibility of the loosely compacted soil.

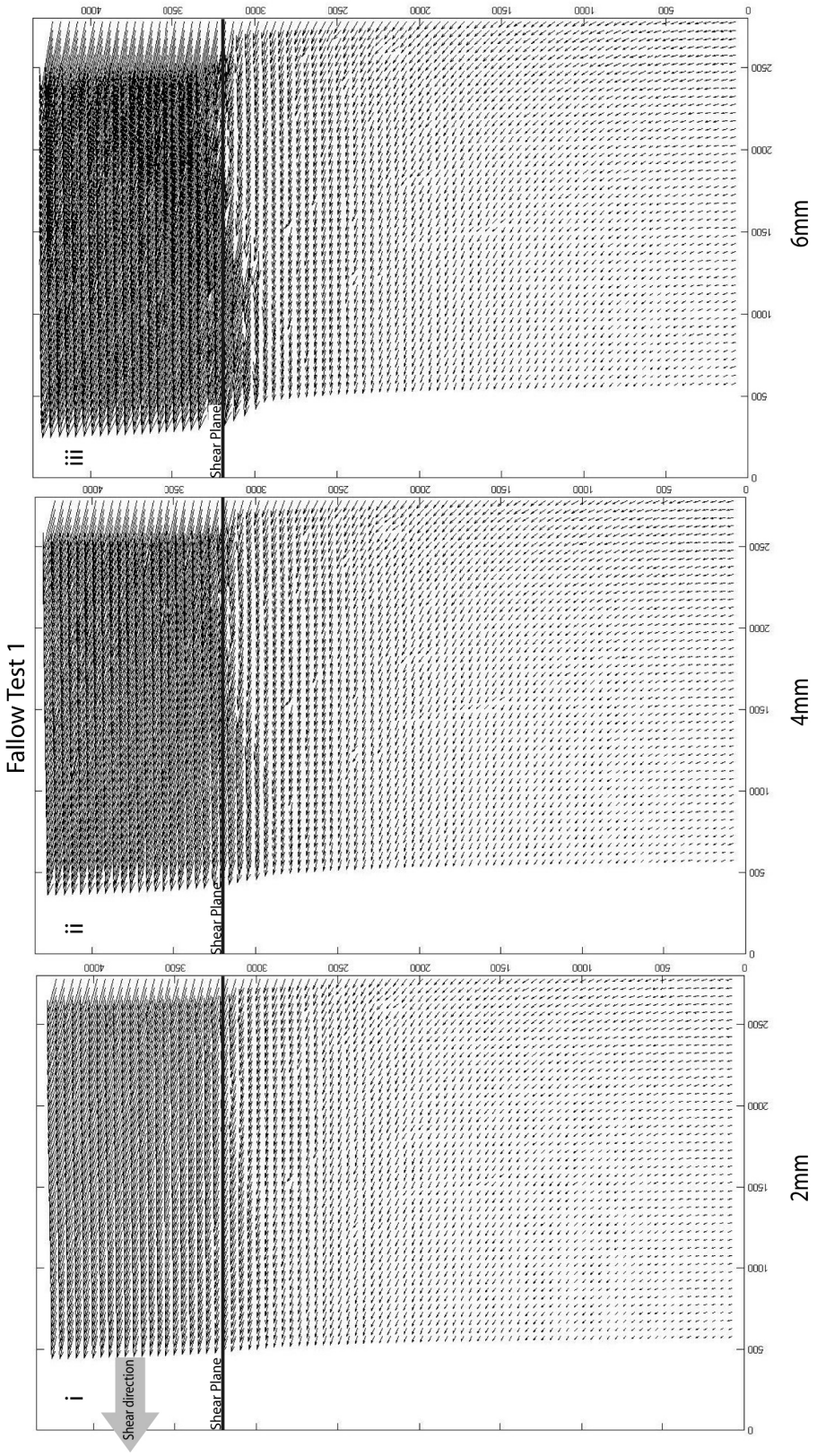

Figure 6-9: Soil displacement vector plots for fallow shear box test 1: **i** = 2mm displacement; **ii** = 4mm displacement; **iii** = 6mm displacement

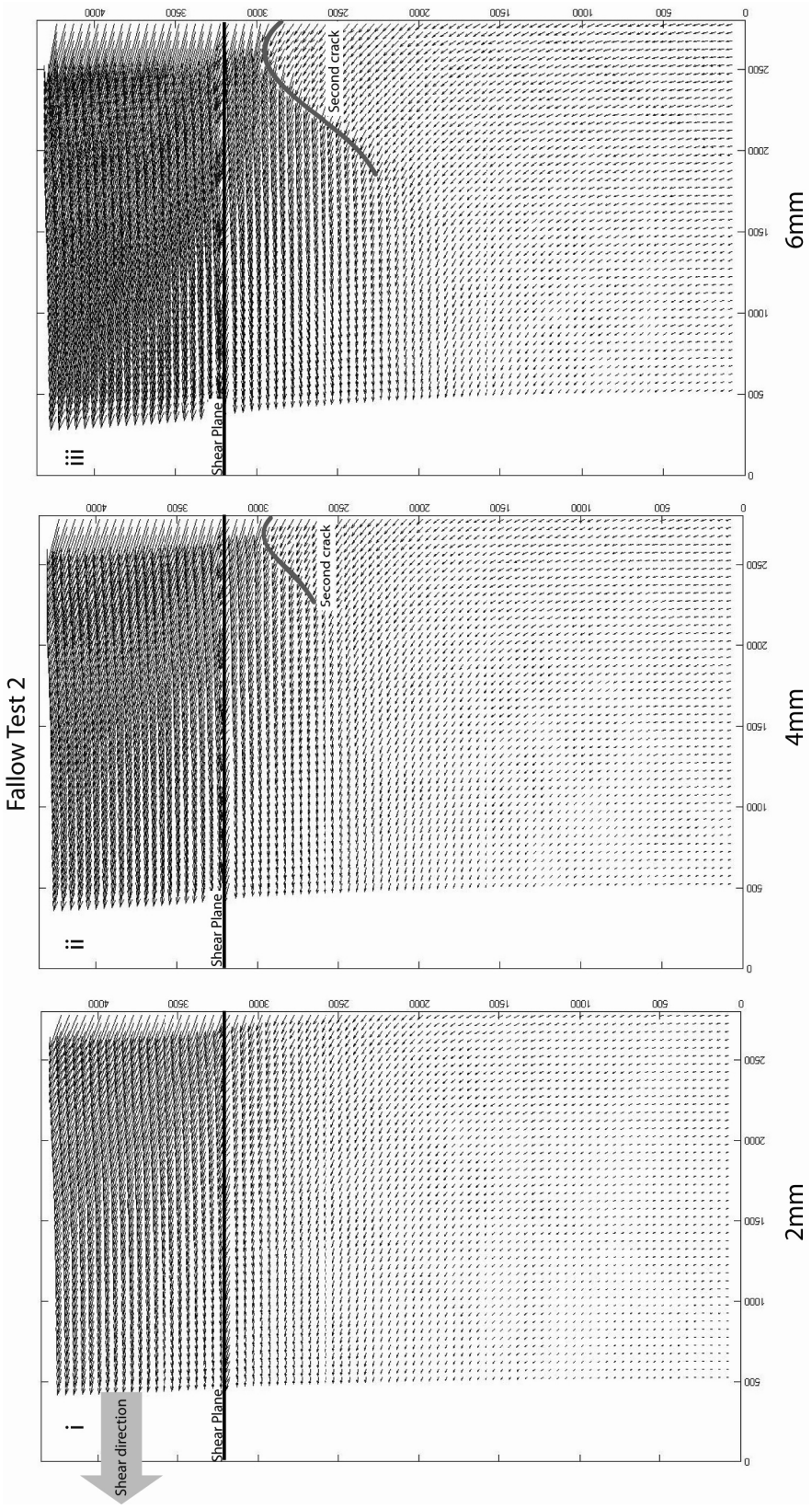

Figure 6-10: PIV vector plots for fallow shear box test 2: **i** = 2mm displacement; **ii** = 4mm displacement; **iii** = 6mm displacement

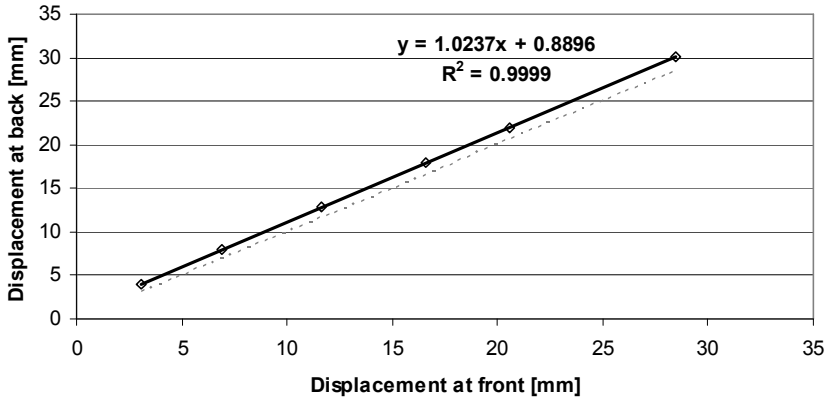

Figure 6-11: Example of soil displacement at front and rear of shear boxes, dashed line indicates 1:1 slope

Shear zones in the fallow tests were observed to extend approximately 10 mm below the shear plane with little disturbance above the shear plane (Figure 6-12). Shear zones developed to a greater extent at the front of the box due to reduced soil contact at the back caused by the top box section moving across the bottom.

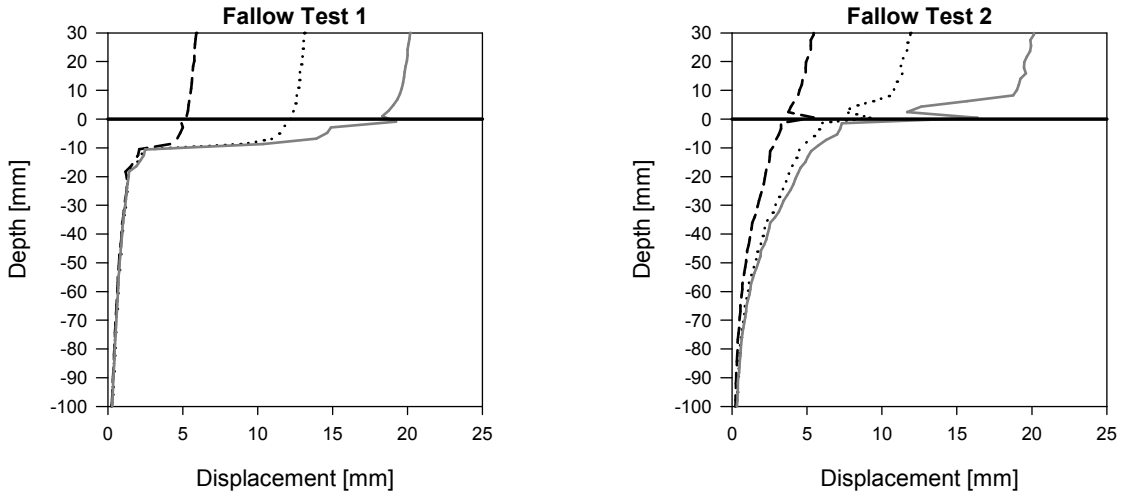

Figure 6-12: Fallow soil displacement plots with depths following PIV analysis. Plots shown at three levels of displacement, 7mm, 14mm and 21mm. Plots highlight shear zone development during direct shear, ─ = shear plane

6.3.2 Root deformation

Shear deformation zones in boxes containing root segments (Figure 6-13) extended between 5 mm and 10 mm above the shear plane and between 10 mm and 20 mm below the shear plane. Values were very similar to those observed during fallow tests. The placement of root segments only on the soil surface, as opposed to growing through the entire soil block meant reinforcement was insufficient to modify soil deformation during shear.

Vector plots demonstrated visually how the roots responded to shear displacement. Roots bent and straightened during shear, with displacement vectors highlighting both lateral and vertical movement. An example of vector root plots, using roots in three orientations, may be found in Figures 6-14, 6-15 and 6-16. The initiation point of each vector was on the root and therefore shows the original location of the roots. Lateral movement indicates the root being displaced horizontally with vertical movement indicating both root straining and also pull-out failure occurring during the test. Root movement below the shear plane was not initiated very quickly when roots were orientated vertically through the shear plane (Figure 6-14). Roots orientated in tension (Figure 6-15) and compression (Figure 6-16), however, appear to initially move more below the shear plane at smaller displacements than that observed for roots orientated vertically. Movement of roots orientated in tension and compression also appear to move more at greater displacements. Roots were observed to straighten, through loading, before the frictional connection between root and soil failed, resulting in pull-out failure. In some instances the frictional resistance between root and soil exceeded root strength and roots were observed to break. The stage and extent at which this occurred differed depending on root orientation, root type and age.

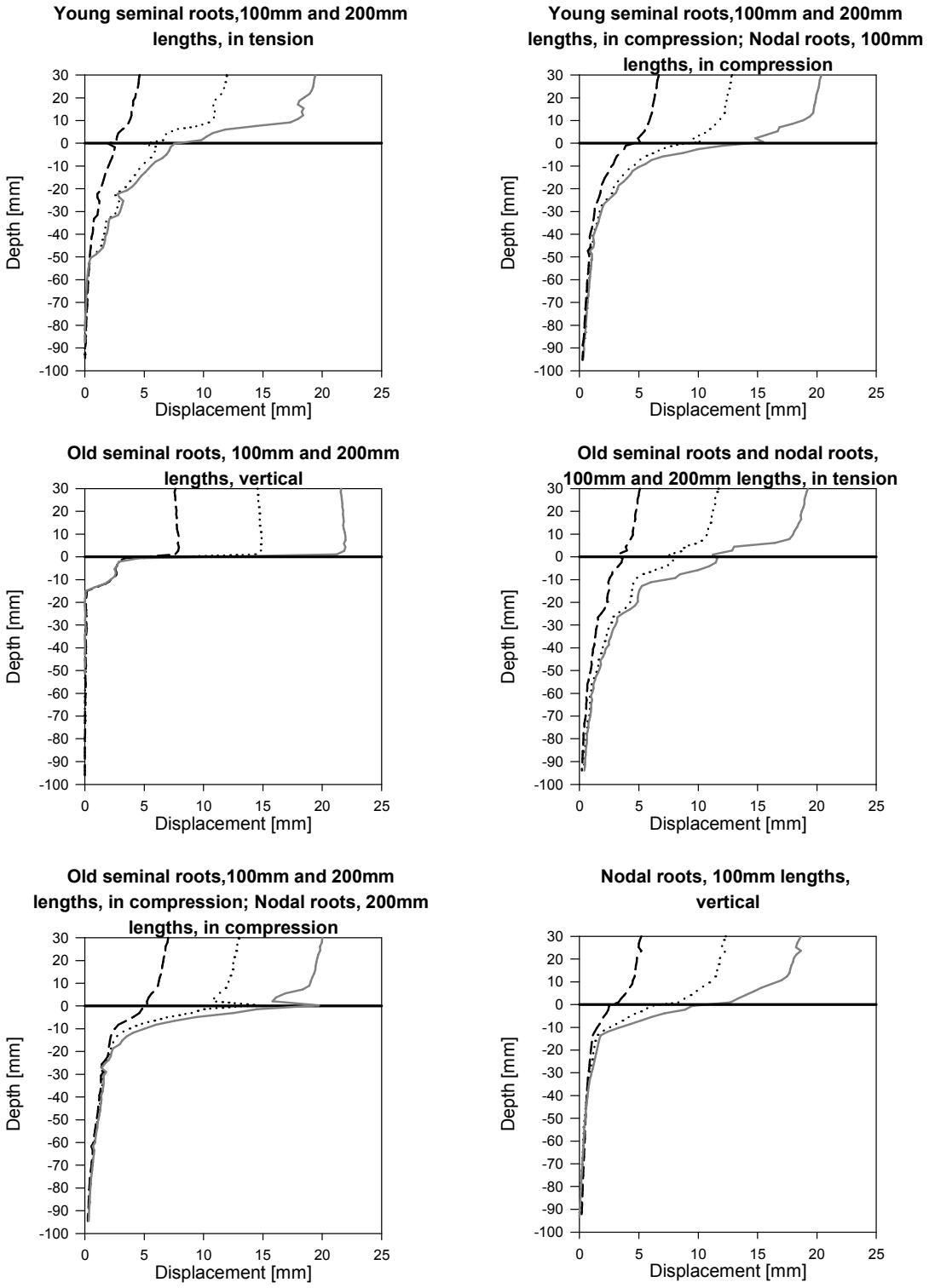

Figure 6-13: Displacement plots of soil from PIV analysis of all rooted shear tests used within this study for assessing root failure. Plots shown for three displacements: 7 mm (- - - - -), 14 mm (····) and 21 mm(——). Plots highlight shear zone development during direct shear, ─ = shear plane

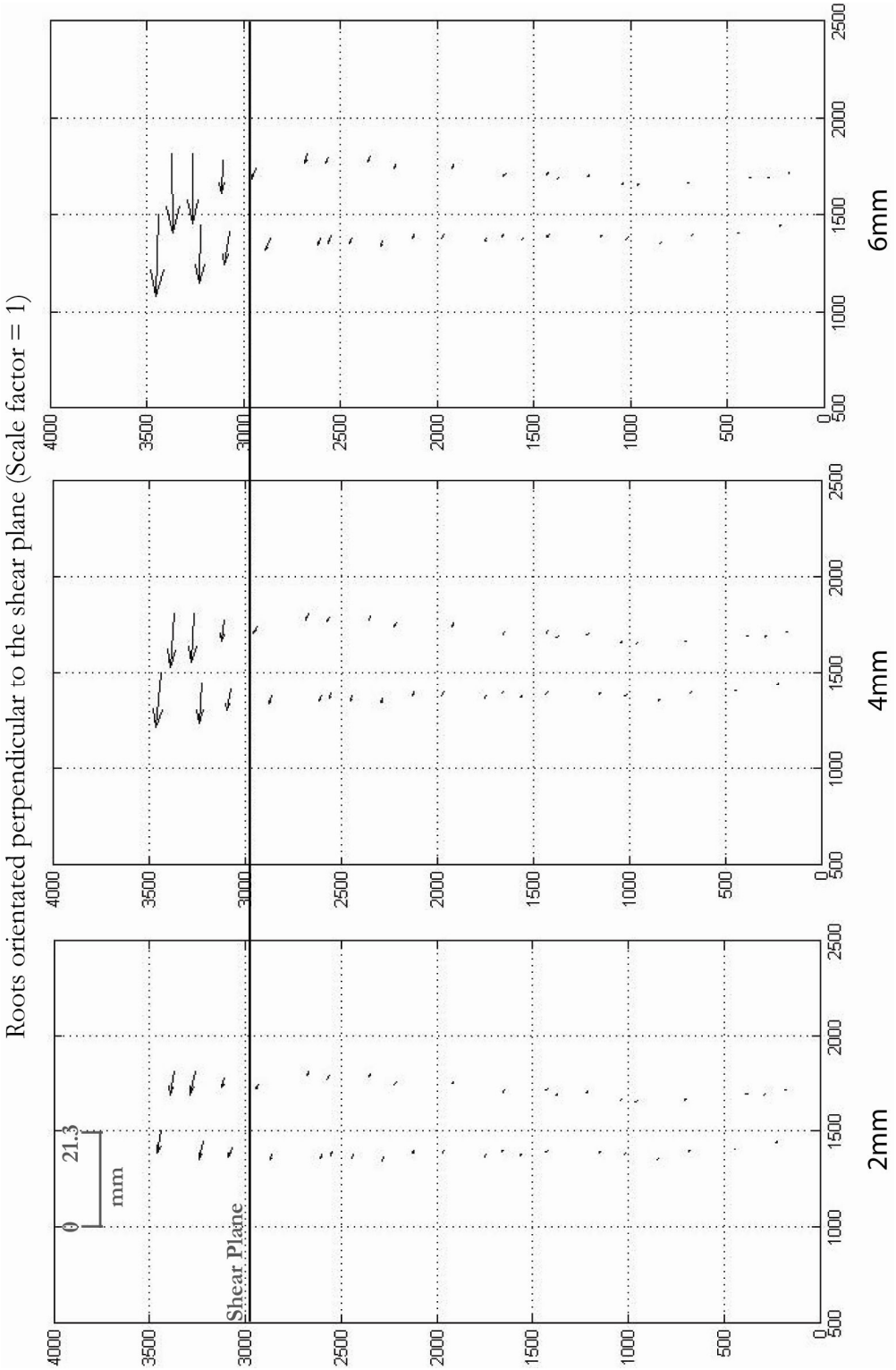

Figure 6-14: Example of vector plots of patch movement during direct shear of roots perpendicular to the shear plane. Plots derived from co-ordinate data produced by running PIV analysis

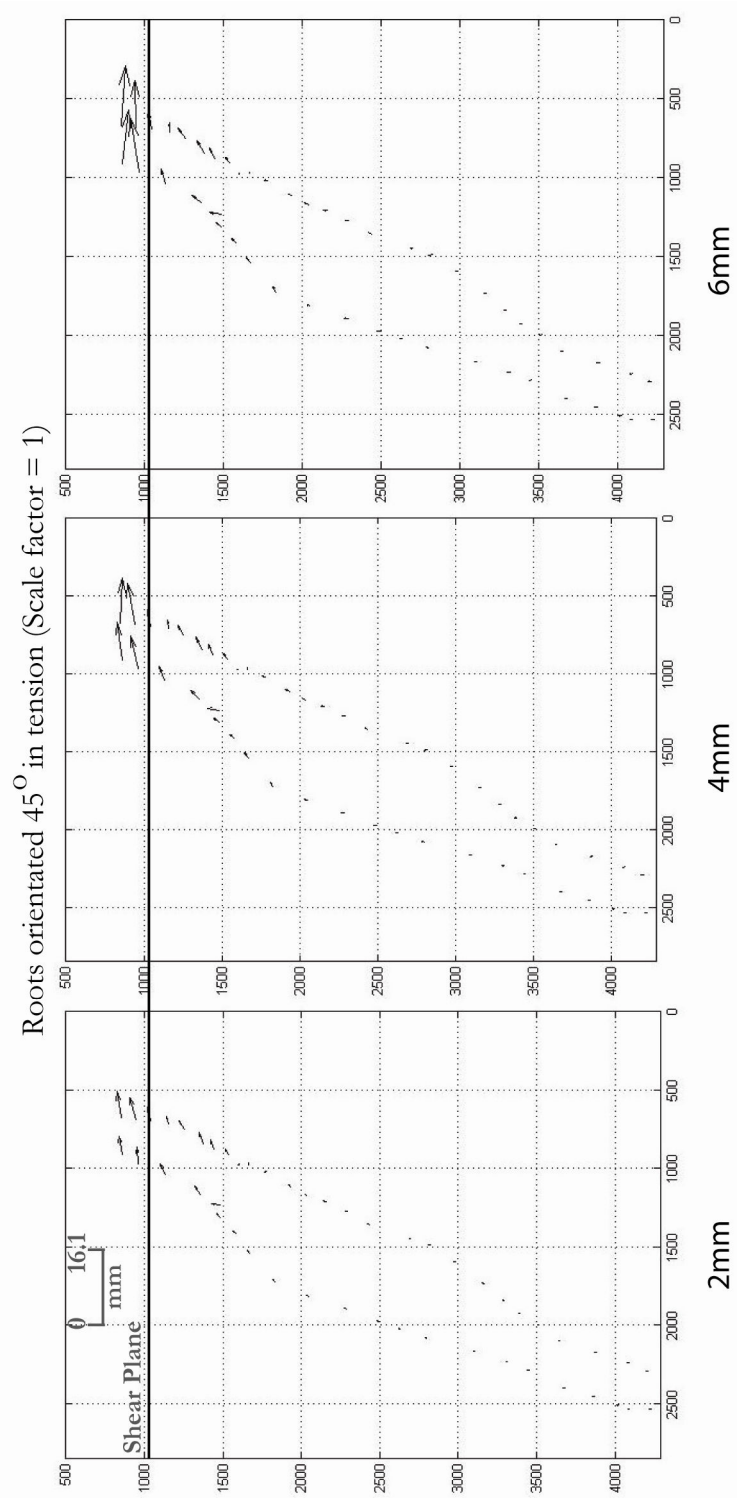

Figure 6-15: Example of vector plots of patch movement during direct shear of roots orientated 45° in tension through the shear plane. Plots derived from co-ordinate data produced by running PIV analysis

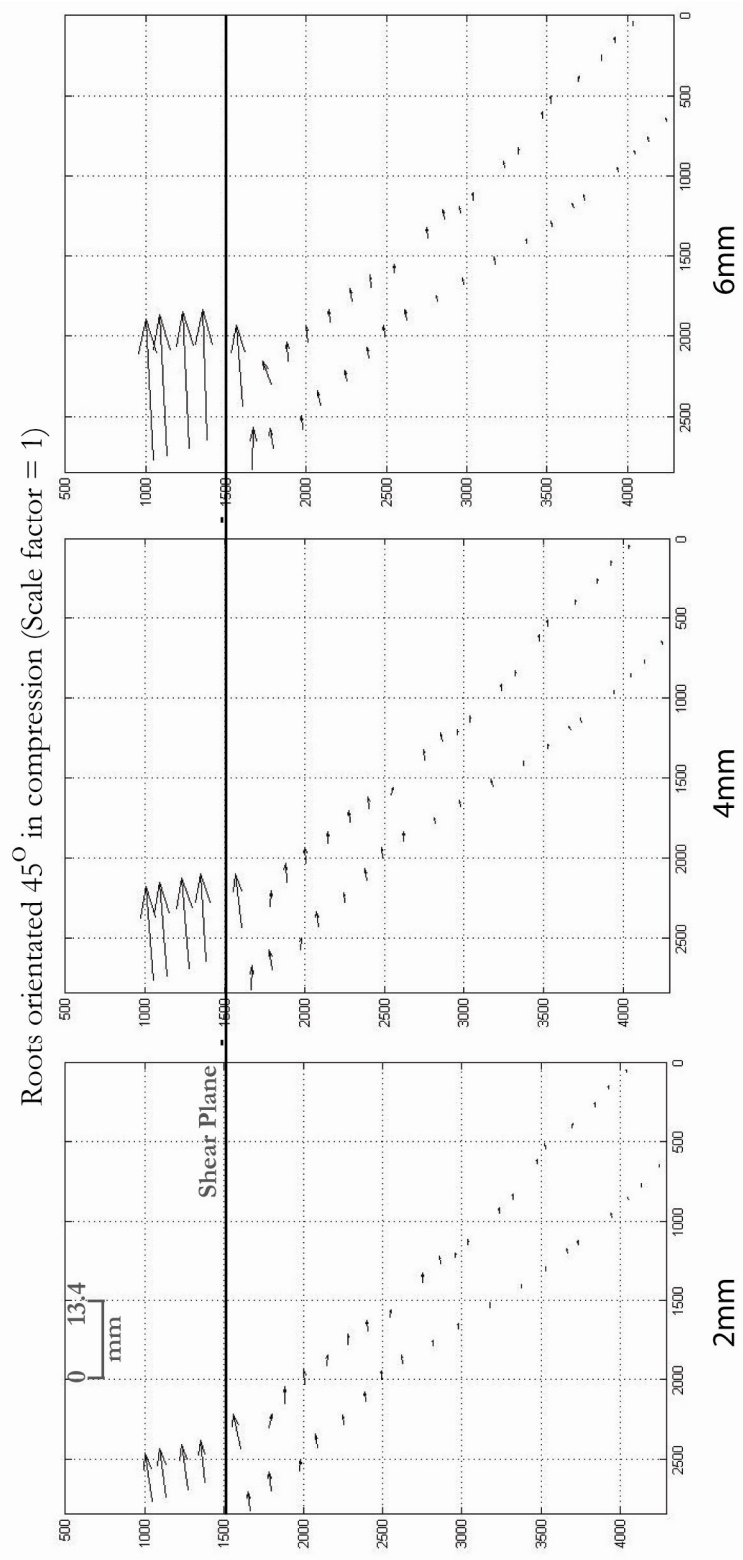

Figure 6-16: Example of vector plots of patch movement during direct shear of roots orientated 45° in compression through the shear plane. Plots derived from co-ordinate data produced by running PIV analysis

Vector plots have shown general trends in root movement. However, values for root movement in *x* and *y* directions are not quantified using this technique. Root movement during shear was assessed further by plotting specific changes in *x* and *y* co-ordinates of patches produced by GEOPIV8. Three levels of displacement were analysed for each shear test in order to examine root movement during the duration of the shear tests to the maximum displacement of 21mm. Lateral root movement resulting from shear displacement was greatest above the shear plane with lateral displacement decreasing with increasing distance below the shear plane (Figure 6-17). Horizontal movement was not observed to be influenced by root orientation. However, plots show potential soil block movement, as commented on in fallow soil tests (section 6.3.1). Following initial horizontal movement, plotted after 7mm displacement, no further movement is observed >40mm below the shear plane, further indicating soil block movement only occurred at the initial stages of the shear tests.

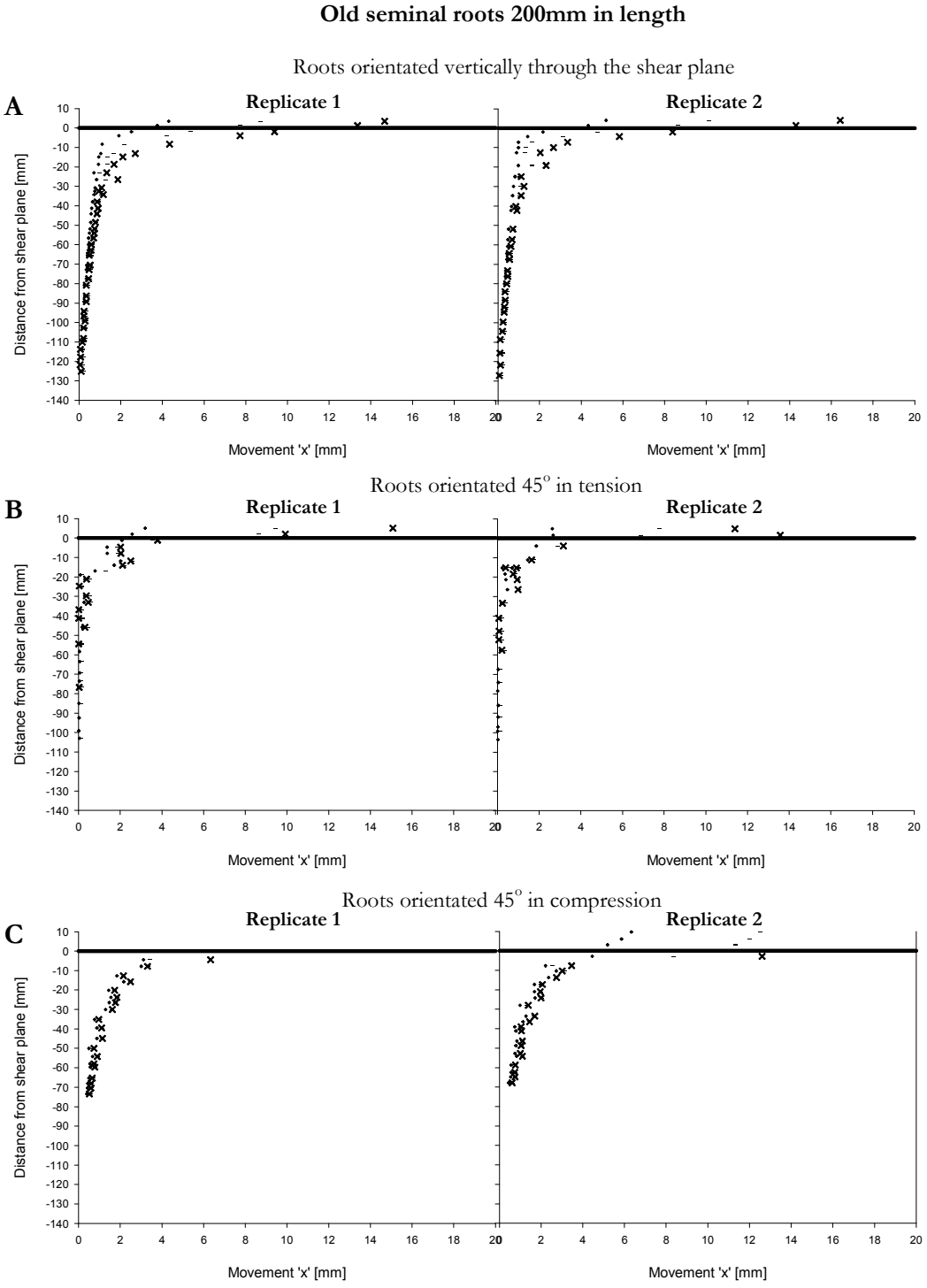

Figure 6-17: Lateral patch movement as a function of distance below the shear plane. • = 7mm displacement; - = 14 mm displacement; x = 21 mm displacement

The movements of patches vertically (*y*) appeared to depend on root orientation (Figure 6-18). Roots orientated vertically through the shear plane showed evidence of strain

within 30mm of the shear plane (Figure 6-18 (A)). This is unlikely to be pull-out failure but may have been influenced by soil dilation. However, previously the shear zone was shown to be approximately 15mm below the shear plane (Figure 6-13), indicating that root movement was unlikely to have been influenced by shear distortion. The vertical movement of patches increased when roots were orientated in tension (Figure 6-18 (B)), with evidence of increasing pull-out failure with increasing displacement. As with roots orientated vertically through the shear plane, the greatest vertical movement of roots in tension was found approximately 30 mm below the shear plane**.** The shear zone region was shown to be 20 mm below the shear plane (Figure 6-13) with roots potentially affected by dilation. Little vertical movement was found when roots were orientated in compression (Figure 6-18 (C)). However, replicate 2 did move vertically above the shear plane. This again may have been attributable to dilation or root buckling during shear. Plots also suggest that Replicate 2 was forced vertically into the soil, with negative '*y*' values recorded after 14 mm and 21 mm of displacement.

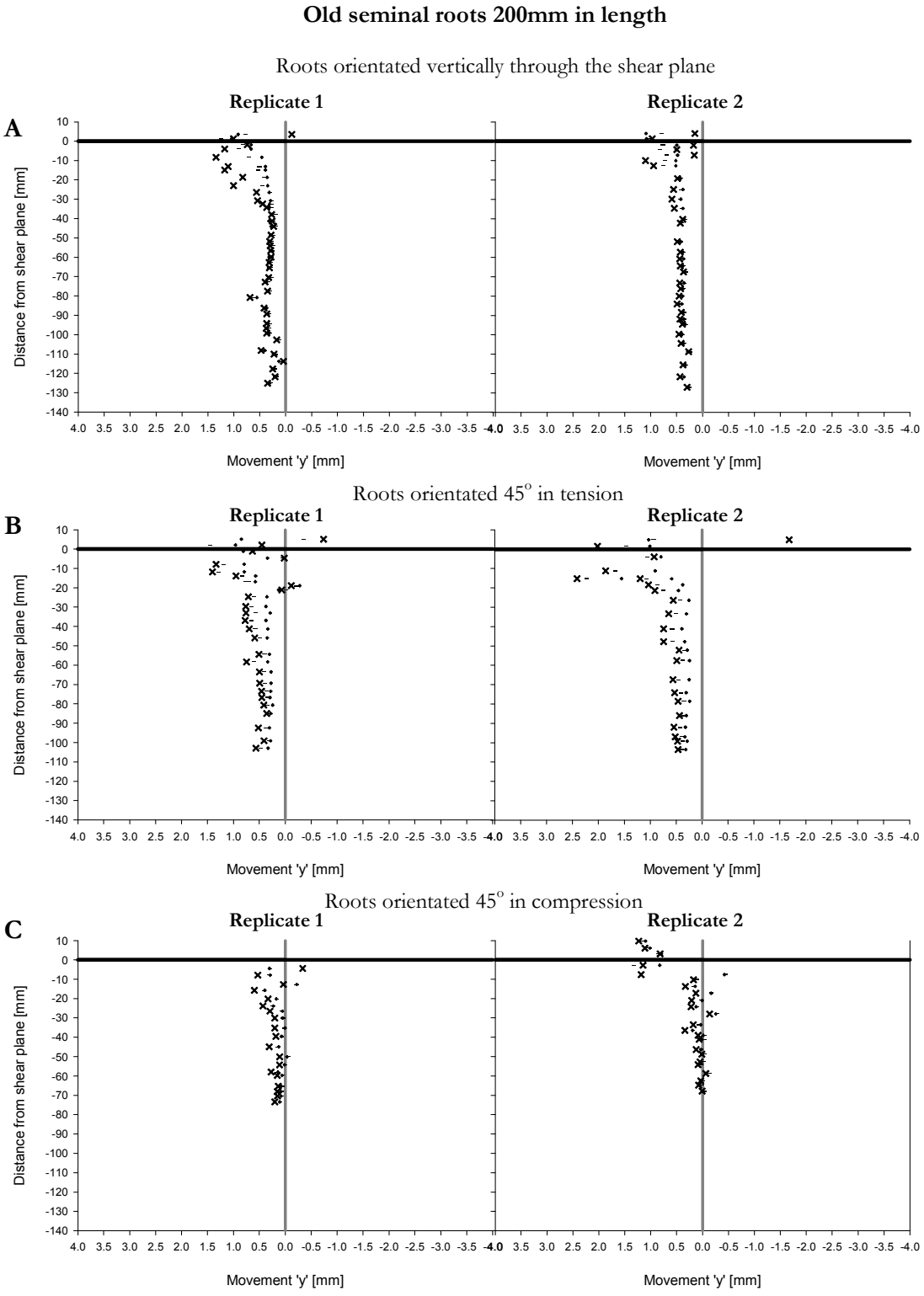

Figure 6-18: Vertical patch movement as a function of distance below the shear plane.• = 7mm displacement; - = 14mm displacement; x = 21mm displacement

6.3.3 Root strain development

Although strain development within root lengths could be calculated from co-ordinate data, the results were disappointing. The assessment of patch movement in '*x*' any '*y*' directions indicated differences between root orientations, with evidence of possible strain development along the root length during direct shearing. Shear strain between patches was then calculated against distance from the shear plane. Strain values for 200 mm lengths of old seminal root were both negative and positive, ranging from +40% to -45% (Figure 6-19). Strain was heterogeneous along the length of all roots, with the greatest strains within the region 30 mm below the shear plane when roots were orientated in tension (Figure 6-19 (A). This was similar to the trends of vertical root movement observed in Figure 6-18(A). Roots orientated vertically through the shear plane contained two regions where strain was greatest and also the most heterogeneous; the region 30mm below the shear plane and also at the distal end of the roots, 90mm+ from the shear plane (Figure 6-19 (B; Replicate 1)). Roots in compression did not exhibit strains as heterogeneous as those orientated vertically or in tension. The variation in strain for roots in compression was generally observed to be ±10%. Strains were both negative and positive indicating roots were both in tension and compression during direct shearing (Figure 6-19 (C)). In summary, the least strain was observed in roots orientated in compression. However, in general strain was observed to be highly variable along root lengths.

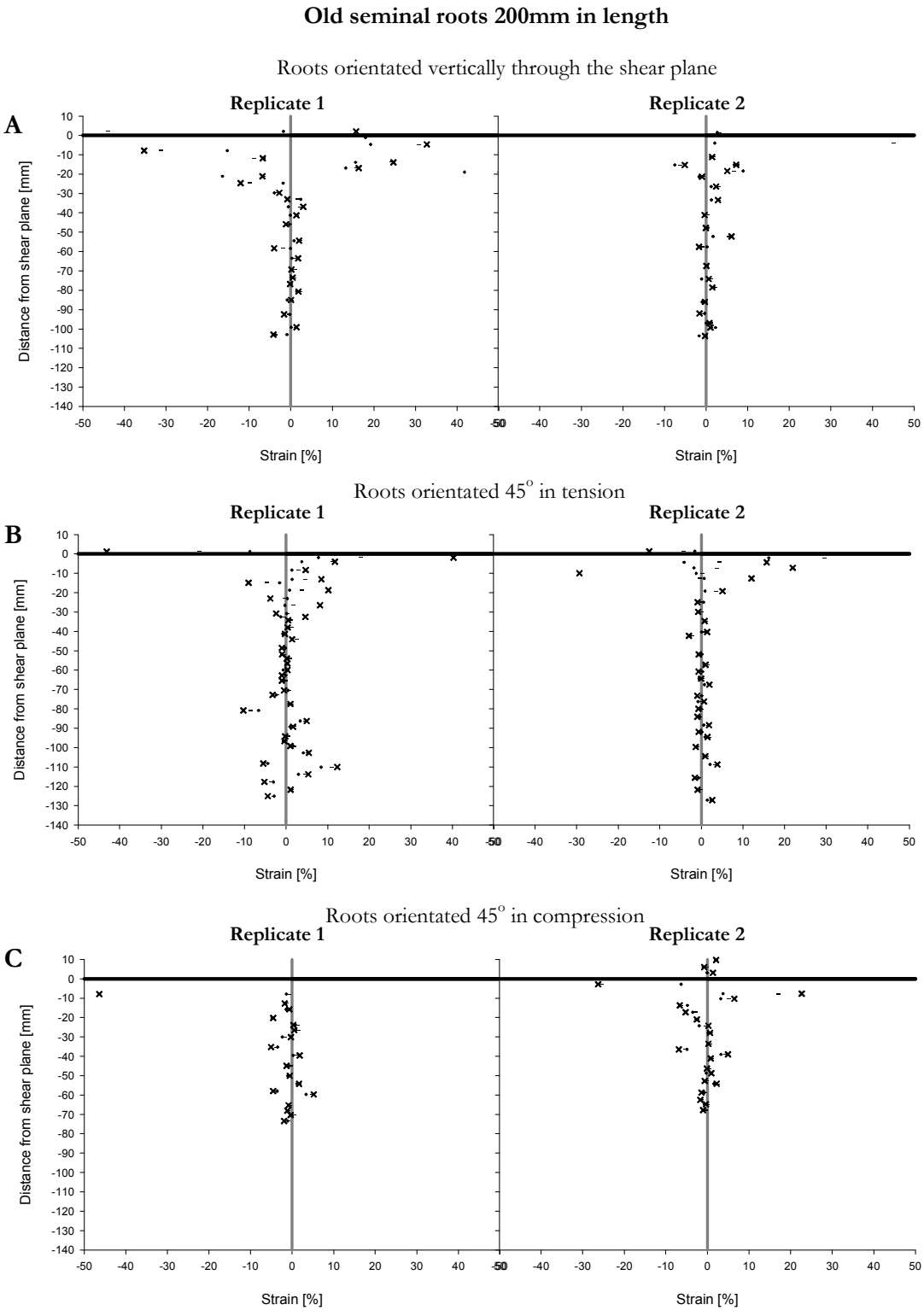

Figure 6-19: Calculated strain development as a function of distance from shear plane during direct shear. • = 7mm displacement; - = 14mm displacement; x = 21mm displacement.

Old seminal roots 200 mm in length were the only group of tests that enabled full comparisons between the three different root orientations. This was due to scatter in the plotted values of strain and vertical/compressive patch movement during shear in the other tests. Other analyses of different root types and orientations highlighted potential problems and noise within data derived from PIV analysis (Figure 6-20). Figures for all tests have been included in Appendix 2. In general, test results using output co-ordinates produced by GEOPIV8 were disappointing with potential explanations for this discussed later.

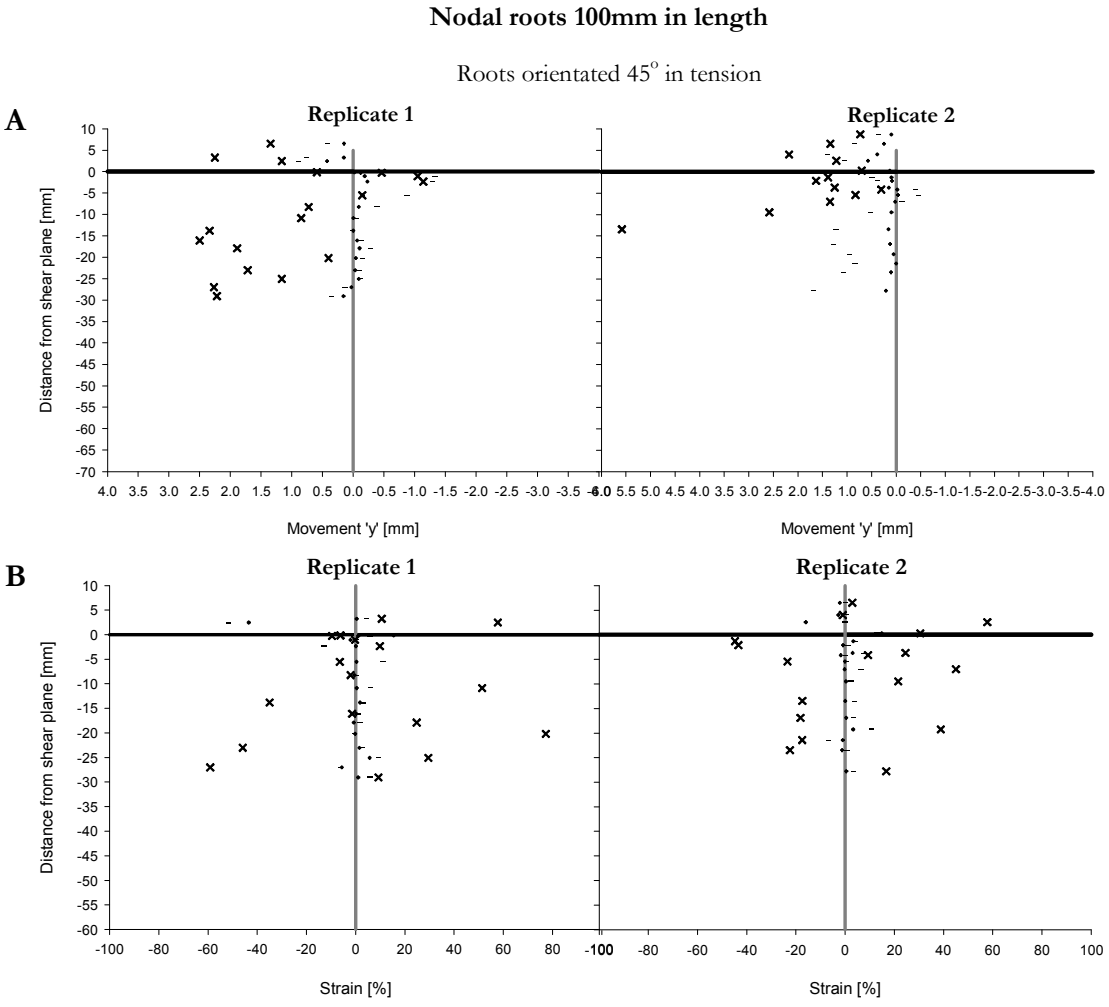

Figure 6-20: Inaccurate plots of patch movement in '*y*' direction (A) and strain development (B) along nodal roots 100mm in length

An analysis of patch movement did not provide a graphical representation of how roots changed orientation and form during shear. In order to resolve this, the co-ordinates of patches along root lengths were plotted for a series of images at their original location and at three subsequent displacements (Figure 6-21). Changes in co-ordinate location demonstrated changes in root form during direct shear. Roots orientated vertically through the shear plane and also in tension can be seen to straighten between their original position and after 21mm displacement (Figure 6-21 (A and B)). Roots orientated in compression both bent and also compressed during shear (Figure 6-21 (C)). Although it was possible to visualise changes in root form from these plots, they do not provide quantitative data that can be incorporated into models. Were stress and strain data of the roots recorded during shear testing, more accurate modelling of root contributions to reinforcement during intermediary failure stages could possibly be performed.

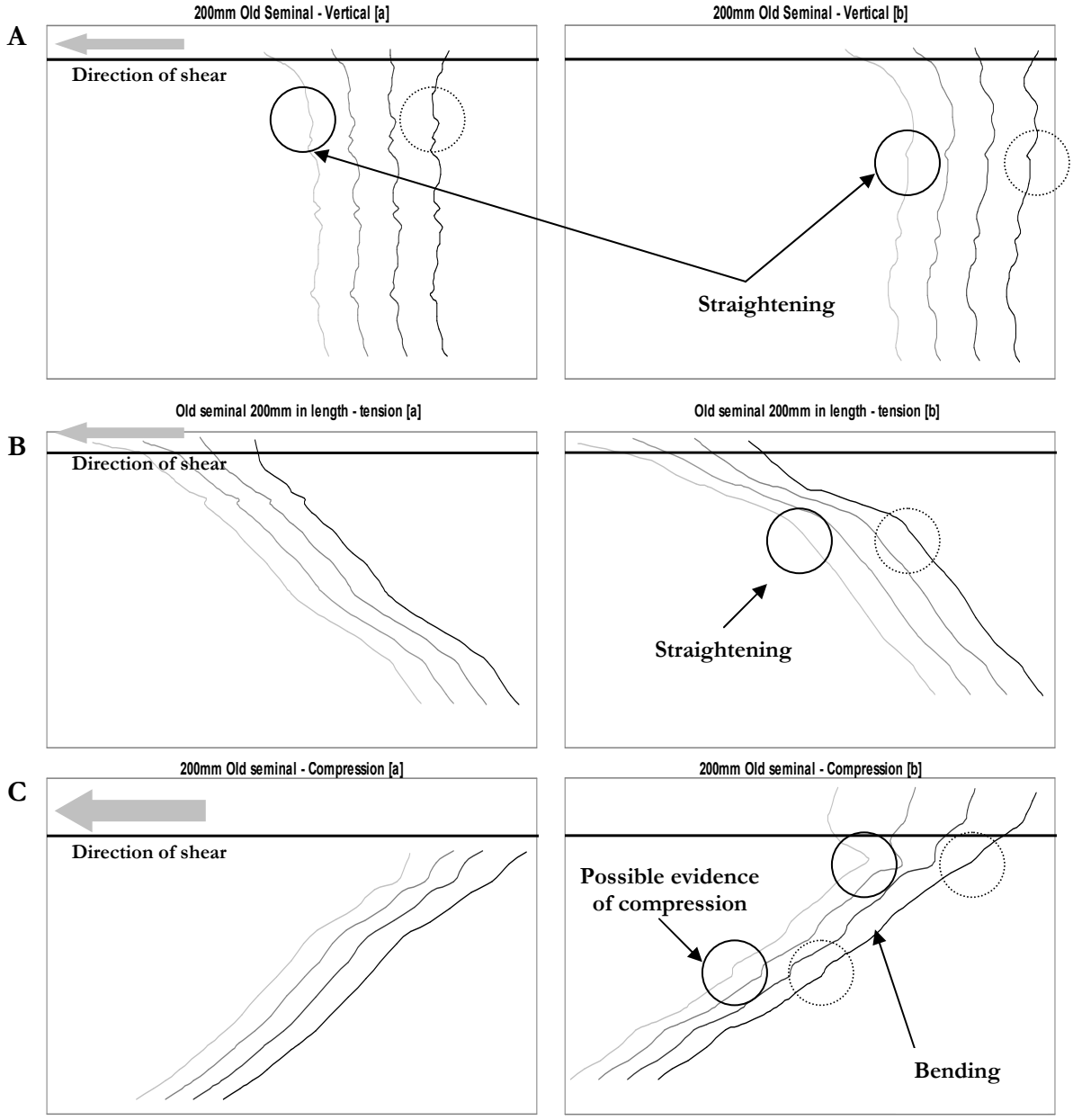

Figure 6-21: Direct shear effects on 200mm long old seminal roots orientated vertically, in tension and compression through the shear plane. Gray scale defines shear displacements from original position (darkest) and at three subsequent displacements. Roots were orientated vertically (A), in tension (B) and in compression (C) and have been offset to allow changes in root form to be fully visualised in figures

6.3.4 Root observations during direct shear

Visualisation by eye observed roots failing through both breaking and also through the root soil bond being broken resulting in pull-out failure. Various intermediary stages prior to ultimate failure were observed, with roots straightening, bending, stretching and compressing under direct shear (Table 6-3). The intermediate failure type was found to be dependant on root orientation, length and also type. All roots were found to straighten during shearing when orientated vertically and in tension, with only old seminal roots showing evidence of straightening when orientated in compression. Roots were also observed to bend when orientated vertically and in compression, with little or no observed bending when roots were in tension. Roots in compression were observed to physically compress, e.g. force the root down into the soil. However, old seminal roots also showed a similar response when orientated vertically through the shear plane (Table 6-3).

Root type	Orientation	Root length [mm]	Intermediary failure stages observed			
			Straightens	*Bends*	*Stretches*	*Compresses*
Young seminal	Vertical	100	n/a	n/a	n/a	n/a
	Tension	100	✓	×	✓	×
	Compression	100	✓	✓	×	×
Old seminal	Vertical	100	✓	✓	×	✓
	Tension	100	✓	×	✓	×
	Compression	100	×	✓	×	✓
Nodal	Vertical	100	n/a	n/a	n/a	n/a
	Tension	100	✓	×	✓	×
	Compression	100	×	✓	×	✓
Young seminal	Vertical	200	n/a	n/a	n/a	n/a
	Tension	200	✓	×	✓	×
	Compression	200	×	✓	×	×
Old seminal	Vertical	200	✓	✓	✓	×
	Tension	200	✓	×	✓	×
	Compression	200	✓	✓	×	×
Nodal	Vertical	200	n/a	n/a	n/a	n/a
	Tension	200	✓	×	✓	×
	Compression	200	×	✓	×	✓

Table 6-3: Summary of observed intermediary root failure during direct shear, *x* = no; ✓ = yes

The ultimate failure of the root-soil frictional bond during direct shear was previously assumed to be through pull-out or breakage. Significantly, only younger seminal roots in tension failed through breakage, whereas all other orientations and root types failed either by pull-out or experienced displacement with no failure (Table 6-4). A full description of each test performed may be found in the Appendix, whilst only summary data are presented within this chapter.

Root type	Orientation	Root length [mm]	Ultimate failure observed	
			Pull-out	***Breakage***
Young seminal	Vertical	100	n/a	n/a
	Tension	100	✓	✓
	Compression	100	×	×
Old seminal	Vertical	100	×	×
	Tension	100	✓	×
	Compression	100	×	×
Nodal	Vertical	100	n/a	n/a
	Tension	100	✓	×
	Compression	100	×	×
Young seminal	Vertical	200	n/a	n/a
	Tension	200	✓	✓
	Compression	200	×	×
Old seminal	Vertical	200	✓	×
	Tension	200	✓	×
	Compression	200	×	×
Nodal	Vertical	200	n/a	n/a
	Tension	200	✓	×
	Compression	200	×	×

Table 6-4: Summary of observed ultimate root failure during direct shear

6.4 Discussion

6.4.1 Root deformation mechanisms

Using shear boxes with clear surfaces for viewing, it was possible to visualise root movement during direct shear testing. The method proved reliable for visualising root and soil movement during shear, with observations of root failure by both pull-out and breakage. Successfully applying the approach used by White et al. (2003) has enabled the use of PIV to demonstrate the complexity of root response to direct shear. There were some difficulties in applying the approach to shear tests on soil containing roots. There was evidence of complex soil movement at the commencement of shear tests, which may be due to either the shear box itself moving or an affect of initial soil stress on the soil block. The shear boxes were secured to minimise box movement during shear, so it was therefore likely that the initial movement was caused by the soil block moving. Intermediary stages of failure were also observed and these are vital for increasing the understanding of the deformation behaviour of roots during shear.

Roots responded to shear displacements in different ways depending on root orientation across the shear plane and root age (Figure 6-22). Roots orientated vertically through the shear zone undergo straightening, bending, stretching and finally pull-out. Roots orientated in tension predominantly straighten, stretch and then finally pull-out or in some incidences break. Although roots are generally classified as *failing* through pull-out or breakage (Ennos, 1990), *compression*, *straightening*, *bending* or *stretching* may all occur and influence the mechanical response with differing contributions to reinforcement (Thomas and Pollen-Bankhead, 2010). Therefore, the derived reinforcement from different root types, orientations and shear displacement will be dependant on root

properties other than tensile strength or stiffness. Roots that were shown to fail through pull-out may have been affected by the shear zone depth. With deeper shear zones the interface strength between root and soil may decrease because of changes in normal contact distribution, reducing friction, increasing likelihood of pull-out (Abe and Ziemer, 1991).

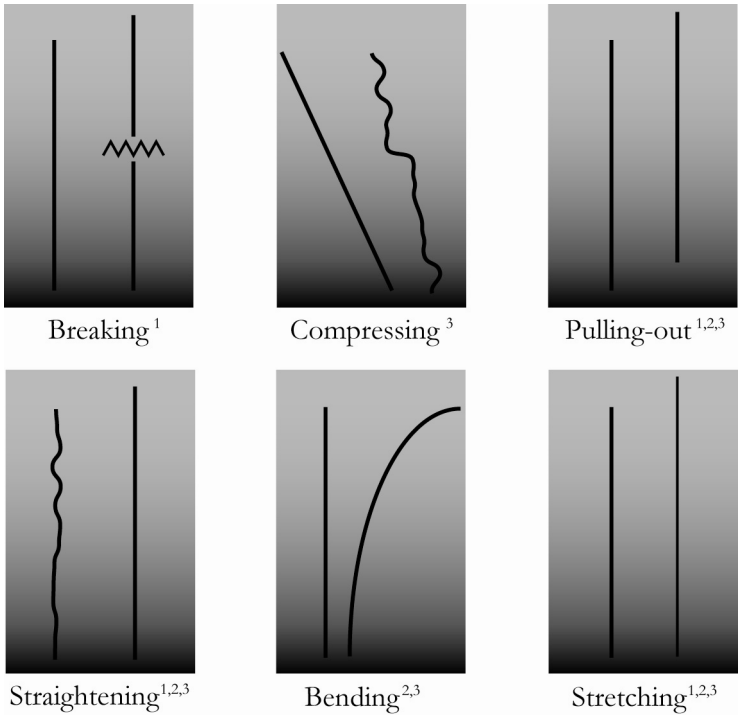

Figure 6-22: Root responses to shear strain visualised during direct shear testing. Superscript numbers refer to response observed when roots orientated 45^0 in tension (1), vertically (2) and 45^0 in compression (3) through the shear plane

Ennos (1990) showed that the mechanical properties of roots were influenced by age, with earlier work in this thesis (Chapter 5) agreeing with these findings. My study has shown that in some tests, younger seminal roots broke during shear testing, whereas older roots were only observed to fail through pull-out. This further highlights that the potential failure mechanisms are affected by root age and changing root mechanics.

6.4.2 Strain measurements in roots

Along the length of a root, there were differences in strain localisation due to distance from the shear plane and bending during shear. Surface asperities on roots and structural variability along the length of roots could also influence strain localisation (Hamza, 2006). The initial buckling of roots followed by tension could exacerbate localised strain, however, bending stiffness indicates that this effect would probably be greater for woody roots with a larger bending modulus than the fibrous roots tested here.

Although fibrous root movements were measured, there were difficulties in applying PIV because of the importance of patch size and the size of the element being examined. Fibrous roots, by definition, may be defined as very fine ranging from 0.3 mm to 1.0 mm in diameter (Bohm, 1979; Stokes et al., 2009). This presents a great challenge in defining a small enough patch size that will remain on the particular root section of interest, whilst still containing enough texture to be tracked accurately. Previous work using PIV by Hamza et al. (2007) increased texture through the application of graphite powder prior to performing tensile tests on tobacco roots. The roots they studied, however, also had a greater diameter then those studied in this thesis, potentially explaining good measurements of strain. In Mickovski et al. (2007), pull-out was observed on root analogues of 1.7 and 2.3mm in diameter, making it possible to optimise patch size versus root diameter. In my study the strain calculations may have been improved through capturing images covering a smaller segment of the root, but it was important to capture the whole root to visualise root failure during shear along the entire length of the root. Focusing on a smaller section of each root, increasing resolution, would result in better greyscale variation on photographed root sections. Better greyscale contrast between root and soil would allow patches to be located entirely on the root resulting in better tracking

between images. It was possible to see roots straining during shear by eye, but this response was not clearly seen in strain or displacement plots. Values of localised strain between patches were calculated as ranging from 350% to -100%, which are not realistic. In Chapter 3 (field and glasshouse) a number of tensile tests were performed on roots collected from field plots after 5 and 20 weeks growth. Strain at tensile failure for these samples was found to be <10%.

Vector plots can be used to summarise and visualise root movement, as done by Hamza et al. (2007) for element tests on individual roots and Mickovski et al. (2007) for pull-out tests of roots from soil. The quantification of vectors was unfortunately not possible because soil block rotation made it impossible to separate specific root movement from soil movement. Through further work it may be possible to produce vector plots for quantitative calculations of root movement through the use of co-ordinate data. Better shear box design may eliminate problem associated with the observed rotation of the soil block during shear.

6.4.3 Implications of findings

This work has developed a new method of enabling PIV to be used during direct shear testing to investigate root movement and strain localisation. Analogue roots have been used to investigate root strain during pull-out failure and effects of root architecture, branching (Mickovski et al., 2007) previously. However, studies utilising real roots, and observation of their responses to direct shear, have been limited. Pull-out tests have been shown to be useful (Mickovski et al., 2007), but only show strain development during vertical uprooting and not intermediary stages of root strain development observed

during direct shear. Investigation into antecedent strain conditions prior to breakage failure will enable better understanding of initial stress/strain relationships.

The increased understanding of root-soil mechanical interactions from this study opens up challenging research questions for the future. For instance, although many studies have investigated the impact of root architecture on root resistance to pull-out, the mechanisms during shear failure are poorly understood. Models of root reinforcement of soil under shear incorporate the influence of bending stiffness (EI) and axial stiffness (EA), but more work is required to also consider the contributions through root straightening and buckling/compression. Analysis of root stress and strain during the process of root straightening may provide a better value for incorporation into root reinforcement models. Stress along the root length will develop as a result of root straightening during direct shear testing with highly sinuous roots possibly localising stress slower than those that are less sinuous. This *quasi* Young's Modulus (Figure 6-23) during straightening ('E' = $\Delta F/(A\ \Delta l^{Q}/l_o^{Q})$, where Δl^{Q} is the overall apparent root length change measured using the root end positions only and l_o^{Q} is the apparent length between the ends) may be a more realistic term for initial root stress localisation during shear than the Young's modulus measured from straight root element tests. Further work is required to investigate potential differences in this *quasi* Young's modulus in response to changes in root sinuosity with stress increasing during the root straightening phase (Figure 6-24). Contributions to soil reinforcement and sinuosity will also be affected significantly by root stiffness. Tortuosity has previously been shown to be affected by soil moisture (Konopka et al., 2008), highlighting one of the many factors that may contribute to the way in which roots localise strain. It has only been very recently that attempts have been made to include tortuosity in models as a factor affecting

reinforcement. A recent review by Stokes et al. (2009), however, has highlighted a total of fifteen other desirable root traits with potential to increase resistance to landslides.

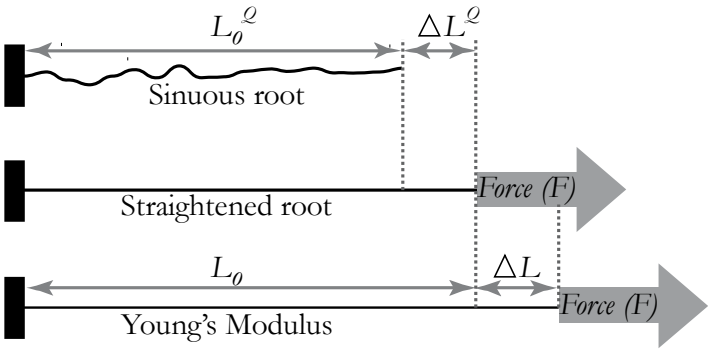

Figure 6-23: Measurement of *Quasi* Young's Modulus and Young's Modulus

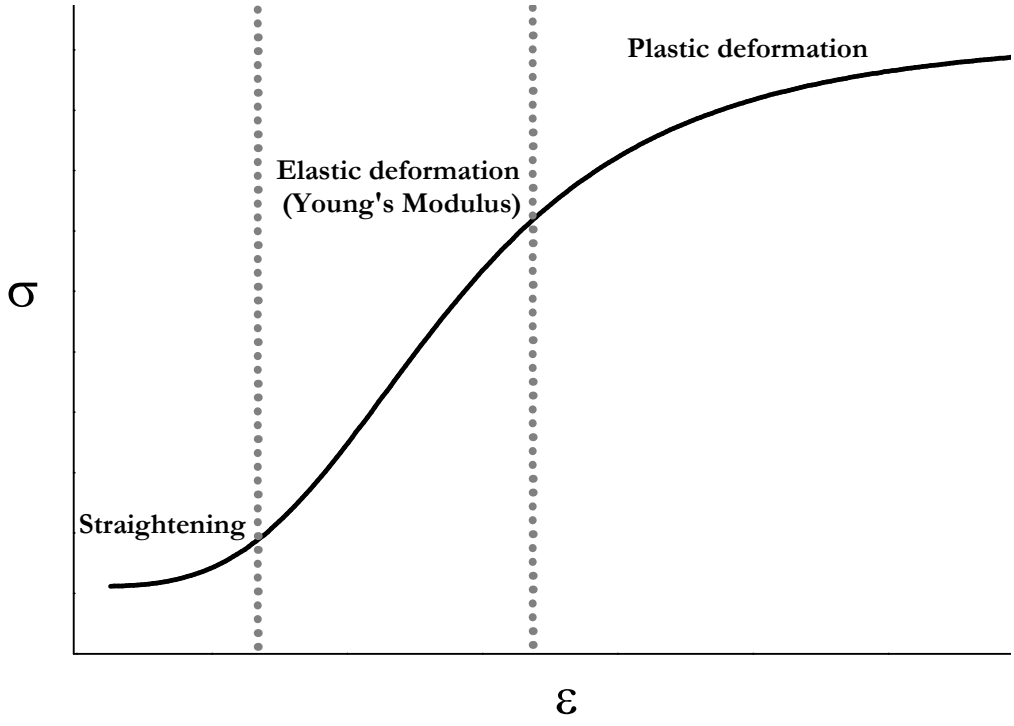

Figure 6-24: Simulated stress vs. strain behaviour of tortuous root during direct shear

6.4.4 Conclusions and further work

The visualisation of root-soil interactions during shear has shown the impact of root age and orientation on how roots respond to displacement. This first direct observation of shearing in root-reinforced soil has added considerably to our knowledge of how roots reinforce soil. Particle image velocimetry was a useful tool for analysing root movement during shear. Displacement trajectory plots showed root movement at very fine resolution for small diameter fibrous roots. Roots were observed to fail through pull-out and breakage in this study, with the transfer of shear strain from testing observed along root lengths.

Due to the different root behaviours during shear, dependant on root orientation and age, further work is required regarding 3D modelling of root system architecture. Such research may better predict reinforcement as noted previously by other authors (Danjon et al., 2007; Reubens et al., 2009). Roots were only placed on the soil surface not allowing for natural processes of root soil bonding through actions of root exudation (Ennos, 1990; Mickovski et al., 2009) and also root hairs penetrating the soil (Bailey et al., 2002; Bengough and Mullins, 1990) to develop. Root hairs may have increase the soil root bond, however, root hairs of *Arabidopsis thaliana* have not been shown to increase pull-out resistance when compared to those roots with hairs (Bailey et al., 2001). Investigating soil movement in the region surrounding roots would further increase our understanding of the root soil interface. Although this cannot be reported on in this study, due to the spatial resolution of the images and roots not having been grown in shear boxes, the method proposed could be adapted to investigate this further. Capture of smaller segments of root sections, capturing higher resolution images, will lead to a better understanding of these key interfaces. However, through the use of X-ray scanning three-

dimensional (3-D) visualisation of changes in root form during shear maybe possible in the future. Until recently image resolution has hampered the use of this technique for fine roots (Tracy et al., 2010). Increasing resolution from >100μm to <500nm has enabled the visualisation of very fine roots, such as those of *Arabadopsis thaliana,* in soil (Tracy et al., 2010) with root-tracing software able to reconstruct the 3-D architecture of the root system (Jassogne, 2009 in Tracy et al., 2010).

BLANK PAGE

7. Root reinforcement modelling and discussion

Some of the modelling within this chapter has been published with Chapter 3 in:

Loades, K. W, Bengough, A.G., Bransby, M.F. and Hallett, P.D. (2010), Planting density influence on fibrous root reinforcement of soils. Ecological Engineering Vol. 36 (3), pp 276-284 (APPENDIX 1).

7.1 Introduction

Predicting reinforcement derived from root inclusions in soil allows for extrapolation of research findings to large scale applications, such as slope stability analysis and the integration of models into Geographical Information Systems (GIS) software. Soil strength, or shear resistance (S_f), can be predicted using the Mohr Coulomb equation:

$$S_f = c + \sigma_N \tan\varphi$$

where c = soil cohesion; σ_N= applied normal stress and φ= internal angle of friction.

Waldron (1977) developed one of the earliest models to predict changes in shear strength from root inclusions through integration of a root cohesion term (c_r) into the Mohr-Coulomb equation for soil shear strength:

$$S_f = c + c_r + \sigma_N \tan\varphi .$$

c_r is a function of root tensile strength (T_r) and root area ratio (RAR) derived from the Area of root (A_r)/ Shear surface area (A). If root inclination, θ, is also included, c_r can be evaluated by:

$$c_r = T_r (A_R / A)(\sin\theta + \cos\theta \tan\varphi)$$

This equation assumes that all roots fail simultaneously. Waldron's initial model was further developed by Wu et al. (1979) who simplified the c_r component. It was found that a variation in θ from 48-72° had little impact, so the equation could be simplified to:

$$c_r = 1.2(T_R(A_R / A))$$

where 1.2 is a constant to account for root inclination.

More recently, fibre bundle models have been utilised by Pollen and Simon (2005), with roots viewed as fibres bearing load with load redistributed as fibres break (Daniels, 1945) resulting in progressive failure. Whereas Wu et al. (1979) assumed that roots fail catastrophically (i.e. all at the same time), with soil strength heavily reliant on the RAR, the fibre bundle model (FBM) proposed by Pollen and Simon (2005) used the relationship between the diameter and mechanical behaviour of roots to describe progressive failure of roots from weakest to strongest. In the FBM, load is redistributed as each root breaks. This approach is more realistic as progressive failure has been observed during the failure of root systems (Mickovski et al., 2009).

Pollen and Simon (2005) developed a computer program named 'RipRoot', which uses an FBM approach to predict soil reinforcement by plant roots based on progressive failure (Chapter 2, Figure 2.13). Key to the use of this model is root strength data that must be incorporated. It is possible to use Rip-Root to predict reinforcement using data from numerous studies on the strength of roots of woody species used in forestry and also riparian species (Abernethy and Rutherfurd, 1999; O'Loughlin and Ziemer, 1982; Wu et al., 1979). These species, however, have measured predominantly larger diameter roots. Missing are data on fine roots (0-5mm in diameter) that are essential for the application of FBM models (Pollen-Bankhead and Simon, 2009).

Another challenge with FBM models are assumptions used about the mechanical behaviour of roots. Rip-Root assumes stiffness scaling of E/d, where E is stiffness and d is diameter, based on Daniell's (1945) earlier work on more idealised materials. Whether this scaling relationship is correct for plant roots has never been quantified. Other FBM approaches are stress based, so stiffness is not considered. For woody species, Mickovski et al. (2009) showed that stress-based FBM approaches are not appropriate as they predict failure of the largest roots first and smallest roots last. It is possible to incorporate stiffness into FBM so that failure is strain rather than stress dependent. Rather than making an assumption about the scaling of stiffness, the relationship is obtained from stiffness vs. diameter data obtained from tensile tests. To our knowledge, this approach has been not been used to describe soil reinforcement by plant roots.

This chapter incorporates data obtained in Chapter 2 to model the reinforcement of soil by plant roots. Different modelling approaches are investigated using a wide range of data: simultaneous breakage model of Wu et al. (1979) and the two stress and strain based FBMs. A smaller data-set is used to compare Rip-Root to stress-based and strain-based FBM approaches. It is hypothesised that the accuracy of the prediction will increase as models incorporate more realistic failure conditions. The strain-based FBM is anticipated to provide the most accurate prediction because it incorporates data on root stiffness and strength, as well as the progressive failure of roots. With the data collected in this thesis, it will also be possible to identify weaknesses in different modelling approaches, such as the assumption about stiffness scaling in Rip-Root. A major aim of this chapter is to identify weaknesses in modelling approaches that need to be incorporated in the development of future models.

7.1. *Methods*

7.1.1. Root biomechanics and rooted soil shear data

Root data used within models was that derived from the field and glasshouse experiment (Chapter 3). Using data from Chapter 3 allows for observed shear strength to be compared to that of model predictions to verify model accuracy. Cofie and Koolen (2001) recommended that due to the influence of strain rate on root biomechanical data (strength and modulus), root data should be derived from tensile tests performed at the same displacement rates. Shear tests within this thesis have all been performed at a shear rate of 1mm/min, which was the same rate used throughout this thesis when assessing root tensile strength and stiffness.

7.1.2. Shear plane root diameter distribution

Within Chapter 3 root diameters at the shear plane were measured using a microscope. Method used are found in section 3.2.4.

7.1.3. Reinforcement models used

Three models were used to predict reinforcement, those proposed by Wu et al., (1979) and Pollen and Simon (2005). A stress-based FBM was used by Mickovski et al. (2009) and a strain-based FBM was developed in conjunction with my supervisors. Information collected on root diameter distribution on the shear surfaces and the relationship between root diameter and strength from the glasshouse and field experiment were incorporated in the root reinforcement models of Wu et al. (1979), Pollen and Simon (2005) and Mickovski et al. (2009). The strain-based FBM also incorporated data on the

relationship between root diameter and stiffness. The models chosen predict reinforcement in different ways. Wu et al. (1979) assumed that all roots fail catastrophically through breakage. Shear reinforcement was calculated from the sum of the forces required to break each individual root, crossing the shear plane by:

$$c_r = \frac{1.2}{A_{shearplane}} \sum_{i=1}^{n} T_{ri} A_i$$

where 1.2 is a correction factor for root orientation described previously.

Rip-Root, developed by Pollen and Simon (2005), derives reinforcement from the distribution of stress over all the roots with stress redistributed as each root fails allowing progressive failure to be observed. This approach extends Daniel's (1945) FBM approach by using T_r x d to define the critical failure condition for roots. Although it is not explicit in their paper (Pollen and Simon, 2005), this correction accounts for decreasing root stiffness with increasing diameter. The load sharing rule becomes:

$$F_i = \sum F(D_i / \sum D)$$

so that the force distribution depends on the root diameter which is from Daniels (1945). With this approach, stiffness scales as E/d. Roots are ordered from weakest to strongest, with the weakest root removed at each step. The failure process was repeated with the diminishing unbroken root population. The peak root reinforcement, c_r was the result of the calculation that provided the maximum reinforcement effect as:

$$c_r = \max(\sigma_{rj})$$

where σ_{rj} is the overall stress applied to the core that is taken up by roots to cause root j to fail.

Predicted reinforcement using the models of Wu et al. (1979) and both stress and strain based FBM models plotted against observed reinforcement for both field and glasshouse to test these models. The stress-based FBM is derived by:

$$\sigma_{rj} = T_{rj} \frac{\sum_{i=1}^{j} A_i}{A_{shearplane}}$$

where σ_{rj} is the overall stress applied to the core that is taken up by roots to cause root j to fail, T_{rj} is the strength of the weakest remaining root, and A is the area of each root. In the strain-based FBM, roots are ordered from smallest to largest strain required to failure. Increasing strain, rather than stress, is applied to the roots, with failing roots removed at each step and the load redistributed amongst remaining roots. On a subset of data, consisting only of the field experiment for 5 weeks growth, the Rip-Root model proposed by Pollen and Simon (2005) was also tested.

7.2. *Results*

7.2.1. Root diameter distributions

7.2.1.1. Field cores

The models being tested require the root diameter populations and power-law regressions of root strength to predict reinforcement. Root diameter distributions in the field cores sampled after 5 weeks growth had >90% of all root diameters in two diameter classes or 0-0.2mm and 0.2-0.4mm (Figure 7-1). Root diameters measured after 20 weeks growth showed similar trends with >90% falling in diameter classes 0-0.2mm and 0.2-0.4mm (Figure 7-2). Increases in total root number, with increasing planting density, at 20 weeks was not as pronounced as that observed at 5 weeks. RAR was highest in field

plots 5 weeks after sowing however, there was large scatter (Figure 7-3), after 20 weeks growth RAR decreased, compared to after 5 weeks growth, with little variability in RAR within planting densities (Figure 7-3).

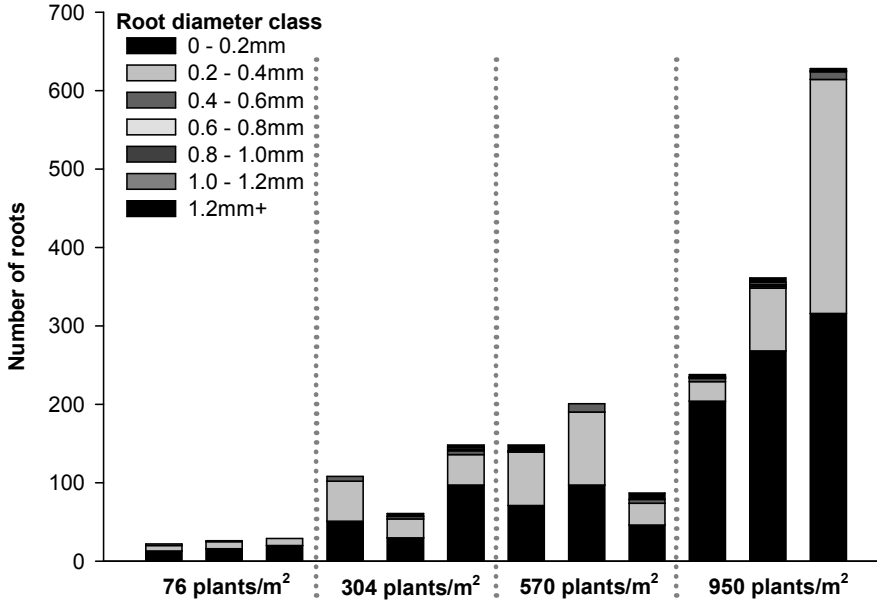

Figure 7-1: Root diameters and number of roots measured at the shear plane for field sampled cores after 5 weeks growth at four different planting densities, three replicates for each planting density. The stacked bars are ordered with the smallest diameter on the bottom and largest diameters at the top

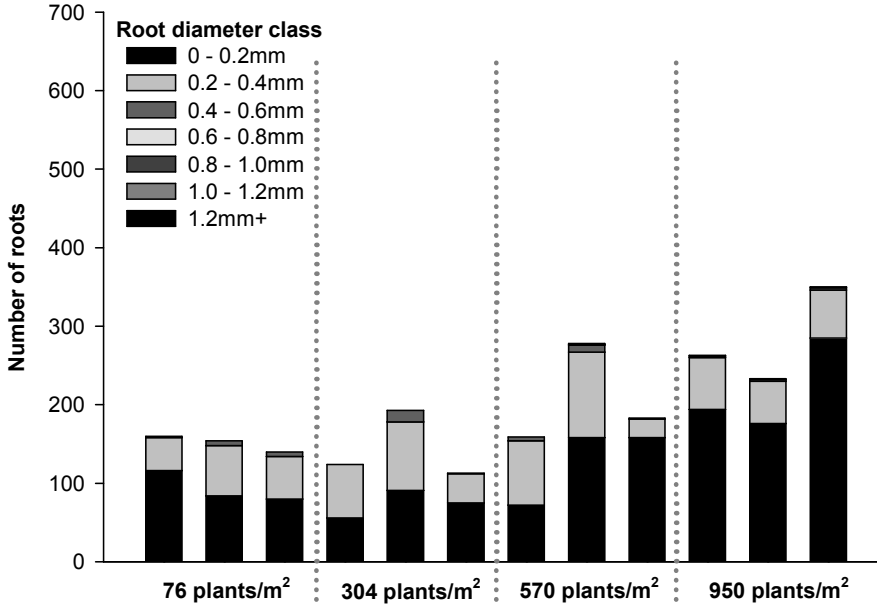

Figure 7-2: Root diameters and number of roots measured at the shear plane for field sampled cores after 20 weeks growth at four different planting densities, three replicates for each planting density. The stacked bars are ordered with the smallest diameter on the bottom and largest diameters at the top

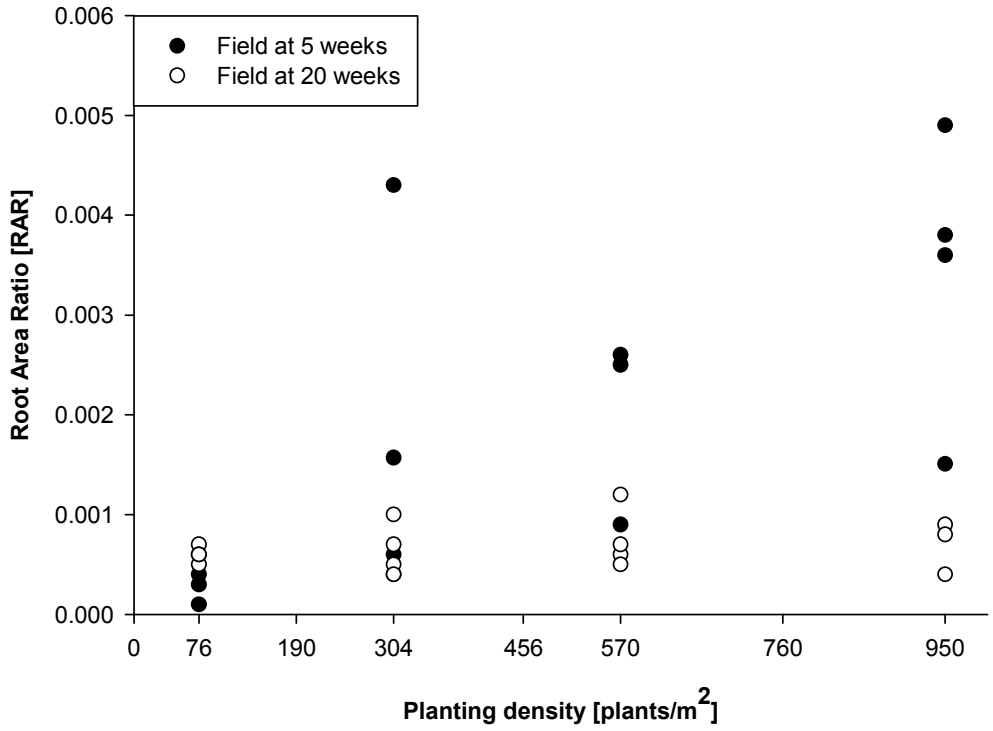

Figure 7-3: Changes in root area ratio (RAR) in field cores 5 and 20 weeks after sowing

7.2.1.2. Glasshouse cores

Root diameter distributions in the glasshouse cores followed similar trends to those observed in field plots. >90% of all root diameters fell within size classes 0.0-0.2mm and 0.2-0.4mm (Figure 7-4). Unlike field plots, however, the total root number was only found to increase up to a planting density to 570 plants/m^2, beyond which total root number decreased. RAR did not exhibit the trends observed within the field grown cores with very little variability between cores and planting density (Figure 7-5).

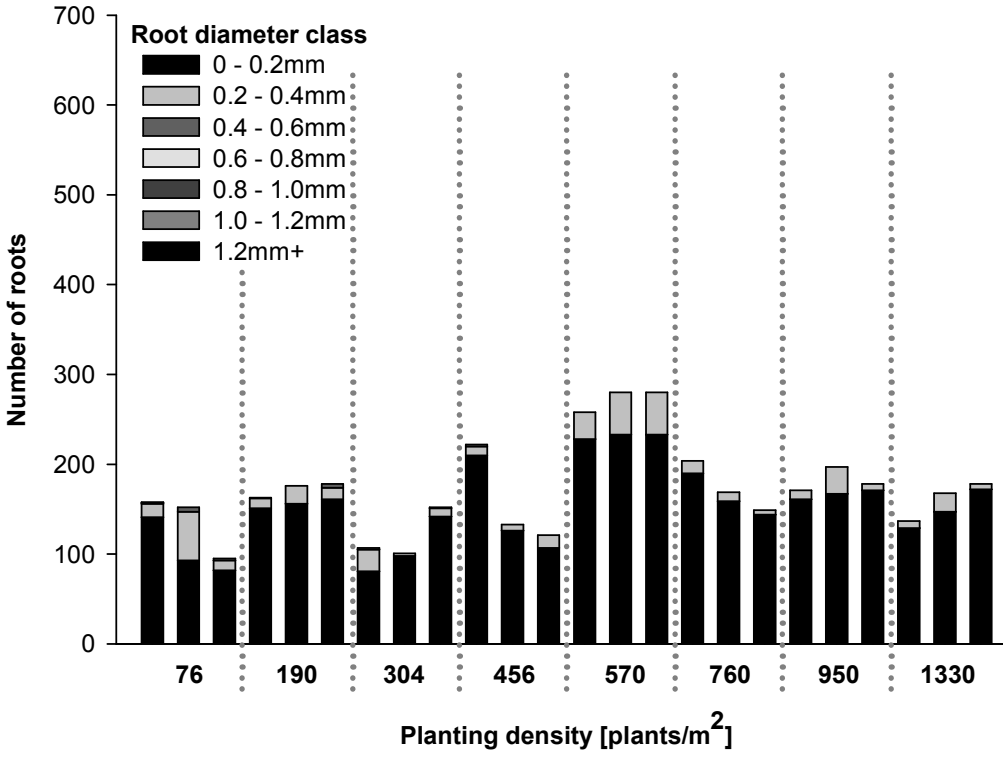

Figure 7-4: Root diameters and number of roots measured at the shear plane for cores grown in the glasshouse at eight different planting densities, three replicates for each planting density. The stacked bars are ordered with the smallest diameter on the bottom and largest diameters at the top

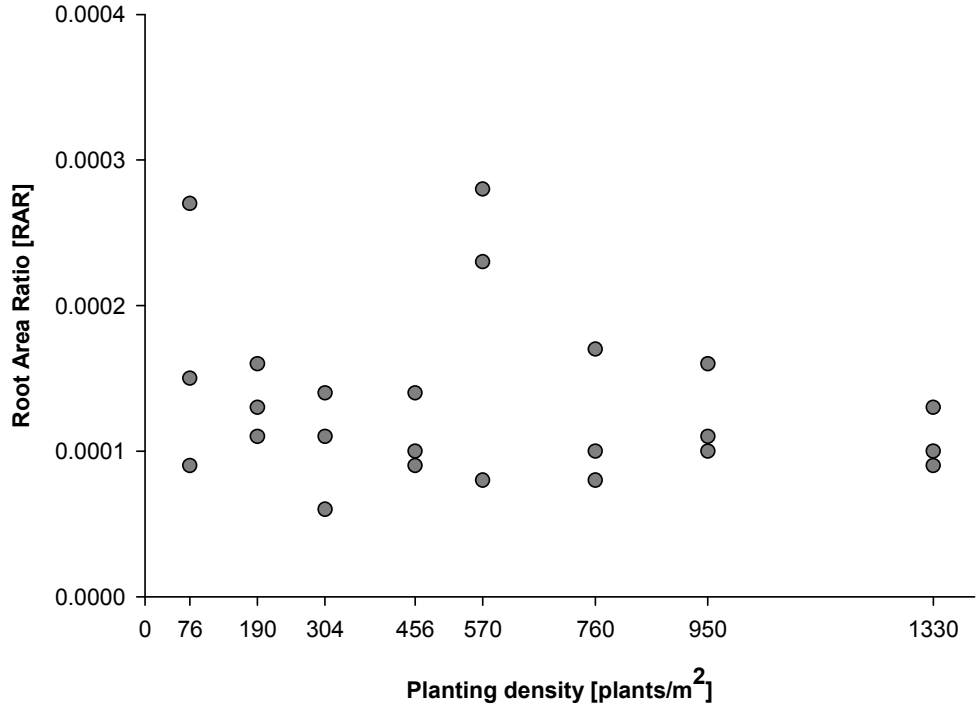

Figure 7-5: Root Area Ratio (RARs) for glasshouse grown cores

7.2.2. Model outputs

7.2.2.1. Field plots

Modelling of reinforcement from data collected shows differing levels of accuracy depending on plant age and planting density but showed a large degree of scatter in nearly all cases. Field results show reinforcement was either overestimated or accurately predicted by the strain based FBM at lower planting densities during early growth, 5 weeks after sowing (Figure 7-6). Planting density affected model accuracy with reinforcement predicted in sparsely planted plots closer to those observed. As plants matured, 20 weeks after sowing, the strain based FBM over-predicted reinforcement for all planting densities, with density not affecting model accuracy (Figure 7-6).

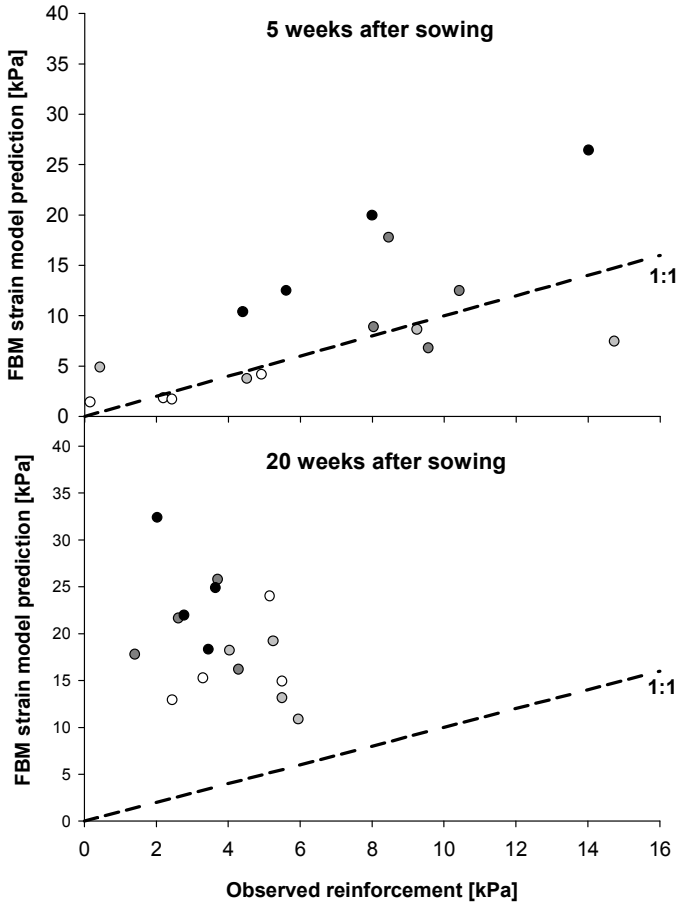

Figure 7-6: Strain based FBM predicted reinforcement plotted against observed reinforcement within field cores after 5 weeks growth and 20 weeks. Gray scale colours represent planting density (76 plants/m², white to 950 plants/m², black)

Results from the stress based FBM were similar to the strain based FBM with reinforcement both over and under predicted after 5 weeks growth (Figure 7-7). Five of the seven predictions over estimated were in those planted at the two highest densities. Reinforcement was again over predicted for all planting densities 20 weeks after sowing (Figure 7-7) with planting density again not found to affect model accuracy unlike that observed after 5 weeks growth.

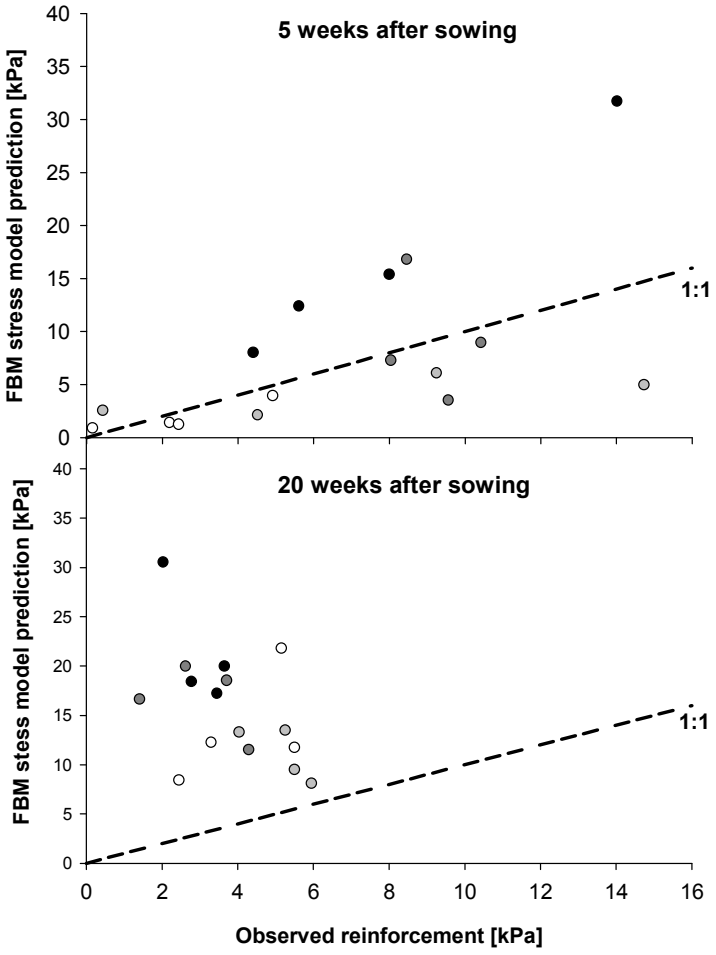

Figure 7-7: Stress based FBM predicted reinforcement plotted against observed reinforcement within field cores after 5 weeks growth and 20 weeks. Gray scale colours represent planting density (76 plants/m², white to 950 plants/m², black)

Predictions using the Wu et al. (1979) model overestimated reinforcement for all planting densities and sampling times. After 5 weeks growth, only one prediction of

reinforcement was underestimated, despite lower planting densities being over-estimated they were closer to the observed reinforcement than those at higher planting densities (Figure 7-8). Reinforcement predicted for mature plants was again over-predicted, similar to that observed within both the strain and stress based FBMs, with planting density not affecting model accuracy (Figure 7-8).

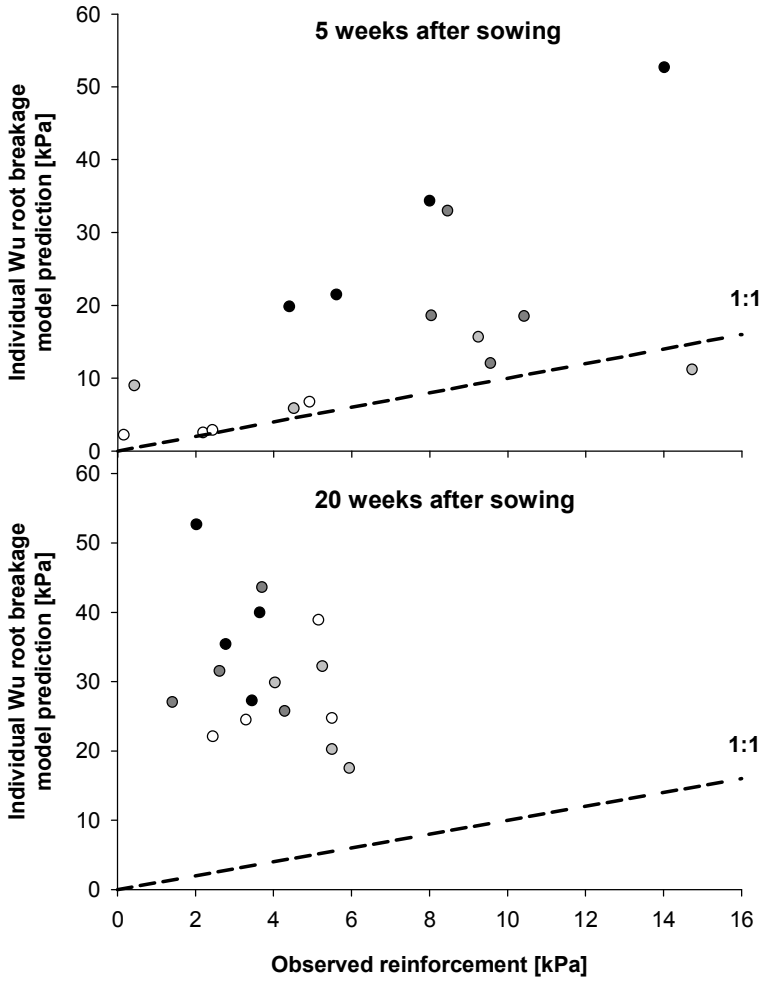

Figure 7-8: Individual root break Wu et al. (1979) model of predicted reinforcement plotted against observed reinforcement within field cores after 5 weeks growth and 20 weeks. Gray scale colours represent planting density (76 plants/m^2, white to 950 plants/m^2, black)

Results from the stress based FBM under predicted reinforcement in nine out of sixteen field cores after 5 weeks growth (Figure 7-9). Of the seven over predicted, five were from

the two highest planting density plots, showing again reduced model accuracy with increasing planting density.

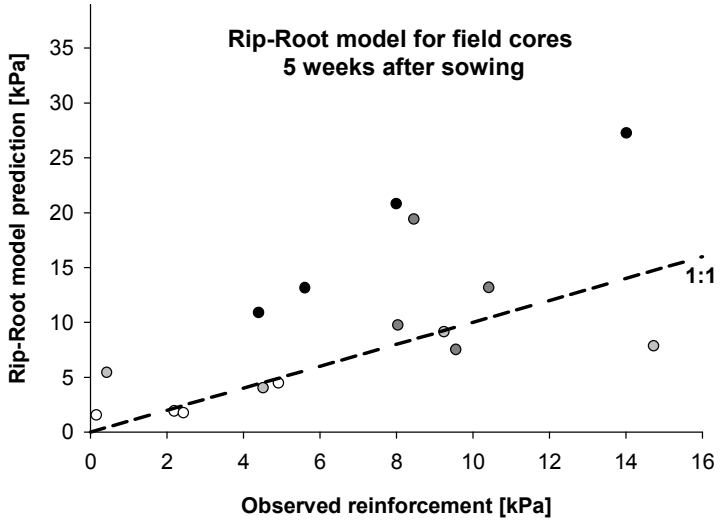

Figure 7-9: Rip-Root model results of predicted reinforcement plotted against observed reinforcement within field cores after 5 weeks growth. Gray scale colours represent planting density (76 plants/m^2, white to 950 plants/m^2, black)

The FBM models and Rip-Root model allow progressive failure of roots to be plotted whilst showing changes in reinforcement during these failures. Root failure within the stress based FBM occurred at lower values of reinforcement when compared to both Rip-Root and the strain based FBM (Figure 7-10). Root failures in both the Rip-Root model and strain based FBM were very similar highlighting only small changes between them associated with changes in calculating strain within the models (Figure 7-10).

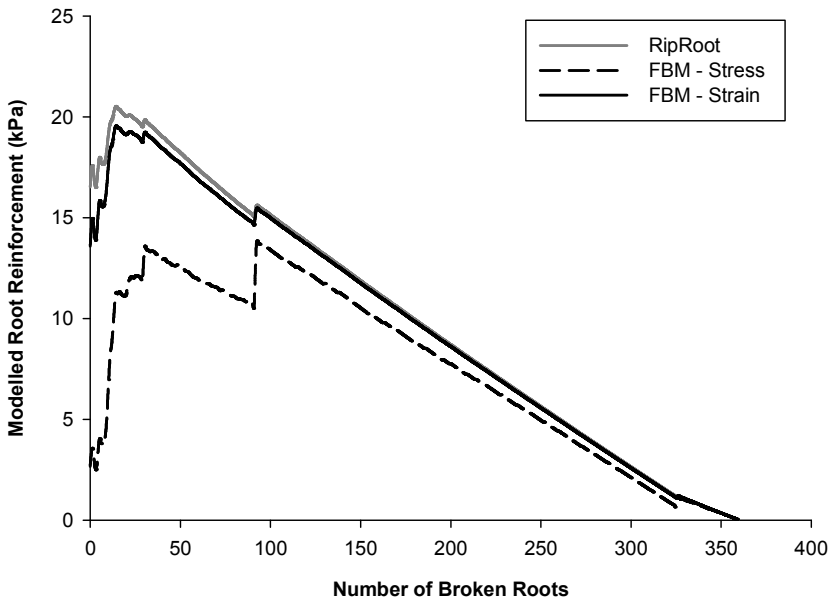

Figure 7-10: Progressive root breakage during Rip-Root and both stress and strain based FBMs. Results are for a field plot planted at 304 plants/m^2

7.2.2.2. Glasshouse cores

Both the strain based FBMs and Wu et al. (1979) model generally over-predicted reinforcement at lower planting densities, with cores at higher planting densities under-predicted. Reinforcement within 70% of the cores was over-predicted by the strain based FBM (Figure 7-11) compared to 75% of those predicted using the Wu et al. (1979) model (Figure 7-11). The Wu et al. (1979) model and the strain based model only under-predicted reinforcement within cores planted at densities >950 plants/m^2. The stress based FBM only over-predicted 46% of the cores, again with those of the lowest planting densities (Figure 7-11).

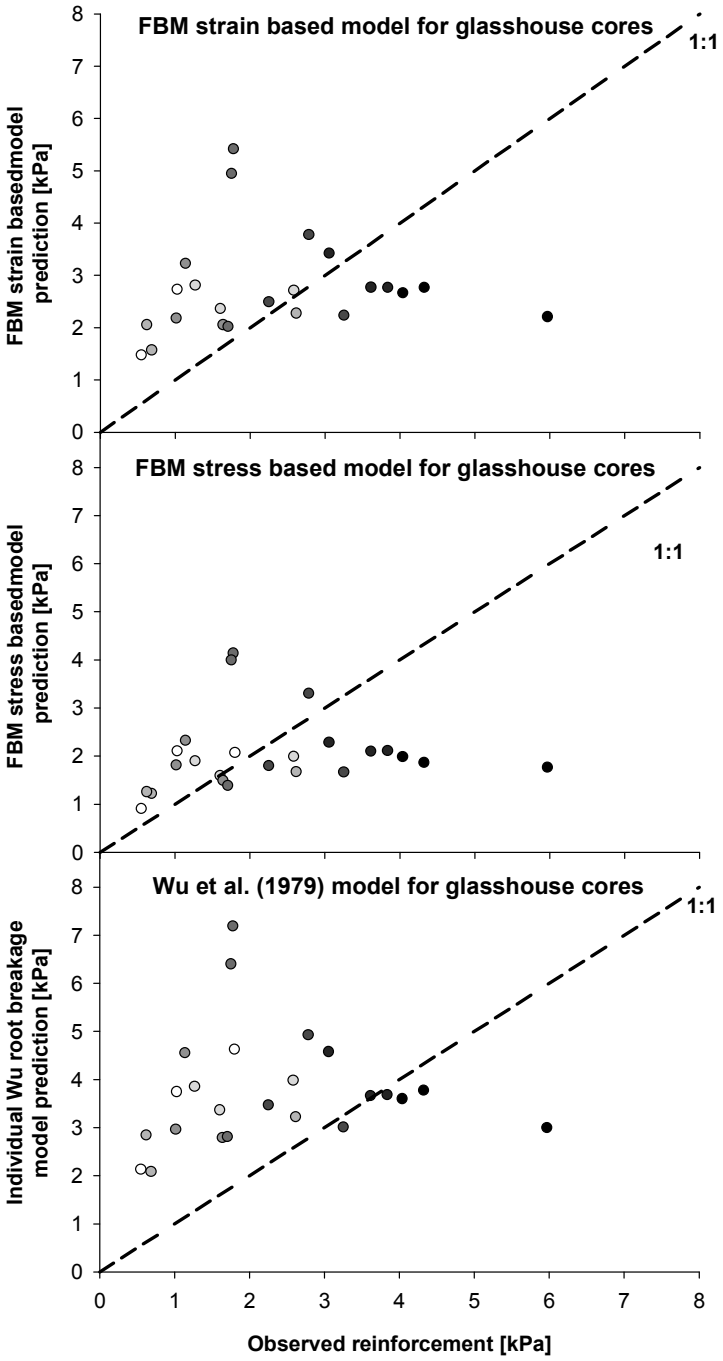

Figure 7-11: Strain and stress based FBMs and individual root break Wu et al. (1979) model predicted reinforcement plotted against observed reinforcement within glasshouse cores. Gray scale colours represent planting density (76 plants/m^2, white to 1330 plants/m^2, black**)**

7.3. *Discussion*

7.3.1. Model outputs

Model results showed that Wu et al. (1979) over-predicted root reinforcement, as has been observed in other studies (Pollen and Simon, 2005). This model works with an unrealistically large RAR due to catastrophic failure, as the progressive breakage of the weakest roots was not considered in this model. The stress based FBM worked better for controlled glasshouse conditions and younger plants in the field, but at 20 weeks in the field the predictions were poor. The strain based models, strain based FBM and Rip-Root, under predicted reinforcement greater than the stress based model. Within the stress based models roots the largest diameter roots broke first, due to them being weaker than the smaller diameter roots. This is unrealistic however due to the smallest roots being stiffer and therefore able to localise stress quicker and break first. When the relationship between stiffness and root diameter was incorporated into the strain based model, reinforcement was predicted to increase with smaller roots breaking first.

All the models used are relatively simplistic, but they did predict reinforcement surprisingly well. One of the major flaws, however, is that they do not incorporate many major factors responsible for reinforcement. Ideally models need to incorporate the influence of roots on bonding and aggregation mechanisms in soil, but the complexity and uncertainty of these processes presents a considerable challenge. The influence of root orientation also needs to be considered, particularly in the FBM where all roots are assumed to be perpendicular to the shear plane. It must also be noted that the development of these reinforcement models has been performed with measurements of root intersection number, which can be substantially underestimated when measured in the field (Bengough et al., 1992).

8. Thesis summary, conclusions and future work

8.1 Summary and conclusions

Interactions between roots and soil that drive mechanical reinforcement have been shown in previous literature to be highly complex. Research has emphasised the contributions of woody rooted plant species to reinforcement (Bischetti et al., 2005; Mickovski et al., 2009; Norris, 2005) with limited research into fibrous roots. This thesis has focussed on fibrous root systems, extremely important for the stabilisation of surface soils against erosion. Fibrous roots may also reinforce soils against crack propagation where cracking may cause slope destabilisation and lead to the preferential flow of contaminants to groundwater. The aim of this thesis was to develop an understanding of fibrous root derived reinforcement by isolating some of the root soil interactions through a range of controlled experiments. Experiments were conducted through manipulation of environmental conditions or the use of novel model plant lines with differing root properties.

Root reinforcement modelling has previously been performed through the use of the root area ratio (RAR), or the amount of root crossing the failure region of interest, with an average value for root strength (Waldron, 1977; Wu et al., 1979). Root strength has widely been reported in publications through negative power-law fits between strength and diameter (Bischetti et al., 2005; Genet et al., 2005; Mickovski et al., 2009; Pollen and Simon, 2005). Initial investigations in Chapter 3 aimed to test the hypothesis that increasing planting density increases root derived reinforcement due to increasing RAR. Experiments were conducted in both the field and under glasshouse conditions using

barley (*Hordeum vulgare*), as a model fibrous root systems, planted at a range of densities. Results from the field experiment showed that RAR can change seasonally, with observations in the field showing decreases in RAR after 20 weeks of growth when compared to that after 5 weeks of growth at a depth of 50mm below the soil surface. Root diameter distribution also showed signs of being influenced by planting density when grown under glasshouse conditions. This may be in response to nutrient availability and potentially a factor within low nutrient soils. Root strength was also observed to decrease with increasing diameter, as previously shown by other authors (Bischetti et al., 2005; Genet et al., 2005; Mickovski et al., 2009; Pollen and Simon, 2005). Chapter 3 highlighted that modelling reinforcement based on RAR may be overly simplistic due to potential effects of low nutrient conditions on root diameter and variability in root strength associated with changing root diameter. Also, with changes in root diameter RAR may not decrease, with plants producing more, finer roots and potential for reinforcement to increase due to relationships between root diameter and strength. Such a relationship was observed in the glasshouse study with reinforcement observed to increase with planting density with limited differences in RAR.

Rooted cores subjected to direct shear testing in Chapter 3 failed within the soil due to either pull-out or breakage failure. Failure mechanisms are difficult to predict and influenced by a variety of factors including soil physical conditions, root architecture, root diameter and stress development within the root during direct shearing. When assessing root architectural effects on increased resistance of roots to pull-out failure, some work has used fabricated root analogues (Mickovski et al., 2007; Sonnenberg, 2008). Chapter 4 attempted to take this a step further by growing plants in soil and manipulating soil effective stress conditions to assess root characteristics and their

effects on the development of either pull-out or breakage failure. No changes in reinforcement were observed between soil treatments, effective stress, and root trait. Further investigations into failure mechanism will be discussed later and future work recommended.

Root age, composition and the environment in which roots grow are fundamental in modelling reinforcement, however, little is known on the impacts to root biomechanics. With climate change predictions forecasting changes in weather patterns, significant effects from plant roots on soil stabilisation could occur. For predicting long term soil stabilisation, the effects of root age requires quantifying. Root cell structure is known to change over time (Zeier et al., 1999) with cellulose and lignin key to root biomechanics (Genet et al., 2005; Niklas, 1992). Chapter 5 highlighted the potential for changes in root biomechanics, rooting depth and root architectural structure resulting from changes in the growth environment. The study highlighted significant impacts on root biomechanics resulting from water logging and also changes in soil bulk density, increasing mechanical impedance. It is widely accepted that root elongation is impeded within soil of a high bulk density (Bengough and Mullins, 1990; Lipiec et al., 2009) but little was known on the likely effects on root strength and stiffness. Data on changing root stiffness and strength as a function of root age further highlighted an important factor not incorporated into reinforcement models. Previous authors have collected root strength data from particular depths in the soil and incorporated these into existing models (e.g. Pollen and Simon, 2005). Collection of root strength data is therefore likely to include both old and young roots, the ratios of which may change over time. This was the first study to investigate specific changes in fibrous root biomechanics as a function

of age and growth environment allowing for data to be incorporated into future root architecture models.

Chapter 5 utilised model mutant barley cultivars to investigate root composition using plants previously shown to contain reduced quantities of lignin. Plants were grown within a growth room environment in both soil and also in an 'ideal' hydroponic setup. Results did not show any clear effects of reduced lignin on root biomechanics. It is possible that this is due to plants not having received any stimulation to above ground biomass. Stimulation may have increased lignin and cellulose content as previously reported by Scippa et al. (2006) and Hales et al. (2009) resulting in a change to plant tissue biomechanics (Cipollini, 1997; Saidi et al., 2009). Changes in agriculture and silviculture may, in future, change plant composition with research into such impacts essential in order for models to be used for land use planning facilitated through large scale mapping applications. Understanding the composition and structures of plant roots will also enable screening of a variety of plant species. Such screening would allow for root biomechanical properties and architecture to be predicted and plant species chosen dependant on the application.

As mentioned previously Chapter 4 investigated root failure mechanisms, Chapter 6 took this further through the visualisation of root failure during direct shear. The effects of root age, type, orientation to the shear plane and length were shown to affect root movement during direct shear. Primarily roots were observed to pull-out of the soil with only young roots observed to break. Prior to ultimate root failures of pull-out and breakage, several other stages relating to strain development were observed. Research by others has concentrated on the mechanical strain generated during pull-out failure during

vertical uprooting (Hamza et al., 2006; Mickovski et al., 2007) with this research the first to investigate strain during direct shear. Also, this is the first study to visualise strain on roots orientated in tension, compression and perpendicular to the shear plane. Development of PIV analysis during direct shear has thus now been developed opening up a variety of opportunities in the future to examine strain during direct shear further.

Key to all of the work conducted was an assessment of root models developed on the principles proposed by Waldron (1977), Wu et al. (1979) and more recently the fibre bundle model (FBM) proposed by Pollen and Simon (2005). Chapter 7 showed that both the stress and strain based FBMs generally predicted root reinforcement more accurately than the model proposed by Wu et al. (1979). Considering the factors affecting root reinforcement the accuracy of the FBMs was surprising however predictions were only good in some, not all, of the studies. This highlights the necessity for future models to incorporate more factors than just root strength, elasticity and diameter.

Key to all of the studies in this thesis has been the use of real plant roots grown in a field soil, as opposed to the use of analogue roots and packed sands (Mickovski et al., 2007). Using real roots and natural soil inherently increases variability due to natural biological and environmental factors in both glasshouse and field studies. However, major processes that drive root reinforcement of soil may not occur in model systems, such as bonding processes in the rhizosphere.

8.2 Incorporation of findings in root reinforcement models

Throughout this thesis, experiments have been conducted in order to increase our understanding of root reinforcement of soils. Chapter 3 highlighted the importance of both the number of roots and also the root diameter in affecting measured reinforcement. Modelling and predicting reinforcement derived from the roots, however, has highlighted that existing models may be over simplistic. A major problem is that models are based entirely on root reinforcement, and fail to incorporate other factors driven by roots that are responsible for increases in soil shear strength. Root area ratio (RAR) has been widely used in the past to predict the reinforcement from roots. However, Chapter 3 has shown increases in reinforcement not associated with increasing RAR.

Fundamental to all models is the strength of roots, with previous literature highlighting the trends in decreased tensile strength with increasing root diameter. More than 550 tensile tests were performed on roots as part of this thesis. Negative power-law relationships, widely adopted within published literature, between strength and diameter were fitted. Strength curve fits were highly variable with r^2 values ranging from 0.048 (Chapter 4) to 0.95 (Chapter 5). Some aspects of fit variability may be attributable to the environment in which the roots were grown, which in itself highlights the requirement to increase research on environmental contributions to root strength. Within the glasshouse experiment conducted in Chapter 3 potential impacts of nutrient availability were observed on root diameters, with roots generally being smaller when competition for nutrients was greater due to increases in planting density. Regression curves relating diameter to strength suggested that reinforcement would be greater as result of stronger, finer roots. This was supported by the finding of RAR remaining constant with

increasing planting density in glasshouse cores, whilst shear strength was observed to increase. Despite similar RAR, a shift towards a greater number of finer roots with increased planting density, probably caused this increase in shear strength.

8.3 Importance of the mechanical behaviour of soil

The role of soil mechanics and the contribution to reinforcement by fibrous roots has not been discussed within this thesis. It was decided that roots alone presented a complex challenge so the experiments were designed that focussed only on root properties. Soil physical properties have significant impacts on root reinforcement, for example that of effective stress discussed in Chapter 4. Early models of root reinforcement incorporated a root contribution to models of soil shear strength simply by adding to the cohesion parameter. More recent models, such as the FBM, remove soil shear resistance, focussing on predicting the contribution of roots alone. Fully coupled models, with soil and roots included, need to be developed. However the complexities of this task cannot be underestimated. Coupling models would, however, allow for failure mechanism to be incorporated through the addition effective stress in relation to the root soil frictional bond. In order to achieve this a better understanding of the switch from pull-out to breakage failure is required and also quantification of the role unbroken roots play in providing strength to soils (Hales et al., 2009).

8.4 Complexity of root-soil interactions

Chapter 5 showed root age was important to root strength, with older roots stronger than younger roots. Root age was examined as a function of the distance from the root tip. Root strength increased with distance from the root tip, thereby translating to the strongest root sections being those closest to the stem base. Such an observation suggests that thigmomorphogenesis may play a role in root strength, with roots strongest at the stem base in order to support the above ground biomass. Chapter 5 also demonstrated the effects of the environment on plant growth and biomechanics. Roots in waterlogged or compacted soil, for instance, did not penetrate soil as deeply as observed in well drained soil or less compacted soil. Due to the root system of barley (*Hordeum vulgare*) being composed of lateral, nodal and seminal roots, different structures in the plant root tissue exist and were shown to result in different biomechanics. To date, changes in root biomechanics have not been reported by root type, with previous work generally reporting per species. Such knowledge of differing root strength, dependant on root type and growth environment, will further increase the potential accuracy of models. Moreover, these data provide fascinating insight into the mechanical interactions between roots and soil based on the whole root system. The failure to examine this in previous research omits the behaviour of large portions of the root system that could drive reinforcement and anchorage. Incorporation of changing root strengths into root growth architecture models has the potential to allow soil shear strength to be predicted dependant on environment and architectural composition.

8.5 Major weaknesses of root reinforcement models

Chapter 7 demonstrated that the most commonly used model of root reinforcement developed by Wu et al. (1979) provides a poor prediction due to the assumptions of simultaneous root breakage and does not describe the observed failure mechanism. This supports the work of Pollen & Simon (2007), but the work presented here could be compared directly to shear tests conducted under controlled conditions. Moreover, the information on root diameters and abundance crossing the shear plane was unique.

A major requirement in future root reinforcement models in the incorporation of root stiffness to predict root breakage with increasing shear displacement. Root biomechanical tensile tests have shown root elasticity to exhibit power-law relations to root diameter, as observed with root strength. Chapter 6 enabled strain development to be visualised during direct shear, highlighting different responses dependant on root orientation and root age. Limitations of the study were that it was not possible to grow roots in the soil, eliminating the potential effects of rhizosphere processes in increasing root resistance to pull-out failure. However, these data did show that orientation influences how shear displacement induces strain in plant roots. Rather than accounting directly for strain, as done in Chapter 7, a correction may be needed to include the influence of root re-orientation and partial pull-out.

Another great challenge to modelling is the variability in the mechanical properties of roots. Although power-laws relationships could be fitted to root stiffness and strength, earlier discussion in this Chapter has highlighted the variability in the fitted data. This thesis used only one plant species, (barley, *Hordeum vulgare*) with root strength highly variable and influenced by environmental conditions. Attempting to predict the

contributions of a biologically diverse assemblage of plants to reinforcement is therefore, at this stage, not possible without further work. Greater research focus needs to be placed on whether root strength is influenced greater by the environment than assuming root populations have a specific strength relationship to root diameter. Within all of the research chapters one or more environmental condition may have been responsible for changes in root biomechanical properties or contributions made by plants to reinforcement.

8.6 Future work

Work in this thesis has highlighted areas of research that need to be assessed further. More research will enable development of more holistic models incorporating more factors thereby increasing model accuracy. Such areas of research in the future may incorporate:

- Root strain during direct shear. A better understanding of the difficulties of measuring strain during shear has been highlighted in this thesis. Further work can build on these foundations with more accurate measurement of strain development along root lengths and the effects of root orientation.

- Changes in root orientation during direct shear. Currently it is very difficult to view the manner in which roots have failed, through either breakage or pull-out, or changed orientation during direct shearing of soil. Visualising root architecture through the use of X-ray scanning is work that could significantly increase modelling accuracy on multiple levels. Previously such work has been

compromised by issues of image resolution however techniques have now been developed allowing fine roots to be visualised within soil cores (Tracy et al., 2010). Root orientation could be assessed prior to direct shear testing and changes assessed following different amounts shearing, up to failure. Non-invasive investigations into root failure mechanisms could also be assessed without potential root damage through root excavation. This is critical due to the fine nature of fibrous roots where roots may break during the root washing process.

- Effects of rhizosphere processes on root failure and potential effects on soil reinforcement. No research has yet investigated the role of rhizosphere processes in contributing to the failure mechanism. Papers have demonstrated the benefits in improving soil structure through root growth (Angers and Caron, 1998; Hallett et al., 2009), but the effects on the frictional resistance of roots shear failure has not been addressed.

- Thigmomorphogenesis and its effect on root biomechcnics. Previous research has shown that plant biomechanics is significantly affected (Cipollini, 1997; Saidi et al., 2009) but little is known on the effects below ground. Many plants in research are grown in glasshouses where plants are protected from natural perturbation, such as wind. Investigations into the effects of mechanical stimulation on root strength may yield important information in both how far down the root length stress is transferred and also quantify the effects on root strength.

- Root decomposition and root biomechanics were found to change with age with older roots being stronger. Less is known on the effects of root degradation on the biomechanics of smaller diameter roots. Although studies have investigated degradation impacts in woody species, less is understood regarding fine root biomechanics and therefore a weakness when attempting to model long-term soil stability.

- The interactions of multiple plants, or assemblages of plants, on reinforcement is another area requiring further investigation. Root systems of different plant species inhabit different depths in the soil (Jackson et al., 1996) with little known on the effects of root interactions between different species. Research currently examines each root as an individual element where each element has different architecture increasing the resistance of the root to failure. It is possible that even single tap root like elements may become intertwined with other single tap root elements, thereby increasing failure resistance. This is a simplistic interaction, however, one that may significantly increase soil shear strength.

References

Abe K and Ziemer R R 1991 Effect of tree roots on a shear zone - Modeling reinforced shear-stress. Canadian Journal of Forest Research 21, 1012-1019.

Abernethy B and Rutherfurd I D 1999 The distribution and strength of riparian tree roots in relation to riverbank reinforcement. Hydrological Processes 15, 63-79.

Adrian R J 1991 Particle-imaging techniques for experimental fluid-mechanics. Annual Review of Fluid Mechanics 23, 261-304.

Aggarwal P, Choudhary K K, Singh A K and Chakraborty D 2006 Variation in soil strength and rooting characteristics of wheat in relation to soil management. Geoderma 136, 353-363.

Angers D A and Caron J 1998 Plant-induced changes in soil structure: Processes and feedbacks. Biogeochemistry 42, 55-72.

Bailey P H J, Currey J D and Fitter A H 2002 The role of root system architecture and root hairs in promoting anchorage against uprooting forces in *Allium cepa* and root mutants of *Arabidopsis thaliana*. Journal of Experimental Botany 53, 333-340.

Barlow P W and Baluska F 2000 Cytoskeletal, perspectives on root growth and morphogenesis. Annual Review of Plant Physiology and Plant Molecular Biology 51, 289-322.

Baruch Z and Merida T 1995 Effects of drought and flooding on root anatomy in four tropical forage grasses. International Journal of Plant Sciences 156, 514-521.

Bates, B.C., Z.W. Kundzewicz, S. Wu and J.P. Palutikof, Eds., 2008: Climate change and water. Technical paper of the Intergovernmental Panel on Climate Change, IPCC Secretariat, Geneva, Switzerland.

Bauhus J and Messier C 1999 Evaluation of fine root length and diameter measurements obtained using RHIZO image analysis. Agronomy Journal 91, 142-147.

Beek L, Wint J, Cammeraat L and Edwards J 2005 Observation and simulation of root reinforcement on abandoned Mediterranean slopes. Plant and Soil 278, 55-74.

Bengough A G and Mullins C E 1990 Mechanical impedance to root-growth - a review of experimental-techniques and root-growth responses. Journal of Soil Science 41, 341-358.

Bengough A G, Bransby M F, Hans J, McKenna S J, Roberts T J and Valentine T A 2006 Root responses to soil physical conditions; growth dynamics from field to cell. Journal of Experimental Botany 57, 437-447.

Berry P M, Sterling M, Spink J H, Baker C J, Sylvester-Bradley R, Mooney S J, Tams A R and Ennos A R 2004 Understanding and reducing lodging in cereals. Advances in Agronomy 84, 217- 271.

Bilbro J D, Undersander D J, Fryrear D W and Lester C M 1991 A survey of lignin, cellulose, and acid detergent fiber ash contents of several plants and implications for wind erosion control. Journal of Soil and Water Conservation 46, 314-316.

Bischetti G B, Chiaradia E A, Epis T and Morlotti E 2009 Root cohesion of forest species in the Italian Alps. Plant and Soil 324, 71-89.

Bischetti G B, Chiaradia E A, Simonato T, Speziali B, Vitali B, Vullo P and Zocco A 2005 Root strength and root area ratio of forest species in Lombardy (Northern Italy). Plant and Soil 278, 11-22.

Bohm W 1979 Root parameters and their measurement. In Methods of studying root systems. 125-138. Springer-Verlag, Berlin.

Boudet A M, Kajita S, Grima-Pettenati J and Goffner D 2003 Lignins and lignocellulosics: a better control of synthesis for new and improved uses. Trends in Plant Science 8, 576-581.

Campbell M M and Sederoff R R 1996 Variation in lignin content and composition - Mechanism of control and implications for the genetic improvement of plants. Plant Physiol. 110, 3-13.

Caravaca F, Alguacil M M, Azcon R and Roldan A 2006 Formation of stable aggregates in rhizosphere soil of *Juniperus oxycedrus*: Effect of AM fungi and organic amendments. Applied Soil Ecology 33, 30-38.

Cheng H and Liu A P 2003 Comparison of root strength of different plant species. Water-Saving Agriculture and Sustainable Use of Water and Land Resources, Volumes 1 and 2, Proceedings 149-152.

Cipollini D F 1997 Wind-induced mechanical stimulation increases pest resistance in common bean. Oecologia 111, 84-90.

Cipollini D F 1998 The induction of soluble peroxidase activity in bean leaves by wind-induced mechanical perturbation. American Journal of Botany 85, 1586-1591.

Cofie P and Koolen A J 2001 Test speed and other factors affecting the measurements of tree root properties used in soil reinforcement models. Soil & Tillage Research 63, 51-56.

Coppin N J and Richards I G 1990 Use of Vegetation in Civil Engineering. CIRIA (Construction Industry Research and Information Association). Publisher: Butterworth-Heinemann, Oxford, United Kingdom.

Costa C, Dwyer L M, Hamel C, Muamba D F, Wang X L, Nantais L and Smith D L 2001 Root contrast enhancement for measurement with optical scanner-based image analysis. Canadian Journal of Botany 79, 23-29.

Crook M J, Ennos A R and Sellers E K 1994 Structural development of the shoot and root systems of two winter wheat cultivars, *Triticum aestivum L.* Journal of Experimental Botany 45, 857-863.

Dakora F D and Nelwamondo A 2003 Silicon nutrition promotes root growth and tissue mechanical strength in symbiotic cowpea. Functional Plant Biology 30, 947-953.

Daniels H E 1945 The statistical theory of the strength of bundles of threads. Proceedings of the Royal Society of London Series A - Mathematical and Physical Sciences 183, 405-435.

Danjon F, Barker D H, Drexhage M and Stokes A 2008 Using three-dimensional plant root architecture in models of shallow-slope stability. Annals of Botany 101, 1281-1293.

De Baets S, Poesen J, Knapen A and Galindo P 2007 Impact of root architecture on the erosion-reducing potential of roots during concentrated flow. Earth Surface Processes and Landforms 32, 1323-1345.

De Baets S, Torri D, Poesen J, Salvador M P and Meersmans J 2008 Modelling increased soil cohesion due to roots with EUROSEM. Earth Surface Processes and Landforms 33, 1948-1963.

de Leon-Gonzalez F, Celada-Tornel E, Hidalgo-Moreno C I, Etchevers-Barra J D, Gutierrez-Castorena M C and Flores-Macias A 2006 Root-soil adhesion as affected by crop species in a volcanic sandy soil of Mexico. Soil and Tillage Research 90, 77-83.

Dickin E and Wright D 2008 The effects of winter waterlogging and summer drought on the growth and yield of winter wheat (*Triticum aestivum L.*). European Journal of Agronomy 28, 234-244.

Docker B B and Hubble T C T 2008 Quantifying root-reinforcement of river bank soils by four Australian tree species. Geomorphology 100, 401-418.

Easson D L, Pickles S J and White E M 1995 A study of the tensile force required to pull wheat roots from soil. Annals of Applied Biology 127, 363-373.

Ennos A R 1990 The anchorage of leek seedlings - the effect of root length and soil strength. Annals of Botany 65, 409-416.

Ennos A R 1991 The mechanics of anchorage in wheat *triticum-aestivum*. The anchorage of wheat seedlings. Journal of Experimental Botany 42, 1601-1606.

Epstein E 1994 The anomaly of silicon in plant biology. Proceedings of the National Academy of Sciences of the United States of America 91, 11-17.

Escobar J C, Lora E S, Venturini O J, Yáñez E E, Castillo E F and Almazan O 2008 Biofuels: Environment, technology and food security. Renewable and Sustainable Energy Reviews 13, 1275-1287.

Fan C C and Su C F 2008 Role of roots in the shear strength of root-reinforced soils with high moisture content. Ecological Engineering 33, 157-166.

Fredlund D G, Xing A Q, Fredlund M D and Barbour S L 1996 The relationship of the unsaturated soil shear strength to the soil-water characteristic curve. Canadian Geotechnical Journal 33, 440-448.

Genet M, Kokutse N, Stokes A, Fourcaud T, Cai X, Ji J and Mickovski S 2008 Root reinforcement in plantations of *Cryptomeria japonica* D. Don: effect of tree age and stand structure on slope stability. Forest Ecology and Management 256, 1517-1526.

Genet M, Stokes A, Salin F, Mickovski S, Fourcaud T, Dumail J F and van Beek R 2005 The influence of cellulose content on tensile strength in tree roots. Plant and Soil 278, 1-9.

Glade T 2003 Landslide occurrence as a response to land use change: a review of evidence from New Zealand. CATENA 51, 297-314.

Goodman A M and Ennos A R 1999 The effects of soil bulk density on the morphology and anchorage mechanics of the root systems of sunflower and maize. Annals of Botany 83, 293-302.

Gray D H and Ohashi H 1983 Mechanics of fiber reinforcement in sand. Journal of Geotechnical Engineering 109, 335-353.

Guo L B, Halliday M J and Gifford R M 2006 Fine root decomposition under grass and pine seedlings in controlled environmental conditions. Applied Soil Ecology 33, 22-29.

Gyssels G, Poesen J, Bochet E and Li Y 2005 Impact of plant roots on the resistance of soils to erosion by water: a review. Progress in Physical Geography 29, 189-217.

Hackett C 1968 A study of the root system of barley. I. Effects of nutrition on two varieties. New Phytologist 67, 287-299.

Hales T C, Ford C R, Hwang T, Vose J M and Band L E 2009 Topographic and ecologic controls on root reinforcement. Journal of Geophysical Research-Earth Surface 114.

Hallett P D, Feeney D S, Bengough A G, Rillig M C, Scrimgeour C M and Young I M 2009 Disentangling the impact of AM fungi versus roots on soil structure and water transport. Plant and Soil 314, 183-196.

Hamza M A and Anderson W K 2005 Soil compaction in cropping systems - A review of the nature, causes and possible solutions. Soil & Tillage Research 82, 121-145.

Hamza O, Bengough A G, Bransby M F, Davies M C R and Hallett P D 2006 Biomechanics of plant roots: estimating localised deformation with particle image velocimetry. Biosystems Engineering 94, 119-132.

Hamza O, Bengough A G, Bransby M F, Davies M C R, Halpin C and Hallett P D 2007 Novel biomechanical analysis of plant roots. In: Eco- and Ground Bio-Engineering: The Use of Vegetation to Improve Slope Stability, Proceedings of the First International Conference on Eco-Engineering 13-17 September 2004 13-20.

Hathaway R and Penny D 1975 Root strength in some *Populus* and *Salix* clones. New Zealand Journal of Botany 13, 333-344.

Hepworth D G and Vincent J F V 1998 The mechanical properties of xylem tissue from tobacco plants (*Nicotiana tabacum* 'Samsun'). Annals of Botany 81, 751-759.

Hidalgo R C, Moreno Y, Kun F and Herrmann H J 2002 Fracture model with variable range of interaction. Physical Review E 65, article 046148 2002.

Horn R and Smucker A 2005 Structure formation and its consequences for gas and water transport in unsaturated arable and forest soils. Soil & Tillage Research 82, 5-14.

Hu W J, Harding S A, Lung J, Popko J L, Ralph J, Stokke D D, Tsai C J and Chiang V L 1999 Repression of lignin biosynthesis promotes cellulose accumulation and growth in transgenic trees. Nature Biotechnology 17, 808-812.

Jackson R B, Canadell J, Ehleringer J R, Mooney H A, Sala O E and Schulze E D 1996 A global analysis of root distributions for terrestrial biomes. Oecologia 108, 389-411.

Jaffe M J 1973 Thigmomorphogenesis - Response of plant-growth and development to mechanical stimulation - with special reference to *Bryonia-Dioica*. Planta 114, 143-157.

Kohler L 2000 Biphasic mechanical behaviour of plant tissues. Materials Science & Engineering C-Biomimetic and Supramolecular Systems 11, 51-56.

Kohler L and Spatz H C 2002 Micromechanics of plant tissues beyond the linear-elastic range. Planta 215, 33-40.

Konopka B, Pages L and Doussan C 2008 Impact of soil compaction heterogeneity and moisture on maize (*Zea mays L.*) root and shoot development. Plant, Soil and Environment 54, 509-519.

Li Y Y and Shao M A 2006 Change of soil physical properties under long-term natural vegetation restoration in the Loess Plateau of China. Journal of Arid Environments 64, 77-96.

Lipiec J, Wojciga A and Horn R 2009 Hydraulic properties of soil aggregates as influenced by compaction. Soil & Tillage Research 103, 170-177.

Loades K W, Bengough A G, Bransby M F and Hallett P D 2010 Planting density influence on fibrous root reinforcement of soils. Ecological Engineering 36, 276-284.

Lobo I 2008 Pleiotropy: One gene can affect multiple traits. Nature Education 1. Available online at: http://www.nature.com/scitable/topicpage/Pleiotropy-One-Gene-Can-Affect-Multiple-Traits-569 [Accessed January 2010].

Lopez-Bucio J, Cruz-Ramirez A and Herrera-Estrella L 2003 The role of nutrient availability in regulating root architecture. Current Opinion in Plant Biology 6, 280-287.

Materechera S A, Dexter A R and Alston A M 1992 Formation of Aggregates by Plant-Roots in Homogenized Soils. Plant and Soil 142, 69-79.

Mattia C, Bischetti G B and Gentile F 2005 Biotechnical characteristics of root systems of typical Mediterranean species. Plant and Soil 278, 23-32.

Mickovski S B, Bengough A G, Bransby M F, Davies M C R, Hallett P D and Sonnenberg R 2007 Material stiffness, branching pattern and soil matric potential affect the pullout resistance of model root systems. European Journal of Soil Science 58, 1471-1481.

Mickovski S B, Bengough A G, Bransby M F, Davies M C R, Hallett P D and Sonnenberg R 2006 The root-soil interface during uprooting (poster), Scottish Crop Research Institute, Dundee, United Kingdom.

Mickovski S, Hallett P D, Bengough A G, Bransby M F, Davies M C R and Sonnenberg R 2009 The effect of willow roots on the shear strength of soil. Soil Science Society of America Journal 73, 1276-1285.

Milleret R, Le Bayon R C, Lamy F, Gobat J M and Boivin P 2009 Impact of roots, mycorrhizas and earthworms on soil physical properties as assessed by shrinkage analysis. Journal of Hydrology 373, 499-507.

Mooney S J, Morris C and Berry P M 2006 Visualization and quantification of the effects of cereal root lodging on three-dimensional soil macrostructure using X-ray computed tomography. Soil Science 171, 706-718.

Niklas K J 1992 Some biological and physical preliminaries. In Plant biomechanics: An engineering approach to plant form and function 1-47, The University of Chicago Press, London.

Niklas K J 1998 Effects of Vibration on Mechanical Properties and Biomass Allocation Pattern of *Capsella bursa-pastoris* (Cruciferae). Annals of Botany 82, 147-156.

Norris J 2005 Root reinforcement by hawthorn and oak roots on a highway cut-slope in Southern England. Plant and Soil 278, 43-53.

O'Loughlin C and Ziemer R R 1982 The importance of root strength and deterioration rates upon edaphic stability in steepland forests. pp. 70-78. Oregon State University, Corvallis, Oregon.

Operstein V and Frydman S 2000 The influence of vegetation on soil strength. Ground Improvement 4, 81-89.

Osman N and Barakbah S S 2006 Parameters to predict slope stability - Soil water and root profiles. Ecological Engineering 28, 90-95.

Pardo A, Amato M and Chiaranda F Q 2000 Relationships between soil structure, root distribution and water uptake of chickpea (*Cicer arietinum L.*). Plant growth and water distribution. European Journal of Agronomy 13, 39-45.

Pedersen J F, Vogel K P and Funnell D L 2005 Impact of reduced lignin on plant fitness. Crop Science 45, 812-819.

Pierret A, Doussan C, Capowiez Y, Bastardie F and Pages L 2007 Root functional architecture: A framework for modeling the interplay between roots and soil. Vadose Zone Journal 6, 269-281.

Pollen N 2007 Temporal and spatial variability in root reinforcement of streambanks: Accounting for soil shear strength and moisture. CATENA 69, 197-205.

Pollen N and Simon A 2005 Estimating the mechanical effects of riparian vegetation on stream bank stability using a fiber bundle model. Water Resources Research 41, W07025.

Pollen-Bankhead N and Simon A 2010 Hydrologic and hydraulic effects of riparian root networks on streambank stability: Is mechanical root-reinforcement the whole story? Geomorphology 116, 353-362.

Reubens B, Pannemans B, Danjon F d r, De Proft M, De Baets S, De Baerdemaeker J, Poesen J and Muys B 2009 The effect of mechanical stimulation on root and shoot development of young containerised *Quercus robur* and *Robinia pseudoacacia* trees. Trees - Structure and Function 23, 1213-1228.

Reubens B, Poesen J, Danjon F, Geudens G and Muys B 2007 The role of fine and coarse roots in shallow slope stability and soil erosion control with a focus on root system architecture: a review. Trees - Structure and Function 21, 385-402.

Ryden P, Sugimoto-Shirasu K, Smith A C, Findlay K, Reiter W D and McCann M C 2003 Tensile properties of *Arabidopsis* cell walls depend on both a xyloglucan cross-linked microfibrillar network and rhamnogalacturonan II-borate complexes. Plant Physiology 132, 1033-1040.

Saidi I, Ammar S, mont-Caulet N, Thevenin J, Lapierre C, Bouzid S and Jouanin L 2009 Thigmomorphogenesis in *Solanum lycopersicum*: Morphological and biochemical responses in stem after mechanical stimulation. Plant Science 177, 1-6.

Scippa G S, Di Michele M, Di Iorio A, Costa A, Lasserre B and Chiatante D 2006 The response of *Spartium junceum* roots to slope: Anchorage and gene factors. Annals of Botany 97, 857-866.

Shewbridge S E and Sitar N 1996 Formation of shear zones in reinforced sand. Journal of Geotechnical Engineering 122, 873-885.

Silva S d, Castro E and Soares A 2003 Effects of different water regimes on the anatomical characteristics of roots of grasses promising for revegetation of areas surrounding hydroelectric reservoirs. Ciencia e Agrotecnologia 27, 393-397.

Sonnenberg R 2008 PhD Thesis: Centrifuge modelling of root reinforced slopes. University of Dundee, Scotland.

Stephens J 2008 Personal communications. Scottish Crop Research Institute, Dundee, United Kingdom.

Stokes A and Mattheck C 1996 Variation of wood strength in tree roots. Journal of Experimental Botany 47, 693-699.

Stokes A, Atger C, Bengough A G, Fourcaud T and Sidle R C 2009 Desirable plant root traits for protecting natural and engineered slopes against landslides. Plant and Soil 324, 1-30.

Swinnen J, Van Veen J A and Merckx R 1994 Rhizosphere carbon fluxes in field-grown spring wheat: Model calculations based on 14C partitioning after pulse-labelling. Soil Biology and Biochemistry 26, 171-182.

Thomas R E and Pollen-Bankhead N 2010 Modeling root-reinforcement with a fiber-bundle model and Monte Carlo simulation. Ecological Engineering 36, 47-61.

Tisdall J M and Oades J M 1982 Organic-Matter and Water-Stable Aggregates in Soils. Journal of Soil Science 33, 141-163.

Tobias S 1995 Book: Vegetation and slopes- stabilisation, protection and ecology; Title of paper: Shear strength of the soil root bond system. Proceedings of the international conference held at the University Museum, Oxford, 29-30th September 1994 280-286.

Tosi M 2007 Root tensile strength relationships and their slope stability implications of three shrub species in the Northern Apennines (Italy). Geomorphology 87, 268-283.

Toukura Y, Devee E and Hongo A 2006 Uprooting and shearing resistances in the seedlings of four weedy species. Weed Biology and Management 6, 35-43.

Tracy S, Roberts J, Black C, McNeill A, Davidson R and Mooney S 2010 The X-factor: visualizing undisturbed root architecture in soils using X-ray computed tomography. Journal of Experimental Botany 61.

Vincent C D and Gregory P J 1989 Effects of Temperature on the Development and Growth of Winter-Wheat Roots .1. Controlled Glasshouse Studies of Temperature, Nitrogen and Irradiance. Plant and Soil 119, 87-97.

Waldron L and Dakessian S 1981 Soil reinforcement by roots: calculation of increased soil shear resistance from root properties. Soil Science 132.

Waldron L J 1977 Shear resistance of root-permeated homogeneous and stratified soil. Soil Science Society of America Journal 41, 843-849.

Wang J, Zhu J M, Lin Q Q, Li X J, Teng N J, Li Z S, Li B, Zhang A M and Lin J X 2006 Effects of stem structure and cell wall components on bending strength in wheat. Chinese Science Bulletin 51, 815-823.

Watson A, Marden M and Rowan D 1997 Root-wood strength deterioration in Kanuka after clearfelling. New Zealand Journal of Forestry Science 27, 205-215.

Watson A, Phillips C and Marden M 1999 Root strength, growth, and rates of decay: root reinforcement changes of two tree species and their contribution to slope stability. Plant and Soil 217, 39-47.

Watt M, Magee L J and McCully M E 2008 Types, structure and potential for axial water flow in the deepest roots of field-grown cereals. New Phytologist 178, 135-146.

Watt M, McCully M E and Kirkegaard J A 2003 Soil strength and rate of root elongation alter the accumulation of Pseudomonas spp. and other bacteria in the rhizosphere of wheat. Functional Plant Biology 30, 483-491.

Welbank P J, Gibb M J, Taylor P J and Wiliams W D 1973 Root growth of cereal crops. Rothamsted Report for 1973 Part 2 26-66.

White D J and Take W A 2002 GeoPIV: Particle Image Velocimetry (PIV) software for use in geotechnical engineering. Cambridge University Engineering Department, Cambridge, United Kingdom.

White N A, Hallett P D, Feeney D, Palfreyman J W and Ritz K 2000 Changes to water repellence of soil caused by the growth of white-rot fungi: Studies using a novel microcosm system. Microbiology Letters 184, 73-77.

Wrobel-Kwiatkowska M, Starzycki M, Zebrowski J, Oszmianski J and Szopa J 2007 Lignin deficiency in transgenic flax resulted in plants with improved mechanical properties. Journal of Biotechnology 128, 919-934.

Wu T H, Mckinnell W P and Swanston D N 1979 Strength of tree roots and landslides on Prince-Of-Wales-Island, Alaska. Canadian Geotechnical Journal 16, 19-33.

Wynn T M, Mostaghimi S, Burger J A, Harpold A A, Henderson M B and Henry L A 2004 Variation in root density along stream banks. Journal of Environmental Quality 33, 2030-2039.

Zeier J, Ruel K, Ryser U and Schreiber L 1999 Chemical analysis and immunolocalisation of lignin and suberin in endodermal and hypodermal/rhizodermal cell walls of developing maize (*Zea mays L.*) primary roots. Planta 209, 1-12.

Zeier J, Ruel K, Ryser U and Schreiber L 1999 Chemical analysis and immunolocalisation of lignin and suberin in endodermal and hypodermal/rhizodermal cell walls of developing maize (*Zea mays L.*) primary roots. Planta 209, 1-12.

Zhang L Z, Li B G, Yan G T, Van der Werf W, Spiertz J H J and Zhang S P 2006 Genotype and planting density effects on rooting traits and yield in cotton (*Gossypium hirsutum L.*). Journal of Integrative Plant Biology 48, 1287-1293.

Ziemer R 1981 The role of vegetation in the stability of forrested slopes. Proceedings of the International Union of Forestry Research Organizations, XVII World Congress, 6-17 September 198l, Kyoto, Japan. Vol. I: 297-308.

Zobel R W 2003 Sensitivity analysis of computer-based diameter measurement from digital images. Crop Science 43, 583-591.

Zobel R W, Kinraide T B and Baligar V C 2007 Fine root diameters can change in response to changes in nutrient concentrations. Plant and Soil 297, 243-254.

BLANK PAGE